

Aspects of Electroweak Symmetry Breaking in Physics Beyond the Standard Model

Peter Athron

Department of Physics and Astronomy

University of Glasgow

Presented as a thesis for the degree of Ph.D.
in the University of Glasgow, University Avenue,
Glasgow, G12 8QQ.

© P. Athron, September 2008

November 26, 2008

Abstract

Fine tuning in the Standard Model (SM) is the basis for a widespread expectation that the minimal model for electroweak symmetry breaking, with a single Higgs boson, is not realised in nature and that new physics, in addition to (or instead of) the Higgs, will be discovered at the Large Hadron Collider (LHC). However constraints on new physics indicate that many models which go beyond the SM (BSM) may also be fine tuned (although to a much lesser extent). To test this a reliable, quantitative measure of tuning is required. We review the measures of tuning used in the literature and propose an alternative measure. We apply this measure to several toy models and a constrained version of the Minimal Supersymmetric Standard Model.

The Exceptional Supersymmetric Standard Model (E_6 SSM) is another BSM motivated by naturalness. As a supersymmetric theory it solves the SM hierarchy problem and by breaking a new gauged $U(1)$ symmetry it also solves the μ -problem of the MSSM. We investigate the Renormalisation Group Evolution of the model and test for radiative electroweak symmetry breaking in two versions of the model with different high scale constraints. First we briefly look at scenarios with non-universal Higgs masses at the GUT scale and present a particle spectrum that could be observed at the LHC. Secondly we study the constrained E_6 SSM (CE_6 SSM), with universal scalar (m_0), trilinear (A_0) and gaugino ($M_{1/2}$) masses. We reveal a large volume of CE_6 SSM parameter space where the correct breakdown of the gauge symmetry can be achieved and all experimental constraints can be satisfied. We present benchmark points corresponding to different patterns of the particle spectrum. A general feature of the benchmark spectra is a light sector of SUSY particles consisting of a light gluino, two light neutralinos and a light chargino. Although the squarks, sleptons and Z' boson are typically much heavier, the exotic color triplet charge $1/3$ fermions as well as the lightest stop can be also relatively light leading to spectacular new physics signals at the LHC.

Acknowledgements

I want to thank all the staff and students in the particle physics theory group at Glasgow University for their help and support and for putting up with my bizarre questions, random rants and general noise pollution. In particular I would like to thank my supervisor David J. Miller for helping me find and work on such interesting projects and for all the other help and support he has provided during my studies. I also want to give special thanks to my office mate and collaborator Roman Nevzorov for providing informative answers to my endless questions, and working with me on exciting projects.

I'm also very grateful to David Sutherland for listening to and discussing my wilder speculations on particle physics and to Dave Thompson for offering some of his own. Thanks to John Campbell, Craig McNeile, Erik Gregory for support in the latter years of my PhD, to Christine Davies, Colin Froggatt and Kit Wong who have provided support and especially to Andrew Davies who helped me work through Peskin and Schroeder. Luo Rui, Ian Kendall, Ian Allison and Dan Guise have also had listen to my random queries and ideas so thanks to them and especially to Dan for reading an early draft of my Standard Model chapter.

I am extremely grateful to my collaborators in Southampton, Steve F. King and Stefano Moretti, with whom I have really enjoyed working and hope to continue doing so. Many thanks as well to Ben Allanach for making his SOFTSUSY program publicly available and also for answering my questions about it.

I wish also to say thanks to Dominik Stötckinger both for his support and help during his brief time in Glasgow and for giving me the opportunity to continue to do interesting research, by offering me the job at Dresden. I look forward to working with him.

Finally thanks to my friends and family who have been there when I needed them.

Declaration

I declare that none of the material presented in this this thesis has previously been presented for a degree at this or any other university.

Chapter 1 provides an overview of my research and the content of the thesis. The material in chapters 2,3,4 and 7 are drawn from background material. Chapters 5,6,8 and 9 describe original work and chapter 10 summarises the thesis. Chapters 5 and 6 are drawn from work carried out in collaboration my supervisor Dr David J. Miller. Chapters 8 and 9 are drawn from work carried out in collaboration with Prof. Steve F. King, Dr David J. Miller, Dr Stefano Moretti and Dr Roman Nevzorov. With the exception of references to the derivation of E_6 SSM Renormalisation Group Equations in chapters 8 and 9 which were derived by my collaborator, Dr Roman Nevzorov, and elsewhere where it is explicitly stated in the text, the content of chapters 5,6,8 and 9 are my own work. My work described here has appeared in the following publications,

- P. Athron and D. J. Miller, “A New Measure of Fine Tuning,”
Phys. Rev. D **76**, 075010 (2007), arXiv:0705.2241 [hep-ph].
- P. Athron and D. J. Miller, “Fine tuning in supersymmetric models,”
AIP Conf. Proc. **903**, 373 (2007).
- P. Athron and D. J. Miller, “Measuring Fine Tuning In Supersymmetry,”
arXiv:0710.2486 [hep-ph].
- P. Athron, S. F. King, D. J. Miller, S. Moretti and R. Nevzorov,
“Electroweak Symmetry Breaking in the E_6 SSM,”
J. Phys. Conf. Ser. **110**, 072001 (2008) arXiv:0708.3248 [hep-ph].

Contents

1	Introduction	1
2	The Standard Model	5
2.1	Particles in the Standard Model	8
2.1.1	Fermions	8
2.1.2	Gauge Bosons	12
2.2	SM Interactions and the Local Gauge Invariance Principle	13
2.3	Electroweak Symmetry Breaking	17
2.3.1	The Higgs Mechanism	17
2.3.2	Higgs Mechanism in the Standard Model	18
2.4	Renormalisation and Renormalisation Group Equations	22
2.5	Hierarchy Problem	26
2.6	Other Motivations to go beyond the Standard Model	28
3	Supersymmetry	30
3.1	Solution to the Hierarchy Problem	32

3.2	Further Motivations	33
3.3	SUSY Lagrangians and Superpotentials	36
3.4	Softly Breaking Supersymmetry	39
3.5	R-Parity	44
3.6	Experimental Constraints on Supersymmetry	45
4	Minimal Supersymmetric Standard Model	47
4.1	Description of the model	47
4.2	Electroweak Symmetry Breaking in the MSSM	49
4.3	Tree level Masses in the MSSM	51
4.4	CMSSM	54
4.4.1	Softsusy	55
5	Quantifying Fine Tuning	58
5.1	Motivation	58
5.1.1	Little Hierarchy Problem	59
5.2	Tuning Measures In literature	60
5.3	Limitations of Traditional Measure	61
5.4	Constructing Tuning Measures	63
5.5	New Tuning Measure	66
5.6	Relation To Other Measures	68
6	Applying New Tuning Measure	70

6.1	Toy Models	70
6.1.1	SM Hierarchy Problem Revisited	70
6.1.2	Other Toy Models with one parameter	73
6.1.3	Proton Mass	75
6.1.4	Toy SM with two parameters	76
6.1.5	Toy Model with three parameters and four observables	78
6.2	CMSSM	80
6.2.1	Procedure	80
6.2.2	Preliminary Study	82
6.2.3	Further Study	84
6.3	Conclusions	92
7	Exceptional Supersymmetric Standard Model	94
7.1	Motivation and Background	94
7.1.1	The μ -problem	95
7.1.2	Light Higgs Mass	96
7.1.3	Gauge Coupling Unification	97
7.1.4	Connection to Superstring theory	97
7.1.5	Neutrinos and Leptogenesis	99
7.2	E_6 SSM Model	100
7.2.1	Superpotential	101
7.2.2	Soft Breaking Terms	103

7.3	Electroweak Symmetry Breaking in the E_6 SSM	104
8	The Non Universal Higgs Mass E_6SSM	111
8.1	Motivation	111
8.2	RG flow of the soft SUSY breaking terms	113
8.3	Electroweak Constraints	115
8.4	Results	117
8.5	Conclusions	119
9	The Constrained E_6SSM	121
9.1	RG flow of the soft SUSY breaking terms	121
9.2	RG flow of the SUSY preserving sector	124
9.3	Low Energy Constraints	126
9.4	Results	129
9.4.1	Exclusion Plots	129
9.4.2	Benchmark Scenarios	137
9.5	Conclusions	154
10	Summary, Conclusions and Outlook	156
A	Superfields	160
A.1	Chiral Superfields	161
A.2	Vector Superfields	161

B Construction of the E_6SSM	163
B.1 Gauge Structure	163
B.2 Matter content	163
B.3 Superpotential	165
C E_6SSM Renormalisation Group Equations	169
D One loop corrections to the Higgs masses in the E_6SSM	178
D.1 Single Derivatives	179
D.2 Double derivatives	180
E Benchmark Spectra	182
E.1 Benchmark Point A1	182
E.2 Benchmark Point A2	184
E.3 Benchmark Point A3	185
E.4 Benchmark Point A4 (Z' mass < 936 GeV)	186
E.5 Benchmark Point B1	187
E.6 Benchmark Point B2	188
E.7 Benchmark Point B3	189
E.8 Benchmark Point C1	190
E.9 Benchmark Point C2	191
E.10 Benchmark Point C3	192
E.11 Benchmark Point D1	193

E.12 Benchmark Point D2	194
E.13 Benchmark Point F1	195
E.14 Benchmark Point F2	196

List of Figures

2.1	SM particle content	6
2.2	Perturbative expansion of the Higgs particles' propagator	23
3.1	Correction to the Higgs propagator from a scalar particle	32
3.2	Comparison of SM and MSSM gauge couplings RGE evolution	34
4.1	SOFTSUSY Flow chart	57
5.1	Illustration for constructing tuning measures	64
5.2	Two dimensional illustration of our tuning measure	67
6.1	SM tuning with one parameter	71
6.2	SM tuning with two parameters	77
6.3	Tuning in a 3 parameter toy model	79
6.4	Flow chart showing the modified iterative routines of our altered version of SOFTSUSY.	81
6.5	$\Delta_{M_{\frac{Z}{2}}}$ for the SPS 1a slope.	83
6.6	Tuning variation in $M_{\frac{Z}{2}}^2$	85

6.7	Δ in the CMSSM	86
6.8	Unnormalised tunings in $m_{\tilde{t}_2}^2$ and m_h^2	87
6.9	$\Delta_{M_A^2}$ in the CMSSM	88
6.10	Point NP1 with a “natural” spectrum	89
6.11	Point NP2 with a “natural” spectrum	89
7.1	Two loop upper bounds on the lightest Higgs mass.	96
7.2	Comparison of RGE Evolution of gauge couplings in the MSSM and E ₆ SSM	98
8.1	NUHM E ₆ SSM exclusion plots	118
8.2	Sample NUHM E ₆ SSM spectrum	119
9.1	Threshold dependence of two-loop RG flow of gauge couplings within the E ₆ SSM	123
9.2	CE ₆ SSM exclusion plot for $\tan\beta = 10$	130
9.3	CE ₆ SSM exclusion plot for $\tan\beta = 10$ and $s = 3$ TeV.	132
9.4	CE ₆ SSM exclusion plot for $\tan\beta = 30$	133
9.5	CE ₆ SSM exclusion plot for $\tan\beta = 10$ and $s = 3$ TeV	134
9.6	CE ₆ SSM exclusion plot for $\tan\beta = 3$	135
9.7	CE ₆ SSM exclusion plot for $\tan\beta = 3$ and $s = 4$ TeV	136
9.8	CE ₆ SSM Benchmark point A1	137
9.9	CE ₆ SSM Benchmark point A2	139
9.10	CE ₆ SSM Benchmark point A3	140

9.11	CE ₆ SSM Benchmark point A4	141
9.12	CE ₆ SSM Benchmark point B1	142
9.13	CE ₆ SSM Benchmark point B2	143
9.14	CE ₆ SSM Benchmark point B3	144
9.15	CE ₆ SSM Benchmark point C1	146
9.16	CE ₆ SSM Benchmark point C2	147
9.17	CE ₆ SSM Benchmark point C3	148
9.18	CE ₆ SSM Benchmark point D1	149
9.19	CE ₆ SSM Benchmark point D2	150
9.20	CE ₆ SSM Benchmark point F1	151
9.21	CE ₆ SSM Benchmark point F2	152

List of Tables

2.1	Chiral fields of the Standard Model	10
2.2	Properties of the Standard Model fermions	11
4.1	Chiral supermultiplets of the MSSM	48
4.2	Gauge supermultiplets of the MSSM, and gauge group representations.	49
4.3	The MSSM particle content yet to be discovered	50
6.1	Tuning measures for models with only one parameter and one observable.	71
6.2	Unnormalised tunings for NP1 and NP2.	90
6.3	Relative tunings with respect to NP1 and NP2	90
7.1	$U(1)_Y$ and $U(1)_N$ charges of E_6 SSM.	104
9.1	Threshold dependence of g_0 and M_X in the CE_6 SSM	124

Chapter 1

Introduction

This thesis describes my research activities carried out during the course of my Ph.D studies. I have a general interest in the phenomenology of both the Standard Model (SM) and physics Beyond the Standard Model (BSM) and the construction of new phenomenologically viable models.

My research has been focused around three related topics, electroweak symmetry breaking, supersymmetry and naturalness. Discovering the mechanism of electroweak symmetry breaking used in nature is essential because it will allow us to understand the origin of the masses of fundamental particles and will either verify the SM, if the simplest version of the Higgs Mechanism is revealed, or provide clues for how the SM must be extended.

For example, in supersymmetric extensions of the SM there are at least two Higgs doublets, leading to at least five physical Higgs particles. One of the major motivations for supersymmetry is that it may solve a naturalness problem with the SM, where the parameters require unnatural fine tuning to keep the Higgs mass light. Naturalness also provides the motivation for most of the BSM physics that provides phenomenology testable at the LHC.

With my supervisor Dr David Miller I carried out research into measuring fine tuning in the Minimal Supersymmetric Standard Model (MSSM) [1–3]. This work

is important because fine tuning is used as a motivating factor for most of the BSM phenomenology and BSM experimental searches at current and future colliders, as well as being the basis for the construction of new exotic physics models. There are a number of difficulties with the tuning measures applied in the literature, including ambiguities in how to combine tunings for individual parameters and observables. Often whether or not a scenario is considered fine tuned depends upon the measure applied. To resolve this we have developed a tuning measure which is directly based on our intuitive notion of tuning and automatically combines tuning from all parameters and observables.

I have also worked on projects on the Exceptional Supersymmetric Standard Model (E_6 SSM) with collaborators Prof. Steve F. King, Dr David J. Miller, Dr Stefano Moretti and Dr Roman Nevzorov. The E_6 SSM model was introduced by S. F. King, S. Moretti and R. Nevzorov in [4–5]. This is a very interesting model because it solves the μ -problem of the MSSM, in a similar way to the NMSSM, but without the accompanying tadpole or domain wall problems. In addition it has a significantly increased upper bound on the mass of the lightest Higgs particle (155 GeV) in comparison to the MSSM, which may ease the Little Hierarchy Problem. It is also very exciting phenomenologically as it predicts the existence of exotic colored objects which may be seen at the LHC.

The projects I have been involved in examine the Constrained Exceptional Supersymmetric Standard Model (CE_6 SSM) [6] and the non-universal Higgs mass (NUHM) E_6 SSM [7] versions of this model to see if electroweak symmetry breaking may be radiatively driven in them in a similar way to the Constrained Minimal Supersymmetric Standard Model (CMSSM). Since radiatively driven electroweak symmetry breaking is viewed as a triumph of the CMSSM, this work provides an important test for the CE_6 SSM and additionally allows us to predict mass spectra which could be seen at the LHC from only three (or six in the case of the NUHM E_6 SSM) soft SUSY breaking parameters.

Chapters 2-4 describe background information on topics which I find interesting and provide information which is important for understanding the research carried out

in later chapters. In chapter 2 a description of the Standard Model is provided with particular emphasis on electroweak symmetry breaking and an introduction to the first naturalness problem in the thesis, the Standard Model Hierarchy problem. Useful pedagogical materials on the topics described here can be found in [8–16].

In much of chapter 2 the language used is deliberately quite basic as it is aimed at as wide an audience as possible. The rest of this thesis is pitched at a postgraduate level student conducting research into theoretical elementary particle physics.

In chapter 3 supersymmetry (SUSY) is introduced. The main motivations for this class of BSM physics are described and basic descriptions of constructing SUSY models and of breaking them are provided. Helpful pedagogical materials may be found in [17–28].

Chapter 4 introduces the MSSM. A description of the particle content and structure of the model are given, followed by a description of EWSB in the MSSM and finally the tree level expressions for the masses of the MSSM particles are presented.

Chapters 5 and 6 describe research I carried out into fine tuning in collaboration with Dr David Miller. In Chapter 5 problems with tuning measures in the literature are identified and a new tuning measure is introduced and its relationship to the other measures revealed.

This new tuning measure and several of the measures in the literature are then applied to the Standard Model and various toy models in chapter 6 and the results compared. Finally the new tuning measure is applied to the CMSSM and the results are analysed.

Chapter 7 describes the E_6 SSM. As such it provides further background material, drawn from papers written by my collaborators [4–5].

Chapters 8 and 9 describe the results of investigations into the radiative electroweak symmetry breaking in the CE_6 SSM and NUHM E_6 SSM. Exclusion plots showing regions of parameter space where no EWSB solutions can be found are presented. The

restrictions from EWSB breaking solutions imply that the gluino is lighter than the squarks, which is unusual and interesting phenomenologically. In addition it is shown that low mass exotic particles are consistent with the model and may be detected at the LHC. Finally detailed particle spectra are presented and discussed

Chapter 2

The Standard Model

The Standard Model (SM) of particle physics is a theoretical construct (called a *Quantum Field Theory*) which is consistent with all current data¹, describing all observed fundamental particles² and their interactions due to the strong, electromagnetic and weak forces.

The particle content of the SM is shown in Fig. 2.1, grouped into matter particles and force mediating particles. The first generation of matter particles are the building blocks of atoms and molecules. The second and third generations are heavier analogues of the first generation, but they do not form stable bound states as they decay too quickly.

Matter particles can also be split up into *quarks* and *leptons*. The quarks interact via the strong, weak and electromagnetic forces. Each generation of quarks contains one particle with positive electric charge, referred to as up type quarks, and one particle with negative electric charge referred to as down type quarks. The first generation of quarks form the bound states, protons and neutrons which make up the nucleus of an

¹Except for the case of neutrino masses as experiments have recently shown that neutrinos have mass [29–31]. The SM has not yet been adapted to include neutrino masses though this could be readily done.

²and one unobserved particle, the *Higgs* boson.

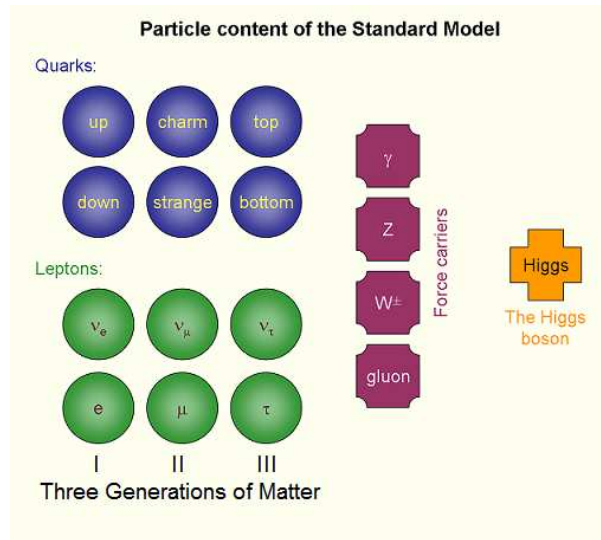


Figure 2.1: The particle content of the Standard Model. Taken from [32]

atom.

The leptons do not interact via the strong force. Instead each lepton generation consists of a lepton which interacts via both the weak force and the electromagnetic force, with negative electric charge and a second type of lepton, termed *neutrino*, which only interacts via the weak force and as such has an electric charge of zero. The first generation charged leptons is the electron. This combines with the positively charged nucleus to form electrically neutral bound states called atoms.

The force mediating particles can be categorised by the force they mediate: the electromagnetic force is mediated by the photon, γ ; the Strong force, by particles called gluons, g , and the weak force by weak particles W^\pm and Z^0 . Gravitational interactions are presumably mediated by a *graviton* but this particle is, so far, undetected due to the relative weakness of gravitation in comparison the other fundamental forces. For this reason gravity (and gravitons) are not included in the SM.

Also shown in Fig. 2.1, and completing the Standard Model is the Higgs particle. The Higgs particle is yet to be observed, but plays a crucial role in the Standard Model as it is responsible for generating masses for the fundamental particles. How fundamental particles obtain mass is currently unknown, but a theoretically consistent

model of the fundamental particles and their interactions cannot be constructed unless it includes a mechanism which generates these masses. In the SM the simplest version of the *Higgs mechanism* (described in Sec. 2.3) plays this role, and this predicts the presence of the Higgs particle.

The construction of the Standard Model is based upon elegant ideas about symmetries of nature. The fundamental forces, which induce the interactions of fundamental particles, are described by groups of symmetry transformations, called *gauge*³ groups, under which the physics is invariant. For example one important family of symmetry groups can be introduced by considering transformations of complex N -component vectors.

The transformations can be represented by $N \times N$ matrices. If these matrices are *unitary* (i. e. $U^\dagger U = I$) the transformations they perform on the vectors will preserve the inner product between them. Such matrices form a unitary group $U(N)$. If the matrices also have a determinant equal to 1 then they form the group of special unitary matrices, $SU(N)$.

Strong interactions are described by *Quantum Chromodynamics* (QCD), which is an $SU(3)$ gauge theory. The electromagnetic and weak forces are described by a unified electroweak theory with gauge group $SU(2) \otimes U(1)$. This electroweak symmetry is broken by the Higgs mechanism to generate masses for the fundamental particles, leaving a different $U(1)$ symmetry associated with the gauge theory *Quantum Electrodynamics* (QED) which describes how light interacts with matter. The full gauge group of the SM, before symmetry breaking, is $SU(3) \otimes SU(2) \otimes U(1)$.

The physics is also invariant when particles in the Standard Model undergo space-time transformations of the Poincaré group. This is a group of translations, rotations and Lorentz boosts. Rotations and boosts make up the Lorentz group of Special Relativity, which is a subgroup of the Poincaré group.

³Gauge transformations are discussed in more detail in 2.2.

2.1 Particles in the Standard Model

In this section the fundamental particles of the Standard Model and their properties are described in more detail. These properties are presented in the Particle Data Book [33] and this has been heavily relied upon as a reference guide here. This information and some updates can be found at the live website [34].

Particles can be classified according to their *spin*, which is an internal quantum number, analogous to angular momentum, though it cannot be described in terms of individual constituents rotating about some fixed axis and is instead an intrinsic property of the particle. Particles with spin values which are odd integer multiples of⁴ $1/2$ are called *fermions*. Particles with integer spin are called *bosons*.

In the Standard model all the fundamental matter particles are fermions and have $\text{spin} = 1/2$.

2.1.1 Fermions

The behaviour of fermions can be conveniently described in the Lagrangian formalism. Just as in classical field theory, the equations of motion (Euler-Lagrange equations) are obtained from the Lagrangian density by finding the path of least action. However unlike classical field theory the fields in the Lagrangian must be quantised.

Free fermions are governed by the Dirac equation,

$$(i\gamma^\mu \partial_\mu - m)\psi = 0. \quad (2.1)$$

which is an Euler-Lagrange equation of the Dirac Lagrangian,

$$\mathcal{L}_{Dirac} = \bar{\psi}(i\gamma^\mu \partial_\mu - m)\psi, \quad (2.2)$$

where ψ the fermion field is a 4-component object, and the adjoint field is given by $\bar{\psi} = \psi^\dagger \gamma^0$. μ runs over the set $\{0, 1, 2, 3\}$ and repeated indices are summed over, m is

⁴Here and throughout this thesis natural units are used in which the reduced Planck constant, \hbar and the speed of light are set equal to 1.

the mass of the fermion and γ^μ are the 4×4 Dirac matrices which satisfy the Clifford algebra, $\{\gamma^\mu \gamma^\nu + \gamma^\nu \gamma^\mu\} = 2g^{\mu\nu}$ and $g^{\mu\nu} = \text{Diag}(1, -1, -1, -1)$ is the Minkowski space-time metric. This can be written in 2x2 block form. Choosing the Weyl representation of the Dirac matrices,

$$\gamma^0 = \begin{pmatrix} 0 & 1 \\ 1 & 0 \end{pmatrix}, \quad \gamma^i = \begin{pmatrix} 0 & \sigma^i \\ -\sigma^i & 0 \end{pmatrix}, \quad (2.3)$$

$$\sigma^1 = \begin{pmatrix} 0 & 1 \\ 1 & 0 \end{pmatrix}, \quad \sigma^2 = \begin{pmatrix} 0 & -i \\ i & 0 \end{pmatrix}, \quad \sigma^3 = \begin{pmatrix} 1 & 0 \\ 0 & -1 \end{pmatrix}, \quad (2.4)$$

$$\Rightarrow L_{Dirac} = (\psi_R^\dagger \ \psi_L^\dagger) \begin{pmatrix} -m & i\sigma \cdot \partial \\ i\bar{\sigma} \cdot \partial & -m \end{pmatrix} \begin{pmatrix} \psi_L \\ \psi_R \end{pmatrix}, \quad (2.5)$$

where ψ_L and ψ_R are two component Weyl spinors and

$$\sigma^\mu = (1, \sigma^1, \sigma^2, \sigma^3) \quad \bar{\sigma}^\mu = (1, -\sigma^1, -\sigma^2, -\sigma^3). \quad (2.6)$$

If $m = 0$ ψ_L and ψ_R decouple and obey independent equations of motion therefore they can be interpreted as separate objects which are coupled by the mass. Fields which obey the ψ_L equation of motion are called left-handed *chiral* fields and those obeying the ψ_R equation, right-handed chiral fields. If the fermion is massless there is no requirement for both the left-handed and right-handed fields to exist.

In addition left-handed and right-handed fields have different interactions. Only left-handed fields interact via the weak force. This means that left-handed fields are placed into electroweak *doublets*, while the right-handed chiral fields are electroweak *singlets*. For a review of the evidence for this see [35–36]. This further suggests that ψ_L and ψ_R really are fundamentally different objects which get coupled by a mass interaction term.

The chiral fields of the Standard Model and their properties are summarised in Table 2.1. These are then mixed by mass couplings into mass eigenstates. The mass eigenstates and properties are shown in Table 2.2.

All of the leptons shown have now been discovered [37–42]. With quarks there

Names		$SU(3)_C$	$SU(2)_L$	$U(1)_Y$
quarks	$Q_i = \begin{pmatrix} u_i \\ d_i \end{pmatrix}_L$	3	2	$\frac{1}{6}$
	u_{Ri}	$\bar{\mathbf{3}}$	1	$\frac{2}{3}$
	d_{Ri}	$\bar{\mathbf{3}}$	1	$-\frac{1}{3}$
leptons	$L = \begin{pmatrix} l_i \\ \nu_i \end{pmatrix}_L$	1	2	$-\frac{1}{2}$
	l_{Ri}	1	1	-1

Table 2.1: The properties of the chiral fields of the Standard Model which apply to all three families, $i = \{1, 2, 3\}$.

is an important subtlety because at low energies the quarks are confined to color neutral bound states called hadrons. There are two types of hadron known as baryons, made up of three quarks each carrying a different color and collectively forming a ‘white’, or color neutral state, and mesons made up of a quark and an anti-quark with the color charges cancelling. The up, down and strange quarks were originally postulated by Gell-Mann and Zweig [43–47] to explain the hadronic spectra. Crucial evidence that quarks really were the substructure of hadrons was obtained when deep inelastic scattering experiments [48–49] verified Bjorken-scaling [50]. Since then the heavier quarks have also been discovered [51–54]. So the existence of all fermions in the Standard Model is well established.

The masses shown in Fig. 2.2 have been extracted from experimental data, and are presented in [33]. In the SM the mass of each fermion is set by its interaction strength with the Higgs (see Sec. 2.3.2) which is a parameter of the model. This means the interaction strength with the Higgs can be fixed by experimentally measured masses, despite no observation of the Higgs to date.

The electric charge shown for the electron is that measured in experiment to be,

Names		charge	mass	Names		charge	mass
quarks	u	$+\frac{2}{3}e$	1.5 – 3 MeV	leptons	e^-	$-e$	0.511 MeV
	d	$-\frac{1}{3}e$	3 – 7 MeV		ν_e	0	< 225 eV
	c	$+\frac{2}{3}e$	1.27 GeV		μ^-	$-e$	105.7 MeV
	s	$-\frac{1}{3}e$	2.5 – 5.5 MeV		ν_μ	0	< 0.19 MeV
	t	$+\frac{2}{3}e$	172.5 GeV		τ^-	$-e$	1.78 GeV
	b	$-\frac{1}{3}e$	4.2 GeV		ν_τ	0	< 18.2 MeV

Table 2.2: Fermions of the Standard Model in their mass eigenstates.. The charges are given in terms of the charge of the electron, $-e = (-1.602176487 \times 10^{-19} \pm 4 \times 10^{-27}) C$.

$-e = (-1.602176487 \times 10^{-19} \pm 4 \times 10^{-27}) C$ [33]. The muon and tauon charges shown are equal to that of the electron as the SM assumes a family symmetry of charges. The neutrinos have strong experimental limits on non-zero charges (see e.g. [55] and more recently [56]). From measurement of the charges of the proton [57] and neutron [58] and the quark model of these baryons one can infer that the charges of the up and down quarks should be $+2/3e$ and $-1/3e$ respectively. Then an assumption of a family symmetry again yields the charges for the second and third generations. There is no experimental evidence of any deviations from this family symmetry of electric charges and in some cases there is very precise experimental confirmation, see e.g. [59] for the muon.

In addition the electric charges of the SM particles are derived from the gauge transformation properties of the left-handed and right-handed chiral fields they are composed of, as will be demonstrated in Sec.2.3.2. In practise this means that experimentally measured electric charges can be used to fix the hypercharge (charge of the $U(1)$ gauge in the SM group $SU(3) \otimes SU(2) \otimes U(1)$) of these fields and conversely any constraints on the hypercharges leads to constraints on the electric charges.

This is important because the charges of the SM particles are also constrained by

anomaly cancellation. The gauge symmetries of the Standard Model are imposed as classical symmetries of the Lagrangian. However it is possible that they could be violated by quantum corrections. In chiral theories there are certain dangerous perturbative quantum corrections, referred to as anomalies, which can violate the classical symmetry in an undesired way. Particular arrangements of the hypercharges can lead to cancellation of these effects preserving the gauge symmetry at the quantum level. The arrangement of electric charges described above does precisely this.

2.1.2 Gauge Bosons

The photon is a spin 0 massless gauge boson, which mediates the electromagnetic force. The mass of the photon is experimentally consistent with zero, the upper limit on its mass being 6×10^{-17} eV [33] and its charge has an upper limit of $5 \times 10^{-30}e$ [33]. The photon is its own anti-particle.

The W^\pm are the charged spin 1 gauge bosons which mediate the weak force, having electromagnetic charge $\pm 1e$. The two different signs represent the particle and the anti-particle. However which sign is associated with the particles and which with the anti-particles is purely a matter of convention. The mass is $m_W = 80.403 \pm 0.029$ GeV [33]. The W was discovered in 1983 at Cern [60].

The Z^0 is a neutral spin 1 gauge boson which mediates the weak force. It has mass $m_Z = 91.1876 \pm 0.0021$ GeV [33]. It was discovered in 1983 [61] just after the W boson.

The gluon is a massless spin 1 gauge boson with zero electric charge which mediates the strong force. From experiment [62] the upper limit on a mass for the gluon is several MeV. There are eight types of gluons commonly labelled by color, with each gluon carrying a color-anticolor charge.

The Higgs particle is a spin 0 boson. Uniquely amongst the particles of the Standard model it is a Lorentz scalar. From searches for the Higgs at LEP the lower bound on the SM Higgs is $m_H > 114.4$ GeV [63]. Recently additional constraints have come from the Tevatron at Fermilab, through search channels $gg \rightarrow h \rightarrow W^+W^-$ and

$q\bar{q} \rightarrow hW^\pm \rightarrow W^\pm W^+ W^-$. The combination of CDF and D0 results now rules out a Higgs mass of 170 GeV [64]. In addition to direct search constraints there are also indirect constraints that can also be used to place bounds on the mass of the Higgs. From electroweak precision test (EWPT) data fitted to the SM an upper bound on the Higgs mass is found, $m_H < 154$ GeV [65].

2.2 SM Interactions and the Local Gauge Invariance Principle

Gauge theories are fundamental to particle physics. As will be shown below the gauge structure of the Standard Model is remarkably successful in describing the interactions of the fundamental particles. For example Quantum Electrodynamics (QED) is a quantum gauge theory which describes how light interacts with matter with remarkably well tested predictions. Integral to the development of QED is the *local gauge invariance principle*.

Classical Electromagnetism is described by Maxwell's Equations. These equations exhibit a *gauge freedom* meaning that a transformation can be made on the scalar or vector fields (electric and magnetic potentials respectively) that leaves the physics invariant. These are termed *gauge transformations*. $A_\mu = (V, \mathbf{A})$ is the electromagnetic 4-vector potential which combines the scalar, V , and vector, \mathbf{A} , potentials of electromagnetism. Using this Maxwell's equations can be derived from,

$$\mathcal{L}_{EM} = -\frac{1}{4}F_{\mu\nu}F^{\mu\nu}, \quad (2.7)$$

$$\text{where } F^{\mu\nu} \equiv \partial^\mu A^\nu - \partial^\nu A^\mu, \quad (2.8)$$

is the Maxwell (or electromagnetic field strength) tensor. This Lagrangian is invariant under gauge transformations, $A_\mu \rightarrow A_\mu - \partial_\mu \alpha(x)$

However if we try to combine this with the Dirac equation (Eq. 2.1) and add an electromagnetic interaction term, then applying only the gauge transformation of classical electromagnetism changes the physics. To leave the physics unaltered the wavefunc-

tion, ψ must be transformed simultaneously with the electromagnetic potentials. Local gauge invariance of the wavefunction is required.

It is more elegant to reverse this argument. The wavefunction ψ describing the field of a particle is not observed, it is $|\psi|$ which has physical meaning. One can adjust the field by phase factors $\psi \rightarrow \exp(i\alpha)\psi$ and observables which are of the form $\int \psi^* \hat{O} \psi dV$, where \hat{O} is an operator, are unchanged.

This is known as ‘global gauge invariance’. The word global is used because the phase factor is the same for all points in space-time. It is also possible to apply a position dependant phase factor $\psi \rightarrow \exp(i\alpha(x))\psi$. However, since derivatives are involved in the Dirac equation, applying this transformation will result in a new term which alters the physics. Demanding local gauge invariance requires modification of the Dirac equation.

To create local gauge invariant terms the derivative ∂_μ is replaced with the *covariant* derivative. For electromagnetism this is written as,

$$D_\mu = \partial_\mu + iqA_\mu, \quad (2.9)$$

where q is the electric charge. Now whenever ψ undergoes an (electromagnetic) gauge transformation, so does the 4-vector potential A_μ . So the formal definition of a local (electromagnetic) gauge transformation is now,

$$\psi \rightarrow \exp(iq\alpha(x))\psi \quad (2.10)$$

$$A_\mu \rightarrow A_\mu - \partial_\mu\alpha(x). \quad (2.11)$$

Combining the free Dirac and electromagnetic Lagrangians and imposing local gauge invariance, leads to the QED Lagrangian,

$$\mathcal{L}_{QED} = \bar{\psi}(i\gamma^\mu D_\mu - m)\psi - \frac{1}{4}F_{\mu\nu}F^{\mu\nu} \quad (2.12)$$

$$= \bar{\psi}(i\gamma^\mu \partial_\mu - m)\psi - \frac{1}{4}F_{\mu\nu}F^{\mu\nu} - q\bar{\psi}\gamma^\mu\psi A_\mu. \quad (2.13)$$

where the γ^μ are the Dirac matrices, defined in Sec. 2.1.1.

Modifying the Dirac equation so that it is locally gauge invariant has led to the inclusion of a new term, $-q\bar{\psi}\gamma^\mu\psi A_\mu$. This term describes interaction between electromagnetic fields and matter, and we now have the Lagrangian of Quantum Electrodynamics!

QED is an extremely well tested theory and has survived since its original inception in the late 1940s [66–72]. Experimental tests of QED are in agreement with theory to a staggering level of precision. For example the anomalous magnetic moment of the electron is:

$$a_e(\text{Experiment}) = 11596521810 \pm 7 \times 10^{-13} \quad (2.14)$$

$$a_e(\text{Standard Model}) = 11596521827.8(0.772)(0.011)(0.026) \times 10^{-13} \quad (2.15)$$

Although this compares experiment with the Standard Model theory prediction [73], a_e is not very sensitive to the strong and weak forces and so this is predominately a test of QED. The number quoted has been calculated by using a value for the fine-structure constant, α determined by experiments using the Rubidium [74] atom.⁵

Since the local gauge invariance principle has led to the remarkably successful gauge theory QED it is reasonable to apply it to interactions involving the weak and strong forces too. The electromagnetic gauge (phase rotations) we have made reference to so far is the abelian group $U(1)_Q$. The subscript Q refers to the charges of the group, which in this case are those of electromagnetism.

To extend this idea we impose local gauge invariance for weak interactions, $SU(2)_W$, where W labels this gauge symmetry as one associated with weak interactions. Then all weakly interacting quarks and leptons are placed into $SU(2)_W$ doublets, to provide a theory of weak interactions. For the strong force we place strongly interacting quarks into $SU(3)_C$ triplets⁶ such that under these $SU(3)_C$ transformations the physics is invariant. This leads to the gauge theory Quantum Chromodynamics (QCD).

⁵An alternative number quoted in [73] can also be obtained by using α measured from experiments using the Caesium [75] atom.

⁶Where C refers to the color charge.

For the standard model we have the gauge group $SU(3)_C \otimes SU(2)_W \otimes U(1)_Y$. From the above discussion one might have expected $U(1)_Q$ to appear in the gauge group instead of the $U(1)_Y$ symmetry describing hypercharge (Y) interactions. However as we shall see the unified electroweak theory with gauge group $SU(2)_W \otimes U(1)_Y$ is in fact broken to the gauge group of electromagnetism, $SU(2)_W \otimes U(1)_Y \rightarrow U(1)_Q$.

The gauge group of the Standard Model leads to predictions of how all the fundamental particles of the SM interact. There is an enormous body of experimental evidence which supports the interactions predicted by the SM.

The $SU(2)_W \otimes U(1)_Y$ theory of electroweak interactions correctly predicts interactions involving neutral and charged Weak currents as well as decays of the Weak bosons. For example see [76] and references therein.

The strength of the QCD interaction increases as the energy scale of the physical process is decreased. This means, as mentioned earlier, that colored objects are confined to bound colorless states, hadrons and mesons, at low energies. Due to this confinement direct probes of QCD are more difficult. Nonetheless perturbative QCD combined with models of hadronisation make predictions which can be testable. These predictions are now well confirmed by experiments.

For example at LEP the processes $e^+e^- \rightarrow$ Four jets, and, $e^+e^- \rightarrow$ Two jets were used to directly probe the gauge structure of QCD [77]. The results are consistent with the $SU(3)_C$ structure of QCD.

Despite the accuracy of these predictions we also have irrefutable experimental evidence for a violation of the $SU(2)_W \otimes U(1)_Y$ symmetry. For example in experiments we observe vector bosons for weak interactions with masses [60–61]. It is not possible to write a mass term for gauge bosons which is invariant under local gauge transformations.

Mass terms are of the form $M^2 B_\mu B^\mu$, where B_μ is the gauge field and M the mass. So for example if B_μ transforms as $B_\mu \rightarrow B_\mu + \partial_\mu \chi(x)$ under the gauge transformation

then,

$$M^2 B_\mu B^\mu \rightarrow M^2 (B_\mu B^\mu + 2B_\mu \partial^\mu \chi(x) + \partial^\mu \chi(x) \partial_\mu \chi(x)). \quad (2.16)$$

The $SU(2)_W \otimes U(1)_Y$ prediction of massless vector bosons is not seen experimentally. Therefore some mechanism of electroweak symmetry breaking should be introduced.

2.3 Electroweak Symmetry Breaking

Electroweak symmetry must be broken to give mass to fundamental particles. However this should be done in a such a way that the predictions for the particle interactions made by the gauge theory are preserved. This can be achieved if the electroweak symmetry is broken *spontaneously*.

To do this in general one takes a continuous symmetry group G of the Lagrangian and adds a potential V which is also invariant under the action of G . Minimising V will determine the minimum energy configuration, or vacuum. If the minimum of V does not respect the full symmetry of Lagrangian, then the symmetry is spontaneously broken in the physical vacuum.

In this case the physical vacuum will not be invariant under all generators of the group. The generators under which the physical vacuum is not invariant are said to have been ‘broken’. A perturbative expansion of the Lagrangian about the physical vacuum is then written. This gives us the Lagrangian of small oscillations ($\mathcal{L}_{f,\lambda}$) about the physical vacuum from which the mass spectrum is obtained.

2.3.1 The Higgs Mechanism

Now we need a continuous symmetry of the Lagrangian and a vacuum, V , which meets the requirements for spontaneous symmetry breaking. It is then possible to determine what happens to the bosons associated with the broken generators, by looking at the mass spectrum of $\mathcal{L}_{f,\lambda}$.

When this is carried out however one does not, in general, obtain mass terms for gauge bosons. Instead massless particles known as Goldstone bosons appear. This phenomenon is known as Goldstone's theorem [78–80]. This theorem is commonly stated (see e. g. [16]) as follows. For every broken global continuous symmetry of the Lagrangian, there is a massless spin zero Goldstone boson which has the same quantum numbers and parity as the 0th component of the symmetry current, j^μ . However when Goldstone's theorem was first formulated it was not clear that local gauge symmetries could evade the basic assumptions it uses. It appeared to be a serious obstacle for developing spontaneously broken gauge theories which describe nature.

As will be shown shortly, a local gauge transformation can remove the Goldstone bosons and therefore, in a local gauge symmetry, the Goldstone bosons cannot be independent physical particles in any gauge. Indeed it is choosing a particular local gauge which leads to a violation of the axioms of Goldstone's theorem.

Peter Higgs first showed this and developed the *Higgs Mechanism* [81–86] to generate masses for gauge bosons. In simple terms this works by postulating a *Higgs Field* which in the minimum energy configuration of the universe (or *vacuum*) is expected to have a non-zero value. This means that the associated Higgs particle is expected to be present in this vacuum. In contrast the fields of fundamental particles are expected to be zero, and the associated particles are not expected to be present in the vacuum.

However, when we move from a vacuum state to an excited one with non-zero values for the field of some fundamental particle, the fundamental particles will appear into space which already contains many Higgs particles. These particles will interact with the Higgs and it will affect their motion according to the strength of this interaction. This effect on the motion of the fundamental particle is what we perceive as mass.

2.3.2 Higgs Mechanism in the Standard Model

In the SM the simplest realisation of the *Higgs Mechanism* which is consistent with data is employed. As was stated in Sec. 2.1.2 the Standard Model has one ingredient

yet to be detected, the *Higgs boson*. This particle is associated with a *Higgs field* postulated in the SM to allow the breakdown of electroweak symmetry into the gauge symmetry of QED, $SU(2)_W \otimes U(1)_Y \rightarrow U(1)_Q$.

The electroweak sector of the SM and its breaking was developed by Glashow, Weinberg and Salam [87,88,89]. The $SU(3)$ symmetry of strong interactions is not broken, as is indicated by the fact that gluons are massless. While the photon is also massless, its physical state is associated with the $U(1)_Q$ symmetry, not the $U(1)_Y$.

The Higgs field in this model is a complex scalar $SU(2)$ doublet,

$$\phi = \begin{pmatrix} \phi^+ \\ \phi^0 \end{pmatrix} \quad (2.17)$$

This appears in Lagrangian for electroweak interactions along with all the matter and gauge fields of the SM,

$$\mathcal{L}_{EW} = (D^\mu \phi)^\dagger (D_\mu \phi) - V(\phi) - \frac{1}{4} [f_{\mu\nu} f^{\mu\nu} + F_{\mu\nu}^l F^{l\mu\nu}] + \mathcal{L}_{matter}, \quad (2.18)$$

where B_μ and $f_{\mu\nu} = \partial_\mu B_\nu - \partial_\nu B_\mu$ are the vector field and field strength tensor, respectively, associated with the $U(1)_Y$ gauge symmetry. W_μ^l , with $l = \{1, 2, 3\}$, are the three vector fields associated with the $SU(2)_W$ gauge symmetry and $F_{\mu\nu}^l = \partial_\nu W_\mu^l - \partial_\mu W_\nu^l + g\epsilon_{jkl} W_\mu^j W_\nu^k$ are the corresponding field strength tensors. \mathcal{L}_{matter} is the part of the Lagrangian from which matter particles derive their mass and interactions and will be discussed later in this section. $V(\phi)$, is the most general renormalisable scalar potential permitted by the SM gauge structure,

$$V(\phi) = \mu^2 |\phi^\dagger \phi| + |\lambda| \left(|\phi^\dagger \phi| \right)^2 \quad (2.19)$$

and D_μ is the covariant derivative

$$D_\mu = \partial_\mu + \frac{ig'}{2} A_\mu Y + \frac{ig}{2} \sigma^l W_\mu^l, \quad (2.20)$$

where σ^l are the Pauli matrices defined in Sec. 2.1.1. Y is the hypercharge and g' and g are dimensionless gauge couplings.

If $\mu^2 < 0$, then the minimum of the potential, is not invariant under $SU(2)_W \otimes U(1)_Y$, leading to spontaneous symmetry breaking. The minimisation condition (or electroweak symmetry breaking condition) for V implies that,

$$|\phi^\dagger \phi| = \frac{\mu^2}{2|\lambda|} \equiv \frac{v^2}{2}. \quad (2.21)$$

This defines a continuous spectrum of minima which could be the physical vacuum, but making the arbitrary choice that one of them is the true physical vacuum,

$$\langle \phi \rangle_0 = \frac{1}{\sqrt{2}} \begin{pmatrix} 0 \\ v \end{pmatrix} \quad (2.22)$$

breaks electroweak symmetry and we have broken generators,

$$\sigma^i \langle \phi \rangle_0 \neq 0, \quad Y \langle \phi \rangle_0 \neq 0. \quad (2.23)$$

So all original generators of $SU(2)_W \otimes U(1)_Y$ are broken, but a linear combination,

$$Q \langle \phi \rangle_0 = \frac{1}{2}(\sigma^3 + Y) \langle \phi \rangle_0 = 0, \quad (2.24)$$

corresponding to the electric charge, is invariant implying a massless boson (the photon) is contained in the model, as required by observation.

Now to find the mass spectrum we need to look at field oscillations about the physical vacuum. Rewriting, $\phi^0 = (h + v)/\sqrt{2}$, expanding the electroweak Lagrangian about the physical vacuum and choosing a specific gauge known as the unitary gauge one obtains,

$$\begin{aligned} L_{s.o} &= \frac{1}{2} \partial^\mu h \partial_\mu h - \mu^2 h^2 + \frac{(v)^2}{8} Z^\mu + \frac{g^2(v)^2}{8} [|W_\mu^+|^2 + |W_\mu^-|^2] \\ &- \frac{1}{4} [f_{\mu\nu} f^{\mu\nu} + F_{\mu\nu}^l F^{l\mu\nu}] + L_{s.o-matter}. \end{aligned} \quad (2.25)$$

where we have defined the fields of the physical gauge bosons,

$$Z_\mu \equiv \frac{gW_\mu^3 - g'B_\mu}{\sqrt{g^2 + g'^2}} \text{ and } W_\mu^\pm \equiv \frac{1}{\sqrt{2}}(W_{1\mu} \mp iW_{2\mu}) \quad (2.26)$$

along with the combination

$$A_\mu \equiv \frac{gB_\mu + g'W_{3\mu}}{\sqrt{g^2 + g'^2}}. \quad (2.27)$$

which defines the field of a massless photon.

So we have an $SU(2) \otimes U(1)$ gauge invariant Lagrangian which after symmetry breaking leads to a particle spectrum containing massive Z_μ, W_μ^+, W_μ^- and Higgs bosons and one massless photon. However to provide a model for nature we also need to include fermions, described by the last term in Eqn. 2.25.

So far the Higgs mechanism has been presented as a method for generating gauge boson masses. However as discussed in Sec. 2.1.1 fermionic fields, ψ are composed of left and right-handed chiral fields, $\psi_{L,R} = (1 \mp \gamma_5)\psi/2$, where $\gamma^5 \equiv i\gamma^0\gamma^1\gamma^2\gamma^3$. These fields are coupled together to form a massive fermion by the mass term in the Lagrangian, $\mathcal{L}_{mass} = -m\bar{\psi}\psi = -m(\bar{\psi}_L\psi_R + \bar{\psi}_R\psi_L)$. Since ψ_L and ψ_R have a different gauge structure, transforming differently under $SU(2)_W$, \mathcal{L}_{mass} violates gauge invariance. So explicit mass terms for the fermions are forbidden.

In the SM the Higgs Mechanism generates mass terms for fermions as well as gauge bosons. A simplified description of this, neglecting generational mixing, can be understood from the following Lagrangian,

$$\begin{aligned}
L_{matter} &= \sum_{j=1}^{j=3} [\bar{L}_j i\gamma^\mu D_\mu L_j + \bar{l}_{Rj} i\gamma^\mu D_\mu l_{Rj} + \bar{Q}_j i\gamma^\mu D_\mu Q_j \\
&+ \bar{u}_{Rj} i\gamma^\mu D_\mu u_{Rj} + \bar{d}_{Rj} i\gamma^\mu D_\mu d_{Rj} - (y_{lj} L_{Lj} \phi l_{Rj} \\
&- y_{uj} \epsilon^{ab} (Q_{Lj})_a (\phi^\dagger)_b u_{Ri} - y_{dj} Q_{Lj} \phi d_{Rj} + h. c.)], \tag{2.28}
\end{aligned}$$

where $h.c.$ stands for hermitian conjugate, j is a generational index, y_f is the trilinear Yukawa coupling between the Higgs field and the right and left-handed chiral fields of the fermion, f . The left-handed electroweak doublets are,

$$Q_1 = \begin{pmatrix} u \\ d \end{pmatrix}_L, \quad Q_2 = \begin{pmatrix} c \\ s \end{pmatrix}_L, \quad Q_3 = \begin{pmatrix} t \\ b \end{pmatrix}_L \tag{2.29}$$

$$L_1 = \begin{pmatrix} \nu_e \\ e^- \end{pmatrix}_L, \quad L_2 = \begin{pmatrix} \nu_\mu \\ \mu^- \end{pmatrix}_L, \quad L_3 = \begin{pmatrix} \nu_\tau \\ \tau^- \end{pmatrix}_L, \tag{2.30}$$

and l_{Rj} , u_{Rj} , and d_{Rj} are the right-handed chiral fields of the j th generation charged lepton, up-type quark and down-type quark respectively. The covariant derivative is defined in Eqn. 2.20, though when acting on quark fields it should include terms with the strong coupling and the $SU(3)_C$ generators, neglected here as they do not take part in the Higgs mechanism.

When we expand about the physical vacuum the last three terms (and their hermitian conjugates) lead to fermion mass terms,

$$\mathcal{L}_{FM} = \sum_{j=1}^{j=3} -\frac{1}{\sqrt{2}}(y_{lj}v)\bar{l}_{Lj}l_{Rj} - \frac{1}{\sqrt{2}}(y_{uj}v)\bar{u}_{Lj}u_{Rj} - \frac{1}{\sqrt{2}}(y_{dj}v)\bar{d}_{Lj}d_{Rj} + h. c. \quad (2.31)$$

To summarise the full particle spectrum described here is two charged gauge bosons W_μ^+ and W_μ^- , sharing a common mass, $gv/2$; two neutral gauge bosons, one A_μ , which is massless, and the other Z_μ^0 having mass $\sqrt{(g^2 + g'^2)}v/2$; fermions with mass $y_f v/\sqrt{2}$ and finally a neutral, scalar boson, h , with mass $\sqrt{-2\mu^2} = v\sqrt{2|\lambda|}$ which is known as the *Higgs boson*.

$$m_\gamma = 0, \quad M_W = \frac{gv}{2}, \quad M_{Z^0} = \frac{(g^2 + g'^2)^{\frac{1}{2}}v}{2}, \quad (2.32)$$

$$m_f = y_f \frac{v}{\sqrt{2}}, \quad m_H = \sqrt{-2\mu^2} = v\sqrt{2|\lambda|} \quad (2.33)$$

2.4 Renormalisation and Renormalisation Group Equations

In the previous sections we have shown how the Standard Model elegantly describes all fundamental particles and their interactions to incredible precision, such as the calculation of the anomalous magnetic moment of the electron in Eq. 2.15. However in some sense we have hidden from view significant complications. Thus far most of the description of the SM has been at the level of classical field theory. While many interesting features of the SM can be explained in this way, the SM is a quantum theory.

The fields are defined through canonical commutation relations. Fourier expansions of the free fields reveal creation and annihilation operators. The creation of a particle at space-time point x and the destruction at space-time point x' is then described by a propagator, for instance the Higgs propagator is written $i/(p^2 - m^2)$. The mass appears as the pole in the particles propagator, and for a non interacting theory this matches the mass which appears as a coefficient of quadratic fields. This relationship breaks down when we try to solve an interacting theory.

The coupled non-linear equations which are obtained from the Lagrangians of interacting quantum field theories like QED or the SM cannot be solved analytically. Instead SM observables are usually calculated using perturbation theory. Observables are written as series expansion in, e. g. $\alpha = e^2/(4\pi^2) \approx 1/137 < 1$, the coupling between photons and fermions. This expansion is commonly done pictorially with Feynman diagrams [71]. The lowest order terms appear as ‘tree level’ diagrams, and higher order terms are drawn as ‘loop’ diagrams, interpreted as being unobserved internal interactions where particles are radiated then reabsorbed.

For example shown below is a diagram representing the propagator of the Higgs particle. On the right hand side of the equality we have explicitly drawn the diagrams for the tree level contribution and two additional diagrams representing one loop corrections due to two different types of particles.

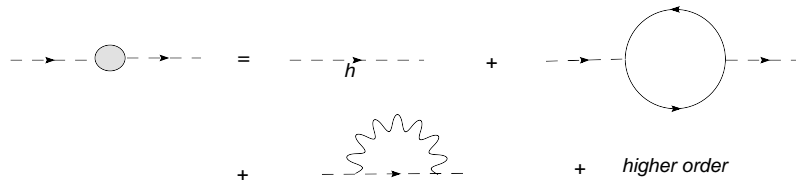


Figure 2.2: Perturbative expansion of the Higgs particles’ propagator

While at tree level the pole in the propagator corresponds to the mass appearing as a quadratic field coupling in the Lagrangian, these corrections disrupt that relationship. We define a pole mass, m_p as the energy in the particle’s rest frame for which the propagator becomes maximal.

$$m_p^2 = m_0^2 + \Sigma, \quad (2.34)$$

where the *bare mass*, m_0 , is the one appearing in the SM Lagrangian and provides the tree level contribution to the propagator. Σ is the real part of the *self energy* of the particle which results from all the radiative corrections

These loops represent integrals which are often formally divergent. However the divergences in the higher order terms can be cancelled by divergences in the bare masses and couplings, in a procedure called renormalisation [90–91]. First the divergent integral is rendered finite by some form of regularisation and then removed by the renormalisation procedure where the divergence is absorbed into the unobservable parameters of the theory.

The most popular regularisation procedure for the Standard Model is *Dimensional Regularisation* (DREG) [92]. In this regularisation scheme the integral is first rendered finite by changing the number of dimensions from 4 where the integral is divergent, to $4 - 2\epsilon$ where the integral is finite. The divergence now appears as a pole when $\epsilon \rightarrow 0$. While this scheme preserves the gauge invariance of the SM it does violence to supersymmetry, which as will be described in chapter 3 requires the number of bosons (n_b) to be equal to the number of fermions (n_f). Changing the dimension of the integral introduces new degrees of freedom spoiling $n_b = n_f$.

Dimensional Reduction (DRED) [93] is a similar scheme to DREG except that only the momenta are of dimension $4 - 2\epsilon$. The gauge fields and γ matrices representing the Clifford algebra remain ordinary 4 dimensional vectors. DRED is frequently used for supersymmetric loop calculations and it has now been shown that it can be formulated in a mathematically consistent way [94–95].

Once the integral has been regularised, renormalisation is carried out. Here certain renormalisation conditions are applied, where some physical processes are defined to take some finite value at a particular momentum, $p^2 = -Q^2$ say. Q is then referred to as the renormalisation scale.

The divergent quantity which has been regularised (i.e. $1/\epsilon$ in DREG and DRED) appears in unobservable shifts relating the finite physical process to “bare” parameters

which appear in the Lagrangian. Since the physical processes are finite this divergence should be cancelled by a divergence in the bare parameters.

If all the divergences arising from higher order corrections can be cancelled by the divergences in the set of bare parameters the theory is then termed renormalisable. In such a theory, once it has been renormalised, the higher order corrections can be treated as small perturbations in a well behaved perturbation series and physical processes can be calculated to the desired order. It has been shown that spontaneously broken gauge theories are renormalisable [92,96] and physical processes in the Standard Model can be calculated using renormalised perturbation theory.

However the removal of the divergences is not enough to guarantee that a process can be calculated using perturbation theory. It must also be possible to express the process as a power series in some quantity < 1 . Feynman diagrams represent a perturbative expansion about the interaction couplings (like α) so it is important that the coupling for a process is small, but it is also important that there is no other large quantity accompanying it in the power series.

An important effect of renormalisation is that different choices of renormalisation scale, Q , lead to different values of the parameters. This variation can be described by a Renormalisation Group Equation (RGE) [97–98],

$$Q \frac{dg}{dQ} = \beta(g) \qquad Q \frac{dM}{dQ} = \beta(M). \qquad (2.35)$$

The equation on the left and right describe the evolution of a dimensionless coupling g and a massive coupling M respectively, with respect to the renormalisation scale. The right hand side of the equations is called the β function of the coupling and may depend on other couplings as well, leading to coupled equations.

When calculating loop corrections to physical processes, power series of, for example, $\alpha |\ln E/Q|$ appear rather than just α , where E is the energy associated with physical process being calculated. These logarithms can be dangerously large, spoiling the perturbation theory even if α is small. To maintain the validity of perturbation theory, Q can be chosen to be of the same order as E , rendering the logarithms small.

So it is usually best to choose a renormalisation scale which is of the same order as the energy which is relevant for the physical process being calculated.

A modern interpretation of these divergences is that the momentum integral is only valid up to the Planck Energy, where new physics should appear. So in carrying out the renormalisation we are not cancelling infinite contributions, but instead terms dependent on the energy scale of new physics. One way of seeing the effect of this is to cut off the momentum in these loops by mimicking the effect of fictitious heavy particles, as happens in *Pauli-Villars regularisation* [99].

In the next section we will simply introduce an arbitrary, ultra-violet cutoff, Λ , for all loop momenta. This is similar to *Pauli-Villars regularisation* but it violates gauge invariance. Nonetheless it has the advantage of being simple and is useful for illustrating the Hierarchy Problem.

2.5 Hierarchy Problem

The fact that gauge theories can absorb the divergences which occur in all the physical processes and at every order is a remarkable result. This makes it possible for the SM to make predictions of the precision described in Sec. 2.2. Despite the beauty and the very precise agreement between experiment and theory of the SM, we know the SM is not a complete description of nature.

The SM does not include the gravitational interaction. While gravity is so weak that it has negligible effect on energies testable in collider physics, at the Planck scale, $\mathcal{O}(10^{19} \text{ GeV})$, gravitational interactions are significant. Therefore one expects new physics to appear at the Planck scale, if not before.

We also expect new physics beyond the Standard Model to appear at low energies $\mathcal{O}(1\text{TeV})$. A major reason for this belief is the Hierarchy Problem. The Higgs mass can be written as,

$$m_H^2 = m_0^2 + \Sigma_H, \tag{2.36}$$

where Σ_H is the real part of the self energy of the Higgs particle.

To calculate the value of such loop diagrams we integrate over all possible momenta for the virtual particles, with a naive cutoff on the Euclidean momentum, Λ , introduced for renormalisation.

For example consider the third diagram shown in Fig. 2.2. It represents the Higgs particle decaying to a fermion–anti-fermion pair which recombine into the Higgs. This can then be evaluated to give,

$$-i\Sigma_f = -i\frac{\lambda_f^2}{2^3\pi^2} \left(\int_0^1 dx 2\Delta \ln \frac{\Lambda^2 + \Delta}{\Delta} - \Lambda^2 \right), \quad (2.37)$$

where $\Delta = -x(1-x)m_H^2 + m_f^2$, m_f is the mass of the fermion and x is an extra parameter introduced for ease of evaluation. Σ_f contains terms quadratic and logarithmic in the cutoff Λ . If the SM really is valid up to the Planck scale, with no new physics entering at lower energies, then $\Lambda \sim M_{Pl}$. Unfortunately this means that the quadratic terms are huge. The one loop corrections, to the Higgs mass, from gauge bosons will also give similar contributions. The total one loop contribution can be expressed as,

$$m_H^2 = m_0^2 - C\Lambda^2 + \dots, \quad (2.38)$$

where the logarithmic terms have been dropped since they are much smaller than the quadratic terms and C is a combination of gauge and Yukawa couplings.

So in order to get weak scale masses $\sim \mathcal{O}(100\text{GeV})$ the bare mass must be very precisely ‘fine tuned’ to be very close to the momentum cutoff. This required tuning seems very unnatural and we feel there needs to be a more natural mechanism for obtaining this hierarchal structure of scales. This is known as the Hierarchy Problem [100–104].

One may believe that Λ is an artifice of the renormalisation prescription and not be concerned about such tunings. However the Higgs will be sensitive to the masses of any new particles which couple to it. Even if the new particles do not couple directly to the Higgs it will be sensitive to them through higher order loop corrections so long as there are common interactions.⁷ So it is expected that if there is new physics at

⁷These arguments are discussed in more detail in e.g. [17]

the Planck scale the Higgs mass will be quadratically sensitive to that scale, and this implies fine tuning.

To remove the problem of fine tuning one could try to lower the cutoff scale and say that new physics comes in much sooner. To do this one should then attempt to construct a realistic model of physics which cuts off the divergent parts of the integral at energies just above the weak scale. Another solution is to postulate new physics to cancel only the quadratic divergences. Supersymmetry does precisely this, as will be discussed in chapter 3.

2.6 Other Motivations to go beyond the Standard Model

Another deficiency of the SM is that it is inconsistent with the observations of *dark matter*, which appears to make up about 85% of the matter content of the universe. Dark matter cannot be seen and is only detected by observing that the motion of the visible matter deviates from the predictions of General Relativity. A dark matter candidate should be a stable particle which only interacts via the weak force and gravity. A review of all the evidence for dark matter is given in [105]. In the SM the only candidate particles for dark matter are the neutrinos. Current upper limits on neutrino masses mean that they cannot account for all the dark matter in the universe (see e. g. [106]).

The anomalous magnetic moment of the muon, a_μ appears to show a $> 3\sigma$ deviation with the SM. At the recent E821 experiment at Brookhaven it has been measured, [107]

$$a_\mu^{\text{exp}} = 11\,659\,208.0(6.3) \times 10^{-10}. \quad (2.39)$$

The SM theory calculation for a_μ has involved many groups working on the various QED, electroweak and hadronic contributions. A recent review [108] obtains

$$a_\mu^{\text{SM}} = 11\,659\,178.5(6.1) \times 10^{-10} \quad (2.40)$$

giving a 3.4σ deviation. The results obtained in [109–111] are slightly different but all obtain a deviation $> 3\sigma$.

It is still possible that this 3σ deviation could simply be a statistical fluctuation. However it is certainly interesting enough to make theorists wonder what types of new physics could explain it.

Neutrinos in the SM are defined as massless. However it has now been established in neutrino experiments [29,30,31,112] that neutrinos have mass, and the SM must be adapted. This can be easily achieved but there is currently insufficient data to restrict theorists to one particular description of the masses.

Chapter 3

Supersymmetry

Supersymmetry (SUSY) was first introduced as the only way to extend the Poincaré algebra, which describes invariant transformations in relativistic space-time [113]. Conserved operators which transform trivially as scalars under the Lorentz group form an internal symmetry group, such as the gauge structure of the SM. Any further extension is highly restricted. The Haag-Lopuszanski-Sohnius [113] extension of the Coleman-Mandula theorem [114] states that SUSY is the only non-trivial extension of the Poincaré group.

Supersymmetry is a special class of graded Lie algebra (or superalgebra) which is consistent with relativistic quantum field theory [113,115]. Graded Lie algebras include group generators S^a which obey anti-commutation relations (like fermion fields), $\{S^a, S^b\} = if^{abc}S^c$, rather just the usual commutation relations, $[T^a, T^b] = if^{abc}T^c$ for generators defining a Lie algebra.

The SUSY generators (or charges) change the spin of a state by a 1/2 integer. So they transform a fermion into a boson and vice-versa,

$$Q|\text{boson}\rangle = |\text{fermion}\rangle \quad Q|\text{fermion}\rangle = |\text{boson}\rangle. \quad (3.1)$$

The supersymmetry charges have half integer spin and are referred to as fermionic operators, while the generators with integer spin, like those of the Poincaré group are bosonic operators. The charges Q (alongwith a conjugate charge \bar{Q}) should also carry

Weyl spinor indices $(\alpha, \beta$ and $\dot{\alpha}, \dot{\beta})$ which all run over the set $\{1,2\}$. There can be more than one copy of the SUSY generators, so supersymmetries are classified according to the number of copies, N , of the generators¹. Due to the requirement that we have chiral fields at low energies $N = 1$ supersymmetry is the only one relevant to low energy phenomenology [25].

The supersymmetry algebra (with vanishing *central charges*².) is,

$$\{Q_\alpha^A, \bar{Q}_{\dot{\beta}B}\} = 2\sigma_{\alpha\dot{\beta}}^\mu P_\mu \delta^A_B \quad (3.2)$$

$$\{Q_\alpha^A, Q_\beta^B\} = \{\bar{Q}_{\dot{\alpha}A}, \bar{Q}_{\dot{\beta}B}\} = 0 \quad (3.3)$$

$$[P_\mu, Q_\alpha^A] = [P_\mu, \bar{Q}_{\dot{\alpha}A}] = 0 \quad (3.4)$$

where P_μ are the generators of space-time translations in the Poincaré group, with $\mu = 0\dots3$ being the index of a Lorentz four-vector. σ^μ is a 4-component object with, $\sigma^0 = I$, the identity matrix and $\sigma^{1,2,3}$ are the three Pauli matrices. Finally the capitalised Roman indices A, B run from $1\dots N$, labelling the different copies of the generators.

Irreducible representations of the supersymmetry algebra are called *supermultiplets* and describe the one particle states of the supersymmetry. In each supermultiplet the number of bosonic degrees of freedom is equal to the number of fermionic degrees of freedom³ ($n_b = n_f$) so they contain both, fermionic and bosonic states, which are the dubbed superpartners. Since the generators of gauge transformations commute with SUSY generators, the superpartners must also have the same gauge transformation properties and consequentially share the quantum numbers, of electric charge, weak isospin and color. SUSY also requires that the superpartners are of equal mass. This is in conflict with experiment since no superpartners of the SM particles have been observed. So if SUSY exists it must be broken. Nonetheless there are many strong motivations to believe that some form of broken supersymmetry exists in nature. In

¹From this it should be understood that N is an integer ≥ 1 . There are however theories termed $N = 1/2$ supersymmetry which are defined on a “non-anti-commutative” superspace, see e. g. [116–118].

²Central charges are excluded for $N=1$ supersymmetry

³This is shown in a relatively simple way in e.g. [17].

the following sections, we describe how many of the problems of the SM outlined in Sec. 2.5 and Sec. 2.6 can be solved if supersymmetry is broken in such a way that the equality of couplings is maintained while the masses of the superpartners to the observed particles are raised high enough to evade current experimental limits. As will be described in Sec. 3.4 supersymmetry can be broken in exactly this way, so all of the motivations below are valid.

3.1 Solution to the Hierarchy Problem

Supersymmetric theories have the correct properties to cancel the quadratic divergences in scalar masses which were discussed in Sec. 2.5. To see how this works consider the one loop correction to the Higgs propagator, shown in Fig. 3.1 due to a single scalar, s , which is the superpartner of one of the SM fermions.

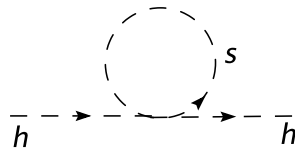


Figure 3.1: Correction to the Higgs propagator from a scalar particle

With a cutoff, Λ , imposed on the Euclidean momentum this gives,

$$-i\Sigma_s = -i\lambda_s \frac{1}{2^4\pi^2} (\Lambda^2 - m_s^2 \ln \frac{\Lambda^2 + m_s^2}{m_s^2}), \quad (3.5)$$

where m_s is the mass of the scalar particle, s and λ_s is a quartic coupling between the Higgs, h , and s . Again both quadratic and logarithmic divergences have appeared. However the quadratic terms have opposite sign and this is a hint for a possible solution. If the coefficients of these terms were equal ($\lambda_f^2/(2^3\pi^2) = \lambda_s/(2^4\pi^2) \Rightarrow \lambda_f^2 = \lambda_s/2$) then the quadratic divergences cancel. Since Supersymmetry requires $n_b = n_f$ in each supermultiplet there are two scalar superpartners for each SM fermion. Furthermore supersymmetry also implies that $\lambda_{s_1} = \lambda_{s_2} = \lambda_f^2$, cancelling the quadratic divergences exactly.

Notice also that the quadratic divergences are independent of the masses of the fermion and the scalar superpartners. So if supersymmetry is broken in such a way that the masses $m_{s_i} > m_f$ the terms with quadratic dependence on the cutoff scale, Λ , do not reappear. However the mass splitting between the superpartners cannot be too large because the terms with logarithmic dependence on Λ , vary quadratically with these masses. Too large a splitting would reintroduce fine-tuning. How tuned a supersymmetric model must be in order to evade current limit on superpartner masses is model dependent. How tuning can be quantified is the subject of Chapter 5 and in Chapter 6 tuning in a particular supersymmetric model, the Constrained Minimal Supersymmetric Standard Model (CMSSM) is examined.

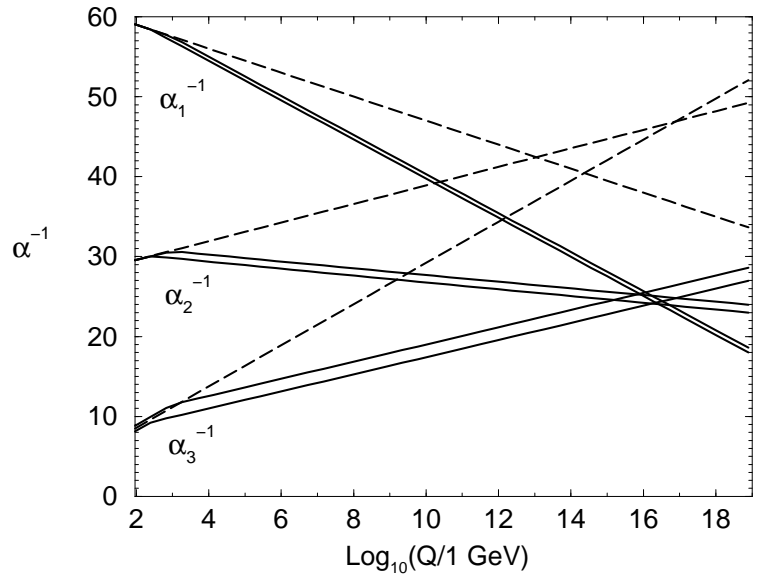
3.2 Further Motivations

Low energy supersymmetry can also explain the deviation between the experimentally measured anomalous magnetic moment and the SM theory prediction. This is a challenge for generic BSM physics as the contributions are suppressed by the mass scale of the new physics and typically masses which are low enough have been ruled out [119–122]. However in supersymmetric models there is a Higgs sector parameter, $\tan\beta$ (see Sec. 4.3 for a definition) which is $\mathcal{O}(10)$ and appears as multiplicative enhancement to the SUSY contribution [123],[119–122]. Since the contribution decreases with the mass scale of the new particles this still requires sparticles which are light.

Another very attractive idea which goes beyond the Standard Model is that of *Grand Unified Theories* (GUT), which provide a unified description of the electromagnetic, weak and strong forces, combining all gauge groups into one, with gauge interaction of strength g_0 . As was described in Sec. 2.4 renormalisation introduces a scale dependence to the couplings and they can be described as evolving according to Renormalisation Group Equations (RGE).

Since GUT have a single unified g_0 it would be nice if the gauge couplings (with appropriate GUT normalisation) evolved to a single point. In the SM when RGE

Figure 3.2: Inverse gauge couplings $\alpha_a^{-1}(Q)$ in the SM (dashed lines) and the MSSM (solid lines) two loop evolution over renormalisation scale, Q . For the MSSM sparticle mass thresholds are varied between 250 GeV and 1 TeV, and $\alpha_3(m_Z)$ between 0.113 and 0.123. Taken from [17].



evolution is plotted the gauge couplings, g_i (or equivalently $\alpha_i = g_i^2/(4\pi^2)$) do not meet at a single point, as shown by the dotted lines in Fig. 3.2 taken from [17]. Threshold corrections to the RGE from new particles associated with the GUT are not known to fix this.

Supersymmetry at or below the TeV scale can improve this, adjusting the running such that gauge couplings unify at a single point. This is shown for the Minimal Supersymmetric Standard Model (MSSM) (which will be described in the next chapter) in Fig. 3.2. However it should be pointed out that recent developments spoil this unification in the MSSM a little, with now a deviation $> 2\sigma$ (see [124] and references therein for an explanation). Nonetheless this discrepancy could be solved by threshold corrections to the RGE from GUT scale physics or in other supersymmetric models like the E_6 SSM [124].

In SUSY models a discrete symmetry called *R-Parity* (see Sec. 3.5) is usually postulated. R-parity conserving SUSY has a natural dark matter candidate, which is the Lightest Supersymmetric Particle (LSP), usually the lightest neutralino (a mass eigenstate formed from superpartners of the neutral gauge and Higgs fields). For the LSP to be dark matter it must be quite light (see e. g. [125]) and if we assume the spectrum is not too hierarchical then this also points to low energy supersymmetry.

It is striking that we now have four separate hints of low energy supersymmetry. While it is certainly possible that some other explanation exists for all of these problems they emphasise the importance of searching for supersymmetric models at forthcoming colliders.

In the Standard Model the shape of the Higgs potential is just postulated to have the correct shape for electroweak symmetry breaking (EWSB). In supersymmetric models one can hope to do better. Various supersymmetry breaking scenarios generate soft masses which break supersymmetry (see Sec. 3.4) at some energy scale far above the electroweak breaking scale where we can do experiments. In addition these breaking schemes often imply some relations between the various soft parameters at the high energy scales.

It is then possible to use the RGE to evolve the parameters from this higher scale down to observable scales and see if the Higgs potential has taken on the required shape for electroweak symmetry breaking. If this happens for generic choices of the parameters at the high scale then one can say that EWSB is radiatively generated, since it is the radiative corrections which dictate how the parameters evolve with scale.

In the MSSM it has been shown that radiative symmetry breaking takes place [126–132] for certain high scale universality prescription on the parameters which have been inspired by SUSY breaking models, e. g. the Constrained MSSM (CMSSM), inspired by the Minimal SuperGRAvity (mSUGRA) breaking scheme.

From Cosmic Microwave Background (CMB) measurements [133] there is a baryon asymmetry in the universe of $(n_b - n_{\bar{b}})/n_\gamma = (6.1 \pm 0.3) \times 10^{-10}$. Explaining the origin of this asymmetry is a theoretical challenge. The SM as defined in Sec. 2 is not sufficient to explain this as it does not have enough CP-violation for electroweak baryogenesis (see e.g. Sec. 7.1 of [19]). However extending the Standard Model to include right-handed neutrinos, which is very reasonable thing to do now that we know neutrinos have mass, can help. This allows an alternative to electroweak baryogenesis, leptogenesis from lepton violating decays.⁴ Supersymmetric models may have some

⁴The lepton asymmetry thus generated is then converted into a baryon asymmetry through the

further advantages over the SM as they have additional sources of CP-violation, improving prospects for Electroweak baryogenesis; may contain new exotic matter with additional lepton number violating decays which can improve prospects for leptogenesis and finally supersymmetric models also admit the possibility of the Affleck-Dine mechanism [135].

3.3 SUSY Lagrangians and Superpotentials

A simple free chiral supersymmetric Lagrangian, can be written as,

$$\mathcal{L}_{\text{free}} = \partial^\mu \phi^{*i} \partial_\mu \phi_i + i \psi^{\dagger i} \bar{\sigma}^\mu \partial_\mu \psi_i + F^{*i} F_i, \quad (3.6)$$

where ϕ is a complex scalar field and ψ is a left-handed 2-component Weyl fermion. The index i is a flavour index. F is auxiliary field which does not describe a physical particle. It is required to balance the fermionic and bosonic degrees of freedom when off shell and has an Euler-Lagrange equation $F_i = 0$.

This Lagrangian is invariant under infinitesimal SUSY transformations,

$$\phi_i \rightarrow \phi_i + \delta\phi_i \qquad \delta\phi_i = \epsilon\psi_i, \quad (3.7)$$

$$(\psi_i)_\alpha \rightarrow (\psi_i)_\alpha + \delta(\psi_i)_\alpha \qquad \delta(\psi_i)_\alpha = i(\sigma^\mu \epsilon^\dagger)_\alpha \partial_\mu \phi_i + \epsilon_\alpha F_i, \quad (3.8)$$

$$F_i \rightarrow F_i + \delta F_i \qquad \delta F_i = i\epsilon^\dagger \bar{\sigma}^\mu \partial_\mu \psi_i, \quad (3.9)$$

where ϵ^α , a 2-component Weyl spinor, is infinitesimal. ϕ_i and ψ_i are superpartners and reside in the same chiral supermultiplet.

Wess and Zumino [136] constructed the first interacting supersymmetry preserving Lagrangian by adding, to the free chiral Lagrangian $\mathcal{L}_{\text{Free}}$, all renormalisable interaction involving chiral supermultiplets that are allowed by supersymmetry,

$$\mathcal{L}_{\text{WZ}} = \partial_\mu \phi^{*i} \partial^\mu \phi_i + \psi^{\dagger i} \bar{\sigma}^\mu \partial_\mu \psi_i - |W_i|^2 - \frac{1}{2} \{W^{ij} \psi_i \psi_j + \text{h.c}\} \quad (3.10)$$

$$W = l^i \phi_i + \frac{1}{2} \mu^{ij} \phi_i \phi_j + \frac{1}{6} y^{ijk} \phi_i \phi_j \phi_k, \quad (3.11)$$

non-perturbative B+L violating sphaleron process [134].

$$W_i = \frac{\partial W}{\partial \phi_i}, \quad W_{ij} = \frac{\partial^2 W}{\partial \phi_i \partial \phi_j}. \quad (3.12)$$

W is the superpotential and μ^{ij} are bilinear couplings of dimension [mass] which are symmetric over the interchange $i \leftrightarrow j$; y_{ijk} are dimensionless trilinear couplings, symmetric in the interchange of i, j and k and the linear coefficients⁵, l^i , are of dimension [mass]². The auxiliary fields have been removed by imposing their Euler-Lagrange equation for the interacting Lagrangian,

$$F_i = -W_i^*, \quad F^{*i} = -W^i. \quad (3.13)$$

So far only spin zero and spin 1/2 fields have been included in the Lagrangian. One can also include spin 1 bosons along with spin 1/2 superpartners, which reside together in gauge supermultiplets. A Lagrangian with gauge supermultiplets can be constructed as,

$$\mathcal{L}_{\text{Gauge}} = -\frac{1}{4} F_{\mu\nu}^a F^{\mu\nu a} - i \lambda^{\dagger a} \bar{\sigma}^\mu D_\mu \lambda^a + \frac{1}{2} D^a D^a, \quad (3.14)$$

where,

$$F_{\mu\nu}^a = \partial_\mu A_\nu^a - \partial_\nu A_\mu^a + g f^{abc} A_\mu^b A_\nu^c \quad (3.15)$$

$$D_\mu \lambda^a = \partial_\mu \lambda^a + g f^{abc} A_\mu^b \lambda^c, \quad (3.16)$$

and the A_μ^a are the gauge fields and their spin 1/2 superpartners λ^a are called gaugino fields. The D^a are auxiliary fields, analogous to the F^i fields for the Wess-Zumino Lagrangian, which are required so that off-shell we maintain $n_b = n_f$ for the gauge supermultiplets and the supersymmetry algebra closes. Roman indices run over the generators of the gauge group, while Greek indices run over the dimensions of space-time for the Lorentz vectors and tensors.

The infinitesimal SUSY transformations are,

$$\delta A_\mu^a = \frac{1}{\sqrt{2}} (\epsilon^\dagger \bar{\sigma}_\mu \lambda^a + \lambda^{\dagger a} \bar{\sigma}_\mu \epsilon), \quad (3.17)$$

$$\delta \lambda_\alpha^a = \frac{i}{2\sqrt{2}} (\sigma^\mu \bar{\sigma}^\nu \epsilon)_\alpha F_{\mu\nu}^a + \frac{1}{\sqrt{2}} \epsilon_\alpha D^a, \quad (3.18)$$

$$\delta D^a = \frac{i}{\sqrt{2}} (\epsilon^\dagger \bar{\sigma}^\mu D_\mu \lambda^a - D_\mu \lambda^{\dagger a} \bar{\sigma}^\mu \epsilon). \quad (3.19)$$

⁵ $l^i \phi_i$ is forbidden unless ϕ_i is a gauge singlet. For this reason the term is often dropped.

Finally we can combine all of this, and adding all renormalisable terms which respect SUSY invariance, we obtain a SUSY invariant Lagrangian containing interacting chiral and gauge supermultiplets,

$$\begin{aligned}
\mathcal{L}_{\text{SUSY}} &= D^\mu \phi^{*i} D_\mu \phi_i + i\psi^{\dagger i} \bar{\sigma}^\mu D_\mu \psi_i - \frac{1}{2} \mu^{ij} \psi_i \psi_j - \frac{1}{2} \mu_{ij}^* \psi^{\dagger i} \psi^{\dagger j} \\
&- \frac{1}{2} y^{ijk} \phi_i \psi_j \psi_k - \frac{1}{2} y_{ijk}^* \phi^{*i} \psi^{\dagger j} \psi^{\dagger k} - \frac{1}{4} F_{\mu\nu}^a F^{\mu\nu a} - i\lambda^{\dagger a} \bar{\sigma}^\mu D_\mu \lambda^a \\
&- \sqrt{2}g(\phi^* T^a \psi) \lambda^a - \sqrt{2}g\lambda^{\dagger a} (\psi^\dagger T^a \phi) - V(\phi, \phi^*)
\end{aligned} \tag{3.20}$$

with,

$$\begin{aligned}
V(\phi, \phi^*) &= F^{*i} F_i + \frac{1}{2} \sum_a D^a D^a = W_i^* W^i + \frac{1}{2} \sum_a g_a^2 (\phi^* T^a \phi)^2 \\
&= \mu_{ik}^* \mu^{kj} \phi^{*i} \phi_j + \frac{1}{2} \mu^{in} y_{jkn}^* \phi_i \phi^{*j} \phi^{*k} + \frac{1}{2} \mu_{in}^* y^{jkn} \phi^{*i} \phi_j \phi_k \\
&+ \frac{1}{4} y^{ijn} y_{kln}^* \phi_i \phi_j \phi^{*k} \phi^{*l} + l^{i*} \mu_{ij} \phi^j + l_i \mu^{ij*} \phi_j^* \\
&+ \frac{1}{2} l^{i*} y_{ijk} \phi^j \phi^k + \frac{1}{2} l_i y^{ijk*} \phi_j^* \phi_k^* + \frac{1}{2} \sum_a g_a^2 (\phi^* T^a \phi)^2.
\end{aligned} \tag{3.22}$$

where we have also used the Euler-Lagrange equations to remove the auxiliary D^a fields ($D^a = -g(\phi^* T^a \phi)$) as well as the F^i fields. D_μ is the covariant derivative for the gauge group of the supermultiplet, T^a are the generators of the gauge group, and g_a are dimensionless gauge couplings. The terms derived from F_i fields in Eqn.(3.21) are referred to as F-terms and terms derived from the D^a fields as D-terms.

Many of the terms in $\mathcal{L}_{\text{SUSY}}$ will vanish if they violate the gauge transformation of the supermultiplet. For example all terms with l_i will vanish unless there is chiral supermultiplet which transforms as a gauge singlet. Most of the terms in the Lagrangian can be determined from the superpotential, W . The other terms are all readily determined from the gauge group of the model, particle content and the transformations. So to specify a SUSY model often the superpotential W , gauge group, particles and the transformation properties of each supermultiplets present in the model are given.

The superpotential is usually written in terms of superfields rather than the scalar fields as was presented here. Eqn. (3.11) can be written instead as,

$$W = l^i \hat{\phi}_i + \frac{1}{2} \mu^{ij} \hat{\phi}_i \hat{\phi}_j + \frac{1}{6} y^{ijk} \hat{\phi}_i \hat{\phi}_j \hat{\phi}_k, \tag{3.23}$$

where $\hat{\phi}_i$ is a superfield and contains the scalar, ϕ_i , fermionic, ψ_i and auxiliary field, F_i . While this is the only knowledge of superfields that is required to understand this thesis a more detailed description of superfields is presented in Appendix A.

3.4 Softly Breaking Supersymmetry

From the non-observation of supersymmetric partners for the SM particles, if supersymmetry exists it must be broken at some scale above energies⁶ which have already been probed at LEP and the Tevatron. However if one wishes to maintain naturalness as a motivation for supersymmetry it must be broken in such a way that the cancellations of the quadratic divergences is maintained.

Therefore the superpartners' equality of dimensionless couplings should be maintained while breaking the mass equalities in such away that the experimental constrains on superpartner masses can be evaded. This is referred to as soft SUSY breaking. The following terms break supersymmetry softly (without re-introducing quadratic divergences at any order in the perturbation theory [137]) if they appear in the Lagrangian:

- Gaugino mass: $M_a \lambda^a \lambda^a$
- Massive trilinear coupling: $a^{ijk} \phi_i \phi_j \phi_k$
- massive bilinear coupling: $b^{ij} \phi_i \phi_j$
- Tadpole term: $t_i \phi_i$
- complex conjugates of all the above terms
- Scalar (mass)² term: $(m^2)_j^i \phi^{j*} \phi_i$

⁶Many of the motivations presented in Secs. 3.1 and 3.2 were for low energy supersymmetry, requiring that superpartners are not too much heavier than the electroweak scale. With respect to fine tuning this will be discussed in much greater detail in Chapters 5 and 6.

where, as with the terms in $\mathcal{L}_{\text{SUSY}}$, further restrictions will be imposed by the gauge groups of the supermultiplets.

With these soft SUSY breaking terms phenomenological studies can be carried out for some particular low energy SUSY model where the soft masses are TeV scale, e.g. the Minimal Supersymmetric Standard Model (MSSM). At high energies supersymmetry is restored but the low energy model incorporating soft breaking terms forms a low energy effective theory. This approach is very general and independent of any particular SUSY breaking mechanism. While this is an entirely valid approach the sheer size of the parameter space makes a thorough survey of all possibilities a daunting task. It is often useful to look to particular breaking mechanisms for some inspiration as to how this parameter space might be constrained.

In any case rather than simply postulate the existence of soft supersymmetry breaking terms without motivation it is preferable to have model of the spontaneous breakdown of supersymmetry. As with EWSB in Sec. 2.3, this occurs when the physical vacuum is not invariant under the action of the generators of the symmetry, in this case supersymmetry generators $Q|0\rangle \neq 0$. This can be achieved when either an F-term or a D-term obtains a vacuum expectation value (vev). The latter is realised in Fayet-Iliopoulos SUSY breaking [138], the former in O’Raifeartaigh SUSY breaking [139].

Typically phenomenological models such as the MSSM, NMSSM and E_6 SSM do not have the right ingredients for a viable breakdown of supersymmetry and need to be augmented in some way. If TeV scale supersymmetry is coupled directly to an O’Raifeartaigh type breaking sector, mass sum rules [140] predict sparticle masses far below the lower bounds set by experiment. Fayet-Iliopoulos type breaking of supersymmetry through tree level couplings to the observed sector fails to produce viable spectra. If the known gauge structure from the SM is used and with an extended $U(1)$ the breaking can reintroduce quadratic divergences unless the trace of the $U(1)$ charges vanishes [141]. Unfortunately requiring the trace of these to vanish returns us to sum rules implying mass spectra ruled out by experiment.

So for SUSY breaking it is normal to postulate a hidden sector, which is secluded from the visible sector (our softly broken, phenomenological SUSY model) having only very small or no couplings with the chiral supermultiplets in the visible sector. Supersymmetry is broken in the hidden sector and then mediated to the visible sector through some common interaction shared by both.

Therefore we have two separate sectors for a complete phenomenologically SUSY model: the hidden sector and the visible sector. SUSY model building then tends to be split into three separate components. The construction of phenomenologically viable SUSY models with explicit soft breaking terms; models of a hidden sector with spontaneous supersymmetry breaking, and models of how this spontaneous breaking is transmitted from the hidden sector to the visible sector via some form of suppressed interaction.

The former has already been discussed in the previous sections and two examples are discussed in much greater detail in chapter 4, the Minimal Supersymmetric Standard Model (MSSM) and in chapter 7 the Exceptional Supersymmetric Standard Model (E_6 SSM).

Since, by construction, the hidden sector has only suppressed interactions with the visible sector it is assumed that hidden sector does not affect the radiative corrections and RG flow in the visible sector. Therefore for phenomenological studies hidden sectors are often neglected, and this is the approach taken in research described in this thesis.

Nonetheless the construction of such models have important implications for naturalness. If supersymmetry is broken dynamically this can actually lead to a hierarchy as a prediction (rather than simply stabilising the Weak scale) [142]. A review of dynamical SUSY breaking models is given in [143]. More recently it has been claimed that dynamical SUSY breaking with a completely stable vacuum (a global minimum) is tough and non-generic (see e. g. [144]). However meta-stable vacua (a local minimum which will eventually decay) are proposed as being easier to construct and generic [144–148]. A useful pedagogical guide is given in [23].

The high scale pattern of the soft masses is largely dictated by the form of mediation. Common types of models for this are gravity mediation, gauge mediation and more recently anomaly mediation has received some interest.

Some breaking schemes predict relations amongst the soft breaking parameters at the high scale. For example gravity mediation with Minimal SuperGRAvity (mSUGRA) inspires certain constrained phenomenological models e.g. CMSSM, CE₆SSM. Since these models are the subject of research described in this thesis, a brief description of their mSUGRA inspiration is given here.

In gravity mediation the soft terms appear through non-renormalisable higher dimensional, Planck suppressed operators of SuperGRAvity (SUGRA) which is a model of local supersymmetry. Global supersymmetry can be promoted to a local symmetry by making the symmetry transformations position dependent (i.e. replace the ϵ with $\epsilon(x)$ in the infinitesimal transformations) as has been done for gauge symmetries. In order to preserve invariance under local SUSY transformations a spin 2 field, $g_{\mu\nu}$ (describing a massless graviton) and a spin 3/2 field ψ^μ (describing a gravitino⁷) must be introduced. Together they form a supergravity supermultiplet which appears in the Lagrangian in non-renormalisable higher dimensional operators which are suppressed by powers of M_{Pl} . In the limit $M_{Pl} \rightarrow \infty$, SuperGRAvity \rightarrow Global supersymmetry.

However the Planck suppressed operators can play an important role in transmitting SUSY breaking to the visible sector. These non-renormalisable operators couple the hidden sector auxiliary F fields to the gaugino and scalar fields of the MSSM. When the F field picks up a vev the soft mass terms, listed at the beginning of this section, are generated as part of a Planck scale effective field theory of broken supersymmetry. They may be generated⁸ as,

- $f_a F \lambda^a \lambda^a / M_{Pl} \rightarrow M_a \lambda^a \lambda^a$ where $M_a = f_a \langle F \rangle / M_{Pl}$

⁷The gravitino obtains a mass through a super-Higgs mechanism when local supersymmetry is broken.

⁸Ignoring the tadpoles as these soft terms are not included in the models discussed in this thesis.

- $h^{ijk}F\phi_i\phi_j\phi_k \rightarrow a^{ijk}\phi_i\phi_j\phi_k$ where $a^{ijk} = h^{ijk}\langle F\rangle/M_{Pl}$
- $\mu'^{ij}F\phi_i\phi_j/M_{Pl} \rightarrow b^{ij}\phi_i\phi_j$ where $b^{ij} = \mu'^{ij}\langle F\rangle/M_{Pl}$
- $FF^*\kappa_j^i\phi_j^*\phi_i/M_{Pl}^2 \rightarrow (m^2)_j^i\phi_j^*\phi_i$ where $(m^2)_j^i = \kappa_j^i\langle F\rangle^2/M_{Pl}^2$

While the soft masses inherit the Planck scale suppression of the non-renormalisable operators, if the auxiliary fields in the hidden sector pick up vevs at a high enough scale the soft masses can be of the desired order (0.1..1 TeV) for phenomenological purposes.

In a very special form of Supergravity, minimal Supergravity (mSUGRA) there are very strong constraints on the couplings appearing in the non-renormalisable Lagrangian. These constraints on the couplings imply constraints on the soft masses generated in mSUGRA leading to a single universal, flavour diagonal, scalar mass, ($m_0^2 = \kappa \frac{|\langle F\rangle|^2}{M_{Pl}^2}$); universal gaugino masses ($M_{1/2} = f \frac{\langle F\rangle}{m_{Pl}}$); universal trilinear softmass ($A = \frac{\alpha\langle F\rangle}{M_{Pl}}$) and finally a universal bilinear mass ($B = \frac{\beta\langle F\rangle}{M_{Pl}}$). κ and f are universal diagonal couplings for the scalar and gaugino masses respectively; β is a constant of proportionality between μ'^{ij} and the bilinear coupling appearing in 3.11 and α is a constant of proportionality between h^{ijk} and y^{ijk} , the Yukawa couplings from 3.11.

Such a scheme has clear phenomenological advantages. It is simple, with only a few parameters making the parameter space much more manageable, enabling phenomenological studies to cover a much greater portion of the space. In addition Flavour Changing Neutral Current (FCNC) constraints (see e.g. [149–151] can be evaded with this universality [152], as well as limits on CP-violating phases (e. g. [153–155]). So the universality conditions are very well motivated from a phenomenological perspective.

The Constrained MSSM (CMSSM) uses the simple high scale parameter scheme motivated by mSUGRA as a postulate, though unlike mSUGRA there is no graviton or gravitino in the model. The masses can be evolved from the high scale down to the TeV and Electroweak scales and the phenomenological consequences can be studied. In this model radiative electroweak symmetry breaking takes place, as the (mass)² of

the up-type Higgs⁹, initially equal to $m_0^2 > 0$ is driven negative by the large top quark Yukawa coupling during the Renormalisation Group evolution between the high scale and the electroweak scale.

It should also be pointed out that strong constraints on the parameter space can also come out of the other breaking mediation schemes. These are not described in detail here as they are not the subject of investigation in this thesis, but it is very important to note that both how supersymmetry is broken and how this breaking is mediated are open questions and the gravity mediation which has inspired the phenomenological models studied in this thesis is just one possibility.

3.5 R-Parity

While in the SM there are no renormalisable terms which could violate baryon number or lepton number, this is not the case in supersymmetric theories. No baryon or lepton number violating decay has been observed experimentally, and the non-observation of the proton decay puts strong constraints on this. While one could impose baryon and lepton number conservation directly to avoid this¹⁰, it is known that non-perturbative effects, significant only at high energies, violate baryon and lepton number [156] and these may be important in the early universe.

Instead a new discrete symmetry is imposed which rules out all the dangerous B and L number violating terms in the Superpotential. This discrete symmetry is often either, Matter parity, or equivalently, R-Parity, which are given by conservation of the multiplicative quantum numbers,

$$P_M = (-1)^{3(B-L)} \quad \text{and} \quad P_R = (-1)^{3(B-L)+2s}, \quad (3.24)$$

respectively and s is the spin of the particle. Due to the conservation of angular

⁹As will be discussed in the next chapter the MSSM contains two Higgs doublets one which gives mass to up-type quarks and other to down-type quarks and charged leptons.

¹⁰In fact proton decay can be avoided simply by imposing *either* baryon or lepton number conservation.

momentum at interaction vertices these two symmetries have the same consequences. All observed SM particles and Higgs particles have $P_R = +1$, while the supersymmetric partners (sparticles) of these have $P_R = -1$.

As a result if a sparticle decays, then there will be an odd number of daughter sparticles. The lightest sparticle (LSP) cannot then decay as any decay into lighter particles would violate R-parity. Therefore, as mentioned earlier, supersymmetric models with R-parity have a stable LSP which can match criteria for dark matter if it is, for example, a neutralino. So R-Parity conserving supersymmetry has the potential to solve the dark matter problem.

In addition to this R-parity implies that sparticles must be pair produced from ordinary matter and this has important consequences for sparticle searches.

3.6 Experimental Constraints on Supersymmetry

Constraining supersymmetry by experiment requires both substantial experimental and theoretical work. In collider experiments an enormous effort must be applied into the construction of the collider, and the detection of the products of the collisions. However, since all supersymmetric particles produced will either decay too quickly or (in the case of the LSP) escape the detector, these particles are not directly observed in the detectors.

Instead the production and decay of the supersymmetric particles must be understood in order to determine an experimental signature for them. For example if charginos had been within the mass reach of LEP they would have been produced through $e^+e^- \rightarrow \gamma, Z \rightarrow \tilde{\chi}^+ \tilde{\chi}^-$. The charginos can then decay via a virtual W boson or a virtual sfermion leading to decays, $\tilde{\chi}^\pm \rightarrow W^{*\pm} \tilde{\chi}_1^0 \rightarrow f \bar{f}' \tilde{\chi}_1^0$ and $\tilde{\chi}^\pm \rightarrow \tilde{f}^* \bar{f}' \rightarrow f \bar{f}' \tilde{\chi}_1^0$ respectively.

Therefore LEP pair production of charginos would have the signature $e^+e^- \rightarrow f \bar{f}' f \bar{f}' + E_T^{miss}$, where E_T^{miss} stands for missing transverse energy due to the light-

est neutralinos escaping the detector. However this signature can also be mimicked by known Standard Model processes, such as W pair production, therefore the SM background must also be carefully predicted.

By comparing the SM predictions and the contribution from the new particles (in this example charginos) it is possible to determine whether or not this signature should yield a statistically significant deviation from the SM for a particular range of masses of the new particles. Finally, assuming this is the case, the data obtained from the detectors is searched for an excess number of events above the expectation value from background processes and, if none is found, limits on the mass of these particles can be obtained.

In general such experimental mass bounds on SUSY particles are both model and parameter space dependent. The bounds on supersymmetric partners of ordinary matter are schematically: squarks and sleptons $\gtrsim 100$ GeV; $\chi_2^0 \gtrsim 60$ GeV; lightest chargino $\gtrsim 100$ GeV [157]; gluino $\gtrsim 150$ GeV [158–159]; the lightest neutralino $\chi_1^0 \gtrsim 45$ GeV [160] and since LEP limits on the SM Higgs usually apply to the lightest neutral Higgs mass, $m_h \geq 114$ GeV. However assuming relations between parameters can dramatically change these bounds. For instance in the CMSSM the gluino $\gtrsim 300$ GeV [158–159].

The bounds on physical particles masses from experiment along with electroweak precision tests can be translated into bounds on the parameter space, [161–169]. More sophisticated analyses combine all experimental data to give a likelihood map of the parameter space [170–177], telling us what our expectations for a particular model are, given the current data.

Chapter 4

Minimal Supersymmetric Standard Model

4.1 Description of the model

The Minimal Supersymmetric Standard Model (MSSM) is a $N = 1$ low energy phenomenological model of supersymmetry, with the minimal possible particle content in order to match data. The MSSM contains a chiral supermultiplet for every observed SM fermion and a gauge supermultiplet for every observed gauge boson. In addition it has two chiral Higgs doublets, which give five physical Higgs particles. The chiral supermultiplets and their gauge transformations are given in Table 4.1 and the gauge supermultiplets are shown in Table 4.2.

The gauge group is the same as the in the SM, $SU(3)_C \otimes SU(2)_W \otimes U(1)_Y$. The superpotential is,

$$W = \epsilon_{\alpha\beta} (y_u^{ij} \hat{H}_u^\alpha \bar{u}_i \hat{Q}_j^\beta - y_d^{ij} \hat{H}_d^\alpha \bar{d}_i \hat{Q}_j^\beta - y_e^{ij} \hat{H}_d^\alpha \bar{e}_i \hat{L}_j^\beta + \mu \hat{H}_u^\alpha \hat{H}_d^\beta), \quad (4.1)$$

where α, β are as usual spinor indices running over $\{1, 2\}$ and the antisymmetric tensor $\epsilon_{\alpha\beta} = -\epsilon_{\beta\alpha}$ and $\epsilon_{12} = -1$. The roman indices are over family space and¹ $\mathbf{y}_u, \mathbf{y}_d, \mathbf{y}_e$

¹Where the bold font is used emphasise that these are matrices when the indices have been dropped.

Supermultiplet	spin 0	spin 1/2	$SU(3)_C$	$SU(2)_L$	$U(1)_Y$
\hat{Q}_i	$(\tilde{u}_L \ \tilde{d}_L)_i$	$(u_L \ d_L)_i$	3	2	$\frac{1}{6}$
\bar{u}_i	\tilde{u}_{Ri}^*	u_{Ri}^\dagger	$\bar{\mathbf{3}}$	1	$-\frac{2}{3}$
\bar{d}_i	\tilde{d}_{Ri}^*	d_{Ri}^\dagger	$\bar{\mathbf{3}}$	1	$\frac{1}{3}$
\hat{L}_i	$(\tilde{\nu} \ \tilde{e}_L)_i$	$(\nu \ e_L)_i$	1	2	$-\frac{1}{2}$
\bar{e}_i	\tilde{e}_{Ri}^*	e_{Ri}^\dagger	1	1	1
\hat{H}_u	$(H_u^+ \ H_u^0)$	$(\tilde{H}_u^+ \ \tilde{H}_u^0)$	1	2	$+\frac{1}{2}$
\hat{H}_d	$(H_d^0 \ H_d^-)$	$(\tilde{H}_d^0 \ \tilde{H}_d^-)$	1	2	$-\frac{1}{2}$

Table 4.1: Chiral supermultiplets of the MSSM, three generations $i = \{1, 2, 3\}$ of left and right-handed quark and lepton supermultiplets and a single generation of Higgs supermultiplets. The representations of $SU(3)_C$ and $SU(2)_W$ as well as the $U(1)_Y$ charges are displayed for each chiral supermultiplet.

are 3×3 matrices of the Yukawa couplings and the superpotential is written using the chiral supermultiplets appearing in Table 4.1 rather than the scalar fields. \hat{H}_u and \hat{H}_d are up and down type Higgs superfields respectively containing spin 0 Higgs bosons and spin 1/2 Higgsino fermions; the \hat{Q}_i are quark superfields containing spin 1/2 quarks and spin 0 squarks; the \hat{L}_i are lepton superfields containing spin 1/2 leptons and spin 0 sleptons.

The soft breaking terms in the MSSM are,

$$\begin{aligned}
-\mathcal{L}_{soft}^{MSSM} &= \frac{1}{2} \left[M_3 \lambda_{\tilde{g}} \lambda_{\tilde{g}} + M_2 \tilde{W}^a \tilde{W}^a + M_1 \tilde{B} \tilde{B} + \text{h.c.} \right] \\
&+ \epsilon_{\alpha\beta} [b H_d^\alpha H_u^\beta - a_{uij} H_u^\alpha \tilde{u}_i \tilde{Q}_j^\beta + a_{dij} H_d^\alpha \tilde{d}_i \tilde{Q}_j^\beta + a_{eij} H_d^\alpha \tilde{e}_i \tilde{L}_j^\beta + \text{h.c.}] \\
&+ m_{H_d}^2 |H_d|^2 + m_{H_u}^2 |H_u|^2 + \tilde{Q}_i^\alpha m_{Q_{ij}}^2 \tilde{Q}_j^{\alpha*} \\
&+ \tilde{L}_i^\alpha m_{L_{ij}}^2 \tilde{L}_j^{\alpha*} + \tilde{u}_{Ri}^* m_{uij}^2 \tilde{u}_j + \tilde{d}_i^* m_{dij}^2 \tilde{d}_j + \tilde{e}_i^* m_{eij}^2 \tilde{e}_j.
\end{aligned} \tag{4.2}$$

These soft masses mix the gauge eigenstates and physical particles (mass eigenstates) are combinations of those fields. Assuming inter-generational mixing is suppressed the

Supermultiplet	Gauge	spin 1/2	spin 1	$SU(3)_C$	$SU(2)_L$	$U(1)_Y$
\hat{G}	$SU(3)_C$	\tilde{g}	g	8	1	0
\hat{W}	$SU(2)_W$	$\tilde{W}^\pm \quad \tilde{W}^0$	$W^\pm \quad W^0$	1	3	0
\hat{B}	$U(1)_Y$	\tilde{B}^0	B^0	1	1	0

Table 4.2: Gauge supermultiplets of the MSSM, and gauge group representations.

physical particles not yet observed are shown in Fig. 4.3.

4.2 Electroweak Symmetry Breaking in the MSSM

As mentioned in the previous section, the MSSM has two Higgs doublets. This is the minimal Higgs sector in a supersymmetric model. The structure of supersymmetry forbids terms like $y_u Q H_d^\dagger u_R$ so separate Higgs doublets are needed: one, H_u , to give mass to the ‘up-type’ fermions and the other, H_d , to give mass to the ‘down-type’ fermions. In addition two Higgs doublets with opposite hypercharge are needed to ensure anomaly cancellation in the model.

The Higgs potential of the MSSM is,

$$\begin{aligned}
V_H = & |\mu|^2 (|H_d|^2 + |H_u|^2) + \frac{1}{8}(g^2 + g'^2) (|H_d|^2 - |H_u|^2)^2 \\
& + \frac{1}{2}g^2 |H_d^* H_u|^2 + m_{H_d}^2 |H_d|^2 + m_{H_u}^2 |H_u|^2 + b(\epsilon_{\alpha\beta} H_d^\alpha H_u^\beta + \text{h.c.}) \quad (4.3)
\end{aligned}$$

where g and g' are the gauge couplings of $SU(2)_W$ and $U(1)_Y$, as defined in Sec. 2.3.2. The first three terms, from the SUSY invariant part of the Lagrangian, are all positive, so soft masses are required for electroweak symmetry breaking to take place. Now examining,

$$\frac{\partial V}{\partial H_d^-} = \frac{\partial V}{\partial H_u^+} = 0 \quad \Rightarrow \langle H_u^+ \rangle = \langle H_d^- \rangle = 0. \quad (4.4)$$

From the Hessian of $V_H(H_u^0, H_u^{0*}, H_d^0, H_d^{0*})$, the origin is not a stable minimum if $b^2 > (m_{H_d}^2 + |\mu|^2)(m_{H_u}^2 + |\mu|^2)$. Additionally the potential is unbounded from below when

	Gauge Eigenstates	Mass Eigenstates
up squarks	$\tilde{u}_L \tilde{u}_R \tilde{s}_L \tilde{s}_R \tilde{t}_L \tilde{t}_R$	$\tilde{u}_1 \tilde{u}_2 \tilde{c}_1 \tilde{c}_2 \tilde{t}_1 \tilde{t}_2$
down squarks	$\tilde{d}_L \tilde{d}_R \tilde{c}_L \tilde{c}_R \tilde{b}_L \tilde{b}_R$	$\tilde{d}_1 \tilde{d}_2 \tilde{s}_1 \tilde{s}_2 \tilde{b}_1 \tilde{b}_2$
charged sleptons	$\tilde{e}_L \tilde{e}_R \tilde{\mu}_L \tilde{\mu}_R \tilde{\tau}_L \tilde{\tau}_R$	$\tilde{e}_1 \tilde{e}_2 \tilde{\mu}_1 \tilde{\mu}_2 \tilde{\tau}_1 \tilde{\tau}_2$
sneutrinos	$\tilde{\nu}_e \tilde{\nu}_\mu \tilde{\nu}_\tau$	$\tilde{\nu}_e \tilde{\nu}_\mu \tilde{\nu}_\tau$
Higgs bosons	$H_u^0 H_d^0 H_u^+ H_d^-$	$h^0 H^0 A^0 H^\pm$
neutralinos	$\tilde{B}^0 \tilde{W}^0 \tilde{H}_u^0 \tilde{H}_d^0$	$\tilde{\chi}_1^0 \tilde{\chi}_2^0 \tilde{\chi}_3^0 \tilde{\chi}_4^0$
charginos	$\tilde{W}^\pm \tilde{H}_u^\pm \tilde{H}_d^\mp$	$\tilde{\chi}_1^\pm \tilde{\chi}_2^\pm$
gluino	\tilde{g}	\tilde{g}

Table 4.3: The MSSM particle content yet to be discovered is displayed. Both gauge eigenstates and mass eigenstates are shown, where it is assumed intergenerational mixing is negligible. First and second generation mixing should also be negligibly small but the mass eigenstates are labelled the same as for the third generation for completeness.

$|H_u^0|^2 = |H_d^0|^2$ if $2b > 2\mu^2 + m_{H_d}^2 + m_{H_u}^2$. So for a finite non-zero vev at tree level we require,

$$(m_{H_d}^2 + |\mu|^2)(m_{H_u}^2 + |\mu|^2) < b^2 \quad (4.5)$$

$$2\mu^2 + m_{H_d}^2 + m_{H_u}^2 > 2b \quad (4.6)$$

Minimising the potential yields,

$$(|\mu|^2 + m_{H_u}^2)v_u = bv_d + \frac{1}{4}(g^2 + g'^2)(v_d^2 - v_u^2)v_u \quad (4.7)$$

$$(|\mu|^2 + m_{H_d}^2)v_d = bv_u - \frac{1}{4}(g^2 + g'^2)(v_d^2 - v_u^2)v_d, \quad (4.8)$$

where $v_u = \langle H_u^0 \rangle$ and $v_d = \langle H_d^0 \rangle$.

4.3 Tree level Masses in the MSSM

Defining Z_μ and W_μ^\pm as for the SM in Eq. 2.26,

$$m_Z^2 = \frac{1}{2}(g^2 + g'^2)(v_u^2 + v_d^2) \quad (4.9)$$

$$m_W^2 = \frac{1}{2}g^2(v_u^2 + v_d^2), \quad (4.10)$$

where the combination $(v_u^2 + v_d^2)^{1/2} = v = \left(\frac{2m_W^2}{g^2}\right)^{1/2} = 174$ GeV is fixed from experiment and $\tan \beta \equiv v_u/v_d$. This allows Eqns. 4.7, 4.8 to be rewritten as,

$$M_Z^2 = \frac{2(m_{H_d}^2 - m_{H_u}^2 \tan^2 \beta)}{\tan^2 \beta - 1} - 2|\mu|^2 \quad (4.11)$$

$$\sin(2\beta) = \frac{2b}{m_{H_u}^2 + m_{H_d}^2 + 2|\mu|^2}, \quad (4.12)$$

The observed fermions' masses are given by,

$$m_{u,c,t} = y_{u,c,t}v \sin \beta, \quad m_{d,s,b} = y_{d,s,b}v \cos \beta, \quad m_{e,\mu,\tau} = y_{e,\mu,\tau}v \cos \beta. \quad (4.13)$$

With three of the eight degrees of freedom from the Higgs scalars being absorbed by the W^\pm and Z bosons, there are five degrees of freedom remaining and these become five physical Higgs particles, with masses,

$$m_A^2 = 2b/\sin(2\beta) \quad (4.14)$$

$$m_{H^\pm}^2 = m_{A^0}^2 + m_W^2, \quad (4.15)$$

$$m_{h,H}^2 = \frac{1}{2} \left(m_A^2 + m_Z^2 \mp \sqrt{(m_A^2 - m_Z^2)^2 + 4m_Z^2 m_A^2 \sin^2(2\beta)} \right). \quad (4.16)$$

where A is a CP-odd, pseudoscalar Higgs boson, H^\pm are charged Higgs bosons and h and H are the light and heavy CP even Higgs bosons.

The superpartners of the W^\pm and the charged Higgs fields are mixed by mass terms and the mass eigenstates are called charginos with mass,

$$m_{\tilde{\chi}_1, \tilde{\chi}_2}^2 = \frac{1}{2} \left[|M_2|^2 + |\mu|^2 + 2m_W^2 \mp \sqrt{(|M_2|^2 + |\mu|^2 + 2m_W^2)^2 - 4|\mu M_2 - m_W^2 \sin 2\beta|^2} \right]. \quad (4.17)$$

The superpartners of the neutral $SU(2)_W$ field, W^0 and the neutral field of the $U(1)_Y$, B , the ‘‘Wino’’ and ‘‘Bino’’ respectively, mix with the superpartners of the neutral Higgs fields into the mass eigenstates called neutralinos. Their masses are determined by diagonalising,

$$\mathbf{M}_{\tilde{\chi}^0} = \begin{pmatrix} M_1 & 0 & -g'v_d/\sqrt{2} & g'v_u/\sqrt{2} \\ 0 & M_2 & gv_d/\sqrt{2} & -gv_u/\sqrt{2} \\ -g'v_d/\sqrt{2} & gv_d/\sqrt{2} & 0 & -\mu \\ g'v_u/\sqrt{2} & -gv_u/\sqrt{2} & -\mu & 0 \end{pmatrix}. \quad (4.18)$$

while the gluino, the superpartner of the gluon, does not mix with any other states and has a mass at tree level which is simply, M_3 .

Finally if intergenerational mixing is assumed negligible so that the soft squark mass matrices are flavour diagonal, and the trilinears are assumed proportional to the Yukawas for each generation,² $a_u = A_u y_u$, $a_d = A_d y_d$, $a_e = A_e y_e$ the sfermion masses are given by,

$$m_{\tilde{u}_1, \tilde{u}_2}^2 = \frac{1}{2} \left[m_Q^2 + m_U^2 + 2m_u^2 + \Delta_Q + \Delta_U \right. \\ \left. \pm \sqrt{(m_Q^2 - m_U^2 + \Delta_Q - \Delta_U)^2 + 4m_u^2 \left(A_u - \frac{\mu}{\tan \beta} \right)^2} \right]. \quad (4.19)$$

for each up-type squark mass, where m_u is the quark mass of the squark’s superpartner, m_Q^2 and m_U^2 are the left-handed and right-handed soft masses, respectively, of the appropriate generation, and Δ_Q , Δ_U are the left-handed and right-handed D-term contributions respectively. For the down-type squark masses,

$$m_{\tilde{d}_1, \tilde{d}_2}^2 = \frac{1}{2} \left[m_Q^2 + m_D^2 + 2m_d^2 + \Delta_Q + \Delta_D \right. \\ \left. \pm \sqrt{(m_Q^2 - m_D^2 + \Delta_Q - \Delta_D)^2 + 4m_d^2 \left(A_d - \mu \tan \beta \right)^2} \right], \quad (4.20)$$

where m_d is the quark mass of the squark’s superpartner, m_Q^2 and m_D^2 are the left-handed and right-handed soft masses, respectively, of the appropriate generation, and

²This is a weaker form of 4.25, but if 4.25 is taken to hold at some high scale far above the squark mass the two relations are consistent, as the RGE running will split the universality of trilinears in exactly this way.

Δ_Q , Δ_D are the left-handed and right-handed D-term contributions respectively. For each charged slepton mass,

$$m_{\tilde{l}_1, \tilde{l}_2}^2 = \frac{1}{2} \left[m_L^2 + m_E^2 + 2m_l^2 + \Delta_L + \Delta_E \right. \\ \left. \pm \sqrt{(m_L^2 - m_E^2 + \Delta_L - \Delta_E)^2 + 4m_l^2 (A_l - \mu \tan \beta)^2} \right], \quad (4.21)$$

where m_l is the lepton mass of the slepton's superpartner, m_L^2 and m_E^2 are the left-handed and right-handed soft masses, respectively, of the appropriate generation, and $\Delta_L + \Delta_E$ are the left-handed and right-handed D-term contributions.

The D-term contributions to these masses appear when the Higgs fields are substituted for their vevs in the D-terms coupling Higgs with sfermions. They depend on the $U(1)_Y$ charges and weak isospin of the sfermions,

$$\Delta_A = (T_{3A}g^2 - Y_A g'^2)(v_d^2 - v_u^2) = (T_{3A} - Q_A \sin^2 \theta_W) \cos(2\beta) m_Z^2. \quad (4.22)$$

With the low energy values of the soft parameters specified, the low energy spectra can be approximated using the formulae presented in this section. For example as a preliminary study prior to the fine tuning project (Chapters 5 and 6) we wrote a program which could take low energy MSSM soft masses and used the tree level relations in this section to calculate all tree level masses in the MSSM. This was tested for several of the benchmark MSSM points, known as Snowmass Points and Slopes³ (SPS) [178] with the low energy parameters taken from [179] and the results for the physical masses compared with the physical masses for the SPS point.

The accuracy of the tree level approximations varies depending on which mass is predicted as well as which SPS point is used. For example the light Higgs mass gets very large corrections from the SUSY breaking sector while its tree level mass is set by the electroweak vev, v . Therefore, in this case, the tree level prediction is a poor approximation, and one loop corrections can be as large as 30%.

³Snowmass Points and slopes are chosen by consensus as representing qualitatively different MSSM scenarios and are very useful for comparison with other work.

Indeed at tree level the upper bound on the light Higgs mass is bounded by M_Z and large radiative corrections are required to evade the LEP bound.

The error on the gluino mass was typically less than 10%. However it is known that the gluino mass corrections can be as large as 30% [180] in some cases. The other masses all had deviations $\lesssim 10\%$, when compared to results in [179] which include one loop corrections. In many cases the corrections were as low as 1 – 2%.

A thorough analysis of the size of one loop corrections can be found in [180].

4.4 CMSSM

As already described in Sec. 3.4 the Constrained MSSM is an mSUGRA inspired form of the MSSM where all soft mass parameters are specified in terms of four parameters, m_0 , $M_{1/2}$, A , B , where,

$$\mathbf{m}_{\tilde{f}_i}^2(M_X) = m_0^2 \mathbf{1} \quad m_{H_u}^2(M_X) = m_{H_d}^2(M_X) = m_0^2 \quad (4.23)$$

$$M_3(M_X) = M_2(M_X) = M_1(M_X) = m_{1/2}, \quad (4.24)$$

$$\mathbf{a}_{\mathbf{u}}(M_X) = A\mathbf{y}_{\mathbf{u}}, \quad \mathbf{a}_{\mathbf{d}}(M_X) = A\mathbf{y}_{\mathbf{d}}, \quad \mathbf{a}_{\mathbf{e}}(M_X) = A\mathbf{y}_{\mathbf{e}}, \quad (4.25)$$

$$b = B\mu, \quad (4.26)$$

where M_X is the high scale at which the universality constraints are postulated and $m_{\tilde{f}_i}^2$ are the sfermion soft mass parameters. Since the gauge couplings unify at a scale $M_{GUT} \approx 10^{16}$, it is usual to take $M_X = M_{GUT}$.

There is also the superpotential mass term μ which mixes the Higgsinos. However $|\mu|$ is fixed by the Z boson mass after imposing the electroweak symmetry breaking conditions. Therefore all unknown masses in the CMSSM can be fixed by just 4 mass parameters and one sign. Since $|\mu|$ is already being fixed by EWSB constraint Eq. 4.11, it is convenient to also swap the parameter B with the ratio of vevs, $\tan \beta$ using Eq. 4.12. A CMSSM point is then specified by the parameter set,

$$\{m_0, \quad M_{1/2}, \quad A, \quad \tan \beta, \quad \text{sign}(\mu)\}. \quad (4.27)$$

In order to link the high scale parameters of the CMSSM with low energies and study the phenomenological consequences of the model, the Renormalisation Group Equations (RGEs) of the MSSM must be employed. In the MSSM the RGEs of the gauge, Yukawa and soft mass couplings form a set of non-linear coupled differential equations which can be solved numerically.

4.4.1 Softsusy

SOFTSUSY [181] is a publicly available program, written by B. C. Allanach which can be used to calculate MSSM mass spectra, to high precision, from MSSM parameters, input at the GUT scale, and experimentally measured data, which is input at low energies. It accepts user inputs of general MSSM parameters, or a smaller set of parameters based on constraints inspired by mSUGRA, Gauge Mediated Symmetry Breaking (GMSB) or Anomaly Mediated symmetry Breaking (AMSB) to generate the spectrum of masses in the MSSM for the user specified point.

The RG evolution between the unification scale and the EWSB scale is controlled by two loop MSSM beta functions. SOFTSUSY employs what is termed an ambidextrous [182] approach to RGE evolution. Soft masses are set at the unification scale, defining high scale boundary conditions (b.c.), while EWSB constraints and low energy data are input at M_Z or the low energy scale most appropriate to their measurement, and these form low energy boundary conditions. Simultaneous solutions to these two sets of b.c.s are then solved iteratively by evolving between the unification scale and low scales. This procedure is summarised in Fig 4.1.

The masses of the observed particles, $\alpha(M_Z)$, $\alpha_3(M_Z)$ and the muon decay constant, G_F^μ , form a set of low energy data used as low energy boundary conditions at M_Z for the procedure. These b.c. are first used to make initial guesses for the Yukawas and gauge couplings of the MSSM. The parameters are RGE evolved up to M_X , where the high scale b.c. are imposed (e.g. those of the CMSSM).

Then all mass parameters and couplings are RG evolved to M_Z , and the tree level

EWSB conditions (Eq. 4.11 and Eq. 4.12) are applied to estimate $|\mu|$ from M_Z , and to replace softmass parameter b with vev parameter $\tan\beta$. The sparticle spectrum and the SUSY scale, $M_S = \sqrt{m_{\tilde{t}_1}(M_S)m_{\tilde{t}_2}(M_S)}$ are also estimated. This concludes the initial part of the procedure illustrated at the top of Fig 4.1 and the main iteration, shown on the bottom left of Fig 4.1, is now entered.

The gauge and Yukawa couplings at M_Z are re-estimated to now accommodate radiative corrections involving the MSSM particles with the masses which have just been estimated. All parameters are then evolved to M_S . The electroweak constraints are again used to determine μ and b , but this time with loop corrections added. For the consistent inclusion of the higher order terms in the EWSB conditions, an iterative procedure is used to determine $|\mu|$. This is shown in the bottom right diagram of Fig 4.1.

With μ determined all parameters are run to M_X and the high scale boundary conditions are reimposed, before running back down to M_Z , where the sparticle spectrum is recalculated. The iteration is then continued until a convergent solution is obtained and the spectrum of SUSY masses is determined and output.

A more complete description of the corrections included and the iteration procedure can be found in the manual [181] or at the website [183] where the program can be downloaded.



Figure 4.1: Flow chart showing how SOFTSUSY finds sparticle spectra consistent with high scale boundary conditions (e.g. those of the CMSSM), correct EWSB and low energy data from experiments.

Chapter 5

Quantifying Fine Tuning

5.1 Motivation

Fine tuning appears in many areas of particle physics and cosmology, such as the Standard Model (SM) Hierarchy Problem and the Cosmological Constant Problem. These problems imply that the universe we live in is a very atypical scenario of the theories we use to describe it. The contortion required to reproduce observation makes such theories seem unnatural, motivating many studies of Beyond the Standard Model (BSM) physics.

However many of the models constructed to solve fine tuning, also exhibit some degree of tuning themselves. In the absence of data, while we await the LHC, naturalness is used to compare models and judge their viability. Great importance has been attached to small differences in the levels of tuning when comparing models, so it is important that naturalness and fine tuning are rigorously understood and measured accurately.

For example the Hierarchy Problem is one of the principle motivations of low energy supersymmetry (SUSY) (see Sec. 2.5 and Sec. 3.1). If the SM is an effective theory, valid up to the Planck scale, then the inclusion of supersymmetric partners for every SM particle leads to the cancellation of quadratic divergences in the loop corrections to

the Higgs mass. This removes the need for fine tuning of $\mathcal{O}(10^{34})$ between the tree-level mass parameter and the Planck Mass, allowing the Higgs boson to be naturally light.

5.1.1 Little Hierarchy Problem

Unfortunately current limits on superpartner masses may imply fine tuning in the most studied model, the Minimal Supersymmetric Standard Model (MSSM). In the previous chapter it was shown that the minimisation of the Higgs potential relates the square of the Z boson mass, M_Z^2 , to the supersymmetry breaking scale. The tree-level expression for this given in Eq. 4.11 and is reproduced here for convenience,

$$M_Z^2 = \frac{2(m_{H_d}^2 - m_{H_u}^2 \tan^2 \beta)}{\tan^2 \beta - 1} - 2|\mu|^2, \quad (5.1)$$

where $\tan \beta$ is the ratio of vacuum expectation values, μ the bilinear Higgs superpotential parameter, and m_{H_u} and m_{H_d} are the up and down type Higgs scalar masses respectively.

Lower bounds on the masses of the supersymmetric particles and the Higgs translate to lower bounds on the parameters appearing on the right hand side of Eq. (5.1). If, for example, one of the parameters is 1 TeV, then to cancel this contribution and give $M_Z = 91.1876 \pm 0.0021$ GeV [33], another parameter (or combination of parameters) would have to be tuned to the order of one part in a hundred.

Including loop corrections to Eq. (5.1) and examining the experimental constraints, one finds that the largest term is from corrections involving the heaviest stop. This can be written as [184],

$$\delta m_{H_u}^2 = -\frac{3y_t^2}{8\pi^2}(m_{\tilde{t}_l}^2 + m_{\tilde{t}_r}^2) \ln \left(\frac{\Lambda}{m_{\tilde{t}}} \right), \quad (5.2)$$

where Λ is the high scale at which the soft stop masses, $m_{\tilde{t}_l}$ and $m_{\tilde{t}_r}$, are generated from the supersymmetry breaking mechanism and y_t is the top Yukawa coupling. A heavy physical stop mass ($m_{\tilde{t}} \gtrsim 500$ GeV) is needed to provide radiative corrections to the light CP even Higgs mass, m_{h^0} of the form,

$$\delta m_{h^0}^2 = \frac{3v^2 y_t^2}{4\pi^2} \sin^4 \beta \ln \left(\frac{m_{\tilde{t}_l} m_{\tilde{t}_r}}{m_t^2} \right), \quad (5.3)$$

which are large enough to evade the LEP constraints on its mass (≥ 114 GeV). So the Little Hierarchy Problem is really about the tension between the masses of the Z boson, the heaviest stop squark and the light Higgs.

The desire to solve this “Little Hierarchy Problem” has motivated a flood of activity in the construction of supersymmetric models [185–191]. There is also increased interest in studying alternative solutions to the SM Hierarchy problem [192–194]. In addition to ensuring such models satisfy phenomenological constraints it is essential that the naturalness is examined using a reliable, quantitative measure of tuning.

5.2 Tuning Measures In literature

In [195] Barbieri and Giudice use a measure of tuning, originally proposed in [196], for an observable, O , with respect to a parameter, p_i ,

$$\Delta_{BG}(p_i) = \left| \frac{p_i}{O(p_i)} \frac{\partial O(p_i)}{\partial p_i} \right|. \quad (5.4)$$

A large value of $\Delta_{BG}(p_i)$ implies that a small change in the parameter results in a large change in the observable, so the parameters must be carefully “tuned” to the observed value. Since there is one $\Delta_{BG}(p_i)$ per parameter, they define the largest of these values to be the tuning for that point in the parameter space,

$$\Delta_{BG} = \max(\{\Delta_{BG}(p_i)\}). \quad (5.5)$$

They then make the aesthetic choice that a tuning, $\Delta_{BG} > 10$ is fine tuned.

This measure has been used extensively in the literature to quantify tuning in the MSSM [197–206] and to examine tuning in other models and theories e.g. [184], [207,211]. However other measures have also been proposed and used.

Motivated by global sensitivity, which will be discussed in the next section, Anderson and Castano [212–215] propose that tuning should be measured with,

$$\Delta_{AC}(p_i) = \frac{\Delta_{BG}(p_i)}{\overline{\Delta_{BG}(p_i)}}, \quad (5.6)$$

where they choose the “average” sensitivity, $\overline{\Delta}_{BG}(p_i)$, not to be the mean, but instead defined by,

$$\overline{\Delta}_{BG}^{-1}(p) = \frac{\int p' f(p') \Delta_{BG}^{-1}(p') dp'}{p f(p) \int dp'}. \quad (5.7)$$

where $f(p)$ is the probability distribution of parameter p . Individual $\Delta_{AC}(p_i)$ are combined in the same manner as the individual $\Delta_{BG}(p_i)$,

$$\Delta_{AC} = \max(\{\Delta_{AC}(p_i)\}). \quad (5.8)$$

There is some dispute within the literature as to whether or not Eq. (5.5) is the best way of choosing a final tuning value from the set $\{\Delta_{BG}(p_i)\}$. In [192],[216–219] the individual $\Delta_{BG}(p_i)$ are be combined as if uncorrelated,

$$\Delta_E = \sqrt{\sum_i \Delta_{BG}^2(p_i)}, \quad (5.9)$$

to give a measure of fine tuning for the parameter space point.

Several other measures have been proposed [220–223], but will not be discussed here.

5.3 Limitations of Traditional Measure

Despite the wide use of Δ_{BG} it has several limitations which may obscure the true picture of tuning:

- variations in each parameter are considered separately;
- only one observable is considered in the tuning measure, but there may be tunings in several observables;
- it does not take account of global sensitivity;
- only infinitesimal variations in the parameters are considered;
- there is an implicit assumption that the parameters come from uniform probability distributions.

Tuning is really concerned with how the parameters are combined to produce an unnatural result. If one measures tunings for each parameter individually, there is no clear guide how to combine these tunings to quantify how unnatural this cancellation is. This has led to two alternative approaches in the literature, Eq. (5.5) and Eq. (5.9); the only way to determine if either Δ_{BG} or Δ_E combines sensitivities correctly is to compare them with a generalisation of $\Delta_{BG}(p_i)$ that varies all of the parameters simultaneously.

Secondly, some theories may contain significant tunings in more than one observable. We want to know how these tunings can be combined to provide a single measure. For example it is reported in [161,224], and more recently in [225–226], that the MSSM also requires tuning in the relic density of the dark matter (ρ). To measure the tuning for some particular set, $S' = \{M'_Z, \rho'\}$, of these observables we should determine how atypical predictions like S' are in the theory. There are four classes of scenario which are significant: the first where both M_Z and ρ are similar to their value in S' ; two more classes where only one of M_Z or ρ is similar to its value in S' ; one with neither observable similar to S' . Tunings in these two observables should be combined in a manner which measures how atypical scenarios in the first class are, without double counting scenarios which appear in the second and third classes. Only a tuning measure which considers the observables simultaneously can achieve this.

A third problem, first mentioned by Anderson and Castano [212] is that the traditional measure picks up global sensitivity as well as true tuning. Δ_{BG} is really a measure of sensitivity. Consider the simple mapping $f : x \rightarrow x^n$, where $n \gg 1$. Applying the traditional measure to $f(x)$ gives $\Delta_{BG} = \Delta_{BG}(x) = n$. Since Δ_{BG} is independent of x , we follow the example of [212] and term this *global sensitivity*. Since $\Delta_{BG}(x_1) - \Delta_{BG}(x_2) = 0$ for all x_1, x_2 , there is no *relative sensitivity* between points in the parameter space.

If we use Δ_{BG} as our tuning measure then $f(x)$ appears fine tuned throughout the entire parameter space. This contrasts with our fundamental notion of tuning being a measure of how atypical a scenario is. A true measure of tuning should only be greater

than one when there is relative sensitivity between different points in the parameter space.

Another concern is that Δ_{BG} only considers infinitesimal variations in the parameters. Since MSSM observables are complicated functions of many parameters, it is reasonable to expect some complicated distribution of the observables about that parameter space. There may be locations where some observables are stable (unstable) locally, but unstable (stable) over finite variations.

Finally, there is also an implicit assumption that all values of the parameters in the effective softly broken Lagrangian \mathcal{L}_{SUSY} are equally likely. However they have been written down in ignorance of the high-scale theory, and may not match the parameters in, for example, the Grand Unified Theory (GUT) Lagrangian, \mathcal{L}_{GUT} . Any non-trivial relation between these different sets of parameters may alleviate or exacerbate the fine tuning problem.

While some of the alternative measures in the literature are motivated by one of these issues, no proposed measure fully addresses all of them.

5.4 Constructing Tuning Measures

A physical theory is fine tuned when generic scenarios of the theory predict very different physics to that which is observed. For the theory to agree with observation the parameters must be adjusted very carefully to lie in an extremely narrow range of values. Insisting that the physics described by the theory is similar to that observed, shrinks the acceptable volume of parameter space. When in this tiny volume even small adjustments to the parameters will dramatically change the physics predicted, so fine tuning may also be characterised by instability. It is this instability which the traditional measure is exploiting.

Instead we wish to construct a tuning measure which determines how rare or atypical certain physical scenarios are. The most direct way to do this is to compare the

volume of parameter space, G , that is *similar* to some given scenario with the *typical* volume, T , of parameter space formed by scenarios which are *similar* to each other.

If all the parameters $\{p_i\}$ are drawn from a uniform probability distribution then the probability of obtaining a scenario in G is, G/V , where V is the volume of parameter space formed by all possible parameter choices. Similarly T/V gives the probability of obtaining a scenario in volume T . We may then define tuning as $\hat{\Delta} = T/G$, to quantify the relative improbability of scenarios *similar* to our given scenario in comparison to the *typical* probability.

To place this within a quantitative framework we must define what we mean by “similar” and “typical”. This will be dealt with later. First, though, consider the toy example presented in Fig. 5.1, showing an observable, O , which depends

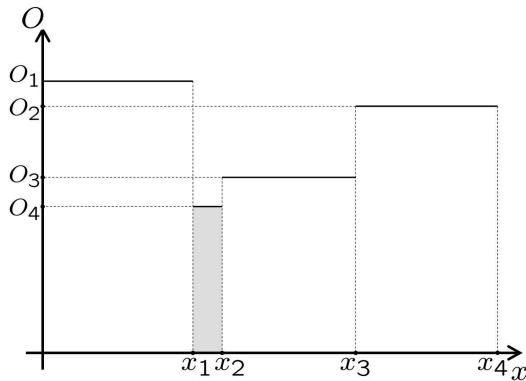


Figure 5.1: A toy example with an observable, O , which depends on a parameter x .

on a parameter, x . Here there are four clearly distinct groups of observable scenario ($O = O_1, O_2, O_3, O_4$) and “similar” can be replaced with equal. Given one of these groups of scenarios, $O = O_i$, the volume G is the length (one dimensional volume) of parameter space with $O = O_i$. For example, for O_4 we have $G = x_2 - x_1$. Next we must define our “typical” volume, T formed by these distinct groups of scenarios. In this simple example an obvious choice is to define T as the mean volume (length) of parameter space formed by scenarios in the same group. So $T = \frac{1}{4}(x_1 + (x_2 - x_1) + (x_3 - x_2) + (x_4 - x_3)) = \frac{x_4}{4}$. The tuning required to get $O = O_4$ is then $\hat{\Delta} = \frac{x_4}{4(x_2 - x_1)}$, which conforms to our intuitive expectation.

In more realistic examples the definitions of “similar” and “typical” will not be so trivial. The definitions must be chosen to fit the type of problem one is considering. In the simple example given above the problem was that scenarios where $O = O_4$ occupied a smaller proportion of the parameter space than other values, $O = O_1, O_2, O_3$.

In hierarchy problems the concern is that one (or more) observable is much smaller than another observable, despite depending on common parameters. The requirement that one observable is large forces the theory into a region of parameter space where generic points also predict a large value for the second observable(s).

So “similar” must be related to the size of the observables. For example, one might consider “similar” to observable O'_i to mean observables “of the same order” as O'_i . A sensible definition of G is then the volume of parameter space where $\frac{1}{10} \leq \frac{O_i}{O'_i} \leq 10$, for all observables O_i . However it is not clear that this is more appropriate than some other choice such as $\frac{1}{2} \leq \frac{O_i}{O'_i} \leq 2$. So generally G can be defined by a class of parameter space volumes formed from dimensionless variations in the observables $a \leq \frac{O_i}{O'_i} \leq b$. Different values of a and b quantify different definitions of “similar” and are therefore different fine-tuning questions. In comparison, the one dimensional measure Δ_{BG} is a ratio of infinitesimal lengths, so implicitly adopts the choice $a, b \rightarrow 1$. One can imagine cases where this would be a bad choice (e.g. an observable which oscillates quickly when the parameter is varied), so care must be taken to choose a and b sensibly (i.e. ask the correct question).

When a large hierarchy between observables requires a large cancellation between parameters, as in the traditional hierarchy problem, the region of parameter space which can provide the correct observables (the volume G) is much smaller than one would expect (i.e. it is “fine-tuned”). We must compare this volume with the “typical volume” of parameter space, T , that one would expect if no fine-tuning were present. The remaining question is then, how do we define this “typical volume”?

One might suggest that this typical volume should be the average of volumes G throughout the whole parameter space, $\langle G \rangle$. However, the measure would then depend only on how far parameters are from some hypothesised upper limits on their values.

For example, an observable O which depends on a parameter p according to $O = \alpha p$ will display fine-tuning for small values of p if one chooses the maximum possible value of p to be large, even though there is no cancellation present. This is not the ‘fine-tuning’ we are trying to probe; we want to gain insight into the unnatural cancellation between parameters, so T must be anchored to the specific parameter point to be tested.

We can do this by adopting the same notion of “similar” that we used to define G . We introduce a volume F which is formed from dimensionless variations $[a, b]$ in the parameters. A comparison of F/G at different points in the parameter space, provides a test of whether G ’s variation is due to a simple scaling with the parameters (as described above for $O = \alpha p$), or due to some “unnatural” effect such as fine-tuning. Consequently one should compare F/G with its average value over the entire space, $\langle F/G \rangle$. Reverting to our previous terminology, the “typical” volume which one would have expected to form from dimensionless variations in the parameters about $\{p'_i\}$, is

$$T = \frac{F(\{p'_i\})}{\langle \frac{F}{G} \rangle}. \quad (5.10)$$

5.5 New Tuning Measure

Following the above discussion and motivated by the limitations of the traditional measure, we propose a new measure of tuning.

We define two volumes in parameter space for every point $P'\{p'_i\}$. Let F be the volume of dimensionless variations in the parameters over some arbitrary range $[a, b]$, about point P' , i.e. the volume formed by imposing $a \leq \frac{p_i}{p'_i} \leq b$. Similarly let G be the volume in which dimensionless variations of the observables fall into the same range $[a, b]$, i.e. the volume constrained by $a \leq \frac{O_j(\{p_i\})}{O_j(\{p'_i\})} \leq b$. Volumes F and G are illustrated for a two dimensional example in Fig. 5.2.

We define an unnormalised measure of tuning with,

$$\Delta = \frac{F}{G}. \quad (5.11)$$

This is sufficient for comparing different regions of parameter space within a given

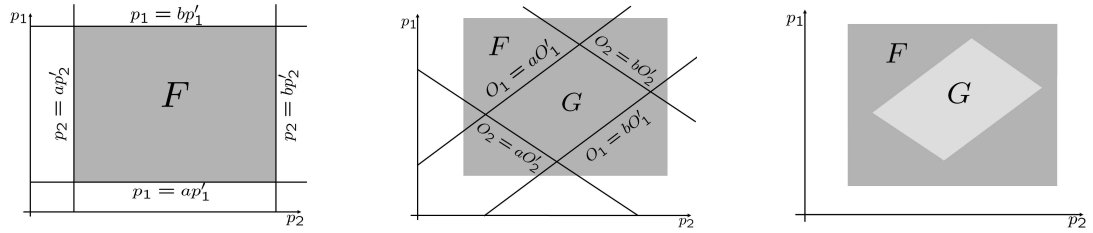


Figure 5.2: *Left*: In two dimensions the bounds placed on the parameters, $a \leq \frac{p_i}{p'_i} \leq b$, appear as four lines in parameter space giving the dark grey area (2d volume), F . *Middle*: Bounds on the two observables, $a \leq \frac{O_j(\{p_i\})}{O_j(\{p'_i\})} \leq b$ introduce four more lines giving the volume G . *Right*: Two dimensional volumes (areas) F (dark grey) and G (light grey).

model as the normalisation factor will be common. To compare tuning in different models we need to include normalisation,

$$\hat{\Delta} = \frac{1}{\overline{\Delta}} \frac{F}{G}, \quad (5.12)$$

with,

$$\overline{\Delta} = \left\langle \frac{F}{G} \right\rangle = \frac{\int dp_1 \dots dp_n \frac{F}{G}(\{p_i\}, \{O_i\})}{\int dp_1 \dots dp_n}. \quad (5.13)$$

Notice that this measure does not depend on experimental constraints. In naturalness problems such constraints should only rule out the point, P' , around which we make variations to test fine tuning. If P' is not experimentally excluded, we should not impose experimental constraints on nearby points $\{P_i\}$ used to probe fine tuning. Fine tuning quantifies how unnatural a region of parameter space is and this is a feature of the theory, not our experimental knowledge.

$\hat{\Delta}$ quantifies the restriction on parameter space. This is more in touch with our intuitive notion of tuning than the stability of the observable. Notice that with only one or two parameters and no global sensitivity, Δ_{BG} also describes restriction of parameter space and yields the same results as our new measure. However it is important to recognise that Δ_{BG} 's ability to do this leads to its utility as a tuning measure there. Equally its failure to do so in many dimensions demonstrates its limitation.

Consider fine tuning for a single observable which depends on more than one parameter, Even though the true tuning for any physical scenario should be described using all available observables, it is often useful to define individual tunings for each observable separately. However, in this case, the volume G is unbounded, since a single observable can only constrain one combination of parameters.

To resolve this difficulty one must either reduce the number of parameters to one or introduce some other bounds on G . The former reintroduces the problem of combining tunings for individual parameters and a better procedure is to restrict G to be within F . Here we are trying to pick up how much of the restriction in parameter space is due to this particular observable. The assumption is made that if all other observables were natural then they would restrict G no more than F does. Therefore we define G_{O_j} to be the volume restricted by $a \leq \frac{O_j(\{p_i\})}{O_j(\{p'_i\})} \leq b$ and $a \leq \frac{p_i}{p'_i} \leq b$. Tuning is then defined by,

$$\hat{\Delta}_{O_j} = \frac{1}{\left\langle \frac{F}{G_{O_j}} \right\rangle} \frac{F}{G_{O_j}}, \quad (5.14)$$

This definition is applied to obtain individual tunings in the MSSM in Section 6.2.1.

Like Δ_{BG} and Δ_{AC} , Δ depends upon the choice of parameterisation. Since tuning is about the restriction of the parameter space this seems unavoidable. To examine different choices of parametrisation one must redefine volumes F and G in terms of the new parameters and normalise the tuning by taking the average over the new parameter space.

5.6 Relation To Other Measures

Since much of the motivation behind developing this measure was to generalise Δ_{BG} so that many parameters and many observables are considered simultaneously, it is interesting to look at how the two measures are related.

Consider a theory with one observable, y which has a linear dependence on a single

parameter, x , with the value of that parameter being drawn from a uniform probability distribution. At the parameter point (x_0, y_0) , notice that, $\Delta_{BG} = |x_0/y_0 \partial y / \partial x|$, while we can see $F = (b - a)x_0$ and $G = \frac{\partial x}{\partial y}(b - a)y_0$, so,

$$\Delta = \frac{F}{G} = \frac{bx_0 - ax_0 \partial y}{by_0 - ay_0 \partial x} = \Delta_{BG}. \quad (5.15)$$

Similarly Anderson and Castano's measure may be written as,

$$\Delta_{AC} = \frac{x_0 \partial y}{y_0 \partial x} \frac{\int dx' y(x') \frac{\partial x'}{\partial y(x')}}{x_0 \int dx'} = \frac{\int dx' y(x')}{y_0 \int dx'} \quad (5.16)$$

Now notice that $\langle G \rangle = \frac{\partial x}{\partial y} \frac{\int dx' (b-a)y(x')}{\int dx'}$, so,

$$\Delta_{AC} = \frac{\langle G \rangle}{G}. \quad (5.17)$$

In Section 5.4, we pointed out the difficulty in using $\langle G \rangle / G$ as a tuning measure and this will be further illustrated in Section 6.1 when we look at results for our measure and Δ_{AC} for a toy version of the SM Hierarchy problem.

Chapter 6

Applying New Tuning Measure

6.1 Toy Models

In this section a comparison is made of some of the tuning measures for various toy models and the implications are discussed. In each of these examples a uniform probability distribution for the parameters is assumed.

Results from this section for toy models with only one parameter are summarised in Table 6.1, comparing the analytical results of various tuning measures for the simple models with only one parameter and one observable. With only one parameter it is trivially the case that $\Delta_E = \Delta_{BG}$, so it is not included.

6.1.1 SM Hierarchy Problem Revisited

As a first test of our measure we apply it to the Standard Model Hierarchy Problem, where we know the tuning is enormous. Here there is only one observable, the physical Higgs mass, m_H . Recall from Sec. 2.5 that at one loop we can write,

$$m_H^2 = m_0^2 - C\Lambda^2. \tag{6.1}$$

	Δ_{BG}	Δ	Δ_{AC}	$\hat{\Delta}$
Toy SM	$1 + \frac{C\Lambda^2}{m_H^2}$	$1 + \frac{C\Lambda^2}{m_H^2}$	$\frac{m_{Hmax}^2 + m_{Hmin}^2}{2m_H^2}$	$\frac{m_0^2}{m_H^2 + \frac{m_0^2 C\Lambda^2}{m_{0max}^2 - m_{0min}^2} \ln \frac{m_{0max}^2 - C\Lambda^2}{m_{0min}^2 - C\Lambda^2}}$
$f(x) = x^n$	n	$\frac{b-a}{b^{1/n} - a^{1/n}}$	$\frac{x_{max} + x_{min}}{2x}$	1
$g(x) = e^{kx}$	$ kx $	$\frac{(b-a) kx }{\ln \frac{b}{a}}$	1	$\frac{2x}{x_{min} + x_{max}}$
Proton Mass	$\frac{16\pi^2}{b_3 g_3^2}$	$\frac{(b-a)}{(\frac{-k}{g_3^2 \ln b - k})^{1/2} - (\frac{-k}{g_3^2 \ln a - k})^{1/2}}$	$\frac{(g_{max} + g_{min})(g_{max}^2 + g_{min}^2)}{4g_3^3}$	$\approx \frac{g_{max} g_{min}}{g_3^2}$

Table 6.1: Tuning measures for models with only one parameter and one observable.

We treat only the bare mass squared, m_0^2 as a parameter. Λ , the Ultra Violet cutoff, is taken to be the Planck Mass or some other fixed scale. C is a positive constant which includes gauge and Yukawa couplings.

To apply our measure we simply vary the tree level mass parameter about m_0^2 , over the arbitrary range $[am_0^2, bm_0^2]$. As is illustrated in Fig.(6.1), this gives the line $F = (b-a)m_0^2$. Doing the same for the observable yields the line $G = (b-a)m_H^2$.

Figure 6.1: One dimensional volume (length) F (dark grey) and the restricted subset, length G (light grey)

$$\Rightarrow \Delta = \frac{F}{G} = 1 + \frac{C\Lambda^2}{m_H^2} = \Delta_{BG}. \quad (6.2)$$

Notice that the arbitrary range $[a, b]$ has fallen out of the result and it matches that obtained using the traditional measure, which we showed must be the case for linear functions like this.

Since $F/G = \Delta_{BG}$ the only difference between the new measure proposed here and

that of Anderson and Castano is how global sensitivity is determined. In both cases some choice needs to be made for the range of possible m_0^2 , so we write $m_{0\max}^2 \geq m_0^2 \geq m_{0\min}^2 > C\Lambda^2$. The new measure then gives,

$$\left\langle \frac{F}{G} \right\rangle = \frac{1}{m_{0\max}^2 - m_{0\min}^2} [m_{0\max}^2 - m_{0\min}^2 + C\Lambda \ln \frac{m_{0\max}^2 - C\Lambda^2}{m_{0\min}^2 - C\Lambda^2}] \quad (6.3)$$

$$\Rightarrow \hat{\Delta} = \frac{m_0^2}{m_H^2 + \frac{m_H^2 C\Lambda^2}{m_{0\max}^2 - m_{0\min}^2} \ln \frac{m_{0\max}^2 - C\Lambda^2}{m_{0\min}^2 - C\Lambda^2}} \quad (6.4)$$

If the chosen range of variation is large, $m_{0\max}^2 - m_{0\min}^2 \gg C\Lambda^2$,

$$\Rightarrow \left\langle \frac{F}{G} \right\rangle \approx 1 \Rightarrow \Delta \approx \frac{m_0^2}{m_H^2} = \frac{F}{G} = \Delta_{BG}. \quad (6.5)$$

Alternatively choosing very narrow range of variation about $C\Lambda^2 + \mu_H^2$, where $\mu_H^2 \approx 150$ GeV, implies Δ is very small and in the limit $m_{0\max}^2 - m_{0\min}^2 \rightarrow 0$, $\Delta \rightarrow 0$.

This is intuitively reasonable. Imagine there was some compelling theoretical reason for the bare mass term to be constrained to lie close to the cutoff. For instance a GUT or a new quantum theory of gravity which gave rise only to a bare mass with, $C\Lambda^2 < m_0^2 \leq C\Lambda^2 + \mu_H^2$. In light of this, the case for new physics at low energies would be dramatically weakened. Indeed it is precisely because there is no such compelling reason that we worry about the hierarchy problem and look to BSM physics such as SUSY to explain how we can have $m_H \ll M_{Planck}$.

Now the measure used by Anderson and Castano is applied to this problem.

$$\overline{\Delta}_{BG}^{-1} = \frac{m_{0\max}^2 + m_{0\min}^2 - 2C\Lambda^2}{2m_0^2}, \quad (6.6)$$

$$\Rightarrow \Delta_{AC} = \frac{m_{0\max}^2 + m_{0\min}^2 - 2C\Lambda^2}{2m_H^2} = \frac{m_{H\max}^2 + m_{H\min}^2}{2m_H^2}. \quad (6.7)$$

Notice that as $m_{0\max}^2 - m_{0\min}^2 \rightarrow 0$, $m_{H\min} \rightarrow m_H$ and $m_{H\max} \rightarrow m_H$, so $\Delta_{AC} \rightarrow 1$. While numerically different from the result given by the new measure in this limit, in both cases the interpretation is that there is no tuning problem.

However a fundamental difference between $\hat{\Delta}$ and Δ_{AC} is that the latter will give a large tuning for any $m_H^2 \ll \frac{1}{2}(m_{0\max}^2 + m_{0\min}^2) - C\Lambda^2$. If the upper bound is chosen

such that, $m_{0max}^2 \gg m_0^2$, then even a Higgs mass of $\mathcal{O}(m_0^2)$ will appear fine tuned. This measure is not sensitive to the unnatural cancellation which causes our concern. Instead it is sensitive to the fact that large values of m_H^2 take up a much larger volume of parameter space than small values of m_H^2 . This would be true even if the Higgs mass was described by $m_H^2 = m_0^2$, with no unnatural cancellation.

The results for this Toy SM are summarised in the first row of Table 6.1.

6.1.2 Other Toy Models with one parameter

Now consider the tuning for a simple function $f(x) = x^n$. Earlier in Sec. 5.3 it was shown that there was no relative sensitivity in $f(x)$, as the traditional tuning measure is $\Delta_{BG} = n, \forall x$. The unnormalised version of the measure proposed here, Δ , also gives a constant value,

$$\Delta = \frac{b - a}{b^{\frac{1}{n}} - a^{\frac{1}{n}}}. \quad (6.8)$$

If instead tuning measures normalised over the range $x_{max} \geq x_{min} \geq 0$ are used, this global sensitivity is removed. It is trivial to obtain the mean value for Δ_{BG} and Δ ,

$$\overline{\Delta_{BG}} = n \Rightarrow \frac{\Delta_{BG}}{\overline{\Delta_{BG}}} = 1, \quad (6.9)$$

$$\left\langle \frac{F}{G} \right\rangle = \frac{b - a}{b^{\frac{1}{n}} - a^{\frac{1}{n}}} \Rightarrow \hat{\Delta} = 1. \quad (6.10)$$

Although in this case the unnormalised sensitivity does depend the size of the variations (our choice of a and b) the final result, $\hat{\Delta}$ is independent of this and implies that there is not a tuning problem here.

Applying Anderson and Castano's tuning measure, Δ_{AC} , to $f(x)$, over the same range, gives,

$$\Delta_{AC} = \frac{x_{max} + x_{min}}{2x}, \quad (6.11)$$

This does substantially reduce the global sensitivity, but nonetheless implies that for naturalness considerations an observable that is as large as possible is preferential.

Another interesting case is $g(x) = \exp(kx)$, where k is taken to be a positive constant for simplicity. Applying the traditional measure we get $\Delta_{BG} = |kx|$. A naive interpretation suggests that only $x = 0$ to $x = \pm 1/k$ is not tuned and any $|x| > 10/k$ is fine tuned. However this means that if x is allowed to extend to large values ($x \gg 1/k$) then most of the parameter space is fine tuned! Rephrased this would imply that far more of the parameter space matches atypical values than typical ones, which is a contradictory statement. This is another clear example of the need to compare against some ‘‘average’’ sensitivity. Δ gives a similar result but with a different constant factor,

$$\Delta = \frac{|k(b-a)x|}{\ln \frac{b}{a}} \quad (6.12)$$

If instead one compares the sensitivity for some given value of $\exp(kx)$ with the mean sensitivity a more sensible answer can be produced. As in the previous examples to do this one must make certain assumptions about the parameter space. Let the allowed values of x be bounded by $x_{max} \geq x \geq x_{min} \geq 0$ with all values of x being equally likely in this range, then,

$$\hat{\Delta} = \frac{\Delta_{BG}}{\overline{\Delta}_{BG}} = \frac{2x}{x_{min} + x_{max}}, \quad (6.13)$$

Note that $\hat{\Delta} < 2$, so $g(x)$ is never fine tuned for any x according to this measure, though $\hat{\Delta}$ does vary a little.

For $g(x)$ Anderson and Castano’s measure gives,

$$\overline{\Delta}_{BG}^{-1} = \frac{1}{|kx|} \Rightarrow \Delta_{AC} = 1. \quad (6.14)$$

It is interesting that our measure considers $f(x)$ to have consistently no tuning ($\hat{\Delta} = 1$), whereas it is for $g(x)$ that $\Delta_{AC} = 1$ for all x . The tuning results for $f(x)$ and $g(x)$, for the case $x_{max} > x_{min} > 0$ are shown in the second and third rows of Table 6.1.

6.1.3 Proton Mass

The original illustration of global sensitivity presented by Anderson and Castano in [212] was for the proton mass. The proton can be much lighter than the Planck Mass without fine tuning because the renormalisation group equations (RGE) lead to only a logarithmic dependence on high scale quantities. However, by using the one loop RGE for the QCD coupling, α_3 , and equating the proton mass to the QCD scale¹

$$M_{\text{Proton}} \sim \Lambda_{QCD} = C \exp \left[-\frac{8\pi^2}{b_3 g_3^2} \right], \quad (6.15)$$

where g_3 is the strong gauge coupling evaluated at the Planck scale, M_{Planck} , and C is a positive constant. As they demonstrated, this gives,

$$\Delta_{BG}(g_3) = \frac{16\pi^2}{b_3 g_3^2} > 100. \quad (6.16)$$

In [212] Δ_{AC} is proposed to solve this problem and for $g_{max} \geq g_3 \geq g_{min} > 0$ the result obtained is,

$$\Delta_{AC} = \frac{(g_{max} + g_{min})(g_{max}^2 + g_{min}^2)}{4g_3^3}. \quad (6.17)$$

If instead one normalises Δ_{BG} with the mean the result is,

$$\frac{\Delta_{BG}}{\overline{\Delta_{BG}}} = \frac{g_{max} g_{min}}{g_3^2}. \quad (6.18)$$

To evaluate our measure, let $k = 8\pi^2/b_3$, so

$$\Delta = \frac{(b-a)}{\left(\frac{-k}{g_3^2 \ln b-k}\right)^{\frac{1}{2}} - \left(\frac{-k}{g_3^2 \ln a-k}\right)^{\frac{1}{2}}}. \quad (6.19)$$

If $g_3^2 \ln b/k \ll 1$ and $g_3^2 \ln a/k \ll 1$, $\forall g_{min} \leq g_3 \leq g_{max}$

$$\Delta \approx \frac{2k(b-a)}{g_3^2 \ln \frac{b}{a}} \quad (6.20)$$

and

$$\Delta \approx \frac{\hat{\Delta}_{BG}}{\overline{\Delta_{BG}}}. \quad (6.21)$$

¹For details see [212].

In these one parameter examples the need for a normalised tuning measure is apparent. However Δ_{AC} diverges significantly from our new measure, which in many of these simple one dimensional models is equivalent to normalising the traditional measure with its mean value.

It is also interesting that even after accounting for global sensitivity some of these one dimensional functions may still show some small degree of tuning. This opens up the possibility that changing the parameterisation of the effective low energy theory might exacerbate or alleviate the tuning problem. Finding choices of parametrisation which reduce tuning could allow us to select high scale theories which are preferential in terms of naturalness. This point has not appeared in the literature and merits investigation. However we do not address this here but leave it for a future study.

6.1.4 Toy SM with two parameters

Now we consider models with more than one parameter. In these cases Δ_E diverges from Δ_{BG} and we must compare each of these with Δ .

First we return to the SM hierarchy problem, but this time treat m_H as a function of two parameters, m_0^2 and Λ^2 . In the one dimensional example the tension between the weakness of gravitation (the large Planck Mass) and a light Higgs mass was examined indirectly by choosing the Planck mass to be a fixed constant in theory. We now take a more direct route with two observables m_H^2 and M_{Planck}^2 (“observed” to be large due to the weakness of gravitation), predicted from the parameters with,

$$M_{\text{Planck}}^2 = \Lambda^2, \quad m_H^2 = m_0^2 - C\Lambda^2. \quad (6.22)$$

We are still predicting m_H^2 from Eq. (6.1) and have not split up any of the terms to introduce new cancellations, so we expect to simply reproduce the same result for Δ as we obtained in the one parameter toy SM model. However, the method applied provides a simple illustration of how our measure works with more than one parameter. We have a two dimensional parameter space, so allowing the parameters to vary about

some point $P'(m_0^2, \Lambda^2)$ over the dimensionless interval $[a, b]$ defines an area, F , in this space. Clearly the bounds from dimensionless variations in M_{Planck}^2 are the same as those from Λ^2 , while the bounds from dimensionless variations in m_H^2 introduce two new lines in the parameter space.

This is shown in Fig. 6.2 for two different points. In the first point, the values of the parameters are of the same order as the observable, m_H^2 , because we have chosen a small value of M_{Planck} . So G is not much smaller than F . For the other point $M_{\text{Planck}}^2 \gg m_H^2$, resulting in an F much larger than G and fine tuning. Of course neither of these points are representative of the weakness of gravitation we observe. A point with $M_{\text{Planck}} = 10^{19}$ GeV and $m_H = 120$ GeV, would have $F \gg G$ to such an extent that a graphical illustration is not possible.

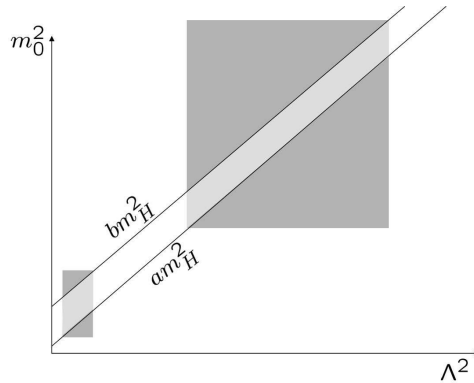


Figure 6.2: The two dimensional volumes (areas) F (dark grey) and G (light grey) for two different points in the two dimensional parameter space.

In general the areas are, $F = (b - a)^2 m_0^2 \Lambda^2$ and $G = (b - a)^2 \Lambda^2 m_H^2$ so,

$$\Delta = 1 + \frac{C\Lambda^2}{m_H^2} = \Delta_{BG}. \quad (6.23)$$

In this simple case we find the same result as the traditional measure. Combining $\Delta_{BG}(\Lambda)$ and $\Delta_{BG}(m_0^2)$ as if they are uncorrelated, gives,

$$\Delta_E = \frac{\sqrt{C^2 \Lambda^4 + m_0^4}}{m_H^2}. \quad (6.24)$$

With $C\Lambda^2$ and m_0^2 both $\gg m_H^2$, i.e. fine tuned scenarios, this gives us $\Delta_E \approx \sqrt{2}\Delta$. While our measure does not deviate from Δ_{BG} in this simple example, models with

additional parameters allow the observable to be obtained from cancellation of more than two terms, complicating the fine tuning picture.

6.1.5 Toy Model with three parameters and four observables

We now look at a model with four observables, M^2 , M_1^2 , M_2^2 , M_3^2 , and three parameters, p_1^2 , p_2^2 , p_3^2 , described by,

$$M^2 = c_1 p_1^2 - c_2 p_2^2 + c_3 p_3^2. \quad (6.25)$$

$$M_1^2 = p_1^2, \quad M_2^2 = p_2^2, \quad M_3^2 = p_3^2. \quad (6.26)$$

For a point (m_1^2, m_2^2, m_3^2) , in the three dimensional parameter space, the traditional measure gives $\Delta_{BG}(p_i) = c_i m_i^2 / M^2$ (no sum over i is implied), so,

$$\Delta_{BG} = \max \left\{ \frac{c_i m_i^2}{M^2} \right\} \quad \text{and} \quad \Delta_E = \frac{\sqrt{\sum_i c_i^2 m_i^4}}{M^2}. \quad (6.27)$$

To apply our tuning measure in the three dimensional case we must determine volumes F and G . For a point, (m_1^2, m_2^2, m_3^2) , with $M^2 = M_0^2 = c_1 m_1^2 - c_2 m_2^2 + c_3 m_3^2$ we have,

$$\frac{\partial^3 F}{\partial p_1^2 \partial p_2^2 \partial p_3^2} = \prod_{i=1}^3 \theta(p_i^2 - a m_i^2) \theta(b m_i^2 - p_i^2), \quad (6.28)$$

$$\frac{\partial^3 G}{\partial p_1^2 \partial p_2^2 \partial p_3^2} = \frac{\partial^3 F}{\partial p_1^2 \partial p_2^2 \partial p_3^2} \theta(M^2 - a M_0^2) \theta(b M_0^2 - M^2), \quad (6.29)$$

where the latter uses $M_i^2 = p_i^2$ and $\theta(x)$ is the usual Heaviside step function. Integrating Eq. (6.28) over all three p_i gives the volume,

$$F = (b - a)^3 m_1^2 m_2^2 m_3^2, \quad (6.30)$$

and similarly Eq. (6.29) gives,

$$\begin{aligned} G &= (b - a)^3 \left\{ \theta(c_3 m_3^2 - c_2 m_2^2) \theta(c_2 m_2^2 - c_1 m_1^2) \left[\frac{1}{c_3} m_1^2 m_2^2 M^2 - \frac{c_1^2}{3 c_2 c_3} m_1^6 \right] \right. \\ &+ \theta(c_1 m_1^2 - c_2 m_2^2) \theta(c_2 m_2^2 - c_3 m_3^2) \left[\frac{1}{c_1} m_2^2 m_3^2 M^2 - \frac{c_3^2}{3 c_2 c_1} m_3^6 \right] \\ &+ \theta(c_3 m_3^2 - c_2 m_2^2) \theta(c_1 m_1^2 - c_2 m_2^2) \left[m_1^2 m_2^2 m_3^2 - \frac{c_2^2}{3 c_1 c_3} m_2^6 \right] \\ &\left. + \theta(c_2 m_2^2 - c_1 m_1^2) \theta(c_2 m_2^2 - c_3 m_3^2) \left[\frac{1}{c_2} m_1^2 m_3^2 M^2 - \frac{1}{3 c_1 c_2 c_3} M^6 \right] \right\}. \quad (6.31) \end{aligned}$$

We find that the analytical expressions for tuning in this model depend on the mass hierarchy of m_1 , m_2 and m_3 .

For $c_1 m_1^2 > c_2 m_2^2 > c_3 m_3^2$ we find,

$$\Delta = \frac{F}{G} = \frac{c_1 m_1^2 m_2^2}{m_2^2 M^2 - \frac{c_3^2}{3c_2} m_3^4} \approx \Delta_{BG} \quad \text{if} \quad c_3 m_3^2 \ll c_2 m_2^2. \quad (6.32)$$

For $c_3 m_3^2 > c_2 m_2^2 > c_1 m_1^2$ we find:

$$\Delta = \frac{F}{G} = \frac{c_3 m_2^2 m_3^2}{m_2^2 M^2 - \frac{c_1^2}{3c_2} m_1^4} \approx \Delta_{BG} \quad \text{if} \quad c_1 m_1^2 \ll c_2 m_2^2. \quad (6.33)$$

For $c_3 m_3^2 > c_1 m_1^2 > c_2 m_2^2$ and $c_1 m_1^2 > c_3 m_3^2 > c_2 m_2^2$:

$$\Delta = \frac{F}{G} = \frac{m_1^2 m_3^2}{m_1^2 m_3^2 - \frac{c_2^2}{3c_1 c_3} m_2^4} \approx 1 \quad \text{if} \quad c_1 m_1^2 c_3 m_3^2 \gg c_2^2 m_2^4. \quad (6.34)$$

For $c_2 m_2^2 > c_1 m_1^2 > c_3 m_3^2$ and $c_2 m_2^2 > c_3 m_3^2 > c_1 m_1^2$:

$$\Delta = \frac{F}{G} = \frac{c_2 m_1^2 m_2^2 m_3^2}{m_1^2 m_3^2 M^2 - \frac{1}{3c_1 c_3} M^6} \approx \Delta_{BG} \quad \text{if} \quad M^4 \ll c_1 m_1^2 c_3 m_3^2. \quad (6.35)$$

Notice that these results do not match Δ_E , but in three dimensions at least Δ_{BG} is a much better approximation, as is shown in Fig. 6.3.

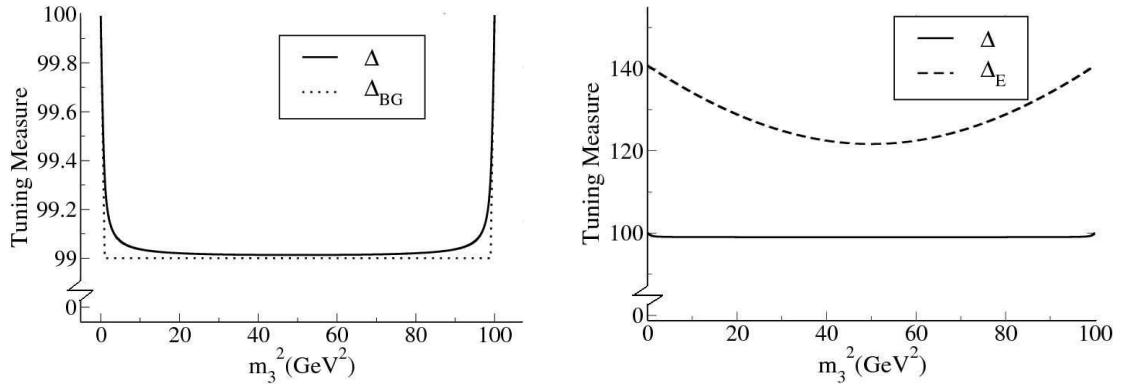


Figure 6.3: Comparison of (unnormalised) tuning measures in the three parameter model with m_3^2 varying from 0 to 100 GeV^2 and $M_0^2 = 1 \text{ GeV}^2$ and $m_2^2 = 99 \text{ GeV}^2$ kept constant. m_1^2 then varies according to Eq. (6.25) to accommodate the changes in m_3^2 . *Left*: between Δ_{BG} and our new measure. *Right*: between Δ_E and our new measure.

However, as we have seen, in moving from two parameters to three parameters these discrepancies appeared, increasing the number of parameters further will increase the divergences between the measures.

6.2 CMSSM

6.2.1 Procedure

The analytical methods described above become increasingly complicated to apply as the number of parameters and observables are increased. For such situations we have also developed a numerical procedure which can be applied to produce approximate results for tuning. Since the MSSM contains many parameters and many observables we chose to apply our numerical approach here.

To do this a modified version of SOFTSUSY 2.0.5 [181] was used. SOFTSUSY was described in Sec. 4.4.1. To apply our new tuning measure we need to input additional high scale constraints, $\mu(M_X) = \mu^{GUT}$ and $b(M_X) = m_3^2$, and be able to calculate M_Z and $\tan \beta$ from $\mu(M_Z)$ and $b(M_Z)$.

In SOFTSUSY 2.0.5, there is a routine to predict M_Z and $\tan \beta$, which was written to apply the traditional tuning measure, Δ_{BG} numerically. However this routine does not provide an iterative solution for M_Z . Instead the Higgs tadpoles and the real part of the transverse self energy of the Z boson for the experimentally measured value of M_Z is used. This approximation is fine for very small deviations about M_Z , but since our new measure uses finite variations, rather than the infinitesimal variations of Δ_{BG} some alteration is required.

We modified SOFTSUSY 2.0.5 so that M_Z was determined through an iterative routine similar to the routine in which μ is iteratively determined. This is illustrated in Fig. 6.4.

The numerical version of our measure can then be applied in the following way.

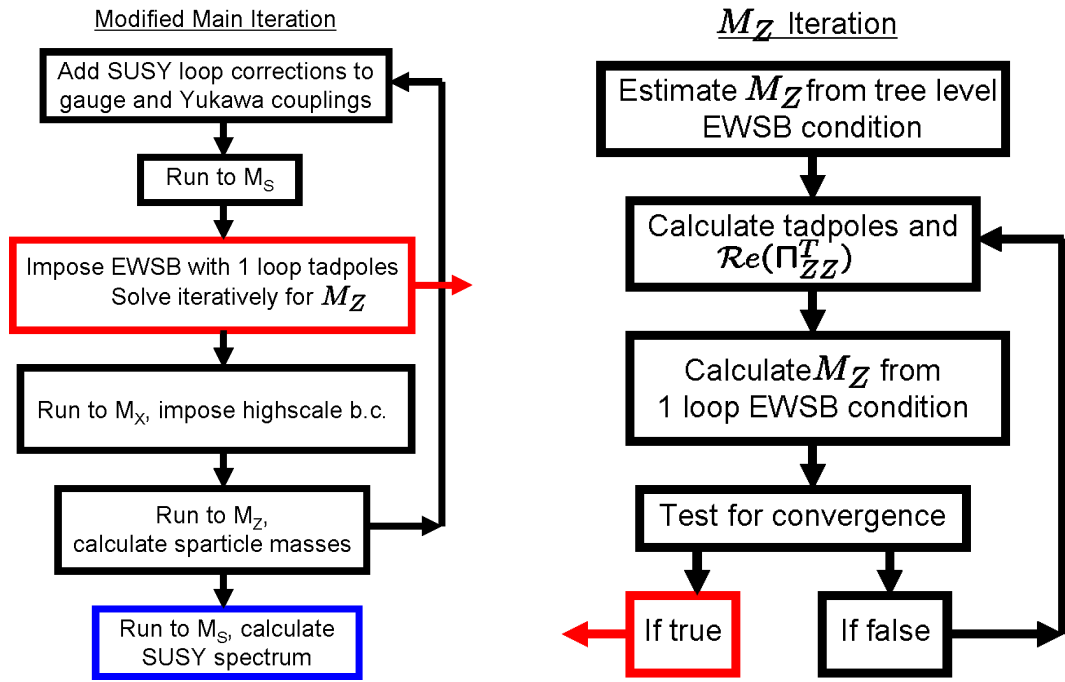


Figure 6.4: Flow chart showing the modified iterative routines of our altered version of SOFTSUSY.

We take random dimensionless fluctuations about an MSSM point at the GUT scale, $P' = \{p_k\}$, to give new points $\{P_i\}$. These are passed to the modified version of SOFTSUSY 2.0.5. Each random point P_i is run down from the GUT scale until electroweak symmetry is broken. An iterative procedure is used to predict M_Z^2 and then all the sparticle and Higgs masses are determined.

As before F is the volume formed by dimensionless variations in the parameters. G_{O_i} is the sub-volume of F additionally restricted by dimensionless variations in the single observable O_i , $a \leq \frac{O_i(\{p_k\})}{O_i(\{p'_k\})} \leq b$. As usual G is the volume restricted by $a \leq \frac{O_j(\{p_k\})}{O_j(\{p'_k\})} \leq b$, for each observable, O_j , where $\{O_j\}$ is the set of masses predicted in SOFTSUSY. For every O_i a count, N_{O_i} , is kept of how often the point lies in the volume G_{O_i} as well as an overall count, N_O , kept of how many points are in G . Tuning is then measured according to,

$$\Delta_{O_i} \approx \frac{N}{N_{O_i}}, \quad (6.36)$$

for individual observables and

$$\Delta \approx \frac{N}{N_O} \quad (6.37)$$

for the overall tuning at that point.

Before describing the results two comments on this approach should be made. Firstly when using SOFTSUSY to predict the masses for the random points, sometimes problems are encountered. We may have a tachyon, the Higgs potential unbounded from below, or non-perturbativity. Such points don't belong in volume G as they will give dramatically different physics. However it is unclear which volumes, G_{O_i} , the point lies in. Such points never register as hits in any of the G_{O_i} and this may artificially inflate the individual tunings, including $\Delta_{M_Z^2}$. Keeping the range small reduces the number of problem points. Therefore we chose $a = 0.9$ and $b = 1.1$ for our dimensionless variations.

Secondly, since we are measuring tuning for individual points numerically and cover only a small sample of points, it is not possible to obtain mean values of Δ and the Δ_{O_i} as we haven't sampled the entire space. When simply comparing how the tuning varies about the parameter space the normalisation factor is not needed, since it is the same for all points. However to compare the tuning between different observables as well as to compare with different models some form of normalisation is essential.

6.2.2 Preliminary Study

We considered points on the Constrained Minimal Supersymmetric Standard Model (CMSSM) benchmark slope, SPS 1a [178]. This slope is defined by,

$$m_0 = -A_0 = 0.4m_{\frac{1}{2}}, \quad \text{sign}(\mu) = +, \quad \tan \beta = 10, \quad (6.38)$$

where m_0 is the common scalar mass, $m_{1/2}$ the common gaugino mass (both at the GUT scale) and $\text{sign}(\mu)$ is the undetermined sign of μ , the magnitude being determined from a loop corrected, inverted form of Eq. (5.1) with M_Z^2 set to its observed value. A_0

is the common multiplicative factor which relates the supersymmetry breaking matrices of trilinear mass couplings to their corresponding Yukawa matrix, e.g. $a_u = A_0 y_u$.

The parameters we vary simultaneously are the set² $\{m_0, m_{1/2}, \mu_{GUT}, m_3^2, A_0, y_t, y_b, y_\tau\}$, where m_3 is the soft bilinear Higgs mixing parameter and y_t, y_b, y_τ are the Yukawa couplings of the top, bottom and tau respectively. The gauge couplings are not included as parameters. Doing so would introduce excessive global sensitivity, increasing the statistics needed to keep the errors under control.

First we applied our tuning measure to the observable M_Z^2 for 13 points on the SPS 1a slope. Moving along this slope in $m_{1/2}$ is an increase in the overall supersymmetry breaking scale, since the magnitude of every soft breaking term is increasing. We have plotted the results of this investigation in Figure 6.5.

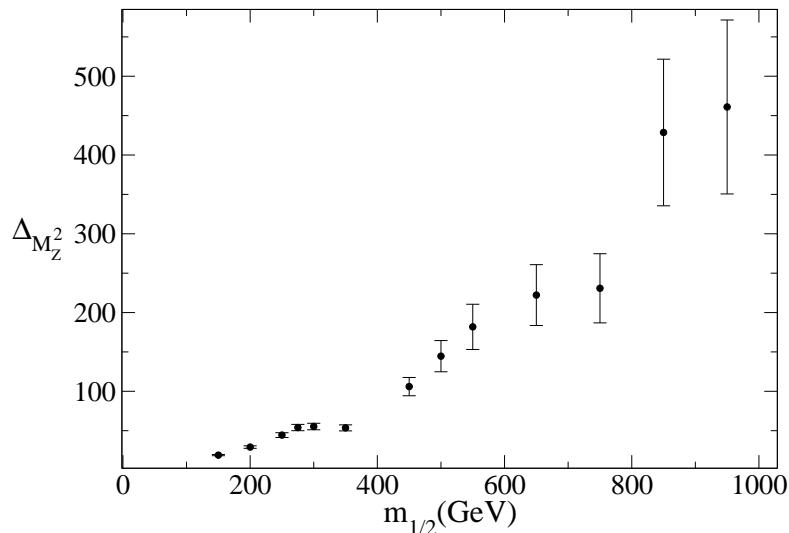


Figure 6.5: $\Delta_{M_Z^2}$ for the SPS 1a slope. Error bars denote a one standard deviation statistical error arising from the numerical procedure.

As expected there is a clear increase in tuning as the supersymmetry breaking scale is raised. The statistical error also increases with the tuning, making the numerical

²Note that since points on the SPS 1a slope have $|\mu|$ set by M_Z^2 , our tuning measure is not sensitive to the μ -problem. However for our random variation about the SPS 1a points we do treat μ_{GUT} as a parameter because we are predicting M_Z^2 from the parameters, not fixing it to its observed value.

approach most difficult to apply when the tuning is large. However precise determinations of tuning are only relevant for moderate and low tunings. With tunings greater than 500, precise values are not required.

6.2.3 Further Study

Due to the difficulty in this approach for measuring large tunings we looked in more detail at points expected to have moderate tuning. We chose a grid of points with,

$$\begin{aligned} A_0 &= -100 \text{ GeV}, & \tan \beta &= 10, & \text{sign}(\mu) &= +, \\ 250 \text{ GeV} &\leq m_{\frac{1}{2}} \leq 500 \text{ GeV}, & 100 \text{ GeV} &\leq m_0 \leq 200 \text{ GeV}. \end{aligned} \quad (6.39)$$

Shown in Fig. 6.6 (top) is a plot of $\Delta_{M_Z^2}$ over this grid of points. While the errors are still significant ($\lesssim 10\%$) there is a clear trend of tuning increasing with $m_{1/2}$. Also shown (bottom left) is $\Delta_{M_Z^2}$ averaged over the five different values of m_0 . This substantially reduces the errors giving a much more stable picture of tuning increasing linearly with $m_{1/2}$. Similarly $\Delta_{M_Z^2}$, averaged over the eleven different values of $m_{1/2}$, is shown (bottom right) as a function of m_0 . $\Delta_{M_Z^2}$ appears insensitive to variations in m_0 . These trends can be understood by looking at the one loop renormalisation group improved version of Eq. (5.1), written in terms of the parameters (with $\tan \beta = 10$),

$$M_Z^2 \approx 2(-|\mu|^2 + 0.076m_0^2 + 1.97m_{\frac{1}{2}}^2 + 0.10A_0^2 + 0.38A_0m_{\frac{1}{2}}), \quad (6.40)$$

where $|\mu|^2$ is the value at M_Z and differs from the parameter at the GUT scale, μ_{GUT} . The large coefficient in front of $m_{1/2}$ explains why variations in this parameter have a much greater impact on $\Delta_{M_Z^2}$ than variations in m_0 whose coefficient is much smaller.

Δ , which includes all of the masses predicted by SOFTSUSY as well as M_Z^2 , is shown in Fig. 6.7. Although the errors are much larger here, a similar pattern to that for M_Z^2 can be seen. Since these are unnormalised tunings, the numerical values of the two measures cannot be compared and one should not assume that $\Delta > \Delta_{M_Z^2}$ implies that the tuning is worse than when only M_Z^2 was considered. In fact the lack

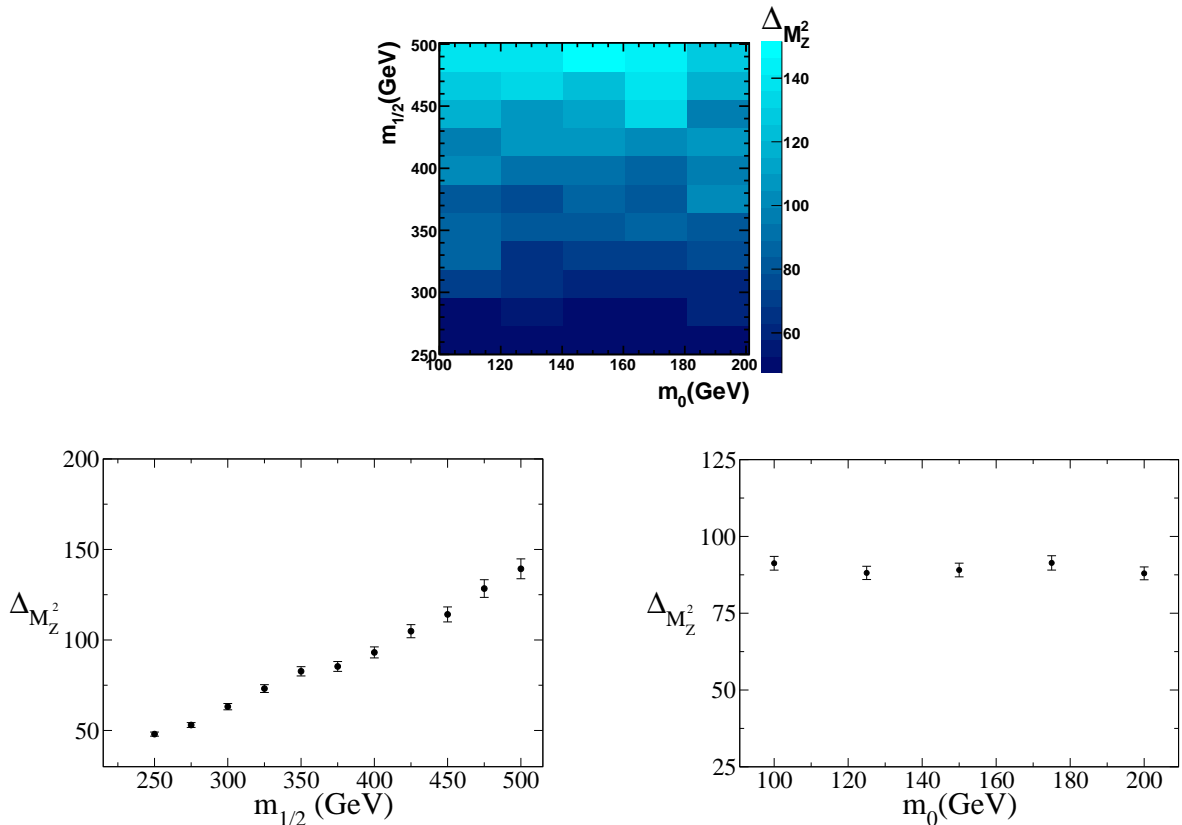


Figure 6.6: Tuning variation in M_Z^2 . *Top*: ΔM_Z^2 for all points on our grid. *Bottom left*: ΔM_Z^2 plotted against $m_{1/2}$. To reduce statistical errors, at each value of $m_{1/2}$, we have taken the mean value ΔM_Z^2 over the five different m_0 values. *Bottom right*: ΔM_Z^2 plotted against m_0 . To reduce statistical errors, at each value of m_0 , we have taken the mean value ΔM_Z^2 over the eleven different $m_{1/2}$ values.

of evidence for distinct patterns of variation in tuning from the Figs. 6.6 and 6.7 is consistent with the conjecture that the large cancellation between parameters in M_Z^2 is the dominant source of the tuning for these points.

Fig. 6.8 shows that $\Delta_{m_{t_2}^2}$ and $\Delta_{m_h^2}$ have similar patterns of variation to ΔM_Z^2 and Δ over $m_{1/2}$, though the gradients are noticeably shallower. While we know m_h^2 and $m_{t_2}^2$ contribute to the Little Hierarchy Problem by giving a large contribution to M_Z^2 , thereby requiring a cancellation to keep M_Z light, this shows there is also some tension in their own masses which restricts the parameter space. It is not clear from our results whether or not dimensionless variations are restricting different regions of parameter

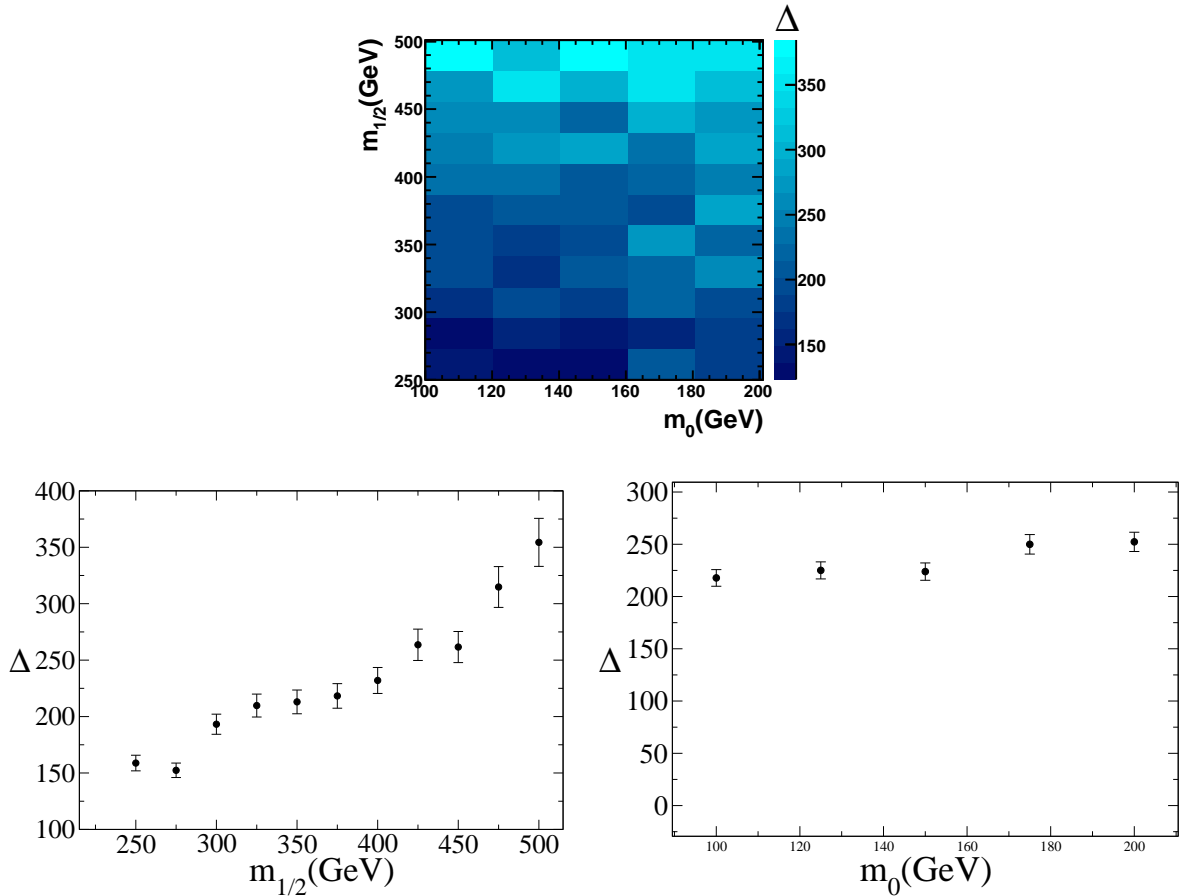


Figure 6.7: Variation in Δ plotted as in Fig. 6.6 for $\Delta_{M_Z^2}$.

space to those in M_Z^2 or if $G_{m_{\tilde{t}_2}^2}$ and $G_{m_{\tilde{h}}^2}$ are merely sub-volumes of $G_{M_Z^2}$, with no influence on Δ . This topic deserves further study.

However our results do show some evidence that the Little Hierarchy Problem is not the only source of tuning. Displayed in Fig. 6.9 is $\Delta_{M_A^2}$. Notice that $\Delta_{M_A^2}$ is very small, so the errors are significantly reduced and we can resolve very small variations in $\Delta_{M_A^2}$. As with the other observables tuning increases with $m_{1/2}$, but it is a distinctly non-linear variation. More surprising is that tuning *decreases* with m_0 . This pattern of variation, distinct from that shown for $\Delta_{M_Z^2}$, shows a different source of tension. It can be understood by examining the one loop RGE solution for M_A ,

$$M_A^2 \approx 2f(|\mu_{GUT}|^2, \{g_i\}, \{y_i\}) + 0.81m_0^2 - 1.55m_{\frac{1}{2}}^2 - 0.022A_0^2 - 0.41A_0m_{\frac{1}{2}}, \quad (6.41)$$

where f is a function of supersymmetry preserving parameters only, arising from the

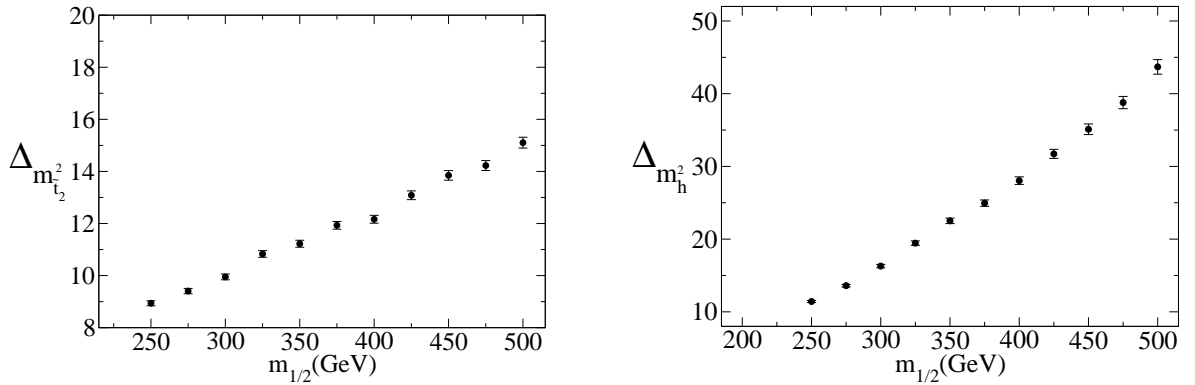


Figure 6.8: Variation of unnormalised tunings in the mass of the heaviest stop ($\Delta_{m_{t_2}^2}$, shown left) and the mass of the light Higgs ($\Delta_{m_h^2}$, shown right) over $m_{1/2}$

evolution of $|\mu|^2$. Notice that there is some opportunity for a cancellation here to make M_A lighter than expected. However the cancellation in the points we have looked at is very small, leading to small values for $\Delta_{M_A^2}$. As m_0^2 increases the already dominant positive part of the equation increases and M_A increases. As this happens the cancellation becomes less significant to M_A further reducing $\Delta_{M_A^2}$ as shown in Fig. 6.9(bottom right). Increasing $m_{1/2}$ increases the size of the cancellation. If all other parameters on the right hand side of Eq. (6.41) were fixed then we would expect to see $\Delta_{M_A^2}$ increase linearly³ with $m_{1/2}$. However each point on our grid has the value of $M_Z = 91.188$ GeV fixed, and the term $f(|\mu|^2, \{g_i\}, \{y_i\}) \approx |\mu^2|$ changes according to an inverted Eq. (6.40). This means M_A^2 is also increasing with $m_{1/2}$ and the balancing act between these two different effects leads to the nonlinear pattern shown.

Although we can't determine the normalisation using this approach it is nonetheless interesting to compare the unnormalised tunings for the points in our study with those obtained for points with more “natural” looking spectra. We present two points for this purpose. NP1 and NP2 are defined by,

$$\text{NP1} : m_{\frac{1}{2}} = M_Z, \quad m_0 = M_Z, \quad A_0 = -M_Z, \quad \text{sign}(\mu) = +, \quad \tan \beta = 3, \quad (6.42)$$

$$\text{NP2} : m_{\frac{1}{2}} = -50 \text{ GeV}, \quad m_0 = 100 \text{ GeV}, \quad A_0 = -50 \text{ GeV}, \quad \text{sign}(\mu) = +, \quad \tan \beta = 10.$$

³The effect of $A_0 m_{1/2}$ can be neglected since $m_{1/2} > A_0$.

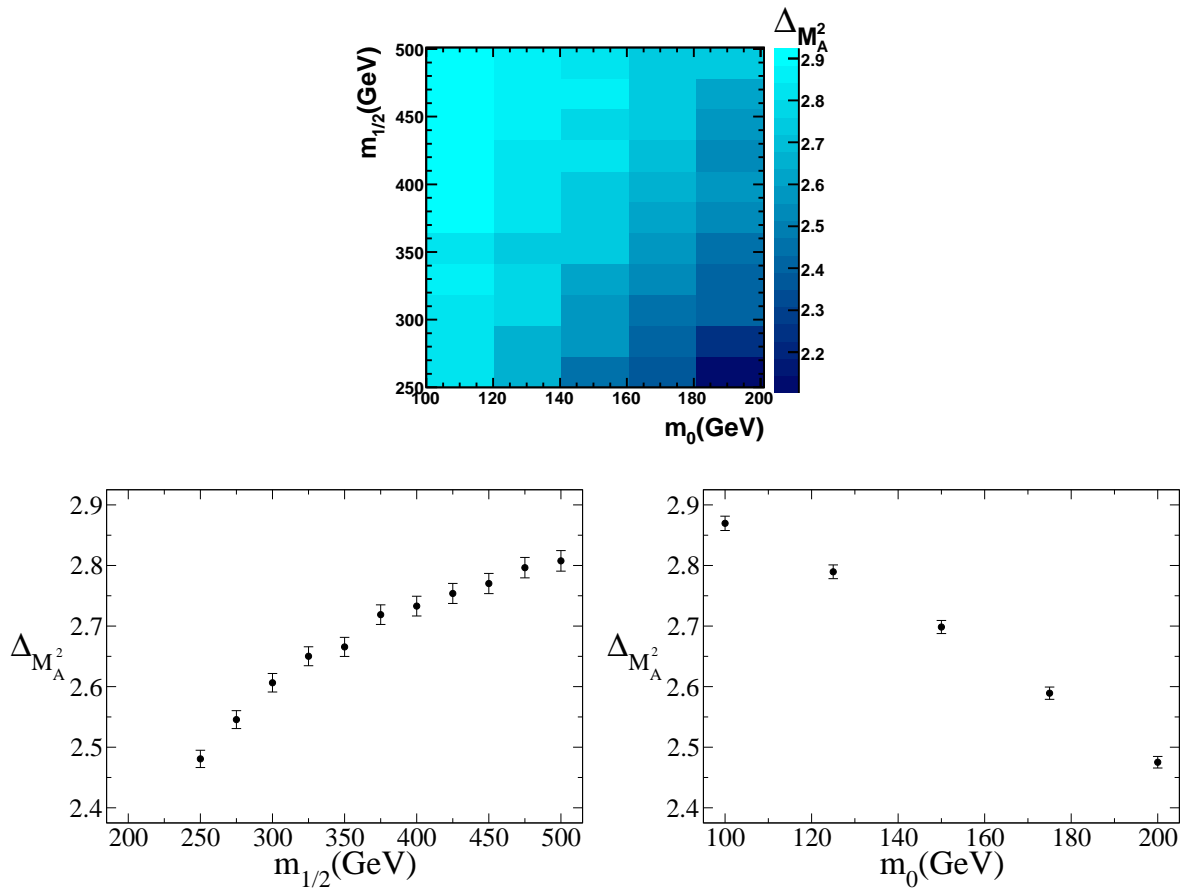


Figure 6.9: Variation in ΔM_A^2 plotted as in Fig. 6.6 for ΔM_Z^2 .

The spectra of these points are displayed in Fig. 6.10 and Fig. 6.11, and the unnormalised tunings are displayed in Table 6.2. Note that these are not intended to be “realistic” scenarios. Indeed both NP1 and NP2 are ruled out by experiment but are simply intended to provide “natural” scenarios for comparison.

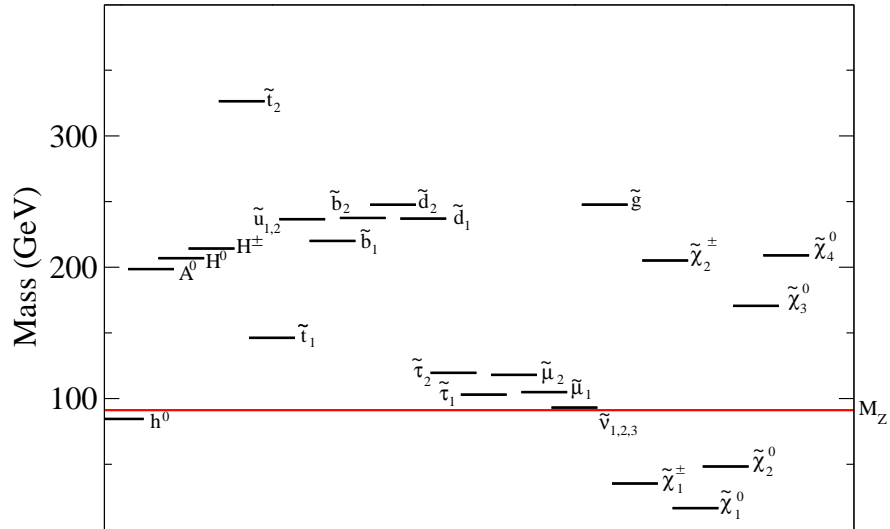


Figure 6.10: Point NP1 with a “natural” spectrum

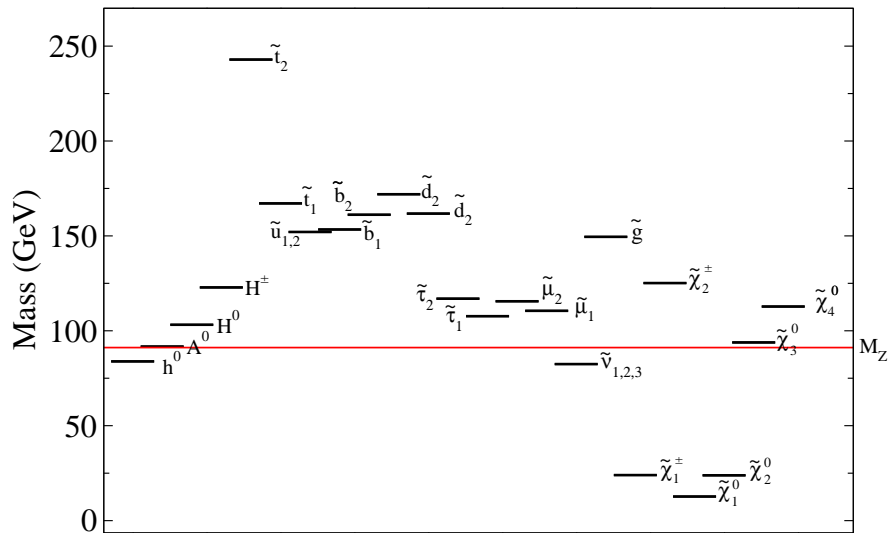


Figure 6.11: Point NP2 with a “natural” spectrum

While NP1 has low values of $\Delta_{M_Z^2}$, $\Delta_{m_h^2}$, $\Delta_{m_{\tilde{t}_2}^2}$ and $\Delta_{M_A^2}$, it has a relatively large tuning in the mass of the lightest neutralino ($\Delta_{m_{\tilde{\chi}_1^0}^2}$). These combine to give a Δ which

	Δ	$\Delta_{M_Z^2}$	$\Delta_{m_{\tilde{t}_2}}$	$\Delta_{m_h^2}$	$\Delta_{M_A^2}$	$\Delta_{m_{\chi_1^0}^2}$
NP1	241_{-26}^{+36}	$14.7_{-0.5}^{+0.5}$	$6.7_{-0.1}^{+0.1}$	$1.72_{-0.02}^{+0.02}$	$2.05_{-0.02}^{+0.02}$	$30.1_{-1.3}^{+1.4}$
NP2	$31.4_{-1.4}^{+1.5}$	$2.92_{-0.04}^{+0.04}$	$2.26_{-0.03}^{+0.03}$	$1.87_{-0.02}^{+0.02}$	$2.23_{-0.03}^{+0.03}$	$2.64_{-0.04}^{+0.04}$

Table 6.2: Unnormalised tunings for the two points, NP1 and NP2, with natural looking spectra.

	$\hat{\Delta}$	$\hat{\Delta}_{M_Z^2}$	$\hat{\Delta}_{m_{\tilde{t}_2}}$	$\hat{\Delta}_{m_h^2}$	$\hat{\Delta}_{M_A^2}$	$\hat{\Delta}_{m_{\chi_1^0}^2}$
Relative to NP1	0.5..1.5	3..10	1..2	7..25	1	0.2
Relative to NP2	5..15	10..50	4..7	6..23	1	2

Table 6.3: Approximate relative tunings for the points in our study, with respect to those for NP1 and NP2.

is similar in size to the values found for our grid of points. In NP2 all of the tunings are relatively small, but the combined tuning is still larger than may naively have been anticipated. This is because many of these small tunings for individual observables are not correlated and are restricting different regions of parameter space. Table 6.3 shows the approximate relative magnitude of the tunings in our grid points with respect to these seemingly natural points.

In attempts to find a CMSSM scenario with a mass spectrum which is manifestly natural we found many scenarios where tuning appeared in the mass of the lightest neutralino. NP1 is a (moderate) example of this. This is because in some parameter choices, the lightest neutralino becomes very light due to large cancellations between the parameters. Other observables may also contain large cancellations between the parameters in certain regions of parameter space. While we have not studied this enough to make definitive claims, this may suggest that mass hierarchies appear in a greater proportion of the parameter space than conventional CMSSM wisdom dictates.

This would reduce the true tuning in the CMSSM as scenarios with hierarchies would be less atypical than previously thought. A reduction in tuning from this effect can only be measured by using our normalised new measure, $\hat{\Delta}$.

Unfortunately the numerical approach we have applied to the MSSM in this paper cannot be used to address this issue. An average measure of Δ , over the whole parameter space, is needed in order to investigate this possibility. A thorough numerical survey of the parameter space would be too expensive, however an analytical study may be more promising. Findings in numerical studies like this may be used to identify which observables and parameters are important for fine tuning and therefore reduce the set $\{O_i\}$ and $\{p_i\}$ to a manageable size. We will not carry out this programme here, but leave it for a future study.

It is not just the possibility of finding a larger than expected global sensitivity which motivates this study. It may be that most of the CMSSM parameter space is hierarchy free and this is not a significant effect. However identifying a region of parameter space where mass hierarchies are common also opens up new possibilities. Past studies (see e.g. [227–228]) have looked for a theoretical basis for relations between parameters which enforce a hierarchy between M_Z and M_{SUSY} . However no search has been made for theoretical relations which simply restrict the parameter space to regions where hierarchies, in general, are common. Such studies may also have the possibility of solving the Little Hierarchy Problem.

Here we have two complimentary approaches. An analytical approach which can determine tuning precisely, but is complicated and unwieldy when applied to a great number of parameters and observables and a numerical approach which can be applied to such situations but is not able to give an unambiguous measure of tuning as global sensitivity cannot be accounted for. Progress can be made by combing our two approaches. Since solving for the tuning analytically with all parameters and observables included would be difficult, one should first apply the numerical method. This might identify which observables are in tension and responsible for the restriction of parameter space and also along which axis in parameter space this restriction takes place. If

these are a sufficiently small set (maybe no more than 5 parameters and 5 observables) then the analytical measure can be applied to this limited set to obtain a reasonably accurate and unambiguous measure of tuning for that model.

6.3 Conclusions

Fine tuning $\approx 10^{34}$ within the Standard Model has motivated many of the BSM theories which are popular within particle physics. In particular it motivates low energy supersymmetry. However constraints from LEP and other searches have placed stringent bounds on new physics which mean that many of the proposed solutions to the SM fine tuning problem also require tuning to some degree. In order to compare the viability of such models and judge whether or not they are satisfactory a reliable measure of tuning is required.

Current measures of tuning have several limitations. They neglect the many parameter nature of fine tuning, ignore additional tunings in other observables, consider local stability only and assume \mathcal{L}_{SUSY} is parametrised in the same way as \mathcal{L}_{GUT} . In the literature there have been different approaches to combine tunings for individual parameters and observables. With no guiding principle to select one particular approach, which models are preferred in terms of naturalness can depend on which tuning measure is used.

In this paper we have presented a new measure of tuning based upon our intuitive notion of the restriction of parameter space. This measure can also be obtained by generalising the traditional measure of tuning to include many parameters, many observables and finite variations in the parameters followed by removing global sensitivity by factoring out the mean value of the unnormalised sensitivity.

From the application of this new measure to various toy models, we have shown that none of the other measures satisfactorily combine individual tunings per parameter. Interestingly though, in the absence of global sensitivity, it is the traditional measure of Barbieri and Giudice which comes closest to our result with deviations for these

simple examples being very small.

A numerical approach for some CMSSM scenarios demonstrated how the tuning in complicated models with many parameters and many observables may be examined and also highlighted some of the complications and issues encountered in doing so.

Our new measure is needed in future studies to examine tuning in the Z boson mass and cosmological relic density simultaneously; to judge the true tuning in the NMSSM in light of [229]; to examine parametrisation choices which alleviate the tuning in different models and to study the global sensitivity of the complete tuning measure to see if this may cause a significant reduction in the tuning problem.

Chapter 7

Exceptional Supersymmetric Standard Model

7.1 Motivation and Background

The Exceptional Supersymmetric Standard Model (E_6 SSM) [4–5] is an E_6 inspired model with an extra gauged $U(1)$ symmetry. It is a very interesting model from a phenomenological point of view because it,

- solves the μ -problem in a similar way to the NMSSM but without the accompanying problems of singlet tadpoles or domain walls;
- allows the light Higgs mass to be as heavy as 155 GeV, which may ease the Little Hierarchy Problem;
- allows unification of the gauge couplings to within 2 standard deviations without relying on threshold corrections;
- predicts a new Z' boson which could be discovered at the LHC if its mass is less than ~ 4 TeV;
- predicts exotic colored objects which may either be diquark or leptoquark in

nature and their supersymmetric partners;

- predicts exotic objects which carry neither lepton nor baryon number which we refer to as *Inert Higgs* and *Inert Higgsinos* and new exotic leptons;
- includes sterile right-handed neutrinos;
- aids successful baryogenesis in the early universe.

From a more theoretical standpoint it also has further advantages due to its E_6 motivation as,

- it could originate from an E_6 Grand Unified Theory;
- E_6 groups arise naturally from the breakdown of $E_8 \times E'_8$ heterotic superstring theory when the extra dimensions are compactified.

Some of these motivations are described in more detail in the following sections.

7.1.1 The μ -problem

The incorporation of the most minimal SUSY extension of the SM, the Minimal Supersymmetric Standard Model (MSSM) into SUGRA or SUSY GUT models lead to the μ -problem [19]. The superpotential of the MSSM contains one bilinear term $\mu \hat{H}_d \hat{H}_u$ which can be present before SUSY is broken. As a result one would naturally expect the parameter μ to be either zero or of the order of the Planck scale. If $\mu \simeq M_{\text{Pl}}$ then the Higgs scalars get a huge positive contribution $\sim \mu^2$ to their squared masses and EWSB does not occur. On the other if $\mu = 0$ at some scale Q the mixing between Higgs doublets is not generated at any scale below Q due to the non-renormalisation theorems [230]. In this case $\langle H_d \rangle = 0$ and down-type quarks and charged leptons remain massless. The correct pattern of EWSB requires μ to be of the order of the SUSY breaking (or EW) scale.

An elegant solution to the μ problem is provided in the E_6 SSM. The low energy gauge group of the E_6 SSM contains an extra gauged $U(1)_N$ symmetry. This forbids the bilinear term, $\mu \hat{H}_d \hat{H}_u$, but allows an interaction of the extra SM singlet superfield \hat{S} with the Higgs supermultiplets \hat{H}_d and \hat{H}_u in the superpotential, $\lambda \hat{S} \hat{H}_d \hat{H}_u$. After EWSB the scalar component of the singlet superfield \hat{S} acquires a non-zero vev breaking $U(1)'$ and an effective μ term of the required size is automatically generated.

7.1.2 Light Higgs Mass

Another striking advantage of this model is that the upper bound on the mass of the lightest Higgs is 155 GeV, significantly larger than in either the MSSM or the NMSSM.

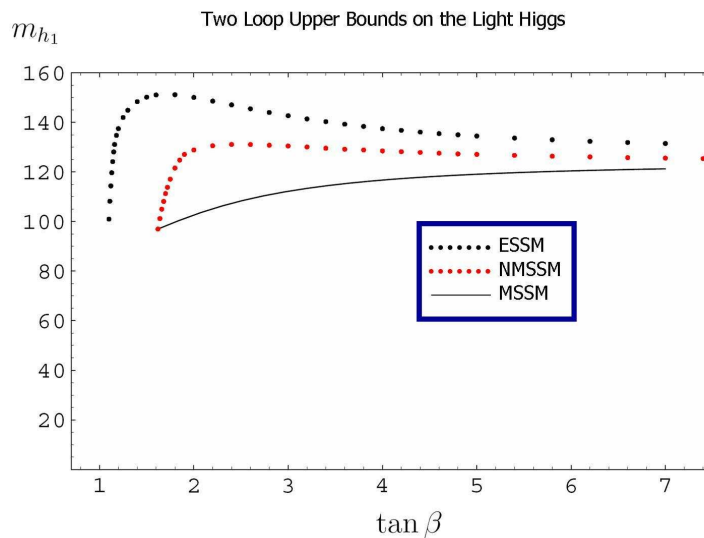


Figure 7.1: Two loop upper bounds on the lightest Higgs mass. Taken from [4].

The upper-bound on the light Higgs mass plays an important role in the Little Hierarchy Problem, as described in Sec. 5.1.1. The accommodation of a heavier SM-like Higgs mass in the E_6 SSM could allow a Higgs mass which is above the LEP limit without the requirement for such a heavy stop, which has led to the perception of a Little Hierarchy problem in the MSSM.

7.1.3 Gauge Coupling Unification

Like the MSSM when the gauge couplings in the E_6 SSM are evolved up to high energies using renormalisation group equations the result is consistent with the gauge couplings unifying at $M_{GUT} \approx 10^{16}$. However, as is described in [124] the gauge couplings of the MSSM no longer meet within 2 standard deviations, following a reduction in the experimental uncertainty in α_3 . This is shown in Fig. 7.2(a) and Fig. 7.2(b). Two loop RGE evolution of the gauge couplings in the E_6 SSM is shown to be consistent within 1 standard deviation, as is shown in, Fig. 7.2(c) and Fig. 7.2(d).

7.1.4 Connection to Superstring theory

The low energy gauge structure of the E_6 SSM may arise naturally from superstring models. Ten-dimensional heterotic $E_8 \times E'_8$ superstring theory [231] could provide an ultraviolet completion of non-renormalisable Supergravity models. The strong coupling behaviour of heterotic $E_8 \times E'_8$ superstring theory is determined by its eleven dimensional supergravity (M-theory) [232] and has been shown to be compatible with the unification scale M_X [233]. When the extra dimensions are compactified this results in breaking of E_8 down to E_6 or one of its subgroups in the observable sector [234]. The matter content of the E_6 SSM fits into the corresponding E_6 multiplets.

The remaining E'_8 only couples to the matter (in the E_6 multiplets) through gravitational interactions and therefore makes up a hidden sector in which the spontaneous breakdown of local supersymmetry can take place, as is often required in phenomenological SUSY models (see Sec. 3.4). At low energies the hidden sector decouples from the observable one due to the weakness of gravity but the spontaneous breaking of local supersymmetry in that sector is transmitted to the visible sector as described in Sec. 3.4. This gives rise to a set of soft SUSY breaking parameters like the ones shown in Sec. 3.4, which spoil the mass degeneracy between bosons and fermions within one supermultiplet.

Superstring inspired E_6 models may lead to low-energy gauge groups with extra

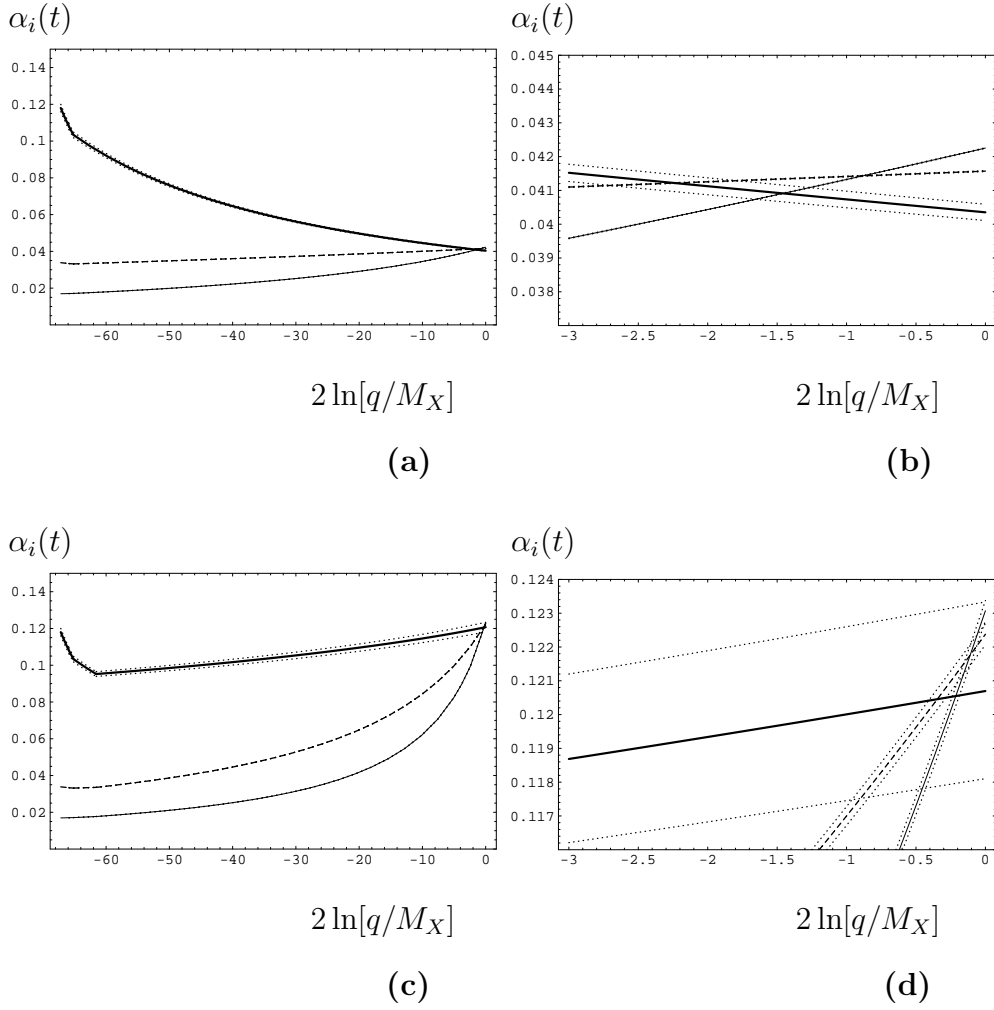


Figure 7.2: Taken from [124]. Renormalisation Group Evolution of gauge couplings: (a) in the MSSM from EW to GUT scale M_X ; (b) in the MSSM close to M_X ; (c) in the E₆SSM from M_Z to M_X ; (d) in the E₆SSM close to M_X . Thick, dashed and solid lines correspond to the running of $SU(3)_C$, $SU(2)_W$ and $U(1)_Y$ couplings respectively. Parameters are $\tan\beta = 10$, an effective SUSY threshold scale $M_S = 250$ GeV, $M_{Z'} = 1.5$ TeV, $\kappa_{1,2,3}(M_Z) = \lambda_{1,2,3}(M_{Z'}) = g_1'(M_{Z'})$, $g_1'^2(M_{Z'}) = 0.2271$, $g_{11}(M_{Z'}) = 0.02024$, $\alpha_s(M_Z) = 0.118$, $\alpha(M_Z) = 1/127.9$ and $\sin^2\theta_W = 0.231$. The dotted lines show the one sigma deviation band about the central values, from the EW scale measurement of α_S .

$U(1)'$ factors. In particular, by means of the Hosotani mechanism [235] E_6 can be broken directly to the subgroup $SU(3)_C \times SU(2)_W \times U(1)_Y \times U(1)_\psi \times U(1)_\chi$, with $U(1)_\psi$ and $U(1)_\chi$ symmetries defined by [236],

$$E_6 \rightarrow SO(10) \times U(1)_\psi, \quad (7.1)$$

$$SO(10) \rightarrow SU(5) \times U(1)_\chi. \quad (7.2)$$

For suitably large vacuum expectation values (vevs) of the symmetry breaking Higgs fields this can be reduced further to an effective model with only one extra gauge symmetry $U(1)'$ which is a linear combination of $U(1)_\chi$ and $U(1)_\psi$:

$$U(1)' = U(1)_\chi \cos \theta + U(1)_\psi \sin \theta. \quad (7.3)$$

This is the extra $U(1)_N$ (with $\theta = \arctan \sqrt{15}$) factor in the gauge group of the E_6 SSM. So the gauge structure and matter content of the E_6 SSM is inspired by the E_6 and Superstring theory.

7.1.5 Neutrinos and Leptogenesis

This particular $U(1)'$ extension of the gauge group set by the choice $\theta = \arctan \sqrt{15}$, is very advantageous. Right-handed neutrinos have zero charge under this gauge group, thus transforming as singlets and do not participate in any gauge interactions. This means with no symmetry protection right-handed neutrinos may be super-heavy and this can help explain the origin of the mass hierarchy in the lepton sector.

The presence of super-heavy right-handed neutrino also allows the generation of lepton and baryon asymmetries of the Universe through leptogenesis [237–238]. The E_6 SSM also contains two generations of *Inert Higgs* fields which carry neither lepton nor baryon number and new lepton doublets with lepton number $L = \pm 1$ and additional exotic matter, exotic colored objects. As well as providing tremendously exciting phenomenology these exotic objects provide new decay channels for the right-handed neutrinos and augment the decay channels already present in the MSSM. This increases the generated CP-asymmetries to such an extent that successful leptogenesis can take

place with a relatively light right-handed neutrino mass in range, $\approx 10^6..10^9 GV$ which is not possible with only MSSM matter content [238].

7.2 E₆SSM Model

The E₆SSM [4–5] is an E₆ inspired model with an extra gauged U(1) symmetry. It provides a low energy alternative to the Minimal (MSSM) and Next to Minimal (NMSSM) Supersymmetric Models. In this section a brief description of the model is given. A more complete description is given in Appendix B.

The gauge group is, $SU(3) \otimes SU(2) \otimes U(1)_Y \otimes U(1)_N$, where $U(1)_N$ is defined by,

$$U(1)_N = \frac{1}{4}U(1)_\chi + \frac{\sqrt{15}}{4}U(1)_\psi, \quad (7.4)$$

with $U(1)_\chi$ and $U(1)_\psi$ in turn, defined by the breaking, shown in 7.2

The matter content is based on three generations of complete 27plet representations of E₆ in which anomalies are automatically cancelled. Each 27plet, $(27)_i$, is filled with one generation of ordinary matter $\hat{Q}_i, \hat{u}_i^c, \hat{d}_i^c, \hat{L}_i, \hat{e}_i^c, \hat{N}_i^c$; a singlet field, \hat{S}_i ; up and down type Higgs like fields, $\hat{H}_{2,i}$ and $\hat{H}_{1,i}$ and exotic colored matter, $\hat{D}_i, \hat{\bar{D}}_i$. In addition to the matter contained in complete 27plets, the model contains two extra SU(2) doublets¹, \hat{H}' and $\hat{\bar{H}}'$ which are components of $27'$ and $\bar{27}'$ E₆ representations that survive to low energies. The inclusion of \hat{H}' and $\hat{\bar{H}}'$ affects the running of the gauge couplings at the one loop level and allows for unification at the GUT scale. So long as μ' (the parameter which sets their masses) is between the EW scale and 30TeV unification can still take place.

To summarise the matter content of the E₆SSM is,

$$3 \left[(\hat{Q}_i, \hat{u}_i^c, \hat{d}_i^c, \hat{L}_i, \hat{e}_i^c, \hat{N}_i^c) + (\hat{S}_i) + (\hat{H}_{2i}) + (\hat{H}_{1i}) + (\hat{D}_i, \hat{\bar{D}}_i) \right] + \hat{H}' + \hat{\bar{H}}', \quad (7.5)$$

¹A slight variant on the E₆SSM, known as the Minimal E₆SSM [239–240], does not contain these extra survival fields and achieves unification of gauge couplings through a two step process.

As mentioned in Sec. 7.1.5, the right-handed neutrinos, \hat{N}_i^c , are expected to gain masses at some intermediate scale. All other matter in the E₆SSM should have masses between the TeV and EW scales near which the gauge group $U(1)_N$ is broken.

7.2.1 Superpotential

Now that the gauge group and matter content has been specified it is time to introduce the superpotential. There is an important subtlety here because the E₆SSM in fact refers to two distinct, though closely related, models, E₆SSMI and E₆SSMII.

The superpotentials of both models originate from the most general renormalisable superpotential which is consistent with low energy E₆SSM gauge structure. This is shown in Appendix B.3, Eq. B.10 where it is divided into E₆ preserving terms and terms which violate E₆, but are allowed by the low energy gauge structure. To forbid dangerous flavour changing processes an approximate Z_2^H symmetry is imposed, under which only one pair of Higgs like superfields \hat{H}_d, \hat{H}_u and one singlet \hat{S} are even and all other superfields are odd. However, to prevent the proton decay, two different discrete symmetries (which are specified below) may be imposed.

In the first model, E₆SSMI, an exact discrete symmetry, Z_2^L , under which lepton² superfields are odd and all other superfields are even is also imposed. In this model all baryon and lepton violating processes are then suppressed³ if the exotic colored objects, \hat{D}_i and $\overline{\hat{D}}_i$ are diquark superfields with baryon number assignment $B_D = -2/3$ and $B_{\overline{D}} = 2/3$.

E₆SSMII has, instead, an exact symmetry, under which the exotic quark and lepton superfields are odd while all the other superfields are even, is imposed. This model

²Recall that exotics \hat{H}' and $\overline{\hat{H}}'$ are lepton superfields, so this applies to them in addition to the lepton superfields of ordinary matter.

³There is one exception to this, $\mu'_{ij} \hat{D}_i \hat{d}_j^c$, coming from the E₆ breaking sector. This term can cause the proton to decay, but it is not certain that explicit E₆ breaking term like this would be generated during the breakdown of E₆, so it is not stressed. This term can be forbidden by an additional Z_2 symmetry, under which only Q_i, u_i^c, d_i^c are odd and all other superfields are even.

is then free from lepton and baryon violating processes if \hat{D}_i and $\hat{\bar{D}}_i$ are leptoquarks, i. e. they carry baryon ($B_D = 1/3$ and $B_{\bar{D}} = -1/3$) and lepton ($L_D = 1$ and $L_{\bar{D}} = -1$) numbers simultaneously.

If the Z_2^H symmetry was exact, then the superpotential of both E₆SSM models would be the same,

$$W_{\text{E}_6\text{SSM I, II}} \rightarrow \lambda_i \hat{S}(\hat{H}_{1i}\hat{H}_{2i}) + \kappa_i \hat{S}(\hat{D}_i\hat{\bar{D}}_i) + f_{\alpha\beta} \hat{S}_\alpha(\hat{H}_d\hat{H}_{2\beta}) \quad (7.6)$$

$$+ \tilde{f}_{\alpha\beta} \hat{S}_\alpha(\hat{H}_{1\beta}\hat{H}_u) + \frac{1}{2} M_{ij} \hat{N}_i^c \hat{N}_j^c + \mu'(\hat{H}'\hat{H}') \quad (7.7)$$

$$+ h_{4j}^E(\hat{H}_d\hat{H}')\hat{e}_j^c + h_{4j}^N(\hat{H}_u\hat{H}')\hat{N}_j^c + W_{\text{MSSM}}(\mu = 0), \quad (7.8)$$

where $\alpha, \beta = 1, 2$ and $i = 1, 2, 3$. By construction the third generation of the Higgs-like scalar fields, $H_u = H_{2,3}$, $H_d = H_{1,3}$ and $S = S_3$, are Higgs fields and develop vevs,

$$\langle H_u^0 \rangle = v_u, \quad \langle H_d^0 \rangle = v_d, \quad \text{and} \quad \langle S \rangle = s, \quad (7.9)$$

where v_u and v_d give mass to ordinary matter, while s both gives mass to the exotic colored fields, $\kappa_i S \rightarrow \kappa_i s = m_{D_i}$ and generates an effective μ -term, $\mu_{eff} = \lambda_3 s$. To ensure that none of the fields $S_{1,2}$, H and H' obtain a vev it is further assumed that,

$$\kappa_i \sim \lambda_3 \gtrsim \lambda_{1,2} \gg f_{\alpha\beta}, \tilde{f}_{\alpha\beta}, h_{4j}^E, h_{4j}^N. \quad (7.10)$$

With the first and second generation singlet couplings $f_{\alpha\beta}$ and $\tilde{f}_{\alpha\beta}$ thus suppressed, the RG equations for soft singlet masses $m_{S_{1,2}}$, as is shown in Eq. C.37 of Appendix C, are dominated by negative contributions from the gaugino mass M'_1 , leading to an increase in mass during RG evolution from the high scale, M_X , to the electroweak scale. Therefore these singlet fields will not develop a vev. Similarly Eq. C.47 and Eq. C.48 show that RG evolution of these survival field are also dominated by negative contributions from gaugino masses preventing them from developing vevs.

Since the approximate Z_2^H symmetry suppresses the Z_2^H violating couplings, this superpotential can in many cases be used to study the model. However the Inert Higgs superfields and the exotic colored superfields only couple to ordinary matter through Z_2^H violating decays. This is why Z_2^H can only be an approximate symmetry

as otherwise the model would contain stable, electromagnetically charged particles. To understand how these exotic particles can be produced and how they decay one must also know the Z_2^H violating couplings present in E₆SSMI and E₆SSMII. These are shown in Appendix B.3, Eq. B.16.

The hierarchical structure of the Yukawa interactions allows substantial simplification of the form of the E₆SSM superpotential. Integrating out heavy Majorana right-handed neutrinos and keeping only Yukawa interactions which will have a significant impact on the RG evolution leaves the Superpotential,

$$W_{\text{E}_6\text{SSM}} \simeq \lambda S(H_d H_u) + \lambda_\alpha S(H_{1,\alpha} H_{2,\alpha}) + \kappa_i S(D_i \overline{D}_i) \quad (7.11)$$

$$+ h_t (H_u Q) t^c + h_b (H_d Q) b^c + h_\tau (H_d L) \tau^c + \mu' (H' \overline{H'}). \quad (7.12)$$

7.2.2 Soft Breaking Terms

Finally to complete this description of the model soft SUSY breaking masses are specified. The most general scalar potential of the E₆SSM that ensures the soft breakdown of supersymmetry is,

$$\begin{aligned} V_{\text{soft}} = & m_{S_i}^2 |S_i|^2 + m_{H_{2i}}^2 |H_{2i}|^2 + m_{H_{1i}}^2 |H_{1i}|^2 + m_{D_i}^2 |D_i|^2 + m_{\overline{D}_i}^2 |\overline{D}_i|^2 \\ & + m_{Q_i}^2 |Q_i|^2 + m_{u_i^c}^2 |u_i^c|^2 + m_{d_i^c}^2 |d_i^c|^2 + m_{L_i}^2 |L_i|^2 + m_{e_i^c}^2 |e_i^c|^2 \\ & + m_{H'}^2 |H'|^2 + m_{\overline{H'}}^2 |\overline{H'}|^2 + [B' \mu' (H' \overline{H'}) + \lambda_i A_{\lambda_i} S(H_{1i} H_{2i}) \\ & + \kappa_i A_{\kappa_i} S(D_i \overline{D}_i) + h_t A_t (H_u Q) t^c + h_b A_b (H_d Q) b^c \\ & + h_\tau A_\tau (H_d L) \tau^c + h.c.]. \end{aligned} \quad (7.13)$$

In addition to the scalar masses appearing in Eq. 7.13 there are also soft SUSY breaking gaugino masses M_1 , M_2 , M_3 , and M'_1 which give mass to the gauginos associated with $U(1)_Y$, $SU(2)_W$, $SU(3)_C$ and $U(1)_N$ gauge groups respectively. So M_3 is a gluino (\tilde{g}) mass, M_2 is a wino (\tilde{W}) mass, M_1 is a bino (\tilde{B}) mass and M'_1 is the mass of the new (with respect to the MSSM) gaugino \tilde{B}' .

	\hat{Q}	\hat{u}^c	\hat{d}^c	\hat{L}	\hat{e}^c	\hat{N}^c	\hat{S}	\hat{H}_2	\hat{H}_1	\hat{D}	$\hat{\bar{D}}$	\hat{H}'	$\hat{\bar{H}'}$
$\sqrt{\frac{5}{3}}Q_i^Y$	$\frac{1}{6}$	$-\frac{2}{3}$	$\frac{1}{3}$	$-\frac{1}{2}$	1	0	0	$\frac{1}{2}$	$-\frac{1}{2}$	$-\frac{1}{3}$	$\frac{1}{3}$	$-\frac{1}{2}$	$\frac{1}{2}$
$\sqrt{40}Q_i^N$	1	1	2	2	1	0	5	-2	-3	-2	-3	2	-2

Table 7.1: Charges of E₆SSM matter fields under gauge symmetries, $U(1)_Y$ and $U(1)_N$. The numerical factors in front of the charges are from E₆ normalisation.

7.3 Electroweak Symmetry Breaking in the E₆SSM

As mentioned in the previous section EWSB takes place in the E₆SSM when the neutral components of H_u and H_d as well as the singlet field S pick up vevs. The interactions between them are defined by the structure of the gauge interactions and the superpotential, Eq. 7.8. The full effective Higgs potential is,

$$\begin{aligned}
V &= V_F + V_D + V_{soft}^H + \Delta V, \\
V_F &= \lambda^2 |S|^2 (|H_d|^2 + |H_u|^2) + \lambda^2 |(H_d H_u)|^2, \\
V_D &= \frac{g^2}{8} \left(H_d^\dagger \sigma_a H_d + H_u^\dagger \sigma_a H_u \right)^2 + \frac{g'^2}{8} (|H_d|^2 - |H_u|^2)^2 + \\
&\quad + \frac{g_1'^2}{2} \left(\tilde{Q}_1 |H_d|^2 + \tilde{Q}_2 |H_u|^2 + \tilde{Q}_S |S|^2 \right)^2, \\
V_{soft}^H &= m_S^2 |S|^2 + m_1^2 |H_d|^2 + m_2^2 |H_u|^2 + \left[\lambda A_\lambda S (H_u H_d) + h.c. \right],
\end{aligned} \tag{7.14}$$

where ΔV includes loop corrections to the Higgs potential. \tilde{Q}_1 , \tilde{Q}_2 and \tilde{Q}_S are effective $U(1)_N$ charges of H_d , H_u and S respectively. The $U(1)_N$ charges are shown in Table 7.1, and the effective charges are related to them by

$$\tilde{Q}_i \equiv Q_i^N + Q_i^Y \frac{g_{11}}{g_1'}, \tag{7.15}$$

where the extra term is a result of gauge kinetic mixing which can arise in loop correction. In fact g_{11} turns out to be rather small and can be neglected for most purposes.

g and g' are the gauge couplings of $SU(2)_W$ and $U(1)_Y$, as defined in Sec. 2.3.2 and g' is not changed by the kinetic mixing. The gauge coupling associated with the $U(1)_N$ symmetry is rescaled by the kinetic mixing, giving g'_1 but since this mixing is small it is reasonable to just consider g'_1 to be the $U(1)_N$ gauge coupling. As usual V_F and V_D contain terms from Auxiliary fields F and D respectively and V_{soft}^H is the Higgs part of Eq. 7.13. V_D contains terms proportional to $g'_1{}^2$, from the extra $U(1)_N$ symmetry, which are not present in the MSSM or NMSSM.

The leading one-loop contributions to the Higgs effective potential [241–242] in Eq. 7.14 come from loops involving the top and stops, and also exotic colored objects if the couplings $\kappa_{1,2,3}$ are large,

$$\begin{aligned} \Delta V^{(1)} = & \frac{3}{32\pi^2} \left[m_{\tilde{t}_1}^4 \left(\ln \frac{m_{\tilde{t}_1}^2}{Q^2} - \frac{3}{2} \right) + m_{\tilde{t}_2}^4 \left(\ln \frac{m_{\tilde{t}_2}^2}{Q^2} - \frac{3}{2} \right) - 2m_t^4 \left(\ln \frac{m_t^2}{Q^2} - \frac{3}{2} \right) \right. \\ & + \sum_{i=1,2,3} \left\{ m_{\tilde{D}_{1,i}}^4 \left(\ln \frac{m_{\tilde{D}_{1,i}}^2}{Q^2} - \frac{3}{2} \right) + m_{\tilde{D}_{2,i}}^4 \left(\ln \frac{m_{\tilde{D}_{2,i}}^2}{Q^2} - \frac{3}{2} \right) \right. \\ & \left. \left. - 2\mu_{D_i}^4 \left(\ln \frac{\mu_{D_i}^2}{Q^2} - \frac{3}{2} \right) \right\} \right] \end{aligned} \quad (7.16)$$

where $m_{\tilde{t}_1}$, $m_{\tilde{t}_2}$ are the masses of the stops, μ_{D_i} are the masses of the exotic fermions and $m_{\tilde{D}_{1,i}}$ and $m_{\tilde{D}_{2,i}}$ are the masses of their scalar superpartners. The physical vacuum is found by minimising the scalar potential (7.14). The Higgs fields have non-zero expectation values in the vacuum (vevs),

$$\langle H_d \rangle = \begin{pmatrix} v_1 \\ 0 \end{pmatrix}, \quad \langle H_u \rangle = \begin{pmatrix} 0 \\ v_2 \end{pmatrix}, \quad \langle S \rangle = s. \quad (7.17)$$

In the E₆SSM the $U(1)_N$ symmetry is broken above (but hopefully not too far above) the EW scale when $m_S^2 < 0$. The requirement for a finite non zero vev for the fields H_u^0 and H_d^0 then becomes the same conditions as in the MSSM, with μ replaced by μ_{eff} and b replaced by b_{eff}

$$(m_{H_d}^2 + |\mu_{eff}|^2)(m_{H_u}^2 + |\mu_{eff}|^2) < b_{eff}^2 \quad (7.18)$$

$$2\mu_{eff}^2 + m_{H_d}^2 + m_{H_u}^2 > 2b_{eff} \quad (7.19)$$

where,

$$\mu_{eff} = \lambda s, \quad b_{eff} = \lambda A_\lambda s. \quad (7.20)$$

Therefore EWSB can be triggered when $m_S^2 < 0$ and $m_{H_u}^2 < 0$.

Stationary points of the Higgs potential, with respect to the Higgs fields, require,

$$m_S^2 s = \frac{\lambda A_\lambda}{\sqrt{2}} v_1 v_2 - \frac{\lambda^2}{2} (v_1^2 + v_2^2) s - \frac{g_1'^2}{2} (\tilde{Q}_1 v_1^2 + \tilde{Q}_2 v_2^2 + \tilde{Q}_S s^2) \tilde{Q}_S s - \frac{\partial \Delta V}{\partial s} \quad (7.21)$$

$$\begin{aligned} m_1^2 v_1 &= \frac{\lambda A_\lambda}{\sqrt{2}} s v_2 - \frac{\lambda^2}{2} (v_2^2 + s^2) v_1 - \frac{\bar{g}^2}{8} (v_1^2 - v_2^2) v_1 \\ &\quad - \frac{g_1'^2}{2} (\tilde{Q}_1 v_1^2 + \tilde{Q}_2 v_2^2 + \tilde{Q}_S s^2) \tilde{Q}_1 v_1 - \frac{\partial \Delta V}{\partial v_1} \end{aligned} \quad (7.22)$$

$$\begin{aligned} m_2^2 v_2 &= \frac{\lambda A_\lambda}{\sqrt{2}} s v_1 - \frac{\lambda^2}{2} (v_1^2 + s^2) v_2 - \frac{\bar{g}^2}{8} (v_2^2 - v_1^2) v_2 \\ &\quad - \frac{g_1'^2}{2} (\tilde{Q}_1 v_1^2 + \tilde{Q}_2 v_2^2 + \tilde{Q}_S s^2) \tilde{Q}_2 v_2 - \frac{\partial \Delta V}{\partial v_2}, \end{aligned} \quad (7.23)$$

where $\bar{g} = \sqrt{g^2 + g'^2}$. Four of the original ten Higgs sector degrees of freedom are absorbed by the W^\pm , Z and Z' gauge bosons. Z_μ and W_μ^\pm can be defined in the same way as in the MSSM and SM in Eq. 2.26 and,

$$M_W = \frac{g}{2} v^2 \quad M_Z^2 = \frac{\bar{g}^2}{2} v^2 \quad (7.24)$$

as before.

However in the E₆SSM Z_μ does not quite coincide with a mass eigenstate. There is a mixing between Z and Z' , the boson associated with the $U(1)_N$ symmetry, with tree level mass,

$$M_{Z'}^2 = g_1'^2 v^2 (\tilde{Q}_1^2 \cos^2 \beta + \tilde{Q}_2^2 \sin^2 \beta) + g_1'^2 \tilde{Q}_S^2 s^2. \quad (7.25)$$

The mass squared mixing matrix is, in the basis (Z, Z') ,

$$M_{ZZ'}^2 = \begin{pmatrix} M_Z^2 & \Delta^2 \\ \Delta^2 & M_{Z'}^2 \end{pmatrix}, \quad (7.26)$$

where

$$\Delta^2 = \frac{\bar{g}g'_1}{2}v^2\left(\tilde{Q}_1\cos^2\beta - \tilde{Q}_2\sin^2\beta\right), \quad (7.27)$$

The eigenvalues of this matrix are

$$M_{Z_1, Z_2}^2 = \frac{1}{2}\left[M_Z^2 + M_{Z'}^2 \mp \sqrt{(M_Z^2 - M_{Z'}^2)^2 + 4\Delta^4}\right]. \quad (7.28)$$

However phenomenological constraints render this mixing negligible [244]. The mass of the extra neutral gauge boson is bounded $M_{Z'} \geq 700$ GeV [261]. These constraints require that S acquires a large vev $s \gtrsim 1.5$ TeV. This large vev implies that the first term of Eq. 7.25 is negligible and

$$M_{Z_2} \simeq M_{Z'} \approx g'_1\tilde{Q}_S s. \quad (7.29)$$

The observed quarks get their masses from, v_u and v_d in the same way as happens in the MSSM.

$$m_{u,c,t} = y_{u,c,t}v\sin\beta, \quad m_{d,s,b} = y_{d,s,b}v\cos\beta, \quad m_{e,\mu,\tau} = y_{e,\mu,\tau}v\cos\beta. \quad (7.30)$$

The remaining six degrees of freedom from the Higgs fields become the physical Higgs bosons. In the E₆SSM the physical Higgs sector consists of two charged Higgs bosons, H^\pm , a neutral CP-Odd pseudoscalar A^0 and three CP-even, neutral Higgs masses. The masses of the pseudoscalar and the charged Higgs at tree level are given by,

$$m_A^2 = \frac{\sqrt{2}\lambda A_\lambda}{\sin 2\varphi}v, \quad \tan\varphi = \frac{v}{2s}\sin 2\beta \quad (7.31)$$

$$m_{H^\pm}^2 = \frac{\sqrt{2}\lambda A_\lambda}{\sin 2\beta}s - \frac{\lambda^2}{2}v^2 + \frac{g^2}{2}v^2. \quad (7.32)$$

The three CP even Higgs masses can be found at tree level by diagonalising the mass matrix of the Higgs scalars, formed from double derivatives of the Higgs potential with respect to the Higgs fields and takes the form,

$$M^2 = \begin{pmatrix} \frac{\partial^2 V}{\partial v_1^2} & \frac{\partial^2 V}{\partial v_1 \partial v_2} & \frac{\partial^2 V}{\partial v_1 \partial s} \\ \frac{\partial^2 V}{\partial v_1 \partial v_2} & \frac{\partial^2 V}{\partial^2 v_2} & \frac{\partial^2 V}{\partial s \partial v_2} \\ \frac{\partial^2 V}{\partial v_1 \partial s} & \frac{\partial^2 V}{\partial s v_2} & \frac{\partial^2 V}{\partial^2 s} \end{pmatrix}, \quad (7.33)$$

or equivalently, noting that tadpole terms vanish, by diagonalising,

$$M^2 = \begin{pmatrix} \frac{\partial^2 V}{\partial v^2} & \frac{1}{v} \frac{\partial^2 V}{\partial v \partial \beta} & \frac{\partial^2 V}{\partial v \partial s} \\ \frac{1}{v} \frac{\partial^2 V}{\partial v \partial \beta} & \frac{1}{v^2} \frac{\partial^2 V}{\partial^2 \beta} & \frac{1}{v} \frac{\partial^2 V}{\partial s \partial \beta} \\ \frac{\partial^2 V}{\partial v \partial s} & \frac{1}{v} \frac{\partial^2 V}{\partial s \partial \beta} & \frac{\partial^2 V}{\partial^2 s} \end{pmatrix} = \begin{pmatrix} M_{11}^2 & M_{12}^2 & M_{13}^2 \\ M_{21}^2 & M_{22}^2 & M_{23}^2 \\ M_{31}^2 & M_{32}^2 & M_{33}^2 \end{pmatrix}. \quad (7.34)$$

where,

$$M_{11}^2 = \frac{\lambda^2}{2} v^2 \sin^2 2\beta + \frac{\bar{g}^2}{4} v^2 \cos^2 2\beta + g_1'^2 v^2 (\tilde{Q}_1 \cos^2 \beta + \tilde{Q}_2 \sin^2 \beta)^2, \quad (7.35)$$

$$M_{12}^2 = \left(\frac{\lambda^2}{4} - \frac{\bar{g}^2}{8} \right) v^2 \sin 4\beta + \frac{g_1'^2}{2} v^2 (\tilde{Q}_2 - \tilde{Q}_1) \times (\tilde{Q}_1 \cos^2 \beta + \tilde{Q}_2 \sin^2 \beta) \sin 2\beta, \quad (7.36)$$

$$M_{22}^2 = \frac{\sqrt{2} \lambda A_\lambda}{\sin 2\beta} s + \left(\frac{\bar{g}^2}{4} - \frac{\lambda^2}{2} \right) v^2 \sin^2 2\beta + \frac{g_1'^2}{4} (\tilde{Q}_2 - \tilde{Q}_1)^2 v^2 \sin^2 2\beta, \quad (7.37)$$

$$M_{23}^2 = M_{32}^2 = -\frac{\lambda A_\lambda}{\sqrt{2}} v \cos 2\beta + \frac{g_1'^2}{2} (\tilde{Q}_2 - \tilde{Q}_1) \tilde{Q}_S v s \sin 2\beta, \quad (7.38)$$

$$M_{13}^2 = M_{31}^2 = -\frac{\lambda A_\lambda}{\sqrt{2}} v \sin 2\beta + \lambda^2 v s + g_1'^2 (\tilde{Q}_1 \cos^2 \beta + \tilde{Q}_2 \sin^2 \beta) \tilde{Q}_S v s, \quad (7.39)$$

$$M_{33}^2 = \frac{\lambda A_\lambda}{2\sqrt{2}s} v^2 \sin 2\beta + g_1'^2 \tilde{Q}_S^2 s^2. \quad (7.40)$$

and the tree level minimisation conditions have been used to substitute soft masses m_1^2 , m_2^2 and m_S^2 .

The charginos have the same expression as for the MSSM,

$$m_{\tilde{\chi}_{1,2}}^2 = \frac{1}{2} \left[|M_2|^2 + |\mu_{eff}|^2 + 2m_W^2 \mp \sqrt{(|M_2|^2 + |\mu_{eff}|^2 + 2m_W^2)^2 - 4|\mu_{eff} M_2 - m_W^2 \sin 2\beta|^2} \right]. \quad (7.41)$$

The E₆SSM has two more neutralinos than the MSSM. This is because there is an extra gauge supermultiplet associated with $U(1)_N$, contributing a gaugino, superpartner to the Z' boson and one extra Higgs supermultiplet, contributing a Higgsino which is the superpartner of the singlet scalar Higgs that picks up vev s . These additional fields get mixed with the others and the masses of the six neutralinos must be determined

by diagonalising,

$$M_{\tilde{\chi}^0} = \begin{pmatrix} M_1 & 0 & -\frac{1}{2}g'v_1 & \frac{1}{2}g'v_2 & 0 & 0 \\ 0 & M_2 & \frac{1}{2}gv_1 & -\frac{1}{2}gv_2 & 0 & 0 \\ -\frac{1}{2}g'v_1 & \frac{1}{2}gv_1 & 0 & -\mu_{eff} & -\frac{\lambda v_2}{\sqrt{2}} & \tilde{Q}_1 g'_1 v_1 \\ \frac{1}{2}g'v_2 & -\frac{1}{2}gv_2 & -\mu_{eff} & 0 & -\frac{\lambda v_1}{\sqrt{2}} & \tilde{Q}_2 g'_1 v_2 \\ 0 & 0 & -\frac{\lambda v_2}{\sqrt{2}} & -\frac{\lambda v_1}{\sqrt{2}} & 0 & \tilde{Q}_S g'_1 s \\ 0 & 0 & \tilde{Q}_1 g'_1 v_1 & \tilde{Q}_2 g'_1 v_2 & \tilde{Q}_S g'_1 s & M'_1 \end{pmatrix}, \quad (7.42)$$

where this has been written in the basis, $(\tilde{B}, \tilde{W}_3, \tilde{H}_1^0, \tilde{H}_2^0, \tilde{S}, \tilde{B}')$ and kinetic mixing has been neglected. As usual M_1, M_2 are the masses for \tilde{B}, \tilde{W}_3 respectively, and M'_1 is the soft gaugino mass for \tilde{B}' .

As in the MSSM the gluino, the superpartner of the gluon, does not mix with any other states and has a mass at tree level which is simply, M_3 .

The sfermions which are superpartners of ordinary matter are also given by the same tree level formulae as their MSSM counterparts, except they have an extra and very significant contribution from the D-terms in the super potential.

$$\begin{aligned} m_{\tilde{u}_1, \tilde{u}_2}^2 &= \frac{1}{2} \left[m_Q^2 + m_U^2 + 2m_u^2 + \Delta_Q + \Delta_U \right. \\ &\quad \left. \mp \sqrt{(m_Q^2 - m_U^2 + \Delta_Q - \Delta_U)^2 + 4m_u^2 \left(A_u - \frac{\mu}{\tan \beta} \right)^2} \right], \end{aligned} \quad (7.43)$$

$$\begin{aligned} m_{\tilde{d}_1, \tilde{d}_2}^2 &= \frac{1}{2} \left[m_Q^2 + m_D^2 + 2m_d^2 + \Delta_Q + \Delta_D \right. \\ &\quad \left. \mp \sqrt{(m_Q^2 - m_D^2 + \Delta_Q - \Delta_D)^2 + 4m_d^2 \left(A_d - \mu \tan \beta \right)^2} \right], \end{aligned} \quad (7.44)$$

$$\begin{aligned} m_{\tilde{l}_1, \tilde{l}_2}^2 &= \frac{1}{2} \left[m_L^2 + m_E^2 + 2m_l^2 + \Delta_L + \Delta_E \right. \\ &\quad \left. \mp \sqrt{(m_L^2 - m_E^2 + \Delta_L - \Delta_E)^2 + 4m_l^2 \left(A_l - \mu \tan \beta \right)^2} \right]. \end{aligned} \quad (7.45)$$

The D-term contributions, Δ_A , to these masses now include contributions from the $U(1)_N$ symmetry. Unlike the D-terms associated with $U(1)_Y$ and $SU(2)_W$ these can be very large as they involve the s vev and s is constrained by phenomenology to be significantly larger than v .

$$\Delta_A = (T_{3A}g^2 - Q_A^Y g'^2)(v_d^2 - v_u^2) + \Delta_A^{(N)}, \quad (7.46)$$

$$\Delta_A^{(N)} = g_1'^2(Q_1 Q_i v_1^2 + Q_2 Q_i v_2^2 + Q_S Q_i s^2). \quad (7.47)$$

The exotic quarks and Inert Higgsinos get their mass from s in a similar manner to ordinary fermions obtaining mass from v_u, v_d .

$$\mu_{D_i} = \kappa_i s, \quad m_{\tilde{H}_{1,j}} = m_{\tilde{H}_{2,j}} = \lambda_j s \quad (7.48)$$

where μ_{D_i} is the mass of the exotic fermion D_i and $i = 1, 2, 3$ is a generational index. and, $m_{\tilde{H}_{1,i}}, m_{\tilde{H}_{2,i}}$ are the masses of the fermion, $\tilde{H}_{1,i}, \tilde{H}_{1,i}$ partners of the scalar Inert Higgs, where in this case generation index j only runs over the first two generations, as the third generation fields $\tilde{H}_{1,3}$ and $\tilde{H}_{1,3}$ play the role of MSSM like Higgsinos and mix in to form neutralinos in Eq. 7.42.

Their scalar super partners get masses in a manner analogous to the sfermion partners to the observed fermions,

$$m_{\tilde{D}_{1i}, \tilde{D}_{2i}}^2 = \frac{1}{2} \left[m_{D_i}^2 + m_{\bar{D}_i}^2 + 2\mu_{D_i}^2 + \Delta_D + \Delta_{\bar{D}} \right. \\ \left. \pm \sqrt{(m_{D_i}^2 - m_{\bar{D}_i}^2 + \Delta_Q - \Delta_U)^2 + 4\mu_D^2 \left(A_{\kappa_i} - \frac{\lambda v_1 v_2}{s} \right)^2} \right], \quad (7.49)$$

$$M_{H_i^d, H_i^u}^2 = \frac{1}{2} \left[m_{H_{1i}}^2 + m_{H_{2i}}^2 + 2m_{\tilde{H}_{1,i}}^2 + \Delta_{H_1} + \Delta_{H_2} \right. \\ \left. \pm \sqrt{(m_{H_{1i}}^2 - m_{H_{2i}}^2 + \Delta_{H_1} - \Delta_{H_2})^2 + 4m_{\tilde{H}_{1,i}}^2 \left(A_{\lambda_i} - \frac{\lambda v_1 v_2}{s} \right)^2} \right], \quad (7.50)$$

Chapter 8

The Non Universal Higgs Mass

E_6 SSM

The Non Universal Higgs Mass (NUHM) E_6 SSM is a version of the E_6 SSM with the GUT scale constraints reducing the number of soft SUSY breaking parameters to a universal gaugino mass ($M_{1/2}$), a universal trilinear (A), a common Higgs singlet mass (m_S^{GUT}), ‘up-type’ Higgs mass ($m_{H_u}^{GUT}$), ‘down-type’ Higgs mass ($m_{H_d}^{GUT}$), and a common scalar mass for all other E_6 SSM scalars (m_0),

$$M_i(M_X) = M_{1/2}, \quad A_i(M_X) = A, \quad m_i(M_X) = m_0 \quad (8.1)$$

$$m_{S_i}(M_X) = m_S^{GUT}, \quad m_{H_{u_i}}(M_X) = m_{H_u}^{GUT}, \quad m_{H_{d_i}}(M_X) = m_{H_d}^{GUT} \quad (8.2)$$

where M_X is defined here as the scale at which the E_6 SSM gauge couplings, g_1 and g_2 appearing in chapter 7 are equal, $g_1 = g_2$.

8.1 Motivation

In this chapter results of the first study into radiative electroweak symmetry breaking in the NUHM E_6 SSM model are presented. This study was presented in [7], proceedings for the European Physical Society Conference in 2007, but has not otherwise been published. The study was carried out as preliminary work while we were studying a

related but more tightly constrained model, the CE_6SSM . Since this was a preliminary study we only tested radiative electroweak symmetry breaking for a sample choice of those E_6SSM Yukawas and vevs which have not been determined from experimental data, so this is far from a complete survey of the model. Additionally as a preliminary study, some effects included in the more thorough study into the CE_6SSM (described in Chapter 9) were not included here. Some of these effects are surprisingly strong so the results presented in this chapter should be interpreted as qualitative rather than quantitative.

Nonetheless this study is interesting in its own right. Although the very strong high scale constraints of universal scalar masses, universal gaugino masses and universal trilinear couplings eliminates a large volume of parameter space which is not phenomenologically viable, it can also restricts parameter space which is viable and therefore such assumptions could be seen as over constraining. In addition while such universality schemes are motivated by minimal SUGRA, there are a much wider variety of SUGRA models which do not lead to these universality constraints. One interesting alternative to the CMSSM which has become popular is the Non Universal Higgs Mass MSSM [245–255]. The NUHM E_6SSM can be seen as a similar alternative to the CE_6SSM .

As described in Sec. 3.2 radiative electroweak symmetry breaking, where EWSB is triggered by the RG flow between the unification and EW scales, occurs in the CMSSM and NUHM MSSM. This is a powerful result as it shows that if SUSY breaking takes place at the TeV scale, then it is natural for EWSB to occur. It is therefore of great interest to see if the same effect is generated in the NUHM E_6SSM . If this occurs the spectrum of particle masses can be determined from the NUHM E_6SSM parameters. As shall be seen some very interesting patterns appear in the particle spectrum which could provide a testable signature for these models.

8.2 RG flow of the soft SUSY breaking terms

Below the Grand Unification scale the RG flow causes the gauge couplings and the soft SUSY breaking parameters to split from the universal values g_0 , m_0^2 , m_S^{GUT} , $m_{H_u}^{GUT}$, $m_{H_d}^{GUT}$, $M_{1/2}$ and A . This splitting is described by the Renormalisation Group Equations (RGE) of the model.

The RGE of the E_6 SSM, derived for these projects by Dr Roman Nevzorov, appear in Appendix C. As this work was carried out earlier than that described in Chapter 9 only two loop beta functions for the SUSY preserving E_6 SSM parameters were available. All soft SUSY breaking parameters were evolved with the one loop RGE.

The complete set of E_6 SSM RGE can be separated into two sectors. The first sector describes the evolution of gauge and Yukawa coupling constants. The corresponding set of equations is nonlinear even in the one-loop approximation. Therefore it is extremely difficult or even impossible to find either exact or approximate solutions of these equations. The remaining subset of RGE describes the running of fundamental parameters which break SUSY in a soft way. If the renormalisation group flow of the gauge and Yukawa couplings is known this part of the RG equations can be considered as a set of linear differential equations for the soft SUSY breaking terms. To solve this set of equations, first one integrates out the equations for the gaugino masses M_i . In the one-loop approximation we get

$$M_i(t) = \frac{g_i^2(t)}{g_0^2} M_{1/2}, \quad M'_1(t) = \frac{g_1'^2(t)}{g_0^2} M_{1/2}, \quad (8.3)$$

where index i runs from 1 to 3, while M_3 , M_2 , M_1 and M'_1 as defined in Sec. 7.2.2 and $t = \ln \frac{Q}{M_X}$, Q being the renormalisation scale at which Eq. 8.3 holds true.

Next one integrates the one-loop renormalisation group equations for the trilinear scalar couplings $A_i(t)$ which can be written as follows

$$\frac{dA_i(t)}{dt} = S_{ij}(t)A_j(t) + F_i(t). \quad (8.4)$$

The dependence of F_i on t comes from the gaugino masses appearing in the one loop RGE of the trilinears. One then finds the solution of this system of linear differential

equations,

$$A_i(t) = \Phi_{ij}(t)A_j(0) + \Phi_{ik}(t) \int_0^t \Phi_{kj}^{-1}(t')F_j(t')dt', \quad (8.5)$$

where we have introduced $\Phi_{ij}(t)$, which is the solution the homogeneous equation $d\Phi_{ij}(t)/dt = S_{ik}(t)\Phi_{kj}(t)$, with the boundary conditions $\Phi_{ij}(0) = \delta_{ij}$. From the universality constraint and exploiting Eq. 8.3 to write $F_i(t) \propto M_{1/2}$, the solution of RG equations for the trilinear scalar couplings takes the form,

$$A_i(t) = e_i(t)A + f_i(t)M_{1/2}. \quad (8.6)$$

The obtained solution Eq. 8.6 can be substituted into the right-hand sides of the RG equations for the soft scalar masses which may be presented in the following form,

$$\frac{dm_i^2(t)}{dt} = \tilde{S}_{ij}(t)m_j^2(t) + \tilde{F}_i(t). \quad (8.7)$$

Due to the scalar mass universality constraints and the fact that the functions $\tilde{F}_i(t)$ contain terms which are proportional to A^2 , $AM_{1/2}$, and $M_{1/2}^2$ the solution of the linear system of differential Eq. 8.7 reduces to,

$$\begin{aligned} m_i^2 &= \alpha_i(t)M_{1/2}^2 + \beta_i(t)A^2 + \gamma_i(t)AM_{1/2} + \delta_i(t)m_0^2 \\ &+ \epsilon_i(t)m_S^{GUT2} + \rho_i(t)m_{H_u}^{GUT2} + \zeta_i(t)m_{H_d}^{GUT2}. \end{aligned} \quad (8.8)$$

The functions, $\alpha_i(t)$, $\beta_i(t)$, $\gamma_i(t)$, $\delta_i(t)$, $\epsilon_i(t)$, $\rho_i(t)$, $\zeta_i(t)$, which determine the evolution of $m_i^2(t)$ and also $e_i(t)$ and $f_i(t)$ for $A_i(t)$, remain unknown, since an exact analytic solution to the full set of E₆SSM renormalisation group equations is unavailable. These functions are strongly dependent on the values of the Yukawa coupling at the Grand Unification scale M_X . At the SUSY breaking scale, M_S , where $t = t_0 = \ln \frac{M_S}{M_X}$, the relations shown in Eq. 8.3, Eq. 8.6 and Eq. 8.8 give the dependence of gaugino masses, trilinear scalar couplings and soft scalar masses on their initial values at the Grand Unification scale.

The RG flow of the soft SUSY breaking terms also depend on the gauge couplings. We find that the running of $g_i(\mu)$ changes dramatically after the inclusion of two-loop effects. In particular, in the one-loop approximation the β function of strong interactions vanishes so $g_3(t)$ would be constant in the one-loop approximation. The vanishing

of the beta function for g_3 also lead to a constant $M_3(t) = M_{1/2}$. Unfortunately as a consequence the two loop contributions to the gaugino masses, not included in this study, are also very large, changing low energy gaugino masses by as much as 20–40%. This is one reason why the results in this chapter can only be considered qualitative.

8.3 Electroweak Constraints

As a test case we chose the new E₆SSM Yukawas and vevs to be,

$$\lambda_3(M_{GUT}) = 0.6, \quad \lambda_{1,2}(M_{GUT}) = 0.46, \quad \kappa_{1,2,3}(M_{GUT}) = 0.162 \quad (8.9)$$

$$\tan \beta = v_u/v_d = 10, \quad s = 3 \text{ TeV} \quad (8.10)$$

with $v^2 = v_u^2 + v_d^2 = (174\text{GeV})^2$ fixed from experiment. The third generation Yukawas h_t , h_b and h_τ are fixed at the electroweak scale by the masses of the top, bottom and τ fermions respectively, using the tree level relations given in Eq. 7.30. The gauge couplings g_1 , g_2 and g_3 are also fixed at the electroweak scale from the experimentally measured values of α_e , $\sin \theta_W$ and α_S . A full set of Yukawas and gauge couplings at the unification scale M_X , consistent with both these EW and M_X constraints, is then found by evolving between the two scales until a stable solution is reached.

Due to the RG flow described in the previous section all low energy soft masses of the E₆SSM can be written in terms of the NUHM E₆SSM GUT scale parameters, as shown in Eq. 8.3, Eq. 8.6 and Eq. 8.8. The dimensionless coefficients appearing in these equations can then be determined numerically by evolving between the unification scale and the EW scale and selectively switching soft GUT scale parameters to zero. This RGE evolution was performed using a version of SOFTSUSY 2.0.5 [181] which we modified to include the E₆SSM RGEs. The EWSB constraints shown in Eq. 7.23 fix the three third generation Higgs masses (m_{H_u} , m_{H_d} and m_S) at the EW scale in terms of the Yukawas, gauge couplings, vevs and A_{λ_3} . Since all vevs and SUSY preserving parameters were either set to their observed values or already chosen, the Higgs masses can be written as functions of A and $M_{1/2}$ after using the RGE solutions to substitute

for A_{λ_3} . This gives,

$$m_{H_d}^2 = p_1 M_{1/2} + q_1 A + h_1 + \Delta_d^{(1)}, \quad (8.11)$$

$$m_{H_u}^2 = p_2 M_{1/2} + q_2 A + h_2 + \Delta_u^{(1)}, \quad (8.12)$$

$$m_S^2 = p_3 M_{1/2} + q_3 A + h_3 + \Delta_s^{(1)}, \quad (8.13)$$

where the one loop contributions, $\Delta_d^{(1)}$, $\Delta_u^{(1)}$ and $\Delta_s^{(1)}$, introduce a more complicated dependence on the soft parameters.

So if the one loop contributions are initially neglected, for each of the Higgs masses we have two constraints which may be equated leaving three low energy constraints and six unification scale parameters. For all choices of $M_{1/2}$, A and m_0 we can then determine what values of $m_{H_d}^2$, $m_{H_u}^2$ and m_S^2 are required to satisfy the constraints.

The rest of the soft mass spectrum can then be determined from Eq. 8.3, Eq. 8.6 and Eq. 8.8 using the coefficients which have been determined numerically. Then the physical masses of the stops and the exotic colored objects are calculated from their tree level relations, Eq. 7.43 and Eq. 7.49 respectively, and their contribution to the one loop effective potential are determined. The leading one loop corrections are then added to Eq. 8.13, and finally the soft mass parameters and particle spectrum are solved iteratively.

In this study the particle spectrum was calculated using the tree level approximations presented in Sec. 7.3. No loop corrections were added to the light Higgs mass as this was not used in constraining the model. Given the large values for soft Higgs parameters and the heavy spectra (particularly stop masses) it seems reasonable to assume that the LEP limit on the light Higgs mass would be evaded in these scenarios and would not restrict our solutions. In addition, since this study was qualitative rather than quantitative, a precise determination of the Higgs mass required to test against the LEP bound seems unrealistic. However it is clear that a full study should include this as a constraint. In addition the gluino mass was only calculated using the very simple tree level expression ($m_{\tilde{g}} = M_3$), though it is also well known that this quantity is also subject to large radiative corrections. This does affect the restrictions on the parameter space, and once again stresses that this is merely a qualitative study.

Finally experimental constraints were applied. We required that charginos were heavier than 100 GeV, neutralinos heavier than 45 GeV, gluinos heavier than 300 GeV, and that the squarks and sleptons of ordinary matter are heavier than 100 GeV. For the exotic quarks and squarks we imposed a lower bound of 300 GeV, to evade HERA constraints on the Leptoquarks [262].

The LEP bound on the light Higgs does not apply to the Inert Higgs bosons as they do not develop vevs and therefore have no HZZ coupling for production via Higgsstrahlung. However they still have HHZ couplings which are fixed by gauge interaction and this means that the charged Inert Higgs bosons (which are degenerate in mass with the neutral Inert Higgs bosons) can be bounded by searches for charged Higgs bosons from LEP [256] and similarly the masses of the Inert Higgsinos can be bounded from below by searches for charginos. To evade these constraints we require that the Inert Higgs and Inert Higgsinos must be heavier than 100 GeV.

8.4 Results

The values obtained for this sample set of SUSY preserving parameters are shown in Fig.8.1(a-c) with the large white regions ruled out by GUT scale tachyons when $(m_{H_d}^{GUT})^2 < 0$, $(m_{H_u}^{GUT})^2 < 0$ or $(m_S^{GUT})^2 < 0$ respectively. From (a) all parameter space accessible at future colliders with $M_{1/2} > 0$ is excluded, but $M_{1/2} < 0$ is valid in our scheme¹. Fig. 8.1(b) and (c) exclude some additional points with $M_{1/2} > 0$. Fig. 8.1(d) shows the combined exclusion region from (a-c) and also a large region of parameter space ruled out by EW scale tachyons and a small slice ruled out by experiment.

The soft Higgs masses at the unification scale are typically much heavier than m_0 and there tends to be some hierarchy amongst them. Indeed none of the points scanned over exhibited a universal scalar Higgs mass, even allowing for it to be very different from m_0 . This indicates the strength of the condition in the CE₆SSM where a full

¹In chapter 9 conventions are chosen such that $M_{1/2} > 0$. This isn't done here but one can perform the transformation, $A \rightarrow -A$, $M_{1/2} \rightarrow -M_{1/2}$, $s \rightarrow -s$, to obtain solutions with $M_{1/2} > 0$.

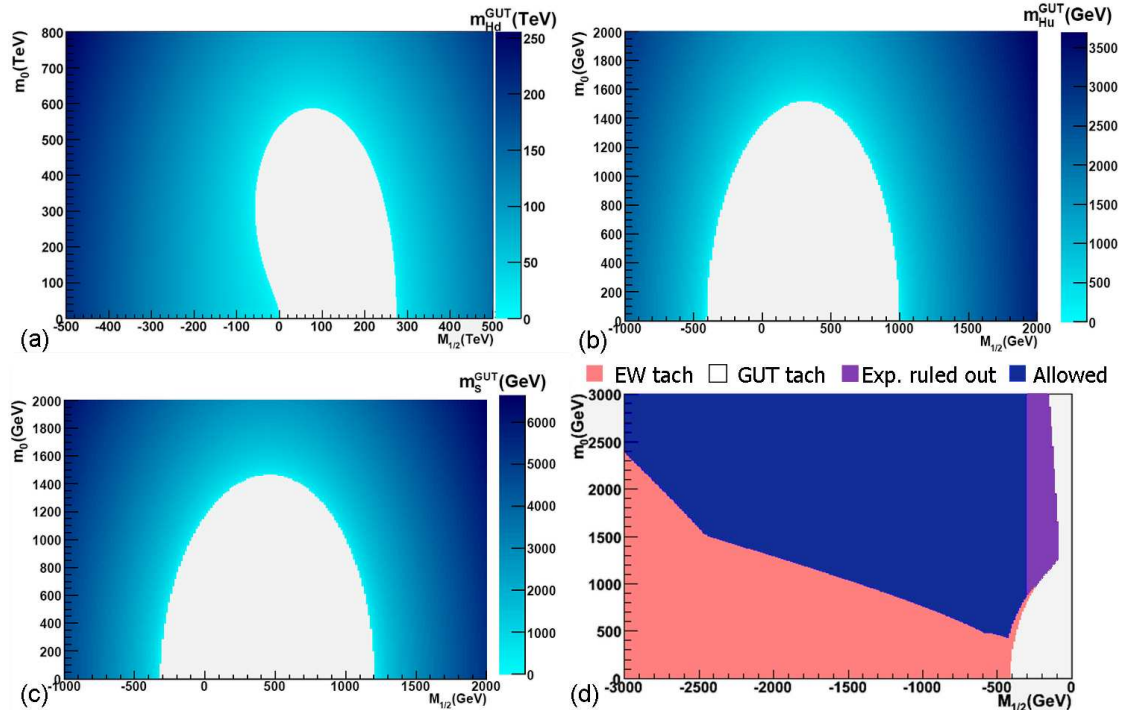


Figure 8.1: EWSB exclusion plots in the m_0 , $M_{1/2}$ plane, with $A = -300$ GeV. (a): $m_{H_d}^{GUT}$ values consistent with the EWSB and NUHM E_6 SSM boundary conditions. The white region is ruled out since $(m_{H_d}^{GUT})^2 < 0$. (b): As (a) but for $m_{H_u}^{GUT}$. (c): As (a) but for m_S^{GUT} . (d): Full exclusion plot. The blue (black) region shows the allowed region of the parameter space, the purple (dark grey) region is ruled out by searches for the charginos and gluinos, while the pink (light grey) and white regions are ruled out by EW and GUT scale tachyons respectively.

universality of scalar masses is imposed.

While EWSB provides strong constraints on the NUHM E_6 SSM, there is a large volume of parameter space which may be physically realised and could be discovered at the LHC. The low energy spectra do have the challenging feature of heavy squarks and sleptons but also have some very interesting phenomenological features. A sample spectrum which might be observed is shown in Fig. 8.2. The presence of the exotic colored particles ($\tilde{D}_{1,2}$ and D) and the new Z' boson at low energies provide interesting experimental signatures for the model. In the spectrum shown, the presence of \tilde{D}_1 at just above 500 GeV offers a tantalising glimpse at what exciting phenomenology may

be discovered at the LHC if nature has chosen this kind of model.

In addition there is a hierarchy in the spectra. The gluino is lighter than most of the squarks, which is unusual and phenomenologically interesting as it affects cascade decays. This is a result of the renormalisation group (RG) running of the soft masses in the E_6 SSM and is typical of points we have looked at in the NUHM E_6 SSM. The smaller the hierarchy amongst the GUT scale soft parameters, the stronger this effect. This also foreshadows results which will be presented in chapter 9. In addition the lightest chargino is lighter than the gluino and the lightest neutralino is lighter still. These features are also due to the RG flow and it would be very challenging if not impossible to find spectra without this hierarchy.

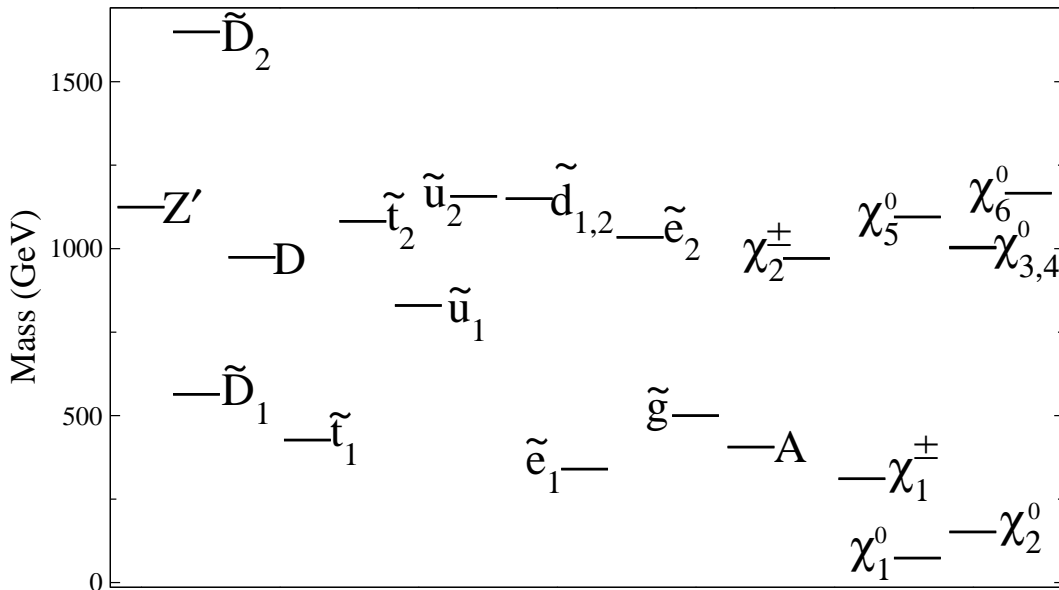


Figure 8.2: A sample NUHM E_6 SSM spectrum that could be seen at the LHC. The soft mass parameters for this point are $m_0 = 600$ GeV, $M_{1,2} = -500$ GeV, $A = -300$ GeV, $m_S^{GUT} = 2.39$ TeV, $m_{H_u}^{GUT} = 2.25$ TeV & $m_{H_d}^{GUT} = 922$ GeV

8.5 Conclusions

In this chapter a qualitative exploration of a small portion of the NUHM E_6 SSM parameter space has been performed. This is the first time any such spectra has been

produced for any version of the E_6 SSM with universality constraints imposed at the unification scale.

For our benchmark choice of E_6 SSM Yukawas and vevs there is no solution with all universal scalar masses at the GUT scale. Indeed the soft GUT scale Higgs masses are generally required to be significantly larger than m_0 for electroweak symmetry breaking to take place, and this feature may be regarded as somewhat disappointing. In addition the spectrum is a little heavy and it may be challenging to detect. Nonetheless we presented a spectra with exotic colored objects ≈ 500 GeV, demonstrating the exciting prospect of such a discovery at the LHC. In addition there is another striking feature of the model. There is clear hierarchy in the spectra. The exotics, squarks, and sleptons are typically significantly heavier than the lighter elements of the gaugino sector. In particular the RG flow implies that the gluino is often lighter than the squarks.

Despite the lack of precision in the study, striking phenomenological features of the model have been uncovered that are generic and should be stable to improvements in the accuracy of the calculations. In addition because these features are driven by the RG flow it is likely that they apply to a wider class of models than just the NUHM E_6 SSM.

This will be seen explicitly when a more thorough study of the CE_6 SSM is provided in the next chapter.

Chapter 9

The Constrained E_6 SSM

The Constrained Exceptional Supersymmetric Standard Model (CE₆SSM) is introduced and studied in this chapter. The model is defined by applying high scale universality constraints to the low energy phenomenological model the E₆SSM, specified in Chapter 7.

These constraints require that at the high scale, M_X , all scalars masses are given by a single flavour diagonal mass, m_0 ; all gaugino masses are specified by a mass $M_{1/2}$ and a single coupling A specifies all trilinear couplings, a_{ijk} through the relation, $a_{ijk} = A y_{ijk}$. So,

$$M_i(M_X) = M_{1/2}, \quad A_i(M_X) = A, \quad m_i(M_X) = m_0. \quad (9.1)$$

As in Chapter 8 M_X is defined as the scale at which the E₆SSM gauge couplings, g_1 and g_2 are equal, $g_1 = g_2$.

9.1 RG flow of the soft SUSY breaking terms

As with the NUHM version of the E₆SSM, the soft SUSY breaking parameters and gauge couplings split from the unified values m_0^2 , $M_{1/2}$, A and g_0 at M_X when evolved to lower energies using the E₆SSM RGE. One loop semi-analytical solutions can be

found for these equation at energies below M_X in a similar manner to that described in Sec. 8.2. The solutions to the gaugino masses, M_i and the trilinear couplings A_i are of the same form,

$$M_i(t) = \frac{g_i^2(t)}{g_0^2} M_{1/2}, \quad M'_1(t) = \frac{g_1'^2(t)}{g_0^2} M_{1/2}, \quad A_i(t) = e_i(t)A + f_i(t)M_{1/2}. \quad (9.2)$$

and again $t = \ln Q/M_X$. For the scalar masses the new more restrictive boundary condition at M_X , in which all scalar masses are take a single unified value, yields the shorter expression,

$$m_i^2(t) = a_i(t)m_0^2 + b_i(t)M_{1/2}^2 + c_i(t)AM_{1/2} + d_i(t)A^2. \quad (9.3)$$

As before the functions $e_i(t)$, $f_i(t)$, $a_i(t)$, $b_i(t)$, $c_i(t)$, and $d_i(t)$, which determine the evolution of $A_i(t)$ and $m_i^2(t)$, are unknown, since an exact analytic solution of the E_6 SSM renormalisation group equations has not been derived.

The sensitivity of these functions to the Yukawa and gauge couplings at M_X is again very strong. In particular it is important to reiterate that the one-loop beta function for the gauge coupling of strong interactions is zero. So the running of g_3 and M_3 is dictated solely by the two loop contributions and these two loop beta functions can change the RG flow substantially. In this study the two loop beta functions for the gaugino masses and trilinear couplings were included. The solution of two loop RG equations for the $M_i(t)$ can be written as follows:

$$M_i(t) = p_i(t)A + q_i(t)M_{1/2}. \quad (9.4)$$

One can see that in the two loop approximation gaugino masses depend not only on the universal gaugino mass, $M_{1/2}$, but also on the trilinear scalar coupling, A . The numerical calculations show that the dependence of $M_i(t)$ on A is rather weak, i.e. $p_i(t_0) \ll 1$. However the change in the co-efficient $q_i(t)$ is substantial and at low-energies the gaugino masses changes by 20-40%.

The general form of the solutions of RG equations for $m_i^2(t)$ and $A_i(t)$ remain intact after the inclusion of two loop effects. At the same time some of the coefficient functions $f_i(t)$, $b_i(t)$ and $c_i(t)$ change significantly. The two loop corrections to the β functions

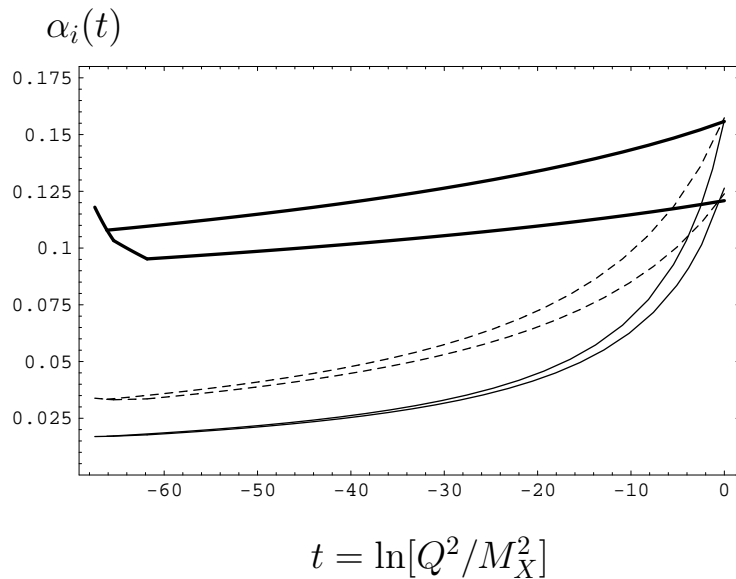


Figure 9.1: Two-loop RG flow of gauge couplings within the E_6 SSM for $T_{MSSM} = T_{ESSM} = M_t = 175$ GeV (upper lines) and $T_{MSSM} = 250$ GeV, $T_{ESSM} = 1500$ GeV (lower lines). Here we fix $\tan\beta = 10$ and $\alpha_3(M_Z) = 0.118$.

have the strongest impact on the RG flow of the soft SUSY breaking terms which are sensitive to the strong interactions.

The RG flow of the gauge couplings, $g_i(t)$, is also quite sensitive to threshold effects. In Fig. 9.1 the running of $\alpha_i(t)$ is presented for two different sets of threshold scales, $T_{MSSM} = T_{ESSM} = 175$ GeV and $T_{MSSM} = 250$ GeV, $T_{ESSM} = 1500$ GeV. The threshold T_{MSSM} is a common scale for the particles of ordinary matter, while T_{ESSM} is a common mass scale for new exotic particles not present in the MSSM. The unified gauge coupling at the M_X changes from 1.24 to 1.4 when these thresholds are changed in this way. This result and also the value of the g_0^2 for several other sets of thresholds, T_{MSSM} and T_{ESSM} , are summarised in Table 9.1.

Since soft SUSY breaking terms depend very strongly on the values of the gauge couplings at the Grand Unification scale, the uncertainty related with the choice of the threshold scales limits the accuracy of our calculations of the particle spectrum. The results of our numerical analysis presented in Table 9.1 and Fig. 9.1 indicate that it is unrealistic to expect an accuracy, in the calculation of the sparticle masses, better than 10%.

T_{MSSM} (GeV)	250	250	250	175	175	175
T_{ESSM} (GeV)	1500	800	250	1500	250	175
g_0^2	1.54	1.60	1.78	1.61	1.88	1.96
M_X (GeV)	$3.5 \cdot 10^{16}$	$3.3 \cdot 10^{16}$	$3.5 \cdot 10^{16}$	$3.7 \cdot 10^{16}$	$4 \cdot 10^{16}$	$4 \cdot 10^{16}$

Table 9.1: The dependence of g_0^2 and M_X on the threshold effects in the exceptional SUSY model. Here we fix $\tan\beta = 10$ and $\alpha_3(M_Z) = 0.118$.

9.2 RG flow of the SUSY preserving sector

To start our analysis we fix effective threshold scales associated with the SUSY and exotic particles as well as the value of $\tan\beta$. Thresholds are used only in the SUSY preserving sector where full two loop RGE are employed and are neglected in the soft SUSY breaking sector where only one loop RGE are used for the scalar masses. The thresholds are chosen before the spectrum is determined and are therefore only an estimate. A more accurate analysis is left for a further study. We chose $T_{MSSM} = 600$ GeV and $T_{ESSM} = 3$ TeV to be the mass scale of the unobserved particles of the MSSM and the new exotic objects in the E_6 SSM respectively, based on studies of the NUHM version and preliminary results for the CE_6 SSM where relatively heavy spectra were observed.

Experimental data is entered at low energies and then the SUSY preserving parameters are evolved up to the unification scale, M_X , using two-loop RG equations. At M_X high scale boundary conditions for the new Yukawas are imposed. An iteration is then performed to find a solution consistent with both sets of boundary conditions. The detail of this procedure is described below.

The gauge couplings are fixed using the experimentally measured values at M_Z . Below the mass of the top quark $SU(2)_W \otimes U(1)_Y$ is broken, therefore between M_Z and m_t the beta functions for QED and QCD are employed to evolve the gauge couplings. A routine to do this is already present in SOFTSUSY 2.0.5 [181] and this was employed

here. At m_t boundary conditions are used to relate the QED and QCD gauge couplings to the gauge couplings of the SM. For each fixed $\tan\beta$ one can find the values of the Yukawa couplings at the electroweak scale using the relation between the running masses of the fermions of the third generation and vevs of the Higgs fields, i.e.

$$\begin{aligned} m_t(M_t) &= \frac{h_t(M_t)v}{\sqrt{2}} \sin\beta, & m_b(M_t) &= \frac{h_b(M_t)v}{\sqrt{2}} \cos\beta, \\ m_\tau(M_t) &= \frac{h_\tau(M_t)v}{\sqrt{2}} \cos\beta. \end{aligned} \tag{9.5}$$

Between m_t and T_{MSSM} the Standard Model RGE which appear in [257] are employed. At T_{MSSM} further boundary conditions are used to relate the Standard model Yukawas and gauge couplings to those of the MSSM. The two loop MSSM beta functions and routines in SOFTSUSY 2.0.5 are then used to evolve between T_{MSSM} and T_{ESSM} . Finally another set of boundary conditions are used to relate the gauge and Yukawa couplings of the MSSM to those of the E_6SSM . The values of the E_6SSM gauge and Yukawa couplings then form a low energy boundary condition for what follows.

The one loop beta functions of the E_6SSM gauge couplings are used to provide a first estimate for the unification scale, M_X , when $g_1 = g_2$. The two loop RGE of the E_6SSM (shown in Appendix C) are used to run the E_6SSM gauge and Yukawa couplings to this estimate of the unification scale. At M_X the chosen high scale values of the new Yukawa couplings λ_i and κ_i are set, and g'_1 is set equal to g_1 and g_2 . The choice of new Yukawas at M_X and the relation $g'_1 = g_1$ form our high scale boundary conditions. The following improved estimate of the scale M_X is then made, based on a routine used in SOFTSUSY 2.0.5.

Defining $t_Q = \ln \frac{Q}{M_Z}$, where Q is the renormalisation scale, a Taylor expansion in t_Q is performed using,

$$g_i(t_Q) = g_i(t_{M_X}) + (t_{M_X} - t_Q) \frac{dg_i}{dt}. \tag{9.6}$$

$$\Rightarrow M_X = Q \exp\left(\frac{g_2(Q) - g_1(Q)}{\beta(g_1)|_Q - \beta(g_2)|_Q}\right). \tag{9.7}$$

where $dg_i/dt = \beta(g_i)$ has been used to replace the derivatives with two loop beta functions. Since two loop beta functions are used, this linear approximation improves on the initial one loop estimate.

An iteration between successively improved estimates of M_X and T_{ESSM} is then performed until convergence is reached. When the iteration is complete the value of all Yukawas and gauge couplings, consistent with unification of the gauge couplings, the low energy constraints from experiment and our choice of $\tan\beta$, are obtained.

9.3 Low Energy Constraints

Now the work in the previous two sections is combined. Semi-analytical expressions for the soft masses at the scale T_{ESSM} are determined as follows. First at the unification scale we set $A = M_{1/2} = 0$ while setting m_0 to some arbitrary non-zero value (in this case 1). The soft masses are RG evolved (using a modified version of SOFTSUSY 2.0.5) down to the low energy scale T_{ESSM} . Eq. 9.3 is then used to fix the coefficients $a_i(t)$, where $t = \ln[T_{ESSM}/M_X^2]$. Similarly unification scale constraints of $m_0 = M_{1/2} = 0$, with A set to a non-zero value and $m_0 = A = 0$, with $M_{1/2}$ set to a non-zero value, are used to fix the two sets of coefficients $\{d_i(t), e_i(t), p_i(t)\}$ and $\{b_i(t), f_i(t), q_i(t)\}$ respectively using Eq. 9.3, Eq. 9.4 and Eq. 9.2.

Once this procedure is carried out all the coefficients $a_i(t)$, $b_i(t)$, $c_i(t)$, $c_i(t)$, $e_i(t)$, $f_i(t)$, $p_i(t)$, and $q_i(t)$ for $t = \ln[T_{ESSM}/M_X^2]$ are known, yielding semi-analytic expressions for all soft mass parameters at T_{ESSM} . As a result all soft scalar masses, trilinear scalar couplings and gaugino masses are determined by $M_{1/2}$, A and m_0^2 only.

This set of low energy constraints on the soft masses are then combined with the tree level low energy EWSB constraints appearing in Eq. 7.23. This leaves three constraints and three soft mass parameters. Two of the equations can be used to eliminate $M_{1/2}$ and m_0 , leaving one quartic equation for one unknown, A . This equation is solved numerically, and the resultant value for A is used to obtain $M_{1/2}$ and m_0 . For fixed values of gauge couplings, Yukawas and vevs, (determined from choices of $\tan\beta$ and s with v known from experiment) there are four sets of soft masses A , $M_{1/2}$ and m_0 . Usually two of the solutions are complex and two are real, but four real or four complex solutions cannot be ruled out. Therefore our routine deals with between 0 and 4 sets

of real solutions to the soft masses.

With a tree level solution for A , $M_{1/2}$ and m_0 determined, the tree level spectrum of masses can be calculated. Leading one loop contributions to the effective potential from stop masses are added and an improved estimate of the electroweak symmetry breaking conditions is made. For the CE₆SSM only stop mass contributions from the one loop contribution to the effective potential are used. This is firstly because we observed during the project on the NUHM E₆SSM that such contributions are small (contributing $\lesssim 5\%$) in comparison to our target accuracy of around 10%. Secondly for higher order contributions to the light Higgs mass (see mass spectra calculations, below) we only included the top-stop sector, so for consistency it was necessary to drop the exotic contributions from the tadpoles.

The stop corrections lead to improved estimates of the three soft mass parameters and then the stop masses themselves can be recalculated to improved accuracy. For each set of tree level solutions an iteration is then performed until stable values for the soft masses are obtained. Finally the mass spectrum is determined and compared with experimental constraints.

The mass spectra are calculated using the tree level expressions given in Sec. 7.3. For the CP-even higgs masses, leading one loop corrections from the effective potential are added. These contributions are listed in Appendix D. However, after a detailed study of the mass spectra for benchmark points, it became apparent that the light Higgs mass could be in conflict with the LEP limit for certain points and that leading two loop corrections were also needed for a reliable estimate.

For approximate two loop corrections we used the expression which appeared in [4] and is a simple generalisation of results in [258,259],

$$m_h^2 \lesssim \left[\frac{\lambda^2}{2} v^2 \sin^2 2\beta + M_Z^2 \cos^2 2\beta + \frac{M_Z^2}{4} \left(1 + \frac{1}{4} \cos 2\beta \right)^2 \right] \times \left(1 - \frac{3h_t^2}{8\pi^2} l \right) + \frac{3h_t^4 v^2 \sin^4 \beta}{8\pi^2} \left\{ \frac{1}{2} U_t + l + \frac{1}{16\pi^2} \left(\frac{3}{2} h_t^2 - 8g_3^2 \right) (U_t + l) l \right\}, \quad (9.8)$$

where $U_t = 2 \frac{X_t^2}{M_S^2} \left(1 - \frac{1}{12} \frac{X_t^2}{M_S^2} \right)$ and $l = \ln \left[\frac{M_S^2}{m_t^2} \right]$.

At tree level the CP-odd pseudoscalar, A and the charged H^\pm Higgs bosons are quasi degenerate in mass with one of the heavier CP-even Higgs (h_2 or h_3). This is assumed to be maintained at the one loop level.

Since it is known that corrections to the gluino mass can be large in the MSSM, we included the one loop contribution to the gluino from the gluon-gluino loops and quark-squark loops, where only quarks and squarks of ordinary matter are included. The contribution from the exotic particles were neglected as preliminary studies suggested they were heavy. With the exotic contributions neglected the gluino correction are the same as those for the MSSM, which have been presented in e.g. [180] and are already present in SOFTSUSY 2.0.5. We use the gluino corrections adapted from SOFTSUSY 2.0.5. In our approximation the gluino mass is evaluated at the E_6 SSM threshold T_{ESSM} as this is where the RG evolution is halted. These corrections are then given by,

$$m_{\tilde{g}} = M_3(T_{ESSM})[1 + \Delta_{\tilde{g}}(T_{ESSM})] \quad (9.9)$$

where

$$\begin{aligned} \Delta_{\tilde{g}}(Q) = & \left(\frac{g_3(Q)}{4\pi} \right)^2 \left[15 + 9 \ln \frac{Q^2}{M(Q)^2} - \sum_q \sum_{i=1}^2 B_1(M_3(Q), m_q, m_{\tilde{q}_i}, Q) \right. \\ & \left. - \sum_{q=t,b} \frac{m_q}{M_3(Q)} \sin(2\theta_q) (B_0(p, m_q, m_{\tilde{q}_1}, Q) - B_0(p, m_q, m_{\tilde{q}_2}, Q)) \right] \quad (9.10) \end{aligned}$$

where the term on the bottom line is only included for the third generation, as mixing, given by the squark mixing angle θ_q , in the first two generations is negligible. The functions B_0 and B_1 are the Passarino-Veltman functions [260] with the divergent part removed using *modified Dimensional Reduction* (\overline{DR}) and may be expressed as [180],

$$B_0(p, m_1, m_2) = -\ln \left(\frac{p^2}{Q^2} \right) - f_B(x_+) - f_B(x_-) \quad (9.11)$$

$$B_1(p, m_1, m_2) = \frac{1}{2p^2} \left[A_0(m_2) - A_0(m_1) + (p^2 + m_1^2 - m_2^2) B_0(p, m_1, m_2) \right] \quad (9.12)$$

$$A_0(m) = m^2 \left[1 - \ln \frac{m^2}{Q^2} \right]. \quad (9.13)$$

and

$$f_B(x) = \ln(1-x) - x \ln(1-x^{-1}) - 1 \quad (9.14)$$

$$x_{\pm} = \frac{s \pm \sqrt{s^2 - 4p^2(m_1^2 - i\varepsilon)}}{2p^2} \quad s = p^2 - m_2^2 + m_1^2 \quad (9.15)$$

The experimental constraints applied in our analysis are, $m_h \geq 114$ GeV, all sleptons and charginos are heavier than 100 GeV, all squarks and gluinos have masses above 300 GeV and Z' boson has a mass which is larger than 700 GeV [261]. We also impose the most conservative bound on the masses of exotic quarks and squarks that comes from the HERA experiments [262]. We assume that our exotic quarks and squarks are heavier than 300 GeV. Finally we require that the Inert Higgs and Inert Higgsinos are heavier than 100 GeV to evade limits on Higgsinos and charged Higgs from LEP, as described in the previous chapter.

In addition to a set of bounds coming from the non-observation of new particles at the experiment we impose a few theoretical constraints. We require that the lightest supersymmetric particle should be a neutralino. We also restrict our consideration by the values of the Yukawa couplings $\lambda_i(M_X)$, $\kappa_i(M_X)$, $h_t(M_X)$, $h_b(M_X)$ and $h_{\tau}(M_X)$ less than 3 to ensure the applicability of perturbation theory up to the Grand Unification scale.

9.4 Results

9.4.1 Exclusion Plots

In our exploration of the CE_6SSM parameter space we looked at scenarios with a universal coupling between exotic colored superfields and the third generation singlet field \hat{S} , $\kappa(M_X) = \kappa_{1,2,3}(M_X)$ and fixed the Inert Higgs couplings $\lambda_{1,2}(M_X) = 0.1$. In fixing $\lambda_{1,2}$ like this we are deliberately pre-selecting for relatively light Inert Higgsinos. The third generation Yukawa $\lambda = \lambda_3$ was allowed to vary along with κ . Splitting λ_3 from $\lambda_{1,2}$ seems reasonable since λ_3 plays a very special role in E_6SSM models in forming the effective μ -term when S picks up a vev.

For fixed values of $\tan\beta = 3, 10, 30$, we scan over s, κ, λ . From these input param-

eters, the sets of soft mass parameters, A , $M_{1/2}$ and m_0 which are consistent with the correct breakdown of electroweak symmetry are found.

We find that for fixed values of the Yukawas the soft mass parameters scale with s . While for fixed s , varying the Yukawas, λ and κ then produces a region of allowed points, as is shown in Figs. 9.3, 9.5 and 9.7, for $(\tan\beta, s)$ values $(10, 3 \text{ TeV})$, $(30, 3 \text{ TeV})$ and $(3, 4 \text{ TeV})$ respectively, with the allowed regions in green and the excluded regions in white. We find that for fixed $\tan\beta$ there is a lower limit on the ratio

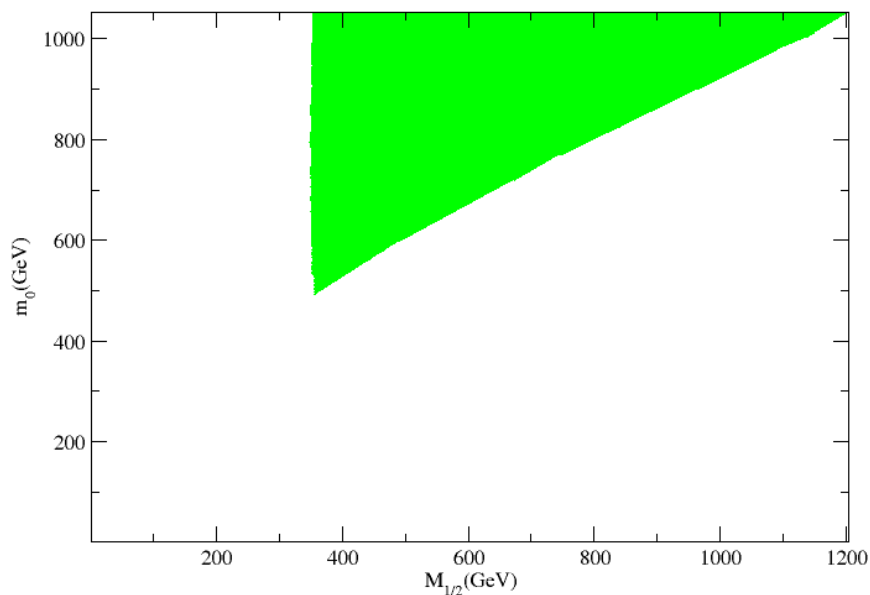


Figure 9.2: Physical solutions with $\tan\beta = 10$ which pass experimental constraints from LEP and Tevatron data. On the left hand side of the allowed region the chargino mass is less than 100 GeV, while underneath and on the lower right quadrant the Inert Higgs are less than 100 GeV or becoming tachyonic.

$m_0/M_{1/2}$ which is a weak function of the singlet vev s . For example consider Fig. 9.2. The region to the left of the allowed space is ruled out by the lightest chargino mass being $< 100 \text{ GeV}$, while the lower right region is ruled out by Inert Higgs bosons with masses below experimental bounds or tachyonic Inert Higgs masses. This boundary

implies that for $\tan\beta = 10$, over the allowed ranges shown, $m_0/M_{1/2}$ varies from ≈ 1.4 to ≈ 0.8 .

This boundary can be understood as follows. For fixed m_0 , maximising $M_{1/2}$ requires the singlet vev s to be increased, as well as varying the Yukawas, λ and κ . However the squared mass values of the Inert Higgs bosons receive a positive contribution from m_0^2 and a negative contribution from the auxiliary D-term which varies with s^2 (see Eq. 7.50). Due to this D-term contribution $m_{1,2}^{d,u2}$ decreases with s and at some point falls below experimental limits, bounding $M_{1/2}$ from above. The larger m_0 is, the larger the negative contribution must be in order to drive the Inert Higgs mass below it's lower limit. Further, if one assumes that $m_0 \sim s$ and $A_\lambda \sim M_{1/2}$ then EWSB conditions imply $s \sim M_{1/2} \tan\beta$. This suggests not only the observed limit on $m_0/M_{1/2}$ but also that it will be more severe for large $\tan\beta$ and shallower for low $\tan\beta$.

In addition, by examining Fig. 9.3 in conjunction with Fig. 9.2, one can see that the lower right boundary in the latter is formed from the bottom right corner of plots like Fig.9.3 which moves upwards and to the right as s is varied. Benchmarks scenarios, shown in Figs. 9.8, 9.9, 9.10 and 9.11 are drawn from these plots. These will be discussed in detail the next section.

The allowed region in Fig. 9.4 is formed from by the same combination of bounds as Fig. 9.3, but in this case $m_0/M_{1/2}$ varies from ≈ 1.9 to ≈ 1.4 , so for this larger $\tan\beta = 30$ the limit on ratio $m_0/M_{1/2}$ is enhanced. The fixed s plot Fig. 9.5 also demonstrates this increased hierarchy as one can see that with $s = 3$ TeV there is a much smaller region which is allowed by EWSB and experimental constraints at low energy. Benchmarks scenarios, shown in Figs. 9.12, 9.13 and 9.14 are drawn from these plots. Again detailed discussion of these is delayed until the next section.

In Fig. 9.6 the region to the left of the allowed parameter space is also ruled out by experimental limits on the chargino mass. However the lower-right region is ruled out not by the Inert Higgs masses but by a light Higgs which is lower than the LEP limit. This change can be understood for two reasons, firstly the Inert Higgs bosons obtain positive contributions to their masses from m_0 (with a coefficient of ≈ 1) and

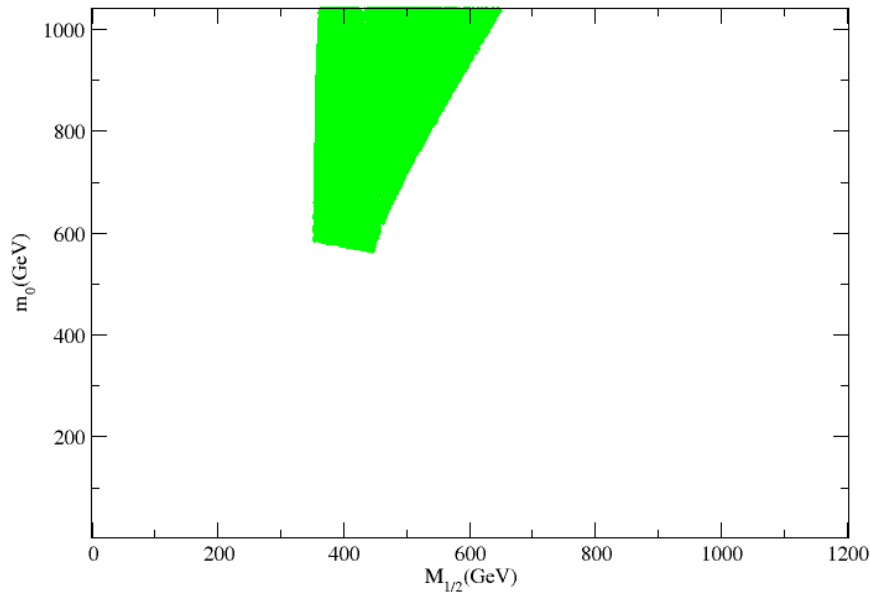


Figure 9.3: Physical solutions with $\tan\beta = 10$ and $s = 3$ TeV fixed, which pass experimental constraints from LEP and Tevatron data. On the left hand side of the allowed region the chargino mass is less than 100 GeV, while underneath the Inert Higgs are less than 100 GeV or becoming tachyonic. The region ruled out immediately to the right of the allowed points is due to $m_h < 114$ GeV.

$M_{1/2}$, while, due to the Auxiliary D-term contribution, the Inert Higgs masses decrease with s . Since decreasing $\tan\beta$ reduces the hierarchy between s and $M_{1/2}$ this negative contribution the mass of the Inert Higgs is smaller and does not decrease their mass as rapidly when m_0 is reduced. Secondly we observe that the light Higgs mass reduces with $\tan\beta$. This occurs because decreasing $\tan\beta$ increases the mixing, which provides a negative contribution to the light Higgs mass.

As with the other values of $\tan\beta$ we also present a plot for $\tan\beta = 3$ with a fixed value of s . However in this case all solutions we obtained with $s = 3$ TeV were ruled out. This is due to experimental constraints on the light Higgs mass, which as already mentioned, decreases when $\tan\beta$ is reduced. Instead a plot for fixed $s = 4$ TeV is

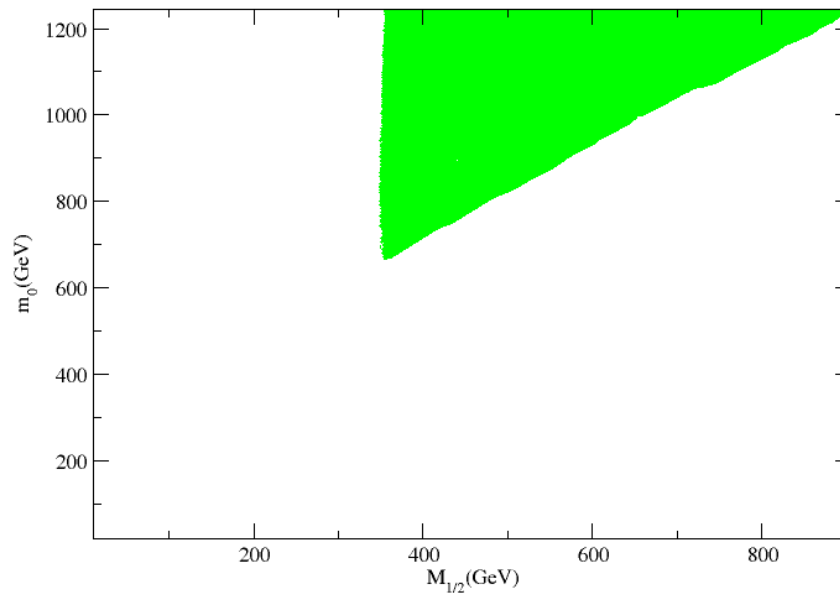


Figure 9.4: Physical solutions with $\tan\beta = 30$ which pass experimental constraints from LEP and Tevatron data. On the left hand side of the allowed region the chargino mass is less than 100 GeV, while underneath and on the lower right quadrant the Inert Higgs are less than 100 GeV or becoming tachyonic.

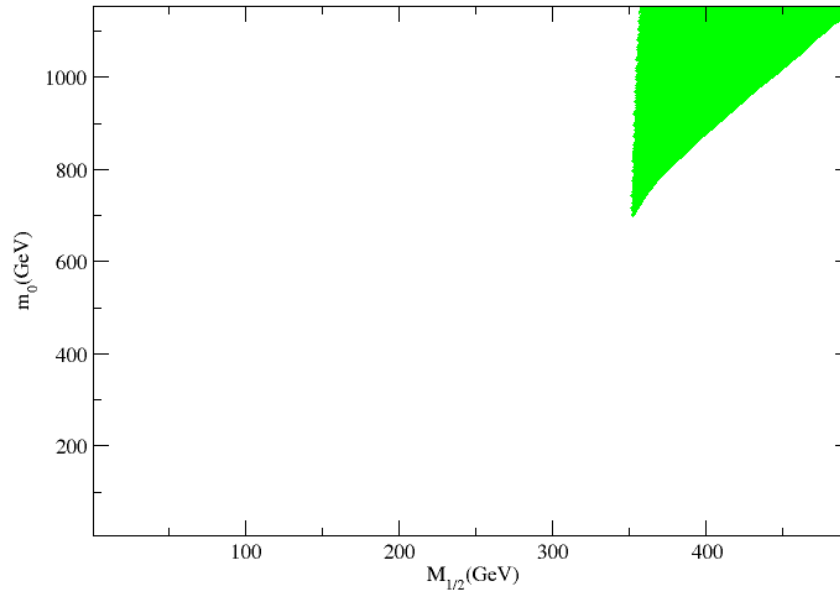


Figure 9.5: Physical solutions with $\tan\beta = 30$ and $s = 3$ TeV fixed, which pass experimental constraints from LEP and Tevatron data. On the left hand side of the allowed region the chargino mass is less than 100 GeV, while points immediately below the lowest (in m_0) allowed point are ruled out by Inert Higgs being less than 100 GeV or becoming tachyonic. The region ruled out immediately to the right of allowed points is due to $m_h < 114$ GeV.

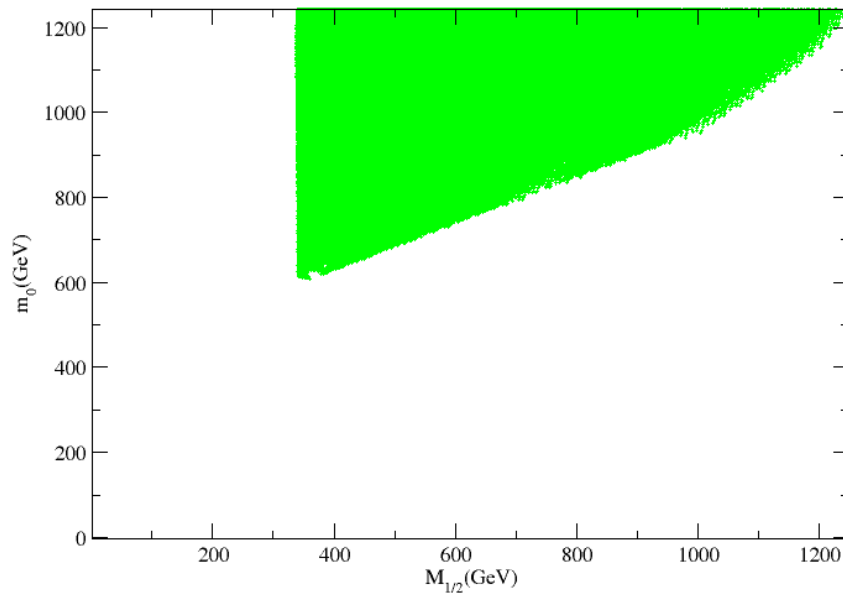


Figure 9.6: Physical solutions with $\tan \beta = 3$ which pass experimental constraints from LEP and Tevatron data. On the left hand side of the allowed region the chargino mass is less than 100 GeV, while underneath and on the lower right quadrant the lightest Higgs mass is less than 114, in violation of the limit set at LEP.

presented in Fig. 9.7.

Even with this value of s the light Higgs mass still provides a strong constraint on the parameter space. Unlike the previous fixed s there is an upper bound on m_0 which is below 1 TeV, and therefore visible on the plot shown. The upper limits on both m_0 and $M_{1/2}$ are due to the light Higgs mass.

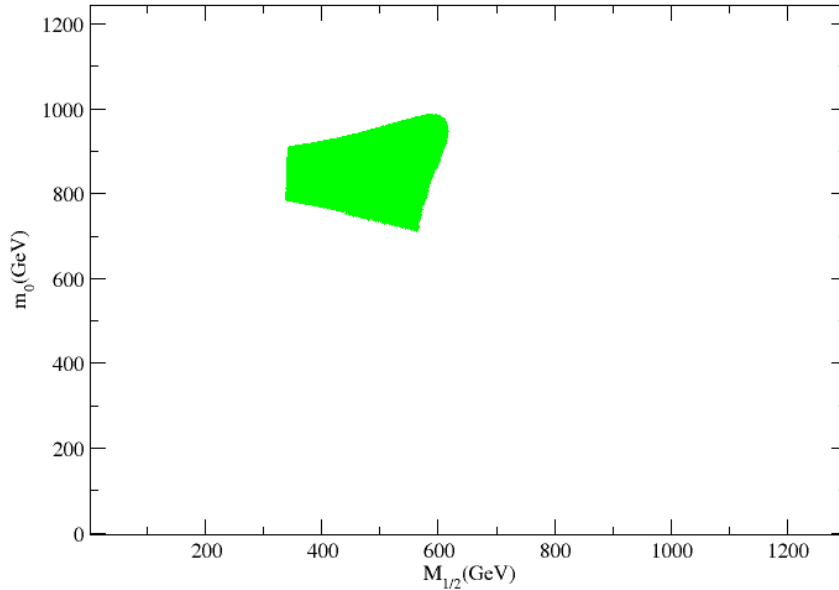


Figure 9.7: Physical solutions with $\tan \beta = 3$ and $s = 4$ TeV fixed, which pass experimental constraints from LEP and Tevatron data. On the left hand side of the allowed region the chargino mass is less than 100 GeV, while points immediately below the lowest (in m_0) allowed point are ruled out by Inert Higgs being less than 100 GeV or becoming tachyonic. The region ruled out immediately to the right and above the allowed points is due to $m_h < 114$ GeV.

Benchmark scenarios, shown in Figs. 9.15, 9.16 and 9.17 are drawn from these plots. A detailed discussion of the benchmark scenarios now follows.

9.4.2 Benchmark Scenarios

In this section the spectra of various benchmark scenarios for the CE_6SSM are shown and discussed. The numerical values for the masses shown the various spectra plot in this section can be found in Appendix E.

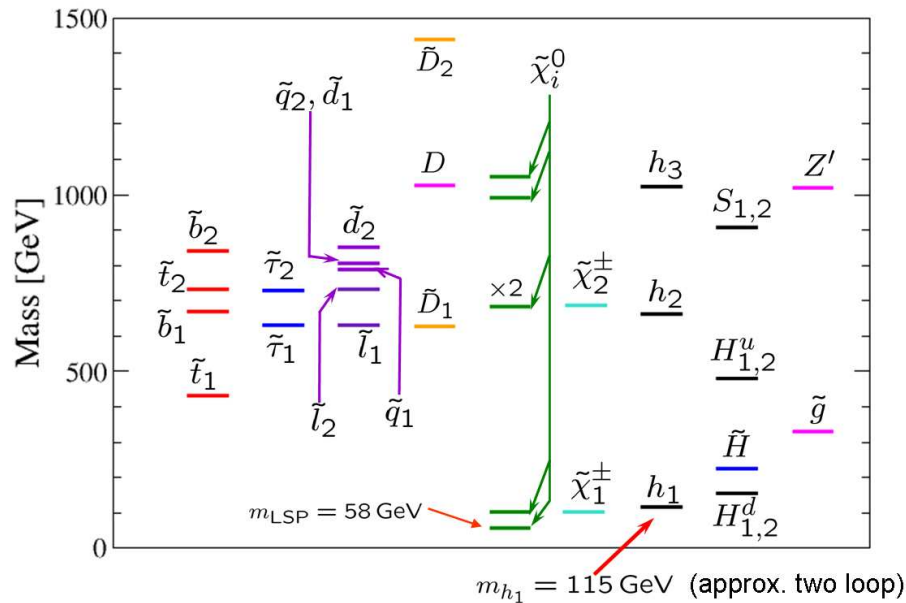


Figure 9.8: The particle mass spectra for CE_6SSM benchmark point A1 with, $\tan\beta = 10$, $s = 2.7$ TeV $M_{1/2} = 363$ GeV, $m_0 = 537$ GeV, $A = 711$ GeV, $\lambda(M_X) = -0.3684$, $\lambda(\mu_S) = -0.3548$, $\lambda_{1,2}(M_X) = 0.1$, $\kappa_{1,2,3}(M_X) = 0.2068$, $\kappa_{1,2,3}(\mu_S) = 0.5385$.

Shown in Fig. 9.8 is Benchmark scenario A1. This CE_6SSM point has been drawn from the lower left corner of the allowed region in Fig. 9.2. This is typical of the light spectra found in that region and it would be difficult to find a significantly lighter CE_6SSM spectra in scenarios with $\tan\beta = 10$, a universal κ coupling and $\lambda_{1,2}(M_X) = 0.1$. Notice that even for this comparatively light spectra the only sfermion below 500 GeV is the lightest stop. The gluino ($m_{\tilde{g}} = 330$ GeV) is lighter than all sfermions and will therefore not decay into a sfermion as in the usual MSSM sparticle

cascade decay chains. The gluino will decay through, $\tilde{g} \rightarrow q\tilde{q}^* \rightarrow q\bar{q} + E_T^{miss}$.

There are also quite light Inert Higgs ($m_{H_{1,2}^d} = 154$ GeV) and Inert Higgsinos ($m_{\tilde{H}} = 244$ GeV) in the spectra. Relatively light Higgsinos were preselected for when $\lambda_{1,2}(M_X) = 0.1$ was set and is not a general prediction of the CE₆SSM.

The light Inert Higgs bosons decay via the Z_2^H violating terms $h_{ijk}^N \hat{N}_i^c \hat{H}_{2j} \hat{L}_k$, $h_{ijk}^U \hat{u}_i^c \hat{H}_{2j} \hat{Q}_k$, $h_{ijk}^D \hat{d}_i^c \hat{H}_{1j} \hat{Q}_k$ and $h_{ijk}^E \hat{e}_i^c \hat{H}_{1j} \hat{L}_k$, where the Inert Higgs superfields are SU(2) doublets with $\hat{H}_{1j} = (\hat{H}_{1j}^0, \hat{H}_{1j}^-)$ and $\hat{H}_{2j} = (\hat{H}_{2j}^+, \hat{H}_{2j}^0)$. These interactions are analogous to the Yukawa interactions of the Higgs superfields, \hat{H}_u and \hat{H}_d . So the neutral Inert Higgs bosons decay predominantly into 3rd generation fermion–anti-fermion pairs like $H_i^{d0} \rightarrow b\bar{b}$. The charged Inert Higgs bosons decays are also into fermion–anti-fermion pairs, but in this case it is the antiparticle of the fermions’ electroweak partner, e.g. $H_i^{d-} \rightarrow \tau\bar{\nu}_\tau$.

The same couplings also govern the decays of the Inert Higgsinos. The electromagnetically neutral Higgsinos predominantly decay into a fermion anti-sfermion pairs (e. g. $\tilde{H}_{2i}^0 \rightarrow t\tilde{t}^*$, $\tilde{H}_{1i}^0 \rightarrow \tau\tilde{\tau}^*$). The charged Higgsinos decays are similar but in this case the sfermion is the supersymmetric partner of the electroweak partner of the fermion, (e. g. $\tilde{H}_{2i}^+ \rightarrow t\tilde{b}^*$, $\tilde{H}_{1i}^- \rightarrow \tau\tilde{\nu}_\tau^*$).

The lightest particles in the spectra are the lightest Higgs ($m_{h_1} = 115$ GeV), the lightest chargino ($m_{\chi_{1\pm}} = 103$ GeV) and the two lightest neutralinos ($m_{\chi_1^0} = 58$ GeV and $m_{\chi_2^0} = 103$ GeV). The second lightest neutralino decays, as in the MSSM, through $\chi_2^0 \rightarrow \chi_1^0 + \bar{l}l$. The lightest chargino will also decay in the way as a light chargino in the MSSM, e.g. $\chi^- \rightarrow \tilde{\tau}^* \nu_\tau$. Although the mass scale of the exotic colored objects is sensitive to s making them typically quite heavy, large mixing in this scenario means that one set of exotic sfermions is comparatively light ($m_{\tilde{D}_1} = 628$ GeV). The decay for this object will be discussed in later benchmarks where it has an even lighter mass.

Benchmark point A2, shown in Fig. 9.9, is also a scenario with $\tan\beta = 10$, a universal κ coupling and $\lambda_{1,2}(M_X) = 0.1$, but with a more exaggerated hierarchy in the mass spectra than A1. This is because the scenario has been chosen from the top

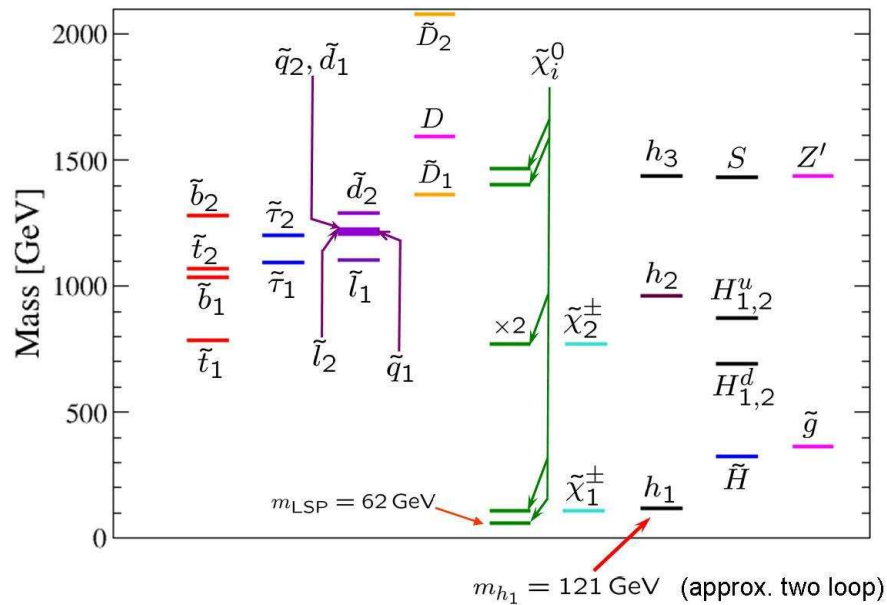


Figure 9.9: Benchmark point A2. $\tan\beta = 10$, $s = 3.8$ TeV, $M_{1/2} = 390$ GeV, $m_0 = 998$ GeV, $A = 768$ GeV, $\lambda(M_X) = -0.3066$, $\lambda(\mu_S) = -0.2845$, $\lambda_{1,2}(M_X) = 0.1$, $\kappa_{1,2,3}(M_X) = 0.2463$, $\kappa_{1,2,3}(\mu_S) = 0.5935$.

left of the allowed region in Fig. 9.2, so that $m_0 \gg M_{1/2}$. the result of raising m_0 has been to push the heavier parts of the spectra up in mass to such an extent that only the gluino, Inert Higgsinos, the lightest Higgs, the lightest chargino and the two lightest neutralinos are below ≈ 700 GeV. With the exception of the lightest Higgs mass, which is bounded from above, these particles are not sensitive to m_0 .

Although the hierarchy in the spectra has increased, the pattern is otherwise quite similar to A1, with a hierarchy amongst the sfermions unchanged. However the lightest set of Inert Higgs bosons are now heavier than the Inert Higgsino as they are sensitive to m_0 . The exotics colored objects are now very heavy.

It is also possible to have a generally heavier spectrum like A2 but with light Inert Higgs bosons. Since the lower right boundary is caused by the inert Higgs bosons becoming too light, a point close to this boundary, with large m_0 and $M_{1/2}$ will have

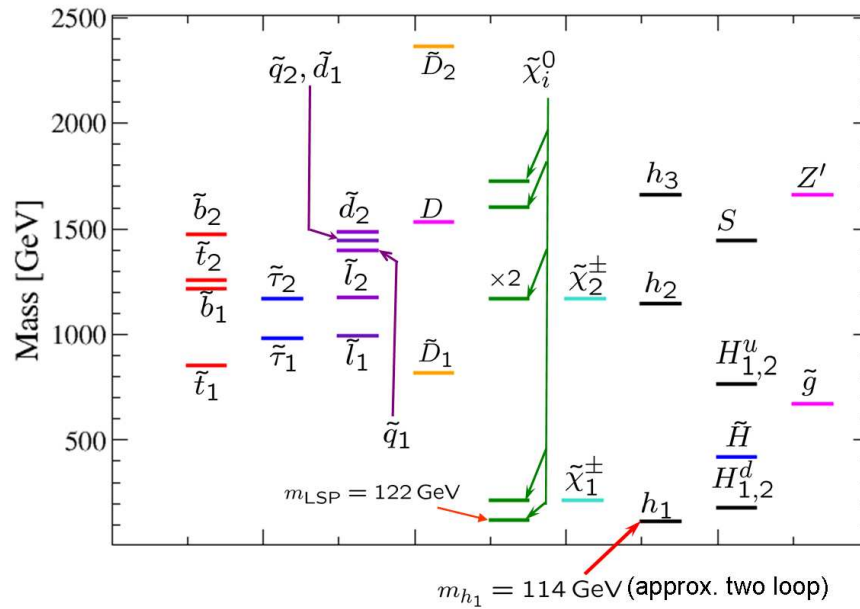


Figure 9.10: Benchmark point A3. $\tan\beta = 10$, $s = 4.4$ TeV, $M_{1/2} = 775$ GeV, $m_0 = 799$ GeV, $A = 919$ GeV, $\lambda(M_X) = -0.3698$, $\lambda(\mu_S) = -0.3736$, $\lambda_{1,2}(M_X) = 0.1$, $\kappa_{1,2,3}(M_X) = 0.1780$, $\kappa_{1,2,3}(\mu_S) = 0.4935$.

light Inert Higgs, but is otherwise expected to have a spectra similar to A2. An example of this is benchmark A3, whose spectra is shown in Fig. 9.10. Notice that since $M_{1/2}$ is also large in this scenario, the light neutralinos and chargino are now a little heavier, with $m_{\chi_1^\pm} = 217$ GeV and $m_{\chi_1^0} = 122$ GeV. The gluino is also significantly heavier, $m_{\tilde{g}} = 673$. Despite this all sfermions are still heavier than the gluino, and the spectrum is still very hierarchical.

All these points drawn from scenarios with $\tan\beta = 10$, a universal κ coupling and $\lambda_{1,2}(M_X) = 0.1$, so far have $M_{Z'} > 1$ TeV. The lower limit on the Z' mass used in this study is 700 GeV and it is interesting to see a spectrum of masses where $M_{Z'}$ is close to this bound. Benchmark A4, whose spectra is shown in Fig. 9.11, is an example of this with $M_{Z'} = 719$ GeV. A light Z' boson can provide a signature through enhanced production of lepton–anti-lepton pairs.

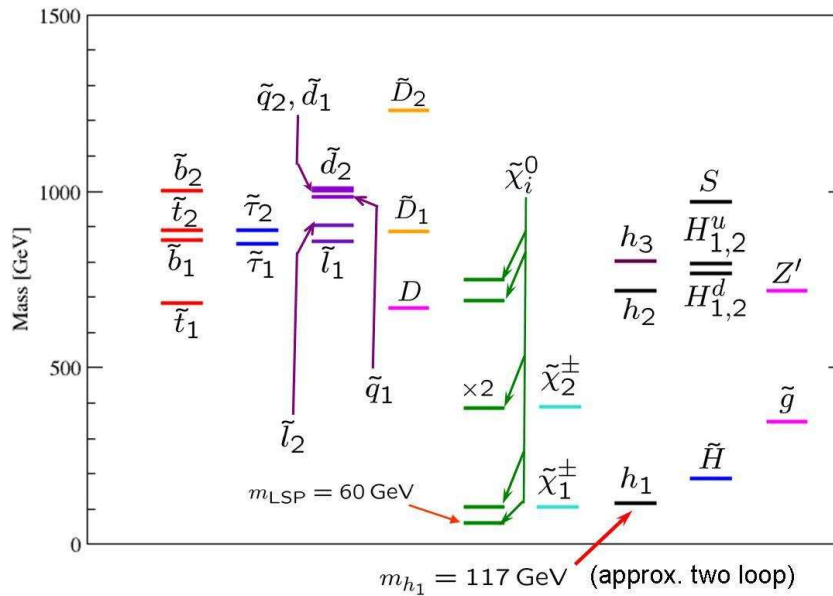


Figure 9.11: Benchmark point A4. $\tan\beta = 10$, $s = 1.9$ TeV, $M_{1/2} = 382$ GeV, $m_0 = 816$ GeV, $A = -19$ GeV, $\lambda(M_X) = -0.2573$, $\lambda(\mu_S) = -0.2780$, $\lambda_{1,2}(M_X) = 0.1$, $\kappa_{1,2,3}(M_X) = 0.1739$, $\kappa_{1,2,3}(\mu_S) = 0.4979$.

This point appears on the left hand side of the $m_0 - M_{1/2}$ plain shown in Fig. 9.2 lying somewhere between A1 and A2. The sfermions are heavier than those in A1 because m_0 is larger. However the heaviest neutralinos and Higgs boson and the exotic D fermions are lighter than in A1 since their masses are set by s . All points with $M_{Z'} < 1$ TeV appear in a similar region of the $m_0 - M_{1/2}$ plane and will have similar spectra. Points with $M_{Z'} < 1$ TeV do not appear in the bottom left corner of the plot from where A1 was drawn.

It is also significant that such points with low Z' masses occupy a region in the $m_0 - M_{1/2}$ plane that is also covered by points with $M_{Z'} > 1$ TeV. This is important because during this project a limit of $M_{Z'} > 936$ GeV [263] was informally announced, though it has not yet been confirmed in a formal publication. All exclusion plots presented in this thesis are, in fact, valid with the new limit on the Z' mass, despite

the fact that we did not impose this as a bound. No other benchmark points with $M_{Z'} < 1$ TeV will be shown here, but if the old limit, in fact, persists the benchmarks associated with different $\tan\beta$ could also have spectra with a pattern similar to A4.

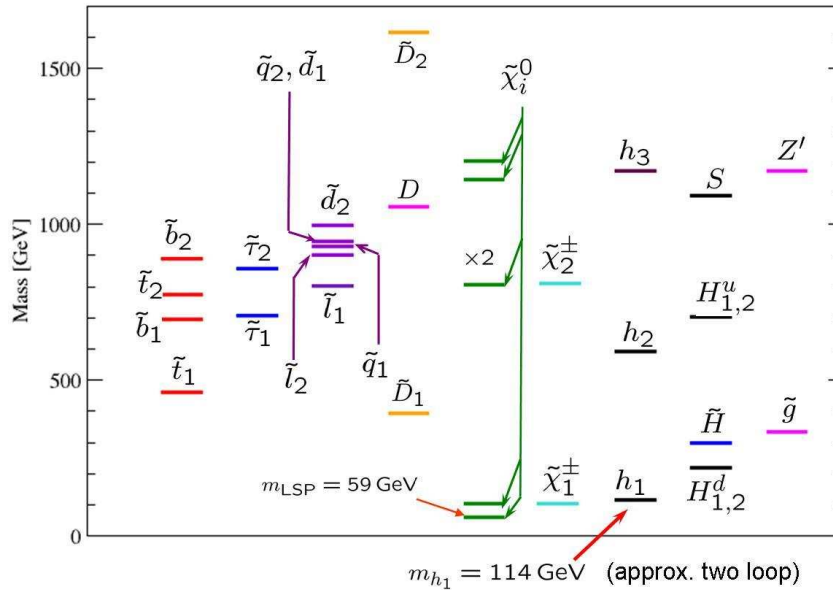


Figure 9.12: Benchmark point B1. $\tan\beta = 30$, $s = 3.1$ TeV, $M_{1/2} = 365$ GeV, $m_0 = 702$ GeV, $A = 1148$ GeV, $\lambda(M_X) = -0.37845$, $\lambda(\mu_S) = -0.3661$, $\lambda_{1,2}(M_X) = 0.1$, $\kappa_{1,2,3}(M_X) = 0.17121$, $\kappa_{1,2,3}(\mu_S) = 0.4813$.

Similar patterns in the mass spectra can be observed for scenarios with a larger $\tan\beta = 30$, but still with a universal κ and fixed $\lambda_{1,2}(M_X) = 0.1$. Benchmark B1, whose mass spectra is shown in Fig. 9.12, is drawn from the lower left corner of Fig. 9.4, and can be seen as an analogous point to A1, but with a larger $\tan\beta$. Also of interest in this spectrum is the lightest sfermion being an exotic D sfermion with $m_{\tilde{D}_1} = 393$ GeV, so light as a result of even larger mixing than in A1. Other than that, the pattern of masses is quite similar to that of A1, but just a little heavier since m_0 and s are larger.

Similarly benchmark B2 (with spectra shown in Fig. 9.13) and B3 (spectra shown in Fig. 9.14) can be seen as larger $\tan\beta$ analogue of benchmarks A2 and A3 respectively.

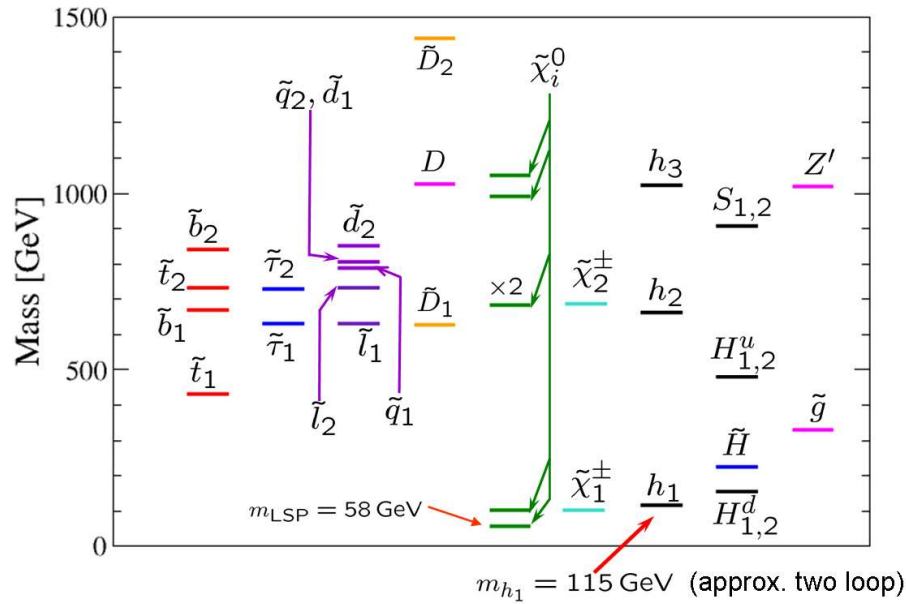


Figure 9.13: Benchmark point B2. $\tan\beta = 30$, $s = 3.4$ TeV, $M_{1/2} = 361$ GeV, $m_0 = 993$ GeV, $A = 1121$ GeV, $\lambda(M_X) = -0.3333$, $\lambda(\mu_S) = -0.3238$, $\lambda_{1,2}(M_X) = 0.1$, $\kappa_{1,2,3}(M_X) = 0.1839$, $\kappa_{1,2,3}(\mu_S) = 0.5078$.

In B3 there is again an increased mixing in the exotic sfermions leading to a very light $m_{\tilde{D}_1} = 312$ GeV. How these objects decay depends on whether they are scalar diquarks or scalar leptoquarks (i.e. whether we are in CE₆SSMI or CE₆SSMII). In CE₆SSMI the exotic scalar diquarks decay through Z_2^H violating terms, $g_{ijk}^Q D_i(Q_j Q_k)$ and $g_{ijk}^a \bar{D}_i d_j^c u_k^c$. Therefore the scalar diquarks decay into an up and a down type quark,¹ like $\tilde{D} \rightarrow tb$.

If instead we are in the CE₆SSMII then the scalar leptoquarks decay through $g_{ijk}^N N_i^c D_j d_k^c$, $g_{ijk}^E e_i^c D_j u_k^c$ and $g_{ijk}^D (Q_i L_j) \bar{D}_k$. This results in decays into quark and lepton pairs like, $\tilde{D} \rightarrow t\tau$.

Since the discrete symmetry forbidding proton decay permits single production of

¹Please recall that in the E₆SSM the discrete symmetry which prevents rapid proton decay ensures that the exotic quarks must decay into a sparticle, while the scalar partners do not.

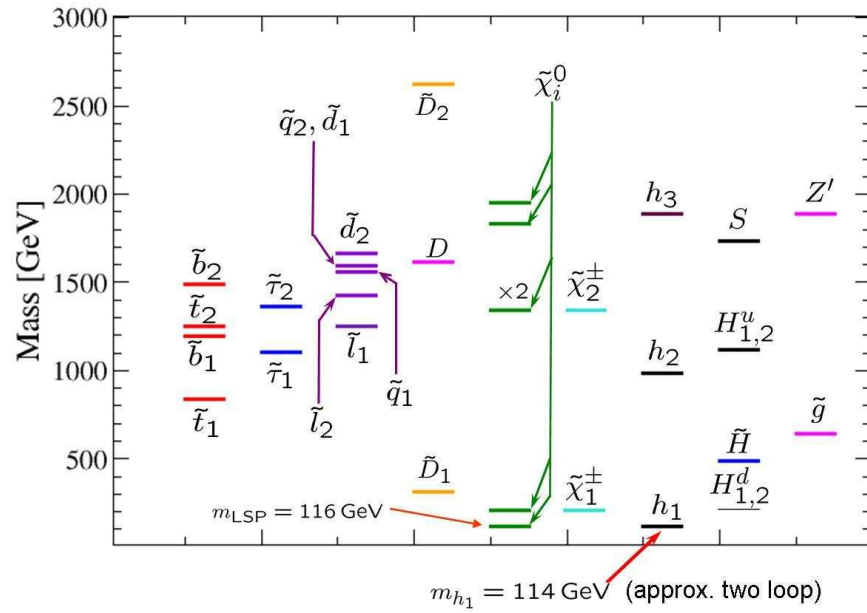


Figure 9.14: Benchmark point B3. $\tan\beta = 30$, $s = 5.0 \text{ TeV}$, $M_{1/2} = 725 \text{ GeV}$, $m_0 = 1074 \text{ GeV}$, $A = 1726 \text{ GeV}$, $\lambda(M_X) = -0.3847$, $\lambda(\mu_S) = -0.3788$, $\lambda_{1,2}(M_X) = 0.1$, $\kappa_{1,2,3}(M_X) = 0.1579$, $\kappa_{1,2,3}(\mu_S) = 0.4559$

these exotic scalars, they can mediate contact interactions between ordinary fermions. However any constraints, coming from such contact interactions, on the masses of these particles depends also on the coupling between these fields and ordinary matter. In the E_6 SSM such interactions are Z_2^H suppressed and contact interactions should not introduce bounds beyond what has already been assumed.

However recent, as yet unpublished, results from Tevatron searches for dijet resonances [264] should apply to the scalar diquarks. This search increases the lower bound on the diquarks to 630 GeV. Therefore in scenarios like B3, where this bound is violated, the exotic scalars should be leptoquarks, with the version of the E_6 SSM model containing diquarks ruled out for such scenarios.

For $\tan\beta = 3$ the spectra benchmark scenarios, C1, C2, C3, with a universal κ and $\lambda_{1,2}(M_X) = 0.1$ are shown in Figs. 9.15, 9.16 and 9.17 respectively. These benchmarks can also be thought of as being lower $\tan\beta$ analogues of the benchmarks A1, A2 and A3, though in the case of C2 and C3 larger values of s were chosen so that an examples of very heavy spectra could be shown.

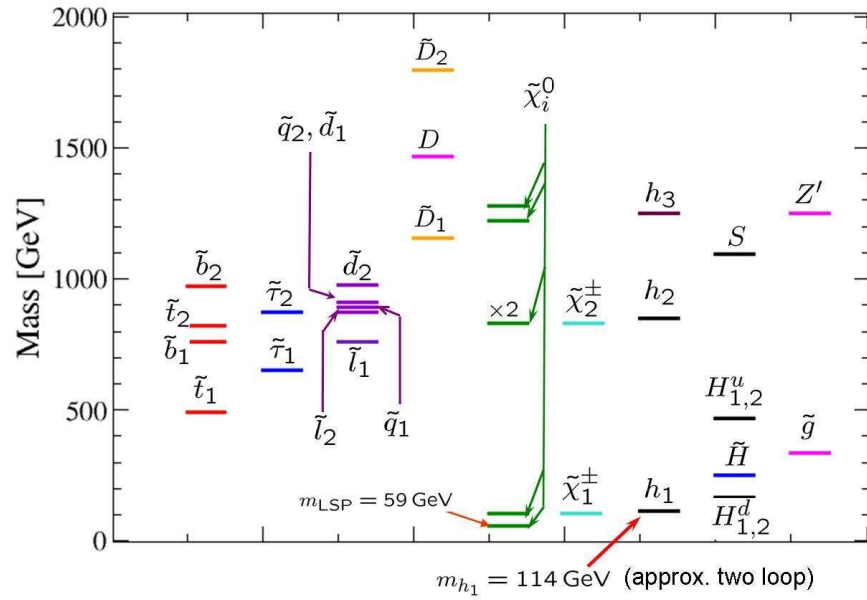


Figure 9.15: Benchmark point C1. $\tan\beta = 3$, $s = 3.3 \text{ TeV}$, $M_{1/2} = 365 \text{ GeV}$, $m_0 = 640 \text{ GeV}$, $A = 798 \text{ GeV}$, $\lambda(M_X) = -0.465$, $\lambda(\mu_S) = -0.354$, $\lambda_{1,2}(M_X) = 0.1$, $\kappa_{1,2,3}(M_X) = 0.3$, $\kappa_{1,2,3}(\mu_S) = 0.628$.

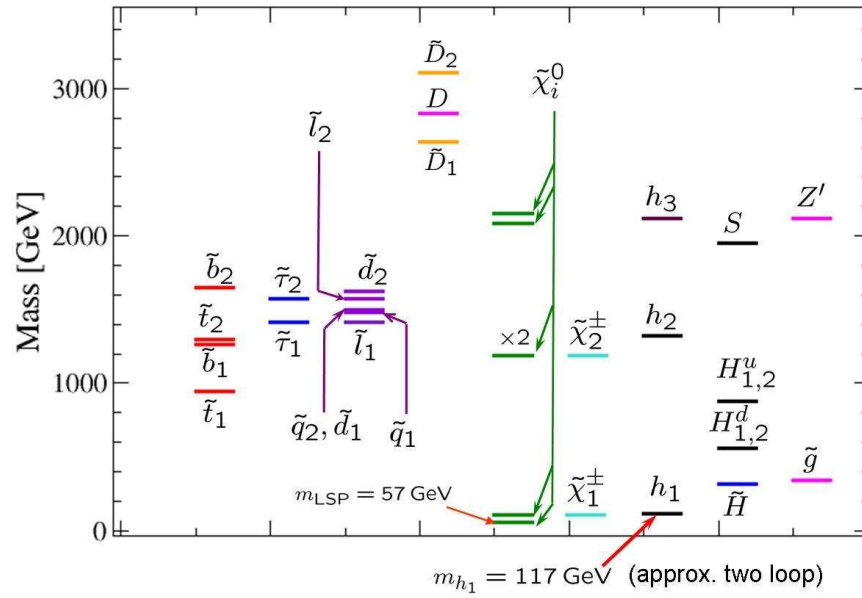


Figure 9.16: Benchmark point C2. $\tan\beta = 3$, $s = 5.6 \text{ TeV}$, $M_{1/2} = 352 \text{ GeV}$, $m_0 = 1238 \text{ GeV}$, $A = 1194 \text{ GeV}$, $\lambda(M_X) = -0.529$, $\lambda(\mu_S) = -0.300$, $\lambda_{1,2}(M_X) = 0.1$, $\kappa_{1,2,3}(M_X) = 0.492$, $\kappa_{1,2,3}(\mu_S) = 0.716$.

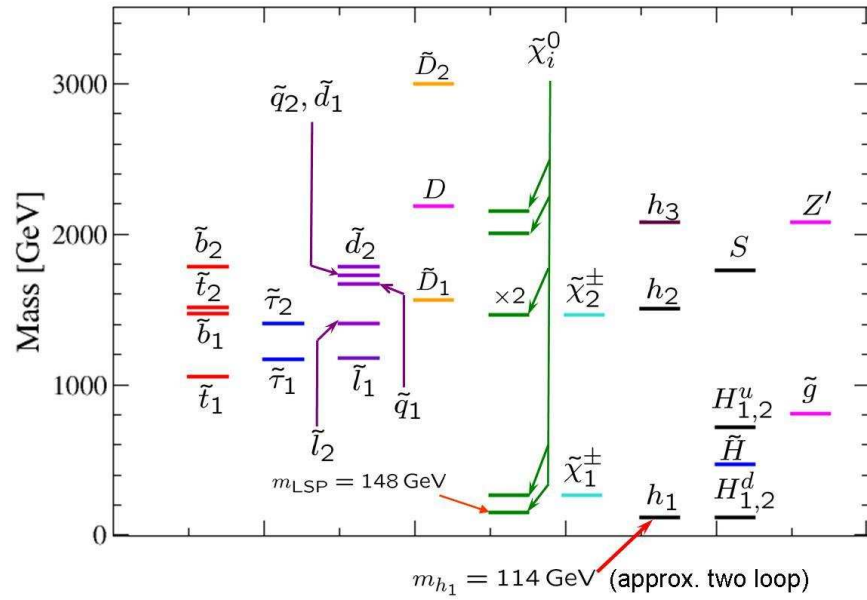


Figure 9.17: Benchmark point C3. $\tan\beta = 3$, $s = 5.5 \text{ TeV}$, $M_{1/2} = 931 \text{ GeV}$, $m_0 = 918 \text{ GeV}$, $A = 751 \text{ GeV}$, $\lambda(M_X) = -0.434$, $\lambda(\mu_S) = -0.375$, $\lambda_{1,2}(M_X) = 0.1$, $\kappa_{1,2,3}(M_X) = 0.23$, $\kappa_{1,2,3}(\mu_S) = 0.56$.

It is also interesting to consider spectra with a hierarchy in the exotic fermion couplings κ_1 , κ_2 and κ_3 . Fixing $\kappa_{1,2} \ll 1$ could provide light first and second generation exotic colored sfermions and fermions. Benchmark D1 (Fig. 9.18) is an example of this with very light exotic fermions with masses $\mu_D^{1,2} = 300$ GeV, which is even lighter than the gluino mass, $m_{\tilde{g}} = 353$ GeV.

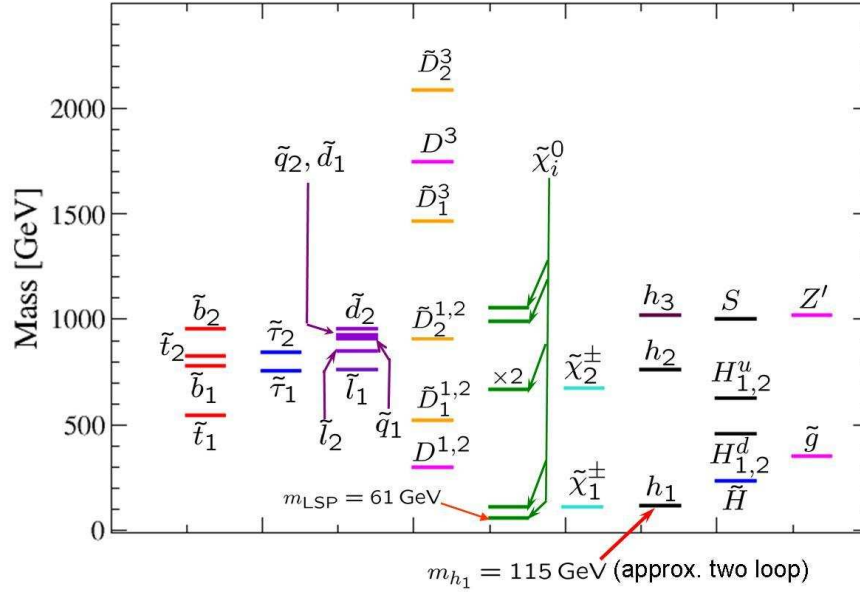


Figure 9.18: Benchmark point D1. $\tan\beta = 10$, $s = 2.7$ TeV, $M_{1/2} = 388$, GeV $m_0 = 681$, GeV $A = 645$, GeV, $\lambda_{1,2}(M_X) = 0.1$, $\lambda_3 = -0.378$, $\lambda(\mu_S) = -0.348$, $\kappa_{1,2} = 0.06$, $\kappa_3(M_X) = 0.42$, $\kappa_3(\mu_S) = 0.915$.

Benchmark D2 is similar to D1 but the spectra, as shown in Fig. 9.19, contains both very light exotic sfermions and fermions, $m_{\tilde{D}_1^{1,2}} = 370$ GeV and $\mu_D^{1,2} = 391$ GeV.

The decays of the light exotic colored sfermions have already been discussed earlier, and are unchanged here. The decays of the exotic colored fermions are governed by the same Z_2^H violating couplings as their sfermion superpartners. Leptoquarks can decay be detected by decay into quark and a slepton, like $D \rightarrow t\tilde{\tau}^*$ or a lepton and a squark, like $\tilde{D} \rightarrow \nu_\tau\tilde{b}^*$. The diquarks decay into a quark and squark, like $\bar{D} \rightarrow t\tilde{b}^*$.

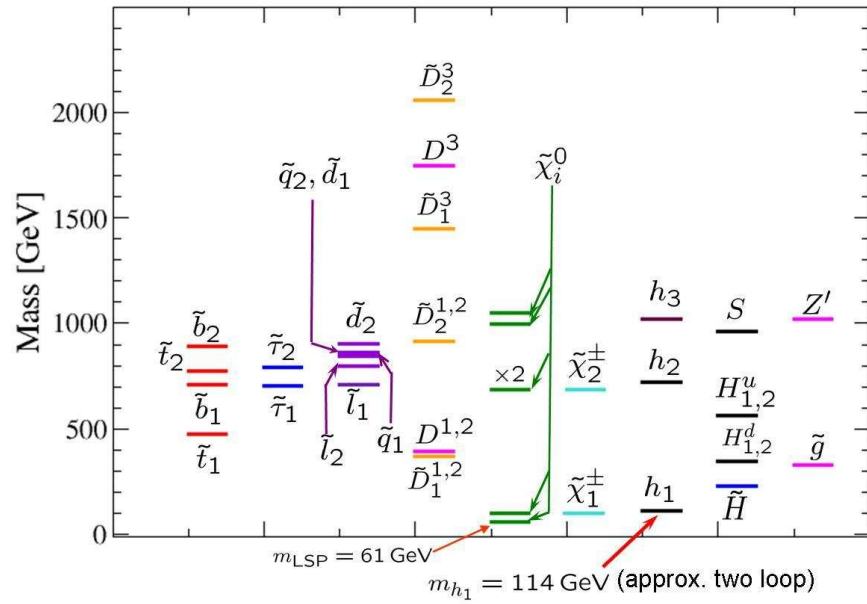


Figure 9.19: Benchmark point D2. $\tan\beta = 10$, $s = 2.7 \text{ TeV}$, $M_{1/2} = 358 \text{ GeV}$, $m_0 = 623 \text{ GeV}$, $A = 757 \text{ GeV}$, $\lambda_{1,2}(M_X) = 0.1$, $\lambda_3 = -0.395$, $\lambda(\mu_S) = -0.355$, $\kappa_{1,2} = 0.08$, $\kappa_3(M_X) = 0.43$, $\kappa_3(\mu_S) = 0.915$.

Finally since in all benchmark scenarios so far, light Inert Higgsinos have been preselected, there has always been some exotic particle (Z' boson, D fermions, sfermions and Inert Higgs and Higgsinos) with a mass lower than 500 GeV in the spectra. This is not necessarily the case. Benchmarks F1 (shown in Fig. 9.20) and F2 (Fig. 9.21) are scenarios where all exotics are heavier than 900 GeV. This demonstrates the range of possibilities in the CE₆SSM model.

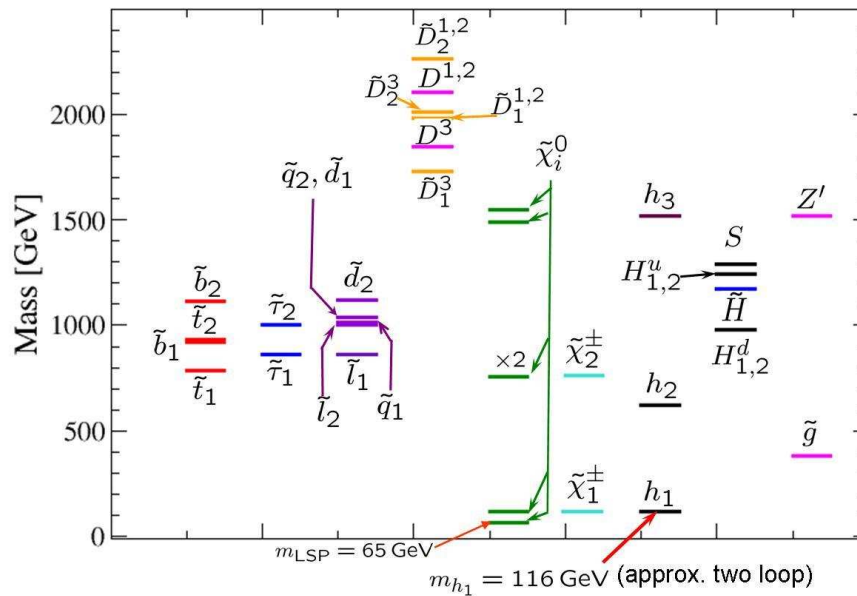


Figure 9.20: Benchmark point F1. $\tan\beta = 10$, $s = 4.0$ TeV, $M_{1/2} = 426$ GeV, $m_0 = 701$ GeV, $A = -1652$ GeV, $\lambda_{1,2}(M_X) = 2.8$, $\lambda_3(M_X) = -2.0$, $\lambda_3(\mu_S) = -0.266$, $\kappa_{1,2} = 2.5$, $\kappa_3(M_X) = 2.0$, $\kappa_3(\mu_S) = 0.652$,

If such a scenario like F1 or F2 is chosen by nature, where the only light sparticles are the gluino, the two lightest neutralinos and the lightest chargino phenomenology signatures can still be obtained. Pair production of $\chi_2^0\chi_2^0$, $\chi_2^0\chi_1^\pm$, $\chi_1^\pm\chi_1^\mp$ and $\tilde{g}\tilde{g}$ should still be detectable at the LHC.

Since the gluino decays through, $\tilde{g} \rightarrow q\bar{q} + E_T^{miss}$, the light gluino provides a signature for the model at the LHC through, $pp \rightarrow q\bar{q}q\bar{q} + E_T^{miss} + X$. In this case a

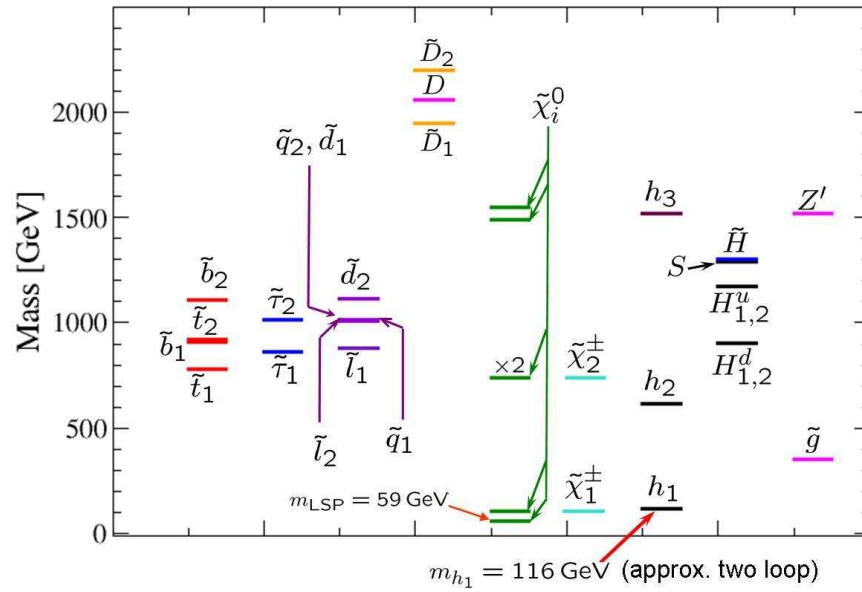


Figure 9.21: Benchmark point F2. $\tan\beta = 10$, $s = 4.0 \text{ TeV}$, $M_{1/2} = 389 \text{ GeV}$, $m_0 = 725 \text{ GeV}$, $A = -1528 \text{ GeV}$, $\lambda_{1,2}(M_X) = 2.6$, $\lambda_3(M_X) = -2.0$, $\lambda_3(\mu_S) = -0.259$, $\kappa_{1,2,3} = 2.5$, $\kappa_3(\mu_S) = 0.728$.

detailed phenomenological study is needed to look at the significance of this signature and how it differs from other SUSY models. This is not included here but is left for further study. The second lightest neutralino decays through $\chi_2^0 \rightarrow \chi_1^0 + \bar{l}l$ and so would produce a signal $pp \rightarrow \bar{l}l\bar{l} + E_T^{miss} + X$, just as in the MSSM.

In this section we have investigated the spectra of the CE₆SSM and have observed that several distinctive patterns present in them. The Z' boson, two heaviest neutralinos and the heaviest CP-even Higgs boson are normally heavier than all the sfermions of ordinary matter. Their masses are almost degenerate around Z' boson mass $M_{Z'}$, i.e.

$$|m_{\chi_5^0}| \simeq |m_{\chi_6^0}| \simeq m_{h_3^0} \simeq M_{Z'} \quad (9.16)$$

This is the case for all but one of the benchmark spectra presented here. In such cases we also find that at tree level,

$$M_{H^\pm} \simeq M_A \simeq m_{h_3^0} \quad (9.17)$$

and we assume, though do not explicitly check that this is maintained at the one loop level.

However if s is very light this can be changed, as is shown in benchmark A4. In this case the degeneracy is with the 2nd heaviest Higgs instead,

$$|m_{\chi_3^0}| \simeq |m_{\chi_6^0}| \simeq m_{h_2^0} \simeq M_{Z'}. \quad (9.18)$$

and in this case the tree level quasi-degeneracy amongst the Higgs is,

$$M_{H^\pm} \simeq M_A \simeq m_{h_2^0}. \quad (9.19)$$

One generation of exotic colored fermions and sfermions also have their mass set by the singlet vev, s , and are therefore usually relatively heavy, though, due to large mixing, sometimes one of the exotic sfermion may be light. If the κ_i couplings are not all equal then light exotics then other generations of sfermions and fermions may be light, as only one κ_i coupling needs to be constrained for EWSB to take place.

The CE_6SSM predicts that the set of the lightest particles always include one CP-even Higgs boson, the lightest neutralino, the lightest chargino and gluino. The masses of the lightest and second lightest neutralinos, the lightest chargino and gluino are determined by the soft gaugino masses M_1 , M_2 and M_3 respectively, i.e.

$$m_{\chi_1^0} \simeq M_1, \quad m_{\chi_2^0} \simeq m_{\chi_1^\pm} \simeq M_2, \quad m_{\tilde{g}} \simeq M_3. \quad (9.20)$$

It also predicts that the gluino is lighter than all sfermions superpartners of the observed SM fermions. As mentioned in chapter 8 this is a result of the RG flow and has strong implications for cascade decays. There is also a stable hierarchy amongst these sfermions, with the heaviest sfermion being one of the down type squarks, \tilde{b}_2 or the quasi-degenerate first and second generation \tilde{d}_2 . Exotic colored sfermions and fermions could appear at low energies providing very exciting collider signatures of the model. This is not however a concrete prediction of the model as it is also possible for all exotics to be relatively heavy.

9.5 Conclusions

In this chapter the CE_6SSM has been introduced and the low energy consequences of the model have been explored. We find it is difficult, if not impossible, to obtain solutions with $m_0 \ll M_{1/2}$ while maintaining $M_{1/2} < 800$ GeV for a light particle spectrum. This makes it very challenging to obtain light sleptons and no scenarios with this feature were found in our study. The squarks of ordinary matter also tend to be quite heavy. The lightest sfermion of ordinary matter in all benchmark scenarios presented here is the lightest stop.

By contrast the gluino can be very light. This should be compared to the CMSSM where the gluino tends to be heavier than most of the sfermions (see e.g. [178]). This feature of the model is a result of the *RGE* evolution. In the E_6SSM the one loop beta-function for the strong coupling (and by implication the soft gluino mass parameter) vanishes, whereas in the MSSM it is < 0 resulting in an increase in the gluino mass

parameter as the RGE are evolved to low energies. A gluino which is lighter than the sfermions is therefore a stable signature of the CE_6 SSM.

In addition to two light neutralinos, a light chargino and a light Higgs should be present. As has been shown in benchmark F2, it is possible that none of the other unobserved particles presented here are lighter than 700 GeV. Nonetheless there are many scenarios where there is light exotic matter below 500 GeV, which would provide a very striking signature of the model.

Chapter 10

Summary, Conclusions and Outlook

Electroweak symmetry breaking is crucial to particle physics, as without this taking place gauge theories cannot provide a correct description of nature. While the mechanism which does this is currently unknown, theoretical models based on gauge theories must include some mechanism for doing this if they are to be consistent with data. In chapter 2 we described how, in the Standard Model, the minimal version of Higgs Mechanism, consistent with data, breaks the electroweak symmetry.

In addition we also explained that we doubt this minimal model will be found in nature as it suffers from the Hierarchy Problem, where the parameters governing the mass of the Higgs boson have to be very delicately fine tuned to maintain a weak scale, which is much lower than the scale at which gravitational interactions become important.

This problem has motivated many new models of beyond the Standard Model physics. These models have more complicated mechanisms for electroweak symmetry breaking, but are considered preferential because they reduce the fine tuning, admitting the possibility that the observed spectrum of masses might be a natural consequence of the model, without some tweaking of the parameters. It is also significant that it appears that any solution to this hierarchy must have new physics which is present at low energies that will be within reach of the LHC, which has just started running as

the finishing touches to this thesis are being made.

If the scale of the new physics is too large this will reintroduce some kind of fine tuning between the mass scale of the new physics and the scale at which electroweak symmetry is broken. This tuning is the first aspect of electroweak symmetry breaking explored in this thesis.

In order to be quantitative about this one must study each model individually and apply some prescription for measuring tuning. In chapter 5 some criticisms of the tuning measures used in the literature are presented and a new measure of fine tuning is introduced and its meaning and relation to other measures expounded.

In chapter 6 this new tuning measure is applied to various models, including a toy version of the SM, in order to demonstrate its use and further elucidate the meaning. It is shown that the new tuning measure picks up the correct features of the Hierarchy Problem while not suffering from any of the problems it was designed to solve. It is also applied to the case of the CMSSM where measures in the literature have indicated that the fine tuning may now be quite severe due to the LEP limits on sparticle masses. The new measure demonstrates that tuning increases with mass scale, as expected. However the results cast doubt on previous claims about the severity of the tuning.

Unfortunately all tuning measures should be normalised in order to remove global sensitivity. This means that a correct normalised measure requires a sampling of the whole parameter space, not just some limited region of it. Doing this went beyond the scope of this study, however from examining points already ruled out by LEP we observed that many such points have larger than expected values for the unnormalised tuning measures, due to different hierarchies in the model. It is possible that in a highly constrained model, such as the CMSSM, any choice of its parameters will lead to some large cancellation amongst them in the expression for one of the masses. Therefore it may be the apparent large tuning in the CMSSM is simply a result of only considering one observable, the Z boson mass.

It is possible that with some sensible bounds on the parameter space and sophis-

licated sampling techniques this work could be expanded and a result for normalised tuning found. This work could be pursued in the future.

The second aspect of electroweak symmetry breaking studied in this thesis is the possibility that EWSB can be driven by radiative corrections. This has already been established for the constrained versions of the MSSM, but in this thesis it is demonstrated that this can also occur in the NUHM E_6 SSM (chapter 8) and the CE_6 SSM (chapter 9).

In the former a qualitative study was performed for a sample choice of new E_6 SSM Yukawa couplings. For this point it was demonstrated that radiative electroweak symmetry breaking can take place for many different values of the NUHM E_6 SSM soft parameters, though there are constraints on m_0 and $M_{1/2}$ requiring them to be $\gtrsim 500$ GeV. A sample spectrum is then shown with masses ranging from ≈ 60 -1700 GeV. The spectrum is very hierarchical with a gluino lighter than most fermions.

A more extensive and quantitative study was carried out in the CE_6 SSM. In this model constraints on the $M_{1/2} - m_0$ plane were obtained for scenarios with universal exotic fermion coupling κ , fixed Inert Higgs coupling $\lambda_{1,2}(M_X) = 0.1$ and fixed values of $\tan\beta = 3, 10, 30$. Sample spectra for these scenarios and also other patterns of the new Yukawa couplings were presented. These show hierarchical spectra with all the sfermions heavier than the gluino. This is a very unusual feature of the model which could provide an interesting signature. A thorough phenomenological study on the process $pp \rightarrow q\bar{q}q\bar{q} + E_T^{miss} + X$ should be carried out in the future.

Additionally the exotic particles of the model, a Z' boson, exotic colored objects and Inert Higgs and Higgsinos could all be detected directly at the LHC if they are light enough.

With the LHC now running and the first collisions anticipated shortly these are very exciting times for particle physics. The mechanism behind electroweak symmetry breaking should be revealed, whatever it may be. In addition a solution to the hierarchy problem requires new physics to appear within the mass ranges ($\mathcal{O}(1 \text{ TeV})$) probed by

the LHC. So assuming the LHC is sensitive to this new physics it will be discovered. The specific models investigated here, the CMSSM, NUHM E₆SSM and CE₆SSM, which have been motivated by naturalness, can be tested directly and either discovered or rejected as solutions to the hierarchy problem.

Appendix A

Superfields

As is described in the body, the Haag-Lopuszanski-Sohnius generalisation of the Coleman-Mandula no-go theorem shows that the most general space-time symmetry also includes fermionic SUSY transformations. Therefore supersymmetry can be viewed as an extension of space-time. This can be made explicit by adding fermionic coordinates, $\theta^a, \bar{\theta}_{\dot{a}}$, which are 2 component Weyl spinors with $a, \dot{a} = \{1, 2\}$ and individual components being anti-commuting Grassman numbers, $\{\theta^a, \theta^b\} = 0$. Including these four new co-ordinates along with the usual four space-time ones gives a superspace with coordinates,

$$z = (x_\mu, \theta^a, \bar{\theta}_{\dot{a}}). \quad (\text{A.1})$$

A superfield is a function of superspace coordinates. Noting identities such as,

$$\theta^a \theta^b \theta^c = 0, \quad (\theta \sigma^\mu \bar{\theta})(\theta \sigma^\nu \bar{\theta}) = \frac{1}{2} g^{\mu\nu} \theta^2 \bar{\theta}^2, \quad \theta \sigma^\mu \bar{\theta} = -\bar{\theta} \bar{\sigma}^\mu \theta \quad (\text{A.2})$$

one can observe that the most general form for a superfield is,

$$\hat{\phi}(z) = \phi(x) + \theta \zeta(x) + \bar{\theta} \bar{\chi}(x) \quad (\text{A.3})$$

$$+ \theta^2 m(x) + \bar{\theta}^2 n(x) + \theta \sigma^\mu \bar{\theta} V_\mu(x) \quad (\text{A.4})$$

$$+ \theta^2 \bar{\theta} \bar{\lambda}(x) + \bar{\theta}^2 \theta \psi(x) + \theta^2 \bar{\theta}^2 d(x). \quad (\text{A.5})$$

where spinor indices are contracted as in $\theta^2 = \theta^a \theta_a = \theta^a \epsilon_{ab} \theta^b$ and $\bar{\theta}^2 = \bar{\theta}_{\dot{a}} \bar{\theta}^{\dot{a}} = \bar{\theta}_{\dot{a}} \epsilon^{\dot{a}\dot{b}} \bar{\theta}_{\dot{b}}$. There are four complex two component spinor fields, $\psi(x)$, $\bar{\lambda}$, $\zeta(x)$ and $\bar{\chi}(x)$ giving

16 fermionic dof. The four complex scalar fields, $\phi(x), m(x), n(x)$ and $d(x)$ make up eight bosonic degrees of freedom (dof). If the vector field $V_\mu(x)$ is complex then this contributes eight more bosonic giving 16 bosonic dof in total. A real Vector field would only contribute four dof, violating $n_b = n_f$.

However this general superfield is not an irreducible representation of supersymmetry. It can be reduced to give chiral superfields or vector superfields by imposing constraints, eliminating certain degrees of freedom.

A.1 Chiral Superfields

Using the SUSY covariant derivatives,

$$D_\alpha = \frac{\partial}{\partial \theta^\alpha} + i\sigma_{\alpha\dot{\beta}}^\mu \bar{\theta}^{\dot{\beta}} \frac{\partial}{\partial x^\mu} \quad \bar{D}_{\dot{\alpha}} = -\frac{\partial}{\partial \bar{\theta}^{\dot{\alpha}}} - i\theta^\beta \sigma_{\beta\dot{\alpha}}^\mu \frac{\partial}{\partial x^\mu}, \quad (\text{A.6})$$

one can define chiral superfields by, $\bar{D}_{\dot{\alpha}} \hat{\phi} = 0$ and anti-chiral fields $D_\alpha \hat{\phi} = 0$. With this constraint a chiral field can be written as,

$$\hat{\phi}(z) = \phi(x) + i\theta\sigma^\mu\bar{\theta}\partial_\mu\phi(x) + \frac{1}{4}\theta^2\bar{\theta}^2\partial_\mu\partial^\mu\phi(x) \quad (\text{A.7})$$

$$+ \sqrt{2}\theta\psi(x) - \frac{i}{\sqrt{2}}\theta^2\partial_\mu\psi(x)\sigma^\mu\bar{\theta} + \theta^2 F(x). \quad (\text{A.8})$$

Alternatively defining $y^\mu \equiv x^\mu - i\theta\sigma^\mu\bar{\theta}$, and relating chiral fields via $\hat{\phi}(y, \theta, \bar{\theta}) = \hat{\phi}_L(x, \theta, \bar{\theta})$ to left-handed chiral fields, $\hat{\phi}_L$, we obtain,

$$\hat{\phi}_L(z) = \phi(x) + \sqrt{2}\theta\zeta(x) + \theta^2 F(x). \quad (\text{A.9})$$

There are no vector fields in these expressions only, two complex scalar fields (4 dof) and one complex Weyl spinor (4 dof), so that $n_b = n_f$.

A.2 Vector Superfields

Vector superfields, V , are formed by imposing the constraint, $V(x, \theta, \bar{\theta}) = V^\dagger(x, \theta, \bar{\theta})$ requiring V to be self-adjoint. This gives,

$$V(z) = C(x) + i\theta\chi(x) - i\bar{\theta}\bar{\chi}(x) + \frac{i}{2}\theta^2[M(x) + iN(x)] \quad (\text{A.10})$$

$$-\frac{i}{2}\bar{\theta}^2 [M(x) - iN(x)] - \theta\sigma^\mu\bar{\theta}V_\mu(x) \quad (\text{A.11})$$

$$+i\theta^2\bar{\theta} \left[\bar{\lambda}(x) + \frac{i}{2}\bar{\sigma}^\mu\partial_\mu\chi(x) \right] - i\bar{\theta}^2\theta \left[\lambda(x) + \frac{i}{2}\sigma^\mu\partial_\mu\bar{\chi}(x) \right] \quad (\text{A.12})$$

$$+\frac{1}{2}\theta^2\bar{\theta}^2 \left[D(x) + \frac{1}{2}\partial_\mu\partial^\mu C(x) \right]. \quad (\text{A.13})$$

where $C(x)$, $M(x)$, $N(x)$, $D(x)$ are real scalar fields, contributing four bosonic dof, $V_\mu(x)$ is a real vector field contributing a further four bosonic dof, while the two complex spinor fields χ , λ give eight fermionic dof. Therefore $n_b = n_f$ again. Nonetheless this vector superfield still has excess dof due to gauge freedom. There is a supersymmetric gauge transformation $\exp(gV) \rightarrow \exp(-ig\hat{\phi}^\dagger)\exp(gV)\exp(ig\hat{\phi})$ which can be made, where $\hat{\phi}$ is a chiral superfield and g is the gauge coupling. For example specialising to the Wess-Zumino gauge removes three scalar dof, C , M , N and the four fermion dof contained in χ . This leaves just the ordinary gauge freedom $V_\mu \rightarrow V'_\mu = G(x)V_\mu G^{-1} + \frac{i}{g}(\partial_\mu G(x))G^{-1}$ where $G = \exp(i\mathbf{T} \cdot \alpha(\mathbf{x}))$, \mathbf{T} is a vector of the generators of the gauge group and $\alpha(\mathbf{x})$ is an arbitrary position dependent vector. When the gauge of V_μ is also fixed, a further bosonic dof is removed and only four fermionic and four bosonic dof remain,

$$V_{WZ}(z) = -\theta\sigma^\mu\bar{\theta}V_\mu(x) + i\theta^2\bar{\theta}\lambda(x) - i\bar{\theta}^2\theta\lambda(x) + \frac{1}{2}\theta^2\bar{\theta}^2 D(x). \quad (\text{A.14})$$

Appendix B

Construction of the E_6 SSM

B.1 Gauge Structure

The gauge group is

$$SU(3) \otimes SU(2) \otimes U(1)_Y \otimes U(1)_N, \quad (\text{B.1})$$

where $U(1)_N$ is defined by,

$$U(1)_N = \frac{1}{4}U(1)_\chi + \frac{\sqrt{15}}{4}U(1)_\psi, \quad (\text{B.2})$$

with $U(1)_\chi$ and $U(1)_\psi$ in turn, defined by the breaking,

$$E_6 \rightarrow SO(10) \times U(1)_\psi, \quad (\text{B.3})$$

$$SO(10) \rightarrow SU(5) \times U(1)_\chi. \quad (\text{B.4})$$

B.2 Matter content

The matter content is based on three generations of complete 27plet representations of E_6 in which anomalies are automatically cancelled. The 27_i multiplets decompose

under the $SU(5) \times U(1)_N$ subgroup of E_6 ,

$$27_i \rightarrow \left(10, \frac{1}{\sqrt{40}}\right)_i + \left(5^*, \frac{2}{\sqrt{40}}\right)_i + \left(5^*, -\frac{3}{\sqrt{40}}\right)_i + \left(5, -\frac{2}{\sqrt{40}}\right)_i + \left(1, \frac{5}{\sqrt{40}}\right)_i + (1, 0)_i, \quad (\text{B.5})$$

where the quantities in the brackets are the $SU(5)$ representation and extra $U(1)_N$ charge, respectively. Index i runs from 1 to 3 in family space. $SU(5)$ can break into the SM gauge group,

$$SU(5) \times U(1)_N \rightarrow SU(3)_C \times SU(2)_W \times U(1)_Y \times U(1)_N \quad (\text{B.6})$$

and the matter multiplets further decompose,

$$\begin{aligned} (10, 1)_i &\rightarrow Q_i \sim \left(3, 2, \frac{1}{6}, 1\right) & (5^*, 2)_i &\rightarrow d_i^c \sim \left(3^*, 1, \frac{1}{3}, 2\right) \\ u_i^c &\sim \left(3^*, 1, -\frac{2}{3}, 1\right) & L_i &\sim \left(1, 2, -\frac{1}{2}, 2\right) \\ e_i^c &\sim (1, 1, 1, 1); \end{aligned} \quad (\text{B.7})$$

$$\begin{aligned} (5^*, -3)_i &\rightarrow H_{1i} \sim \left(1, 2, -\frac{1}{2}, -3\right) & (5, -2)_i &\rightarrow H_{2i} \sim \left(1, 2, \frac{1}{2}, -2\right) \\ \bar{D}_i &\sim \left(3^*, 1, \frac{1}{3}, -3\right) & D_i &\sim \left(3, 1, -\frac{1}{3}, -2\right) \end{aligned} \quad (\text{B.8})$$

where the quantities in the brackets are the $SU(3)$ representations, $SU(2)$ representation, $U(1)_Y$ hypercharge and $U(1)_N$ charges.

So each 27plet, $(27)_i$, is filled with one generation of ordinary matter $(Q_i, u_i^c, d_i^c, L_i, e_i^c, N_i^c)$; a singlet field, S_i ; up and down type Higgs like fields, $H_{2,i}$ and $H_{1,i}$ and exotic colored matter, D_i, \bar{D}_i . In addition to the matter contained in complete 27plets, the model contains two extra $SU(2)$ doublets, H' and \bar{H}' which are components of $27'$ and $\bar{27}'$ E_6 representations that survive to low energies. The inclusion of H' and \bar{H}' affects the running of the gauge couplings at the one loop level and allows for unification at the GUT scale. So long as μ' (the parameter which sets their masses) is between the EW scale and 30TeV unification can still take place.

To summarise the matter content of the E_6 SSM is,

$$3 [(Q_i, u_i^c, d_i^c, L_i, e_i^c, N_i^c) + (S_i) + (H_{2i}) + (H_{1i}) + (D_i, \bar{D}_i)] + H' + \bar{H}', \quad (\text{B.9})$$

As mentioned in Sec. 7.1.5 the right-handed neutrinos, N_i^c , are expected to gain masses at some intermediate scale. All other matter in the E_6 SSM¹ should have masses between the TeV and EW scales near which the gauge group $U(1)_N$ is broken.

B.3 Superpotential

The most general renormalisable superpotential allowed by the low energy gauge structure of the E_6 SSM is,

$$W_{\text{total}} = W_{E_6} + W_{\cancel{E_6}}. \quad (\text{B.10})$$

where, W_{E_6} is the most general renormalisable superpotential which is allowed by the E_6 symmetry,

$$W_{E_6} = W_0 + W_1 + W_2,$$

$$\begin{aligned} W_0 = & \lambda_{ijk} S_i (H_{1j} H_{2k}) + \kappa_{ijk} S_i (D_j \bar{D}_k) + h_{ijk}^N N_i^c (H_{2j} L_k) + h_{ijk}^U u_i^c (H_{2j} Q_k) + \\ & + h_{ijk}^D d_i^c (H_{1j} Q_k) + h_{ijk}^E e_i^c (H_{1j} L_k), \end{aligned} \quad (\text{B.11})$$

$$W_1 = g_{ijk}^Q D_i (Q_j Q_k) + g_{ijk}^q \bar{D}_i d_j^c u_k^c,$$

$$W_2 = g_{ijk}^N N_i^c D_j d_k^c + g_{ijk}^E e_i^c D_j u_k^c + g_{ijk}^D (Q_i L_j) \bar{D}_k.$$

$W_{\cancel{E_6}}$ contains all terms which violate E_6 , are permitted by the low energy gauge structure of the E_6 SSM, $SU(3) \times SU(2) \times U(1)_Y \times U(1)_N$,

$$W_{\cancel{E_6}} = \frac{1}{2} M_{ij} N_i^c N_j^c + W'_0 + W'_1 + W'_2, \quad \text{and} \quad (\text{B.12})$$

¹There is other matter expected to appear at the unification scale, but the E_6 SSM is defined here as a low energy, phenomenological model which is only inspired by E_6 , not an actual E_6 GUT embedded model.

$$\begin{aligned}
W'_0 &= \mu'(H'\overline{H}') + \mu'_i(\overline{H}'L_i) + h_{ij}N_i^c(H_{2j}H') + h_{ij}^{H'}e_i^c(H_{1j}H'), \\
W'_1 &= \frac{\sigma_{ijk}}{3}N_i^cN_j^cN_k^c + \Lambda_k N_k^c + \lambda_{ij}S_i(H_{1j}\overline{H}') + g_{ij}^N N_i^c(\overline{H}'L_j) \\
&+ g_i^N N_i^c(\overline{H}'H') + g_{ij}^U u_i^c(\overline{H}'Q_j) + \mu_{ij}(H_{2i}L_j) + \mu_i(H_{2i}H') + \mu'_{ij}D_i d_j^c, \\
W'_2 &= g_{ij}^{H'}(Q_i H')\overline{D}_j, \quad i, j, k = 1, 2, 3.
\end{aligned} \tag{B.13}$$

Eq. (B.10) includes lepton and baryon number violating couplings which can induce proton decay. In addition the exotic fields in E_6 inspired SUSY models have new Yukawa interactions that will generally induce large non-diagonal flavour transitions in conflict with experiment. To suppress all of these unwanted effects a Z_2^H symmetry can be postulated.

Under this symmetry only one pair of Higgs like fields H_d , H_u and one singlet S are even under this symmetry and all other superfields are odd. We define,

$$H_d \equiv H_{1,3}, \quad H_u \equiv H_{2,3} \quad \text{and} \quad S \equiv S_3. \tag{B.14}$$

With this symmetry imposed only H_d interacts with the down type quarks and charged leptons and only one H_u couples to up type quarks while the couplings of all other exotic particles to the ordinary quarks and leptons are forbidden, eliminating problems with the non-diagonal flavour transitions.

However the Z_2^H symmetry can only be approximate as it results in a Lagrangian, invariant not only with respect to $U(1)_L$ and $U(1)_B$, but also under $U(1)_D$ symmetry transformations $D \rightarrow e^{i\alpha}D$ and $\overline{D} \rightarrow e^{-i\alpha}\overline{D}$.

The $U(1)_D$ invariance ensures that the lightest exotic quark is stable. Theoretical estimations, based on models of the early universe, imply such heavy stable particle should be confined in heavy hadrons which are present in terrestrial matter with a concentration [265] far above experimental limits [266]. So the Z_2^H symmetry in the E_6 SSM has to be broken, but the breakdown of Z_2^H should not give rise to operators leading to rapid proton decay.

This problem is overcome in the E_6 SSM in two different ways, which define two distinct, though closely related, models, E_6 SSMI and E_6 SSMII. One may insist that the resulting Lagrangian must be exactly invariant with respect to either a discrete Z_2^L symmetry, under which all superfields except lepton ones are even (E_6 SSMI), or under a discrete Z_2^B symmetry, which implies that exotic quark and lepton superfields are odd whereas the others remain even (E_6 SSMII). If the Lagrangian is invariant under the Z_2^B symmetry transformations then all terms in W_1 are forbidden and the exotic quarks are leptoquarks, i. e. they carry baryon ($B_D = 1/3$ and $B_{\overline{D}} = -1/3$) and lepton ($L_D = 1$ and $L_{\overline{D}} = -1$) numbers simultaneously. If Z_2^L is imposed then all terms in W_2 are forbidden and the baryon number conservation requires the exotic quarks to be diquarks², i.e. $B_D = -2/3$ and $B_{\overline{D}} = 2/3$. The two possible models can be summarised as,

$$W_{E_6\text{SSMI}} = W_0 + W_1 + \frac{1}{2}M_{ij}N_i^c N_j^c + W'_0, \quad (\text{B.15})$$

$$W_{E_6\text{SSMII}} = W_0 + W_2 + \frac{1}{2}M_{ij}N_i^c N_j^c + W'_0 + W'_2. \quad (\text{B.16})$$

Since Z_2^H symmetry violating operators lead to the non-diagonal flavour interactions, the corresponding Yukawa couplings are expected to be small. Moreover these Yukawa couplings must preserve either Z_2^B or Z_2^L symmetries that ensure proton stability. To guarantee that the contribution of new particles and interactions to the $K^0 - \overline{K}^0$ oscillations and to the muon decay channel $\mu \rightarrow e^- e^+ e^-$ are suppressed in accordance with experimental limits, it is necessary to assume that the Yukawa couplings of exotic particles to the ordinary quarks and leptons are less than $10^{-3} - 10^{-4}$. Since Z_2^H symmetry violating Yukawa couplings are expected to be so small they do not affect the RG flow of other masses and couplings and therefore can be safely ignored in our analysis of the particle spectrum.

The Z_2^H symmetry reduces the structure of the Yukawa interactions in the super-

²The breaking terms include a term a baryon violating $\mu'_{ij} D_i d_j^c$ which can lead to $p \rightarrow \pi^+ \chi^0$. So in E_6 SSMI this must be forbidden by an additional Z_2 symmetry, under which only Q_i , u_i^c , d_i^c are odd and all other superfields are even. This is not stressed here as it is not clear how this E_6 breaking term would be generated if one assumes an E_6 GUT embedding of the model.

potential of the E₆SSM to:

$$W_{E_6SSM I, II} \rightarrow \lambda_i S(H_{1i}H_{2i}) + \kappa_i S(D_i\overline{D}_i) + f_{\alpha\beta} S_\alpha(H_d H_{2\beta}) \quad (B.17)$$

$$+ \tilde{f}_{\alpha\beta} S_\alpha(H_{1\beta}H_u) + \frac{1}{2} M_{ij} N_i^c N_j^c + \mu'(H'\overline{H}') \quad (B.18)$$

$$+ h_{4j}^E (H_d H') e_j^c + h_{4j}^N (H_u H') N_j^c + W_{MSSM}(\mu = 0), \quad (B.19)$$

where $\alpha, \beta = 1, 2$ and $i = 1, 2, 3$. In Eq. (B.19) we choose the basis of $H_{1\alpha}, H_{2\alpha}, D_i$ and \overline{D}_i so that the Yukawa couplings of the singlet field S have flavor diagonal structure.

This model is constructed with the intent that the third generation fields $H_u = H_{2,3}, H_d = H_{1,3}$ and $S = S_3$ will be Higgs fields in this model and develop vevs,

$$\langle H_u^0 \rangle = v_u, \quad \langle H_d^0 \rangle = v_d, \quad \text{and} \quad \langle S \rangle = s, \quad (B.20)$$

where v_u and v_d give mass to ordinary matter, while s both gives mass to the exotic colored fields, $\kappa_i S \rightarrow \kappa_i s = m_{D_i}$ and generates an effective μ -term, $\mu_{eff} = \lambda_3 s$. To ensure that none of the fields $S_{1,2}, H$ and H' obtain a vev it is further assumed that,

$$\kappa_i \sim \lambda_3 \gtrsim \lambda_{1,2} \gg f_{\alpha\beta}, \tilde{f}_{\alpha\beta}, h_{4j}^E, h_{4j}^N. \quad (B.21)$$

For the purposes of Renormalisation Group analysis the couplings $f_{\alpha\beta}, \tilde{f}_{\alpha\beta}, h_{4j}^E, h_{4j}^N$ are sufficiently small that they can be neglected. This leaves a superpotential,

$$W_{E_6SSM} \approx \lambda_i S H_{1,i} H_{2,i} + \kappa_i S D_i \overline{D}_i + h_{ui} H_u Q_i u_{Ri}^c + h_{di} H_d Q_i d_{Ri}^c + h_{ei} H_d L_i e_{Ri}^c, \quad (B.22)$$

where $h_{ui} = \{h_u, h_c, h_t\}$ are the Yukawas for the up type quarks, $h_{di} = \{h_d, h_b, h_c\}$ are the Yukawas for the down type quarks, and $h_{ei} = \{h_e, h_\mu, h_\tau\}$ are the Yukawas for the charged leptons.

Appendix C

E_6 SSM Renormalisation Group Equations

The running of gauge coupling constants from the Grand Unification scale to the electroweak one is determined by the set of renormalisation group (RG) equations. The corresponding RG equations can be written as,

$$\frac{dG}{dt} = G \times B, \quad \frac{dg_2}{dt} = \frac{\beta_2 g_2^3}{(4\pi)^2}, \quad \frac{dg_3}{dt} = \frac{\beta_3 g_3^3}{(4\pi)^2}, \quad (\text{C.1})$$

where $t = \ln [Q/M_X]$ while B and G are 2×2 matrices describing the RG flow of the Abelian gauge couplings which is affected by the kinetic term mixing, i.e.

$$G = \begin{pmatrix} g_1 & g_{11} \\ 0 & g'_1 \end{pmatrix}, \quad (\text{C.2})$$

$$B = \begin{pmatrix} B_1 & B_{11} \\ 0 & B'_1 \end{pmatrix} = \frac{1}{(4\pi)^2} \begin{pmatrix} \beta_1 g_1^2 & 2g_1 g'_1 \beta_{11} + 2g_1 g_{11} \beta_1 \\ 0 & g_1'^2 \beta'_1 + 2g'_1 g_{11} \beta_{11} + g_{11}^2 \beta_1 \end{pmatrix}. \quad (\text{C.3})$$

In the one-loop approximation $\beta_{11} = \frac{\sqrt{6}}{5}$. The two-loop diagonal β functions of the E₆SSM gauge couplings are given by,

$$\beta_3 = -9 + 3N_g + \frac{1}{16\pi^2} \left[g_3^2(-54 + 34N_g) + 3N_g g_2^2 + N_g g_1^2 + N_g g_1'^2 - 4h_t^2 - 4h_b^2 - 2\Sigma_\kappa \right], \quad (\text{C.4})$$

$$\beta_2 = -5 + 3N_g + \frac{1}{16\pi^2} \left[8N_g g_3^2 + (-17 + 21N_g)g_2^2 + \left(\frac{3}{5} + N_g\right)g_1^2 + \left(\frac{2}{5} + N_g\right)g_1'^2 - 6h_t^2 - 6h_b^2 - 2h_\tau^2 - 2\Sigma_\lambda \right], \quad (\text{C.5})$$

$$\beta_1 = \frac{3}{5} + 3N_g + \frac{1}{16\pi^2} \left[8N_g g_3^2 + \left(\frac{9}{5} + 3N_g\right)g_2^2 + \left(\frac{9}{25} + 3N_g\right)g_1^2 + \left(\frac{6}{25} + N_g\right)g_1'^2 - \frac{26}{5}h_t^2 - \frac{14}{5}h_b^2 - \frac{18}{5}h_\tau^2 - \frac{6}{5}\Sigma_\lambda - \frac{4}{5}\Sigma_\kappa \right], \quad (\text{C.6})$$

$$\beta'_1 = \frac{2}{5} + 3N_g + \frac{1}{16\pi^2} \left[8N_g g_3^2 + \left(\frac{6}{5} + 3N_g\right)g_2^2 + \left(\frac{6}{25} + N_g\right)g_1^2 + \left(\frac{4}{25} + 3N_g\right)g_1'^2 - \frac{9}{5}h_t^2 - \frac{21}{5}h_b^2 - \frac{7}{5}h_\tau^2 - \frac{19}{5}\Sigma_\lambda - \frac{57}{10}\Sigma_\kappa \right], \quad (\text{C.7})$$

$$(\text{C.8})$$

where,

$$\Sigma_\lambda = \lambda_1^2 + \lambda_2^2 + \lambda_3^2, \quad \Sigma_\kappa = \kappa_1^2 + \kappa_2^2 + \kappa_3^2, \quad (\text{C.9})$$

The Yukawa couplings appeared in the superpotential of the E₆SSM obey the following system of two-loop renormalisation group equations:

$$\frac{d\lambda_i}{dt} = \frac{\lambda_i}{(4\pi)^2} \left[2\lambda_i^2 + 2\Sigma_\lambda + 3\Sigma_\kappa + (3h_t^2 + 3h_b^2 + h_\tau^2)\delta_{i3} - 3g_2^2 - \frac{3}{5}g_1^2 - \frac{19}{10}g_1'^2 + \frac{\beta_{\lambda_i}^{(2)}}{(4\pi)^2} \right], \quad (\text{C.10})$$

$$\frac{d\kappa_i}{dt} = \frac{\kappa_i}{(4\pi)^2} \left[2\kappa_i^2 + 2\Sigma_\lambda + 3\Sigma_\kappa - \frac{16}{3}g_3^2 - \frac{4}{15}g_1^2 - \frac{19}{10}g_1'^2 + \frac{\beta_{\kappa_i}^{(2)}}{(4\pi)^2} \right], \quad (\text{C.11})$$

$$\frac{dh_t}{dt} = \frac{h_t}{(4\pi)^2} \left[\lambda^2 + 6h_t^2 + h_b^2 - \frac{16}{3}g_3^2 - 3g_2^2 - \frac{13}{15}g_1^2 - \frac{3}{10}g_1'^2 + \frac{\beta_{h_t}^{(2)}}{(4\pi)^2} \right], \quad (\text{C.12})$$

$$\frac{dh_b}{dt} = \frac{h_b}{(4\pi)^2} \left[\lambda^2 + h_t^2 + 6h_b^2 + h_\tau^2 - \frac{16}{3}g_3^2 - 3g_2^2 - \frac{7}{15}g_1^2 - \frac{7}{10}g_1'^2 + \frac{\beta_{h_b}^{(2)}}{(4\pi)^2} \right], \quad (\text{C.13})$$

$$\frac{dh_\tau}{dt} = \frac{h_\tau}{(4\pi)^2} \left[\lambda^2 + 3h_b^2 + 4h_\tau^2 - 3g_2^2 - \frac{9}{5}g_1^2 - \frac{7}{10}g_1'^2 + \frac{\beta_{h_\tau}^{(2)}}{(4\pi)^2} \right], \quad (\text{C.14})$$

where the two-loop contributions to the corresponding β functions are given by,

$$\begin{aligned}
\beta_{\lambda_i}^{(2)} = & -2\lambda_i^2 \left(\lambda_i^2 + 2\Sigma_\lambda - \lambda^2 (3h_t^2 + 3h_b^2 + h_N^2 + h_\tau^2) \right) (2 + \delta_{i3}) \\
& - \left[9h_t^4 + 9h_b^4 + 6h_t^2 h_b^2 + 3h_\tau^4 + 3h_N^4 + 2h_\tau^2 h_N^2 \right] \delta_{i3} + 16g_3^2 \Sigma_\kappa + 6g_2^2 \Sigma_\lambda \\
& + g_1^2 \left(\frac{4}{5} \Sigma_\kappa + \frac{6}{5} \Sigma_\lambda \right) + g_1'^2 \left(\frac{5}{2} \lambda_i^2 - \frac{9}{5} \Sigma_\kappa - \frac{6}{5} \Sigma_\lambda \right) + \left[16g_3^2 (h_t^2 + h_b^2) \right. \\
& + g_1^2 \left(\frac{4}{5} h_t^2 - \frac{2}{5} h_b^2 + \frac{6}{5} h_\tau^2 \right) + g_1'^2 \left(-\frac{3}{10} h_t^2 - \frac{1}{5} h_b^2 - \frac{1}{5} h_\tau^2 \right) \left. \right] \delta_{i3} \\
& + 3g_2^4 \left(3N_g - \frac{7}{2} \right) + \frac{3}{5} g_1^4 \left(3N_g + \frac{9}{10} \right) + \frac{19}{10} g_1'^4 \left(3N_g + \frac{27}{20} \right) \\
& + \frac{9}{5} g_2^2 g_1^2 + \frac{39}{20} g_2^2 g_1'^2 + \frac{39}{100} g_1^2 g_1'^2 + 3\Sigma_\kappa \Big) - 4\Pi_\lambda - 6\Pi_\kappa, \tag{C.15}
\end{aligned}$$

$$\begin{aligned}
\beta_{\kappa_i}^{(2)} = & -2\kappa_i^2 \left(\kappa_i^2 + 2\Sigma_\lambda + 3\Sigma_\kappa \right) - 4\Pi_\lambda - 6\Pi_\kappa - 2\lambda^2 (3h_t^2 + 3h_b^2 + h_N^2 + h_\tau^2) \\
& + 16g_3^2 \Sigma_\kappa + 6g_2^2 \Sigma_\lambda + g_1^2 \left(\frac{4}{5} \Sigma_\kappa + \frac{6}{5} \Sigma_\lambda \right) + g_1'^2 \left(\frac{5}{2} \kappa_i^2 - \frac{9}{5} \Sigma_\kappa - \frac{6}{5} \Sigma_\lambda \right) \\
& + \frac{16}{3} g_3^4 \left(3N_g - \frac{19}{3} \right) + \frac{4}{15} g_1^4 \left(3N_g + \frac{11}{15} \right) \\
& + \frac{19}{10} g_1'^4 \left(3N_g + \frac{27}{20} \right) + \frac{64}{45} g_3^2 g_1^2 + \frac{52}{15} g_3^2 g_1'^2 + \frac{13}{75} g_1^2 g_1'^2, \tag{C.16}
\end{aligned}$$

$$\begin{aligned}
\beta_{h_t}^{(2)} = & -22h_t^4 - 5h_b^4 - 5h_t^2 h_b^2 - 3h_t^2 h_N^2 - h_b^2 h_\tau^2 - h_\tau^2 h_N^2 - 3h_N^4 \\
& - \lambda^2 \left(\lambda^2 + 3h_t^2 + 4h_b^2 + h_\tau^2 + 2\Sigma_\lambda + 3\Sigma_\kappa \right) \\
& + 16g_3^2 h_t^2 + 6g_2^2 h_t^2 + g_1^2 \left(\frac{6}{5} h_t^2 + \frac{2}{5} h_b^2 \right) \\
& + g_1'^2 \left(\frac{3}{2} \lambda^2 + \frac{3}{10} h_t^2 + \frac{3}{5} h_b^2 \right) + \frac{16}{3} g_3^4 \left(3N_g - \frac{19}{3} \right) + 3g_2^4 \left(3N_g - \frac{7}{2} \right) \\
& + \frac{13}{15} g_1^4 \left(3N_g + \frac{31}{30} \right) + \frac{3}{10} g_1'^4 \left(3N_g + \frac{11}{20} \right) + 8g_3^2 g_2^2 + \frac{136}{45} g_3^2 g_1^2 \\
& + \frac{8}{15} g_3^2 g_1'^2 + g_2^2 g_1^2 + \frac{3}{4} g_2^2 g_1'^2 + \frac{53}{300} g_1^2 g_1'^2, \tag{C.17}
\end{aligned}$$

$$\begin{aligned}
\beta_{h_b}^{(2)} = & -5h_t^4 - 22h_b^4 - 5h_t^2 h_b^2 - 3h_b^2 h_\tau^2 - h_t^2 h_N^2 - h_\tau^2 h_N^2 - 3h_N^4 \\
& - \lambda^2 \left(\lambda^2 + 4h_t^2 + 3h_b^2 + h_N^2 + 2\Sigma_\lambda + 3\Sigma_\kappa \right) \\
& + 16g_3^2 h_b^2 + 6g_2^2 h_b^2 + g_1^2 \left(\frac{4}{5} h_t^2 + \frac{2}{5} h_b^2 + \frac{6}{5} h_\tau^2 \right) \\
& + g_1'^2 \left(\lambda^2 + \frac{1}{5} h_t^2 + h_b^2 - \frac{1}{5} h_\tau^2 \right) + \frac{16}{3} g_3^4 \left(3N_g - \frac{19}{3} \right) + 3g_2^4 \left(3N_g - \frac{7}{2} \right)
\end{aligned}$$

$$\begin{aligned}
& + \frac{7}{15}g_1^4 \left(3N_g + \frac{5}{6}\right) + \frac{7}{10}g_1'^4 \left(3N_g + \frac{3}{4}\right) + 8g_3^2g_2^2 + \frac{8}{9}g_3^2g_1^2 + \frac{4}{3}g_3^2g_1'^2 \\
& + g_2^2g_1^2 + \frac{3}{2}g_2^2g_1'^2 + \frac{49}{150}g_1^2g_1'^2, \tag{C.18}
\end{aligned}$$

$$\begin{aligned}
\beta_{h_\tau}^{(2)} = & -9h_b^4 - 3h_t^2h_b^2 - 9h_b^2h_\tau^2 - 3h_t^2h_N^2 - 10h_\tau^4 - 3h_N^4 - 3h_\tau^2h_N^2 - \lambda^2 \left(\lambda^2 + 3h_t^2\right. \\
& + 2h_N^2 + 3h_\tau^2 + 2\Sigma_\lambda + 3\Sigma_\kappa \left.)\right) + 16g_3^2h_b^2 + 6g_2^2h_\tau^2 + g_1^2 \left(-\frac{2}{5}h_b^2 + \frac{6}{5}h_\tau^2\right) \\
& + g_1'^2 \left(\lambda^2 - \frac{1}{5}h_b^2 + \frac{13}{10}h_\tau^2\right) + 3g_2^4 \left(3N_g - \frac{7}{2}\right) + \frac{9}{5}g_1^4 \left(3N_g + \frac{3}{2}\right) \\
& + \frac{7}{10}g_1'^4 \left(3N_g + \frac{3}{4}\right) + \frac{9}{5}g_2^2g_1^2 + \frac{39}{20}g_2^2g_1'^2 + \frac{51}{100}g_1^2g_1'^2, \tag{C.19}
\end{aligned}$$

and

$$\Pi_\lambda = \lambda_1^4 + \lambda_2^4 + \lambda_3^4, \quad \Pi_\kappa = \kappa_1^4 + \kappa_2^4 + \kappa_3^4. \tag{C.20}$$

In the two-loop approximation the RG equations for the gaugino masses and trilinear scalar couplings take a form,

$$\begin{aligned}
\frac{dM_3}{dt} = & \frac{g_3^2}{16\pi^2} \left[(-18 + 6N_g)M_3 + \frac{1}{16\pi^2} \left((-216 + 136N_g)g_3^2M_3 \right. \right. \\
& + 6N_gg_2^2(M_2 + M_3) + 2N_gg_1^2(M_1 + M_3) + 2N_gg_1'^2(M_1' + M_3) \\
& \left. \left. - 8h_t^2(A_t + M_3) - 8h_b^2(A_b + M_3) - 4\Sigma_{A_\kappa} - 4\Sigma_\kappa M_3 \right) \right], \tag{C.21}
\end{aligned}$$

$$\begin{aligned}
\frac{dM_2}{dt} = & \frac{g_2^2}{16\pi^2} \left[(-10 + 6N_g)M_2 + \frac{1}{16\pi^2} \left(16N_gg_3^2(M_3 + M_2) \right. \right. \\
& + (-68 + 84N_g)g_2^2M_2 + \left(\frac{6}{5} + 2N_g\right)g_1^2(M_1 + M_2) \\
& + \left(\frac{4}{5} + 2N_g\right)g_1'^2(M_1' + M_2) - 12h_t^2(A_t + M_2) - 12h_b^2(A_b + M_2) \\
& \left. \left. - 4h_\tau^2(A_\tau + M_2) - 4\Sigma_{A_\lambda} - 4\Sigma_\lambda M_2 \right) \right], \tag{C.22}
\end{aligned}$$

$$\begin{aligned}
\frac{dM_1}{dt} = & \frac{g_1^2}{16\pi^2} \left[\left(\frac{6}{5} + 6N_g\right)M_1 + \frac{1}{16\pi^2} \left(16N_gg_3^2(M_3 + M_1) \right. \right. \\
& + \left(\frac{18}{5} + 6N_g\right)g_2^2(M_2 + M_1) + \left(\frac{36}{25}\right. \\
& \left. \left. + 12N_g\right)g_1^2M_1 + \left(\frac{12}{25} + 2N_g\right)g_1'^2(M_1' + M_1) \right]
\end{aligned}$$

$$\begin{aligned}
& - \frac{52}{5}h_t^2(A_t + M_1) - \frac{28}{5}h_b^2(A_b + M_1) - \frac{36}{5}h_\tau^2(A_\tau + M_1) \\
& - \left. \frac{12}{5}\Sigma_{A_\lambda} - \frac{12}{5}\Sigma_\lambda M_1 - \frac{8}{5}\Sigma_{A_\kappa} - \frac{8}{5}\Sigma_\kappa M_1 \right) \Big], \tag{C.23}
\end{aligned}$$

$$\begin{aligned}
\frac{dM'_1}{dt} &= \frac{g_1'^2}{16\pi^2} \left[\left(\frac{4}{5} + 6N_g \right) M'_1 + \frac{1}{16\pi^2} \left(16N_g g_3^2 (M_3 + M'_1) \right. \right. \\
& + \left. \left(\frac{12}{5} + 6N_g \right) g_2^2 (M_2 + M'_1) + \left(\frac{12}{25} + 2N_g \right) g_1^2 (M_1 + M'_1) \right. \\
& + \left. \left(\frac{16}{25} + 12N_g \right) g_1'^2 M'_1 \right. \\
& - \left. \frac{18}{5}h_t^2(A_t + M'_1) - \frac{42}{5}h_b^2(A_b + M'_1) - \frac{14}{5}h_\tau^2(A_\tau + M'_1) \right. \\
& - \left. \frac{38}{5}\Sigma_{A_\lambda} - \frac{38}{5}\Sigma_\lambda M'_1 - \frac{57}{5}\Sigma_{A_\kappa} - \frac{57}{5}\Sigma_\kappa M'_1 \right) \Big], \tag{C.24}
\end{aligned}$$

$$\begin{aligned}
& + \left(\frac{16}{25} + 12N_g \right) g_1'^2 M'_1 \\
& - \frac{18}{5}h_t^2(A_t + M'_1) - \frac{42}{5}h_b^2(A_b + M'_1) - \frac{14}{5}h_\tau^2(A_\tau + M'_1) \\
& - \left. \frac{38}{5}\Sigma_{A_\lambda} - \frac{38}{5}\Sigma_\lambda M'_1 - \frac{57}{5}\Sigma_{A_\kappa} - \frac{57}{5}\Sigma_\kappa M'_1 \right) \Big], \tag{C.25}
\end{aligned}$$

$$\begin{aligned}
\frac{dA_{\lambda_i}}{dt} &= \frac{1}{(4\pi)^2} \left[4\lambda_i^2 A_{\lambda_i} + 4\Sigma_{A_\lambda} + 6\Sigma_{A_\kappa} + (6h_t^2 A_t + 6h_b^2 A_b + 2h_\tau^2 A_\tau) \delta_{i3} \right. \\
& - 6g_2^2 M_2 - \frac{6}{5}g_1^2 M_1 - \frac{19}{5}g_1'^2 M'_1 + \left. \frac{\beta_{A_{\lambda_i}}^{(2)}}{(4\pi)^2} \right], \tag{C.26}
\end{aligned}$$

$$\begin{aligned}
\frac{dA_{\kappa_i}}{dt} &= \frac{1}{(4\pi)^2} \left[4\kappa_i^2 A_{\kappa_i} + 4\Sigma_{A_\lambda} + 6\Sigma_{A_\kappa} - \frac{32}{3}g_3^2 M_3 - \frac{8}{15}g_1^2 M_1 \right. \\
& - \frac{19}{5}g_1'^2 M'_1 + \left. \frac{\beta_{A_{\kappa_i}}^{(2)}}{(4\pi)^2} \right], \tag{C.27}
\end{aligned}$$

$$\begin{aligned}
\frac{dA_t}{dt} &= \frac{1}{(4\pi)^2} \left[2\lambda^2 A_\lambda + 12h_t^2 A_t + 2h_b^2 A_b - \frac{32}{3}g_3^2 M_3 - 6g_2^2 M_2 \right. \\
& - \frac{26}{15}g_1^2 M_1 - \frac{3}{5}g_1'^2 M'_1 + \left. \frac{\beta_{A_t}^{(2)}}{(4\pi)^2} \right], \tag{C.28}
\end{aligned}$$

$$\begin{aligned}
\frac{dA_b}{dt} &= \frac{1}{(4\pi)^2} \left[2\lambda^2 A_\lambda + 2h_t^2 A_t + 12h_b^2 A_b + 2h_\tau^2 A_\tau - \frac{32}{3}g_3^2 M_3 - 6g_2^2 M_2 \right. \\
& - \frac{14}{15}g_1^2 M_1 - \frac{7}{5}g_1'^2 M'_1 + \left. \frac{\beta_{A_b}^{(2)}}{(4\pi)^2} \right], \tag{C.29}
\end{aligned}$$

$$\begin{aligned}
\frac{dA_\tau}{dt} &= \frac{1}{(4\pi)^2} \left[2\lambda^2 A_\lambda + 6h_b^2 A_b + 8h_\tau^2 A_\tau - 6g_2^2 M_2 - \frac{18}{5}g_1^2 M_1 - \frac{7}{5}g_1'^2 M'_1 \right. \\
& + \left. \frac{\beta_{A_\tau}^{(2)}}{(4\pi)^2} \right], \tag{C.30}
\end{aligned}$$

where the two-loop contributions to the β functions of trilinear scalar couplings are

given by

$$\begin{aligned}
\beta_{A_{\lambda_i}}^{(2)} = & -4\lambda_i^2 \left(\lambda_i^2 + 2\Sigma_\lambda + 3\Sigma_\kappa \right) A_{\lambda_i} - 4\lambda_i^2 \left(\lambda_i^2 A_{\lambda_i} + 2\Sigma_{A_\lambda} + 3\Sigma_{A_\kappa} \right) \\
& -16\Pi_{A_\lambda} - 24\Pi_{A_\kappa} - 2\lambda^2 \left(3h_t^2 + 3h_b^2 + h_\tau^2 \right) (2 + \delta_{i3}) A_\lambda \\
& -2\lambda^2 \left(3h_t^2 A_t + 3h_b^2 A_b + h_\tau^2 A_\tau \right) (2 + \delta_{i3}) \\
& -12 \left[3h_t^4 A_t + 3h_b^4 A_b + h_t^2 h_b^2 (A_t + A_b) + h_\tau^4 A_\tau \right] \delta_{i3} + 32g_3^2 \left(\Sigma_\kappa M_3 + \Sigma_{A_\kappa} \right) \\
& + 12g_2^2 \left(\Sigma_\lambda M_2 + \Sigma_{A_\lambda} \right) + 2g_1^2 \left[\left(\frac{4}{5}\Sigma_\kappa + \frac{6}{5}\Sigma_\lambda \right) M_1 + \frac{4}{5}\Sigma_{A_\kappa} + \frac{6}{5}\Sigma_{A_\lambda} \right] \\
& + 2g_1'^2 \left[\left(\frac{5}{2}\lambda_i^2 - \frac{9}{5}\Sigma_\kappa - \frac{6}{5}\Sigma_\lambda \right) M_1' + \frac{5}{2}\lambda_i^2 A_{\lambda_i} - \frac{9}{5}\Sigma_{A_\kappa} - \frac{6}{5}\Sigma_{A_\lambda} \right] \\
& + 32g_3^2 \left[\left(h_t^2 + h_b^2 \right) M_3 + h_t^2 A_t + h_b^2 A_b \right] \delta_{i3} + 2g_1^2 \left[\left(\frac{4}{5}h_t^2 - \frac{2}{5}h_b^2 + \frac{6}{5}h_\tau^2 \right) M_1 \right. \\
& \left. + \frac{4}{5}h_t^2 A_t - \frac{2}{5}h_b^2 A_b + \frac{6}{5}h_\tau^2 A_\tau \right] \delta_{i3} + g_1'^2 \left[\left(-\frac{3}{5}h_t^2 - \frac{2}{5}h_b^2 - \frac{2}{5}h_\tau^2 \right) M_1' \right. \\
& \left. - \frac{3}{5}h_t^2 A_t - \frac{2}{5}h_b^2 A_b - \frac{2}{5}h_\tau^2 A_\tau \right] \delta_{i3} + 12g_2^4 \left(3N_g - \frac{7}{2} \right) M_2 \\
& + \frac{12}{5}g_1^4 \left(3N_g + \frac{9}{10} \right) M_1 + \frac{38}{5}g_1'^4 \left(3N_g + \frac{27}{20} \right) M_1' + \frac{18}{5}g_2^2 g_1^2 \left(M_2 + M_1 \right) \\
& + \frac{39}{10}g_2^2 g_1'^2 \left(M_2 + M_1' \right) + \frac{39}{50}g_1^2 g_1'^2 \left(M_1 + M_1' \right), \tag{C.31}
\end{aligned}$$

$$\begin{aligned}
\beta_{A_{\kappa_i}}^{(2)} = & -4\kappa_i^2 \left(\kappa_i^2 + 2\Sigma_\lambda + 3\Sigma_\kappa \right) A_{\kappa_i} - 4\kappa_i^2 \left(\kappa_i^2 A_{\kappa_i} + 2\Sigma_{A_\lambda} + 3\Sigma_{A_\kappa} \right) \\
& -16\Pi_{A_\lambda} - 24\Pi_{A_\kappa} - 4\lambda^2 \left(3h_t^2 + 3h_b^2 + h_\tau^2 \right) A_\lambda \\
& -4\lambda^2 \left(3h_t^2 A_t + 3h_b^2 A_b + h_\tau^2 A_\tau \right) + 32g_3^2 \left(\Sigma_\kappa M_3 + \Sigma_{A_\kappa} \right) \\
& + 12g_2^2 \left(\Sigma_\lambda M_2 + \Sigma_{A_\lambda} \right) + 2g_1^2 \left[\left(\frac{4}{5}\Sigma_\kappa + \frac{6}{5}\Sigma_\lambda \right) M_1 + \frac{4}{5}\Sigma_{A_\kappa} + \frac{6}{5}\Sigma_{A_\lambda} \right] \\
& + 2g_1'^2 \left[\left(\frac{5}{2}\kappa_i^2 - \frac{9}{5}\Sigma_\kappa - \frac{6}{5}\Sigma_\lambda \right) M_1' + \frac{5}{2}\kappa_i^2 A_{\kappa_i} - \frac{9}{5}\Sigma_{A_\kappa} - \frac{6}{5}\Sigma_{A_\lambda} \right] \\
& + \frac{64}{3}g_3^4 \left(3N_g - \frac{19}{3} \right) M_3 + \frac{16}{15}g_1^4 \left(3N_g + \frac{11}{15} \right) M_1 \\
& + \frac{38}{5}g_1'^4 \left(3N_g + \frac{27}{20} \right) M_1' + \frac{128}{45}g_3^2 g_1^2 \left(M_3 + M_1 \right) + \frac{104}{15}g_3^2 g_1'^2 \left(M_3 + M_1' \right) \\
& + \frac{26}{75}g_1^2 g_1'^2 \left(M_1 + M_1' \right), \tag{C.32}
\end{aligned}$$

$$\begin{aligned}
\beta_{A_t}^{(2)} = & -88h_t^4 A_t - 20h_b^4 A_b - 10h_t^2 h_b^2 \left(A_t + A_b \right) - 2h_b^2 h_\tau^2 \left(A_b + A_\tau \right) \\
& -2\lambda^2 \left[\left(2\lambda^2 + 3h_t^2 + 4h_b^2 + h_\tau^2 + 2\Sigma_\lambda + 3\Sigma_\kappa \right) A_\lambda + 3h_t^2 A_t + 4h_b^2 A_b + h_\tau^2 A_\tau \right]
\end{aligned}$$

$$\begin{aligned}
& +2\Sigma_{A_\lambda} + 3\Sigma_{A_\kappa} \Big] + 32g_3^2 h_t^2 (M_3 + A_t) + 12g_2^2 h_t^2 (M_2 + A_t) \\
& + 2g_1^2 \left[\left(\frac{6}{5} h_t^2 + \frac{2}{5} h_b^2 \right) M_1 + \frac{6}{5} h_t^2 A_t + \frac{2}{5} h_b^2 A_b \right] \\
& + 2g_1'^2 \left[\left(\frac{3}{2} \lambda^2 + \frac{3}{10} h_t^2 + \frac{3}{5} h_b^2 \right) M_1' + \frac{3}{2} \lambda^2 A_\lambda + \frac{3}{10} h_t^2 A_t + \frac{3}{5} h_b^2 A_b \right] \\
& + \frac{64}{3} g_3^4 \left(3N_g - \frac{19}{3} \right) M_3 + 12g_2^4 \left(3N_g - \frac{7}{2} \right) M_2 \\
& + \frac{52}{15} g_1^4 \left(3N_g + \frac{31}{30} \right) M_1 + \frac{6}{5} g_1'^4 \left(3N_g + \frac{11}{20} \right) M_1' + 16g_3^2 g_2^2 (M_3 + M_2) \\
& + \frac{272}{45} g_3^2 g_1^2 (M_3 + M_1) + \frac{16}{15} g_3^2 g_1'^2 (M_3 + M_1') + 2g_2^2 g_1^2 (M_2 + M_1) \\
& + \frac{3}{2} g_2^2 g_1'^2 (M_2 + M_1') + \frac{53}{150} g_1^2 g_1'^2 (M_1 + M_1'), \tag{C.33}
\end{aligned}$$

$$\begin{aligned}
\beta_{A_b}^{(2)} & = -20h_t^4 A_t - 88h_b^4 A_b - 10h_t^2 h_b^2 (A_t + A_b) - 6h_b^2 h_\tau^2 (A_b + A_\tau) - 12h_\tau^4 A_\tau \\
& - 2\lambda^2 \left[(2\lambda^2 + 4h_t^2 + 3h_b^2 + 2\Sigma_\lambda + 3\Sigma_\kappa) A_\lambda + 4h_t^2 A_t + 3h_b^2 A_b \right. \\
& \left. + 2\Sigma_{A_\lambda} + 3\Sigma_{A_\kappa} \right] + 32g_3^2 h_b^2 (M_3 + A_b) + 12g_2^2 h_b^2 (M_2 + A_b) \\
& + 4g_1^2 \left[\left(\frac{2}{5} h_t^2 + \frac{1}{5} h_b^2 + \frac{3}{5} h_\tau^2 \right) M_1 + \frac{2}{5} h_t^2 A_t + \frac{1}{5} h_b^2 A_b + \frac{3}{5} h_\tau^2 A_\tau \right] \\
& + 2g_1'^2 \left[\left(\lambda^2 + \frac{1}{5} h_t^2 + h_b^2 - \frac{1}{5} h_\tau^2 \right) M_1' + \lambda^2 A_\lambda + \frac{1}{5} h_t^2 A_t + h_b^2 A_b - \frac{1}{5} h_\tau^2 A_\tau \right] \\
& + \frac{64}{3} g_3^4 \left(3N_g - \frac{19}{3} \right) M_3 + 12g_2^4 \left(3N_g - \frac{7}{2} \right) M_2 \\
& + \frac{28}{15} g_1^4 \left(3N_g + \frac{5}{6} \right) M_1 + \frac{14}{5} g_1'^4 \left(3N_g + \frac{3}{4} \right) M_1' + 16g_3^2 g_2^2 (M_3 + M_2) \\
& + \frac{16}{9} g_3^2 g_1^2 (M_3 + M_1) + \frac{8}{3} g_3^2 g_1'^2 (M_3 + M_1') + 2g_2^2 g_1^2 (M_2 + M_1) \\
& + 3g_2^2 g_1'^2 (M_2 + M_1') + \frac{49}{75} g_1^2 g_1'^2 (M_1 + M_1'), \tag{C.34}
\end{aligned}$$

$$\begin{aligned}
\beta_{A_\tau}^{(2)} & = -36h_b^4 A_b - 6h_t^2 h_b^2 (A_t + A_b) - 18h_b^2 h_\tau^2 (A_b + A_\tau) - 40h_\tau^4 A_\tau \\
& - 2\lambda^2 \left[(2\lambda^2 + 3h_t^2 + 3h_\tau^2 + 2\Sigma_\lambda + 3\Sigma_\kappa) A_\lambda + 3h_t^2 A_t + 3h_\tau^2 A_\tau \right. \\
& \left. + 2\Sigma_{A_\lambda} + 3\Sigma_{A_\kappa} \right] + 32g_3^2 h_b^2 (M_3 + A_b) + 12g_2^2 h_\tau^2 (M_2 + A_\tau) \\
& + 4g_1^2 \left[\left(-\frac{1}{5} h_b^2 + \frac{3}{5} h_\tau^2 \right) M_1 - \frac{1}{5} h_b^2 A_b + \frac{3}{5} h_\tau^2 A_\tau \right] \\
& + 2g_1'^2 \left[\left(\lambda^2 - \frac{1}{5} h_b^2 + \frac{13}{10} h_\tau^2 \right) M_1' + \lambda^2 A_\lambda - \frac{1}{5} h_b^2 A_b + \frac{13}{10} h_\tau^2 A_\tau \right]
\end{aligned}$$

$$\begin{aligned}
& +12g_2^4\left(3N_g - \frac{7}{2}\right)M_2 + \frac{36}{5}g_1^4\left(3N_g + \frac{3}{2}\right)M_1 + \frac{14}{5}g_1'^4\left(3N_g + \frac{3}{4}\right)M_1' \\
& + \frac{18}{5}g_2^2g_1^2(M_2 + M_1) + \frac{39}{10}g_2^2g_1'^2(M_2 + M_1') + \frac{51}{50}g_1^2g_1'^2(M_1 + M_1'), \quad (C.35)
\end{aligned}$$

where

$$\begin{aligned}
\Sigma_{A_\lambda} &= \lambda_1^2 A_{\lambda_1} + \lambda_2^2 A_{\lambda_2} + \lambda_3^2 A_{\lambda_3}, & \Sigma_{A_\kappa} &= \kappa_1^2 A_{\kappa_1} + \kappa_2^2 A_{\kappa_2} + \kappa_3^2 A_{\kappa_3}, \\
\Pi_\lambda &= \lambda_1^4 A_{\lambda_1} + \lambda_2^4 A_{\lambda_2} + \lambda_3^4 A_{\lambda_3}, & \Pi_\kappa &= \kappa_1^4 A_{\kappa_1} + \kappa_2^4 A_{\kappa_2} + \kappa_3^4 A_{\kappa_3}.
\end{aligned} \quad (C.36)$$

The one-loop RG equations for the soft scalar masses can be written as

$$\begin{aligned}
\frac{dm_{S_i}^2}{dt} &= \frac{1}{(4\pi)^2} \left[\sum_{j=1..3} 4\lambda_j^2 (m_{H_{2j}}^2 + m_{H_{1j}}^2 + m_S^2 + A_{\lambda_j}^2) \delta_{i3} \right. \\
& \left. + \sum_{j=1..3} 6\kappa_j^2 (m_S^2 + m_{D_j}^2 + m_{\bar{D}_j}^2 + A_{\kappa_j}^2) \delta_{i3} - 5g_1'^2 M_1'^2 + \frac{g_1'^2}{4} \Sigma_1' \right], \quad (C.37)
\end{aligned}$$

$$\begin{aligned}
\frac{dm_{H_{2i}}^2}{dt} &= \frac{1}{(4\pi)^2} \left[2\lambda_i^2 (m_{H_{2i}}^2 + m_{H_{1i}}^2 + m_S^2 + A_{\lambda_i}^2) + 6h_t^2 (m_{H_u}^2 + m_Q^2 + m_{t^c}^2 \right. \\
& \left. + A_t^2) \delta_{i3} - 6g_2^2 M_2^2 - \frac{6}{5}g_1^2 M_1^2 - \frac{4}{5}g_1'^2 M_1'^2 + \frac{3}{5}g_1^2 \Sigma_1 - \frac{g_1'^2}{10} \Sigma_1' \right], \quad (C.38)
\end{aligned}$$

$$\begin{aligned}
\frac{dm_{H_{1i}}^2}{dt} &= \frac{1}{(4\pi)^2} \left[2\lambda_i^2 (m_{H_{2i}}^2 + m_{H_{1i}}^2 + m_S^2 + A_{\lambda_i}^2) + 6h_b^2 (m_{H_d}^2 + m_Q^2 \right. \\
& \left. + m_{b^c}^2 + A_b^2) \delta_{i3} + 2h_\tau^2 (m_{H_d}^2 + m_L^2 + m_{\tau^c}^2 + A_\tau^2) \delta_{i3} \right. \\
& \left. - 6g_2^2 M_2^2 - \frac{6}{5}g_1^2 M_1^2 - \frac{9}{5}g_1'^2 M_1'^2 - \frac{3}{5}g_1^2 \Sigma_1 - \frac{3}{20}g_1'^2 \Sigma_1' \right], \quad (C.39)
\end{aligned}$$

$$\begin{aligned}
\frac{dm_{Q_i}^2}{dt} &= \frac{1}{(4\pi)^2} \left[2h_t^2 (m_{H_u}^2 + m_Q^2 + m_{t^c}^2 + A_t^2) \delta_{i3} + 2h_b^2 (m_{H_d}^2 + m_Q^2 + m_{b^c}^2 \right. \\
& \left. + A_b^2) \delta_{i3} - \frac{32}{3}g_3^2 M_3^2 - 6g_2^2 M_2^2 - \frac{2}{15}g_1^2 M_1^2 - \frac{1}{5}g_1'^2 M_1'^2 \right. \\
& \left. + \frac{1}{5}g_1^2 \Sigma_1 + \frac{g_1'^2}{20} \Sigma_1' \right], \quad (C.40)
\end{aligned}$$

$$\begin{aligned}
\frac{dm_{u_i^c}^2}{dt} &= \frac{1}{(4\pi)^2} \left[4h_t^2 (m_{H_u}^2 + m_Q^2 + m_{t^c}^2 + A_t^2) \delta_{i3} - \frac{32}{3}g_3^2 M_3^2 - \frac{32}{15}g_1^2 M_1^2 \right. \\
& \left. - \frac{1}{5}g_1'^2 M_1'^2 - \frac{4}{5}g_1^2 \Sigma_1 + \frac{g_1'^2}{20} \Sigma_1' \right], \quad (C.41)
\end{aligned}$$

$$\frac{dm_{d_i^c}^2}{dt} = \frac{1}{(4\pi)^2} \left[4h_b^2 (m_{H_d}^2 + m_Q^2 + m_{b^c}^2 + A_b^2) \delta_{i3} - \frac{32}{3}g_3^2 M_3^2 - \frac{8}{15}g_1^2 M_1^2 \right]$$

$$-\frac{4}{5}g_1'^2 M_1'^2 + \frac{2}{5}g_1^2 \Sigma_1 + \frac{g_1'^2}{10} \Sigma_1'] , \quad (\text{C.42})$$

$$\begin{aligned} \frac{dm_{L_i}^2}{dt} &= \frac{1}{(4\pi)^2} \left[2h_\tau^2 (m_{H_d}^2 + m_L^2 + m_{\tau^c}^2 + A_\tau^2) \delta_{i3} + -6g_2^2 M_2^2 - \frac{6}{5}g_1^2 M_1^2 \right. \\ &\quad \left. - \frac{4}{5}g_1'^2 M_1'^2 - \frac{3}{5}g_1^2 \Sigma_1 + \frac{g_1'^2}{10} \Sigma_1' \right] , \end{aligned} \quad (\text{C.43})$$

$$\begin{aligned} \frac{dm_{e_i^c}^2}{dt} &= \frac{1}{(4\pi)^2} \left[4h_\tau^2 (m_{H_d}^2 + m_L^2 + m_{\tau^c}^2 + A_\tau^2) \delta_{i3} - \frac{24}{5}g_1^2 M_1^2 \right. \\ &\quad \left. - \frac{1}{5}g_1'^2 M_1'^2 + \frac{6}{5}g_1^2 \Sigma_1 + \frac{g_1'^2}{20} \Sigma_1' \right] , \end{aligned} \quad (\text{C.44})$$

$$\begin{aligned} \frac{dm_{D_i}^2}{dt} &= \frac{1}{(4\pi)^2} \left[2\kappa_i^2 (m_S^2 + m_{D_i}^2 + m_{\bar{D}_i}^2 + A_{\kappa_i}^2) - \frac{32}{3}g_3^2 M_3^2 - \frac{8}{15}g_1^2 M_1^2 \right. \\ &\quad \left. - \frac{4}{5}g_1'^2 M_1'^2 - \frac{2}{5}g_1^2 \Sigma_1 - \frac{g_1'^2}{10} \Sigma_1' \right] , \end{aligned} \quad (\text{C.45})$$

$$\begin{aligned} \frac{dm_{\bar{D}_i}^2}{dt} &= \frac{1}{(4\pi)^2} \left[2\kappa_i^2 (m_S^2 + m_{D_i}^2 + m_{\bar{D}_i}^2 + A_{\kappa_i}^2) - \frac{32}{3}g_3^2 M_3^2 - \frac{8}{15}g_1^2 M_1^2 \right. \\ &\quad \left. - \frac{9}{5}g_1'^2 M_1'^2 + \frac{2}{5}g_1^2 \Sigma_1 - \frac{3}{20}g_1'^2 \Sigma_1' \right] , \end{aligned} \quad (\text{C.46})$$

$$\frac{dm_{H'}^2}{dt} = \frac{1}{(4\pi)^2} \left[-6g_2^2 M_2^2 - \frac{6}{5}g_1^2 M_1^2 - \frac{4}{5}g_1'^2 M_1'^2 - \frac{3}{5}g_1^2 \Sigma_1 + \frac{g_1'^2}{10} \Sigma_1' \right] , \quad (\text{C.47})$$

$$\frac{dm_{\bar{H}'}^2}{dt} = \frac{1}{(4\pi)^2} \left[-6g_2^2 M_2^2 - \frac{6}{5}g_1^2 M_1^2 - \frac{4}{5}g_1'^2 M_1'^2 + \frac{3}{5}g_1^2 \Sigma_1 - \frac{g_1'^2}{10} \Sigma_1' \right] , \quad (\text{C.48})$$

where

$$\begin{aligned} \Sigma_1 &= \sum_{i=1}^3 \left(m_{Q_i}^2 - 2m_{u_i^c}^2 + m_{d_i^c}^2 + m_{e_i^c}^2 - m_{L_i}^2 + m_{H_{2i}}^2 - m_{H_{1i}}^2 + m_{D_i}^2 - m_{\bar{D}_i}^2 \right) \\ &\quad - m_{H'}^2 + m_{\bar{H}'}^2 , \end{aligned} \quad (\text{C.49})$$

$$\begin{aligned} \Sigma_1' &= \sum_{i=1}^3 \left(6m_{Q_i}^2 + 3m_{u_i^c}^2 + 6m_{d_i^c}^2 + m_{e_i^c}^2 + 4m_{L_i}^2 - 4m_{H_{2i}}^2 - 6m_{H_{1i}}^2 + 5m_{S_i}^2 \right. \\ &\quad \left. - 9m_{D_i}^2 - 6m_{\bar{D}_i}^2 \right) + 4m_{H'}^2 - 4m_{\bar{H}'}^2 . \end{aligned} \quad (\text{C.50})$$

Appendix D

One loop corrections to the Higgs masses in the E_6 SSM

Higgs masses are obtained by taking double derivatives of the effective potential with respect to the Higgs fields.

The tree level Higgs masses for the CP-even Higgs sector were presented in Sec.7.3, Eq. 7.40. The expression for the one loop contribution, $\Delta V^{(1)}$, to the effective potential also appears in Eq. 7.16 and the physical masses of the stops, appearing in this equation, are calculated in the tree level approximation,

$$m_{\tilde{t}_1, \tilde{t}_2}^2 = 0.5 \left[m_Q^2 + m_U^2 + 2m_t^2 + \Delta_Q + \Delta_U \mp \sqrt{(m_Q^2 - m_U^2 + \Delta_Q - \Delta_U)^2 + 4m_t^2 \left(A_t - \frac{\lambda_s}{\sqrt{2} \tan \beta} \right)^2} \right] \quad (\text{D.1})$$

where

$$\Delta_Q = 0.125(g_2^2 - 0.2g_1^2)(v_1^2 - v_2^2) + \frac{g_1'}{80}(-3v_1^2 - 2v_2^2 + 5s^2) \quad (\text{D.2})$$

$$\Delta_T = g_1^2(v_1^2 - v_2^2) + \frac{g_1'}{80}(-3v_1^2 - 2v_2^2 + 5s^2) \quad (\text{D.3})$$

Only including stop/top contributions we find,

$$\frac{\partial \Delta V}{\partial x} = \frac{3}{32\pi^2} \left[2a_0(m_{\tilde{t}_1}) \frac{\partial}{\partial x} m_{\tilde{t}_1}^2 + 2a_0(m_{\tilde{t}_2}) \frac{\partial}{\partial x} m_{\tilde{t}_2}^2 - 4a_0(m_t) \frac{\partial}{\partial x} m_t^2 \right], \quad (\text{D.4})$$

where

$$a_0(m) \equiv m^2 \left[\ln \frac{m^2}{Q^2} - 1 \right]. \quad (\text{D.5})$$

Now defining

$$\Delta_x m_i \equiv a_0(m_i) \frac{\partial}{\partial x} m_i^2, \quad (\text{D.6})$$

$$\Rightarrow \frac{\partial^2 \Delta V}{\partial y \partial x} = \frac{3}{32\pi^2} \left[2 \frac{\partial}{\partial y} \Delta_x m_{\tilde{t}_1} + 2 \frac{\partial}{\partial y} \Delta_x m_{\tilde{t}_2} - 4 \frac{\partial}{\partial y} \Delta_x m_t \right], \quad (\text{D.7})$$

$$\frac{\partial}{\partial x} \Delta_x m = \left(\frac{\partial}{\partial x} m^2 \right)^2 \ln \frac{m^2}{Q^2} + a_0(m) \frac{\partial^2}{\partial x^2} m^2 \quad (\text{D.8})$$

$$\frac{\partial}{\partial y} \Delta_x m = \left(\frac{\partial}{\partial y} m^2 \right) \left(\frac{\partial}{\partial x} m^2 \right) \ln \frac{m^2}{Q^2} + a_0(m) \frac{\partial^2}{\partial y \partial x} m^2 \quad (\text{D.9})$$

Now we obtain single and double derivatives of the masses.

D.1 Single Derivatives

$$m_{\tilde{t}_1, \tilde{t}_2}^2 = 0.5 \left[m_Q^2 + m_U^2 + 2m_t^2 + \Delta_Q + \Delta_U \pm \sqrt{r_t} \right] \quad (\text{D.10})$$

$$r_t \equiv (m_Q^2 - m_U^2 + \Delta_Q - \Delta_U)^2 + 4m_t^2 \left(A_t - \frac{\lambda s}{\sqrt{2} \tan \beta} \right)^2 \quad (\text{D.11})$$

$$\frac{\partial}{\partial s} m_t^2 = \frac{\partial}{\partial v_1} m_t^2 = 0 \quad \frac{\partial}{\partial v_2} m_t^2 = v_2 y_t^2 \quad (\text{D.12})$$

$$\frac{\partial}{\partial s} m_{\tilde{t}_1, \tilde{t}_2}^2 = 0.5 [0.25 g_1'^2 s \pm 0.5 r_t^{-\frac{1}{2}} \left(\frac{\partial}{\partial s} r_t \right)] \quad (\text{D.13})$$

$$\frac{\partial}{\partial s} r_t = -8m_t^2 \left(A_t - \frac{\lambda s}{\sqrt{2} \tan \beta} \right) \frac{\lambda}{\sqrt{2} \tan \beta} \quad (\text{D.14})$$

$$\frac{\partial}{\partial v_1} m_{\tilde{t}_1, \tilde{t}_2}^2 = 0.5 [0.25 (g_2^2 + 0.6 g_1'^2) v_1 - \frac{6}{40} g_1' v_1 \pm 0.5 r_t^{-\frac{1}{2}} \left(\frac{\partial}{\partial v_1} r_t \right)] \quad (\text{D.15})$$

$$\frac{\partial}{\partial v_1} r_t = 0.5 (g_2^2 - g_1'^2) v_1 (m_Q^2 - m_U^2 + \Delta_Q - \Delta_U)$$

$$-8m_t^2(A_t - \frac{\lambda s}{\sqrt{2} \tan \beta}) \frac{s\lambda}{\sqrt{2}v_2} \quad (\text{D.16})$$

$$\frac{\partial}{\partial v_2} m_{\tilde{t}_1, \tilde{t}_2}^2 = 0.5[2v_2 y_t^2 - 0.25(g_2^2 + 0.6g_1^2)v_2 - \frac{1}{10}g_1' v_2 \pm 0.5r_t^{-\frac{1}{2}}(\frac{\partial}{\partial v_2} r_t)] \quad (\text{D.17})$$

$$\begin{aligned} \frac{\partial}{\partial v_2} r_t &= -0.5(g_2^2 - g_1^2)v_2(m_Q^2 - m_U^2 + \Delta_Q - \Delta_U) \\ &+ 4(A_t - \frac{\lambda s}{\sqrt{2} \tan \beta})^2 v_2 y_t^2 + 8m_t^2(A_t - \frac{\lambda s}{\sqrt{2} \tan \beta}) \frac{sv_1 \lambda}{\sqrt{2}v_2^2} \end{aligned} \quad (\text{D.18})$$

D.2 Double derivatives

$$\frac{\partial^2}{\partial s^2} m_{\tilde{t}_1, \tilde{t}_2}^2 = 0.5[0.25g_1'^2 \pm 0.5r_t^{-\frac{1}{2}}(\frac{\partial^2}{\partial s^2} r_t) \mp 0.25(\frac{\partial}{\partial s} r_t)^2 r_t^{-\frac{3}{2}}] \quad (\text{D.19})$$

$$\frac{\partial^2}{\partial s^2} r_t = 8m_t^2(\frac{\lambda}{\sqrt{2} \tan \beta})^2 \quad (\text{D.20})$$

$$\frac{\partial^2}{\partial v_1^2} m_{\tilde{t}_1, \tilde{t}_2}^2 = 0.5[0.25\bar{g}^2 - \frac{6}{40}g_1'^2 \pm 0.5r_t^{-\frac{1}{2}}(\frac{\partial^2}{\partial v_1^2} r_t) \mp 0.25(\frac{\partial}{\partial v_1} r_t)^2 r_t^{-\frac{3}{2}}] \quad (\text{D.21})$$

$$\begin{aligned} \frac{\partial}{\partial v_1} r_t &= 0.5(g_2^2 - g_1^2)(m_Q^2 - m_U^2 + \Delta_Q - \Delta_U) + 0.125(g_2^2 - g_1^2)^2 v_1^2 \\ &+ 8m_t^2(\frac{s\lambda}{\sqrt{2}v_2})^2 \end{aligned} \quad (\text{D.22})$$

$$\frac{\partial^2}{\partial v_2^2} m_{\tilde{t}_1, \tilde{t}_2}^2 = 0.5[2y_t^2 - 0.25\bar{g}^2 - \frac{1}{10}g_1'^2 \pm 0.5r_t^{-\frac{1}{2}}(\frac{\partial^2}{\partial v_2^2} r_t) \mp 0.25(\frac{\partial}{\partial v_2} r_t)^2 r_t^{-\frac{3}{2}}] \quad (\text{D.23})$$

$$\begin{aligned} \frac{\partial^2}{\partial v_2^2} r_t &= -0.5(g_2^2 - g_1^2)(m_Q^2 - m_U^2 + \Delta_Q - \Delta_U) + 0.125(g_2^2 - g_1^2)^2 v_2^2 \\ &+ 4(A_t - \frac{\lambda s}{\sqrt{2} \tan \beta})^2 y_t^2 \\ &+ 8(A_t - \frac{\lambda s}{\sqrt{2} \tan \beta})v_2(\frac{sv_1 \lambda}{\sqrt{2}v_2^2}) + 8m_t^2(\frac{sv_1 \lambda}{\sqrt{2}v_2^2})^2 \end{aligned} \quad (\text{D.24})$$

$$\frac{\partial^2}{\partial v_1 \partial s} m_{\tilde{t}_1, \tilde{t}_2}^2 = 0.5[\pm 0.5r_t^{-\frac{1}{2}}(\frac{\partial^2}{\partial v_1 \partial s} r_t) \mp 0.25(\frac{\partial}{\partial v_1} r_t)(\frac{\partial}{\partial s} r_t)r_t^{-\frac{3}{2}}] \quad (\text{D.25})$$

$$\frac{\partial^2}{\partial v_1 \partial s} r_t = +8m_t^2(\frac{v_1 \lambda}{\sqrt{2}v_2})(\frac{s\lambda}{\sqrt{2}v_2}) - 8m_t^2(\frac{\lambda}{\sqrt{2}v_2^2})(A_t - \frac{\lambda s}{\sqrt{2} \tan \beta}) \quad (\text{D.26})$$

$$\frac{\partial^2}{\partial v_2 \partial s} m_{\tilde{t}_1, \tilde{t}_2}^2 = 0.5[\pm 0.5r_t^{-\frac{1}{2}}(\frac{\partial^2}{\partial v_2 \partial s} r_t) \mp 0.25(\frac{\partial}{\partial v_2} r_t)(\frac{\partial}{\partial s} r_t)r_t^{-\frac{3}{2}}] \quad (\text{D.27})$$

$$\begin{aligned} \frac{\partial^2}{\partial v_2 \partial s} r_t &= -8y_t^2 v_2 \left(A_t - \frac{\lambda s}{\sqrt{2} \tan \beta} \right) \left(\frac{\lambda}{\sqrt{2} \tan \beta} \right) - 8m_t^2 \left(\frac{v_1 \lambda}{\sqrt{2} v_2} \right) \left(\frac{s \lambda v_1}{\sqrt{2} v_2^2} \right) \\ &\quad + 8m_t^2 \left(\frac{v_1 \lambda}{\sqrt{2} v_2^2} \right) \left(A_t - \frac{\lambda s}{\sqrt{2} \tan \beta} \right) \end{aligned} \quad (\text{D.28})$$

$$\frac{\partial^2}{\partial v_2 \partial v_1} m_{\tilde{t}_1, \tilde{t}_2}^2 = 0.5 [\pm 0.5 r_t^{-\frac{1}{2}} \left(\frac{\partial^2}{\partial v_2 \partial v_1} r_t \right) \mp 0.25 \left(\frac{\partial}{\partial v_2} r_t \right) \left(\frac{\partial}{\partial v_1} r_t \right) r_t^{-\frac{3}{2}}] \quad (\text{D.29})$$

$$\begin{aligned} \frac{\partial^2}{\partial v_2 \partial v_1} r_t &= -0.125 (g_2^2 - g_1^2)^2 v_1 v_2 - 8y_t^2 v_2 \left(A_t - \frac{\lambda s}{\sqrt{2} \tan \beta} \right) \left(s \frac{\lambda}{\sqrt{2} v_2} \right) \\ &\quad - 8m_t^2 \left(\frac{s \lambda}{\sqrt{2} v_2} \right) \left(\frac{s \lambda v_1}{\sqrt{2} v_2^2} \right) + 8m_t^2 \left(\frac{s \lambda}{\sqrt{2} v_2^2} \right) \left(A_t - \frac{\lambda s}{\sqrt{2} \tan \beta} \right) \end{aligned} \quad (\text{D.30})$$

Appendix E

Benchmark Spectra

E.1 Benchmark Point A1

$$\tan\beta = 10, \quad s = 2.7 \text{ TeV} \quad M_{1/2} = 363 \text{ GeV} \quad m_0 = 537 \text{ GeV} \quad A = 711 \text{ GeV} \quad (\text{E.1})$$

$$\lambda(M_X) = -0.3683 \quad \lambda(\mu_S) = -0.3548, \quad \lambda_{1,2}(M_X) = 0.1 \quad (\text{E.2})$$

$$\kappa_{1,2,3}(M_X) = 0.2068, \quad \kappa_{1,2,3}(\mu_S) = 0.5384 \quad (\text{E.3})$$

Squark and slepton masses

$$m_{\tilde{t}_1} = 433 \text{ GeV} \quad m_{\tilde{b}_1} = 668 \text{ GeV} \quad m_{\tilde{\tau}_1} = 631 \text{ GeV} \quad (\text{E.4})$$

$$m_{\tilde{t}_2} = 734 \text{ GeV} \quad m_{\tilde{b}_2} = 841 \text{ GeV} \quad m_{\tilde{\tau}_2} = 730 \text{ GeV} \quad (\text{E.5})$$

$$m_{\tilde{u}_{2,d_1}} = 807 \text{ GeV} \quad m_{\tilde{e}_2} = 733 \text{ GeV} \quad (\text{E.6})$$

$$m_{\tilde{u}_1} = 788 \text{ GeV} \quad m_{\tilde{d}_2} = 850 \text{ GeV} \quad m_{\tilde{e}_1} = 631 \text{ GeV} \quad (\text{E.7})$$

Exotic colored masses

$$m_{\tilde{D}_1}(1, 2, 3) = 628 \text{ GeV} \quad m_{\tilde{D}_2}(1, 2, 3) = 1439 \text{ GeV} \quad \mu_D(1, 2, 3) = 1028 \text{ GeV}. \quad (\text{E.8})$$

Neutralinos, charginos, gluino and Z' masses

$$m_{\chi_1^0} = 58 \text{ GeV} \quad m_{\chi_2^0} = 103 \text{ GeV} \quad m_{\chi_3^0} = 684 \text{ GeV} \quad (\text{E.9})$$

$$m_{\chi_4^0} = 684 \text{ GeV} \quad m_{\chi_5^0} = 993 \text{ GeV} \quad m_{\chi_6^0} = 1052 \text{ GeV} \quad (\text{E.10})$$

$$m_{\chi_1^\pm} = 103 \text{ GeV} \quad m_{\chi_1^\pm} = 686 \text{ GeV} \quad M_{Z'} = 1020 \text{ GeV} \quad m_{\tilde{g}} = 330 \text{ GeV} \quad (\text{E.11})$$

CP-Even Higgs masses

$$m_{h_1}^{(2-loop)} = 115 \text{ GeV} \quad m_{h_1}^{(1-loop)} = 119 \text{ GeV} \quad (\text{E.12})$$

$$m_{h_2} = 664 \text{ GeV} \quad m_{h_3} = 1022 \text{ GeV} \quad (\text{E.13})$$

Inert Higgs, Higgsino and Singlet masses

$$m_{H_1}(1, 2) = 479 \text{ GeV} \quad m_{H_2}(1, 2) = 154 \text{ GeV} \quad (\text{E.14})$$

$$m_{Singlet}(1, 2) = 908 \text{ GeV} \quad m_{\tilde{H}_1}(1, 2) = 244 \text{ GeV} \quad (\text{E.15})$$

E.2 Benchmark Point A2

$$\tan\beta = 10, \quad s = 3.8 \text{ TeV} \quad M_{1/2} = 390 \text{ GeV} \quad m_0 = 998 \text{ GeV} \quad A = 768 \text{ GeV} \quad (\text{E.16})$$

$$\lambda(M_X) = -0.306648 \quad \lambda(\mu_S) = -0.284529, \quad \lambda_{1,2}(M_X) = 0.1 \quad (\text{E.17})$$

$$\kappa_{1,2,3}(M_X) = 0.246329, \quad \kappa_{1,2,3}(\mu_S) = 0.593522 \quad (\text{E.18})$$

Squark and slepton masses

$$m_{\tilde{t}_1} = 787 \text{ GeV} \quad m_{\tilde{b}_1} = 1036 \text{ GeV} \quad m_{\tilde{\tau}_1} = 1203 \text{ GeV} \quad (\text{E.19})$$

$$m_{\tilde{t}_2} = 1070 \text{ GeV} \quad m_{\tilde{b}_2} = 1282 \text{ GeV} \quad m_{\tilde{\tau}_2} = 1095 \text{ GeV} \quad (\text{E.20})$$

$$m_{\tilde{u}_{2,\tilde{d}_1}} = 1225 \text{ GeV} \quad m_{\tilde{e}_2} = 1207 \text{ GeV} \quad (\text{E.21})$$

$$m_{\tilde{u}_1} = 1211 \text{ GeV} \quad m_{\tilde{d}_2} = 1292 \text{ GeV} \quad m_{\tilde{e}_1} = 1105 \text{ GeV} \quad (\text{E.22})$$

Exotic colored masses

$$m_{\tilde{D}_1}(1, 2, 3) = 1363 \text{ GeV} \quad m_{\tilde{D}_2}(1, 2, 3) = 2077 \text{ GeV} \quad \mu_D(1, 2, 3) = 1595 \text{ GeV}. \quad (\text{E.23})$$

Neutralinos, charginos, gluino and Z' masses

$$m_{\chi_1^0} = 62 \text{ GeV} \quad m_{\chi_2^0} = 110 \text{ GeV} \quad m_{\chi_3^0} = 771 \text{ GeV} \quad (\text{E.24})$$

$$m_{\chi_4^0} = 771 \text{ GeV} \quad m_{\chi_5^0} = 1405 \text{ GeV} \quad m_{\chi_6^0} = 1469 \text{ GeV} \quad (\text{E.25})$$

$$m_{\chi_1^\pm} = 110 \text{ GeV} \quad m_{\chi_1^\pm} = 773 \text{ GeV} \quad M_{Z'} = 1437 \text{ GeV} \quad m_{\tilde{g}} = 362 \text{ GeV} \quad (\text{E.26})$$

CP-Even Higgs masses

$$m_{h_1}^{(2-loop)} = 121 \text{ GeV} \quad m_{h_1}^{(1-loop)} = 126 \text{ GeV} \quad (\text{E.27})$$

$$m_{h_2} = 963 \text{ GeV} \quad m_{h_3} = 1437 \text{ GeV} \quad (\text{E.28})$$

Inert Higgs, Higgsino and Singlet masses

$$m_{H_1}(1, 2) = 694 \text{ GeV} \quad m_{H_2}(1, 2) = 875 \text{ GeV} \quad (\text{E.29})$$

$$m_{Singlet}(1, 2) = 1430 \text{ GeV} \quad m_{\tilde{H}_1}(1, 2) = 324 \text{ GeV} \quad (\text{E.30})$$

E.3 Benchmark Point A3

$$\tan\beta = 10, \quad s = 4.4 \text{ TeV} \quad M_{1/2} = 775 \text{ GeV} \quad m_0 = 799 \text{ GeV} \quad A = 919 \text{ GeV} \quad (\text{E.31})$$

$$\lambda(M_X) = -0.369832 \quad \lambda(\mu_S) = -0.37357, \quad \lambda_{1,2}(M_X) = 0.1 \quad (\text{E.32})$$

$$\kappa_{1,2,3}(M_X) = 0.177975, \quad \kappa_{1,2,3}(\mu_S) = 0.49349 \quad (\text{E.33})$$

Squark and slepton masses

$$m_{\tilde{t}_1} = 853 \text{ GeV} \quad m_{\tilde{b}_1} = 1216 \text{ GeV} \quad m_{\tilde{\tau}_1} = 1172 \text{ GeV} \quad (\text{E.34})$$

$$m_{\tilde{t}_2} = 1259 \text{ GeV} \quad m_{\tilde{b}_2} = 1473 \text{ GeV} \quad m_{\tilde{\tau}_2} = 982 \text{ GeV} \quad (\text{E.35})$$

$$m_{\tilde{u}_{2,\tilde{d}_1}} = 1446 \text{ GeV} \quad m_{\tilde{e}_2} = 1176 \text{ GeV} \quad (\text{E.36})$$

$$m_{\tilde{u}_1} = 1398 \text{ GeV} \quad m_{\tilde{d}_2} = 1488 \text{ GeV} \quad m_{\tilde{e}_1} = 992 \text{ GeV} \quad (\text{E.37})$$

Exotic colored masses

$$m_{\tilde{D}_1}(1, 2, 3) = 821 \text{ GeV} \quad m_{\tilde{D}_2}(1, 2, 3) = 2363 \text{ GeV} \quad \mu_D(1, 2, 3) = 1535 \text{ GeV} \quad (\text{E.38})$$

Neutralinos, charginos, gluino and Z' masses

$$m_{\chi_1^0} = 122 \text{ GeV} \quad m_{\chi_2^0} = 217 \text{ GeV} \quad m_{\chi_3^0} = 1167 \text{ GeV} \quad (\text{E.39})$$

$$m_{\chi_4^0} = 1167 \text{ GeV} \quad m_{\chi_5^0} = 1603 \text{ GeV} \quad m_{\chi_6^0} = 1727 \text{ GeV} \quad (\text{E.40})$$

$$m_{\chi_1^\pm} = 217 \text{ GeV} \quad m_{\chi_1^\pm} = 1168 \text{ GeV} \quad M_{Z'} = 1663 \text{ GeV} \quad m_{\tilde{g}} = 673 \text{ GeV} \quad (\text{E.41})$$

CP-Even Higgs masses

$$m_{h_1}^{(2-loop)} = 114 \text{ GeV} \quad m_{h_1}^{(1-loop)} = 122 \text{ GeV} \quad (\text{E.42})$$

$$m_{h_2} = 1145 \text{ GeV} \quad m_{h_3} = 1664 \text{ GeV} \quad (\text{E.43})$$

Inert Higgs, Higgsino and Singlet masses

$$m_{H_1}(1, 2) = 182 \text{ GeV} \quad m_{H_2}(1, 2) = 765 \text{ GeV} \quad (\text{E.44})$$

$$m_{Singlet}(1, 2) = 1446 \text{ GeV} \quad m_{\tilde{H}_1}(1, 2) = 418 \text{ GeV} \quad (\text{E.45})$$

E.4 Benchmark Point A4 (Z' mass < 936 GeV)

$$\tan\beta = 10, \quad s = 1.9 \text{ TeV} \quad M_{1/2} = 382 \text{ GeV} \quad m_0 = 816 \text{ GeV} \quad A = -19 \text{ GeV} \quad (\text{E.46})$$

$$\lambda(M_X) = -0.2573 \quad \lambda(\mu_S) = -0.2780, \quad \lambda_{1,2}(M_X) = 0.1 \quad (\text{E.47})$$

$$\kappa_{1,2,3}(M_X) = 0.17385, \quad \kappa_{1,2,3}(\mu_S) = 0.49792 \quad (\text{E.48})$$

Squark and slepton masses

$$m_{\tilde{t}_1} = 682 \text{ GeV} \quad m_{\tilde{b}_1} = 862 \text{ GeV} \quad m_{\tilde{\tau}_1} = 890 \text{ GeV} \quad (\text{E.49})$$

$$m_{\tilde{t}_2} = 890 \text{ GeV} \quad m_{\tilde{b}_2} = 1001 \text{ GeV} \quad m_{\tilde{\tau}_2} = 850 \text{ GeV} \quad (\text{E.50})$$

$$m_{\tilde{u}_2, \tilde{d}_1} = 1001 \text{ GeV} \quad m_{\tilde{e}_2} = 903 \text{ GeV} \quad (\text{E.51})$$

$$m_{\tilde{u}_1} = 985 \text{ GeV} \quad m_{\tilde{d}_2} = 1009 \text{ GeV} \quad m_{\tilde{e}_1} = 857 \text{ GeV} \quad (\text{E.52})$$

Exotic colored masses

$$m_{\tilde{D}_1}(3) = 887 \text{ GeV} \quad m_{\tilde{D}_2}(3) = 1228 \text{ GeV} \quad \mu_D(1, 2, 3) = 669 \text{ GeV} \quad (\text{E.53})$$

Neutralinos, charginos, gluino and Z' masses

$$m_{\chi_1^0} = 60 \text{ GeV} \quad m_{\chi_2^0} = 104 \text{ GeV} \quad m_{\chi_3^0} = 385 \text{ GeV} \quad (\text{E.54})$$

$$m_{\chi_4^0} = 387 \text{ GeV} \quad m_{\chi_5^0} = 690 \text{ GeV} \quad m_{\chi_6^0} = 750 \text{ GeV} \quad (\text{E.55})$$

$$m_{\chi_1^\pm} = 105 \text{ GeV} \quad m_{\chi_2^\pm} = 390 \text{ GeV} \quad M_{Z'} = 719 \text{ GeV} \quad m_{\tilde{g}} = 346 \text{ GeV} \quad (\text{E.56})$$

CP-Even Higgs masses

$$m_{h_1}^{(2-loop)} = 117 \text{ GeV} \quad m_{h_1}^{(1-loop)} = 122 \text{ GeV} \quad (\text{E.57})$$

$$m_{h_2} = 717 \text{ GeV} \quad m_{h_3} = 801 \text{ GeV} \quad (\text{E.58})$$

$$(\text{E.59})$$

Inert Higgs, Higgsino and Singlet masses

$$m_{H_1}(1, 2) = 767 \text{ GeV} \quad m_{H_2}(1, 2) = 797 \text{ GeV} \quad (\text{E.60})$$

$$m_{Singlet}(1, 2) = 970 \text{ GeV} \quad m_{\tilde{H}_1}(1, 2) = 187 \text{ GeV} \quad (\text{E.61})$$

E.5 Benchmark Point B1

$$\tan \beta = 30, \quad s = 3.1 \text{ TeV} \quad M_{1/2} = 365 \text{ GeV} \quad m_0 = 702 \text{ GeV} \quad A = 1148 \text{ GeV} \quad (\text{E.62})$$

$$\lambda(M_X) = -0.37845 \quad \lambda(\mu_S) = -0.3661, \quad \lambda_{1,2}(M_X) = 0.1 \quad (\text{E.63})$$

$$\kappa_{1,2,3}(M_X) = 0.17121, \quad \kappa_{1,2,3}(\mu_S) = 0.4813 \quad (\text{E.64})$$

Squark and slepton masses

$$m_{\tilde{t}_1} = 463 \text{ GeV} \quad m_{\tilde{b}_1} = 694 \text{ GeV} \quad m_{\tilde{\tau}_1} = 858 \text{ GeV} \quad (\text{E.65})$$

$$m_{\tilde{t}_2} = 773 \text{ GeV} \quad m_{\tilde{b}_2} = 890 \text{ GeV} \quad m_{\tilde{\tau}_2} = 706 \text{ GeV} \quad (\text{E.66})$$

$$m_{\tilde{u}_2, \tilde{d}_1} = 945 \text{ GeV} \quad m_{\tilde{e}_2} = 900 \text{ GeV} \quad (\text{E.67})$$

$$m_{\tilde{u}_1} = 929 \text{ GeV} \quad m_{\tilde{d}_2} = 998 \text{ GeV} \quad m_{\tilde{e}_1} = 804 \text{ GeV} \quad (\text{E.68})$$

Exotic colored masses

$$m_{\tilde{D}_1}(3) = 393 \text{ GeV} \quad m_{\tilde{D}_2}(3) = 1617 \text{ GeV} \quad \mu_{\tilde{D}}(1, 2, 3) = 1055 \text{ GeV} \quad (\text{E.69})$$

Neutralinos, charginos, gluino and Z' masses

$$m_{\chi_1^0} = 59 \text{ GeV} \quad m_{\chi_2^0} = 104 \text{ GeV} \quad m_{\chi_3^0} = 808 \text{ GeV} \quad (\text{E.70})$$

$$m_{\chi_4^0} = 809 \text{ GeV} \quad m_{\chi_5^0} = 1143 \text{ GeV} \quad m_{\chi_6^0} = 1203 \text{ GeV} \quad (\text{E.71})$$

$$m_{\chi_1^\pm} = 103 \text{ GeV} \quad m_{\chi_1^\pm} = 810 \text{ GeV} \quad M_{Z'} = 1172 \text{ GeV} \quad m_{\tilde{g}} = 336 \text{ GeV} \quad (\text{E.72})$$

CP-Even Higgs masses

$$m_{h_1}^{(2-loop)} = 114 \text{ GeV} \quad m_{h_1}^{(1-loop)} = 118 \text{ GeV} \quad (\text{E.73})$$

$$m_{h_2} = 593 \text{ GeV} \quad m_{h_3} = 1173 \text{ GeV} \quad (\text{E.74})$$

Inert Higgs, Higgsino and Singlet masses

$$m_{H_1}(1, 2) = 220 \text{ GeV} \quad m_{H_2}(1, 2) = 704 \text{ GeV} \quad (\text{E.75})$$

$$m_{\text{Singlet}}(1, 2) = 1093 \text{ GeV} \quad m_{\tilde{H}_1}(1, 2) = 298 \text{ GeV} \quad (\text{E.76})$$

E.6 Benchmark Point B2

$$\tan \beta = 30, \quad s = 3.4 \text{ TeV} \quad M_{1/2} = 361 \text{ GeV} \quad m_0 = 993 \text{ GeV} \quad A = 1121 \text{ GeV} \quad (\text{E.77})$$

$$\lambda(M_X) = -0.33333 \quad \lambda(\mu_S) = -0.32376, \quad \lambda_{1,2}(M_X) = 0.1 \quad (\text{E.78})$$

$$\kappa_{1,2,3}(M_X) = 0.18394, \quad \kappa_{1,2,3}(\mu_S) = 0.50783 \quad (\text{E.79})$$

Squark and slepton masses

$$m_{\tilde{t}_1} = 694 \text{ GeV} \quad m_{\tilde{b}_1} = 914 \text{ GeV} \quad m_{\tilde{\tau}_1} = 1117 \text{ GeV} \quad (\text{E.80})$$

$$m_{\tilde{t}_2} = 964 \text{ GeV} \quad m_{\tilde{b}_2} = 1133 \text{ GeV} \quad m_{\tilde{\tau}_2} = 973 \text{ GeV} \quad (\text{E.81})$$

$$m_{\tilde{u}_2, \tilde{d}_1} = 1186 \text{ GeV} \quad m_{\tilde{e}_2} = 1165 \text{ GeV} \quad (\text{E.82})$$

$$m_{\tilde{u}_1} = 1211 \text{ GeV} \quad m_{\tilde{d}_2} = 1292 \text{ GeV} \quad m_{\tilde{e}_1} = 1080 \text{ GeV} \quad (\text{E.83})$$

Exotic colored masses

$$m_{\tilde{D}_1}(3) = 884 \text{ GeV} \quad m_{\tilde{D}_2}(3) = 1860 \text{ GeV} \quad \mu_D(1, 2, 3) = 1221 \text{ GeV} \quad (\text{E.84})$$

Neutralinos, charginos, gluino and Z' masses

$$m_{\chi_1^0} = 58 \text{ GeV} \quad m_{\chi_2^0} = 102 \text{ GeV} \quad m_{\chi_3^0} = 784 \text{ GeV} \quad (\text{E.85})$$

$$m_{\chi_4^0} = 785 \text{ GeV} \quad m_{\chi_5^0} = 1256 \text{ GeV} \quad m_{\chi_6^0} = 1316 \text{ GeV} \quad (\text{E.86})$$

$$m_{\chi_1^\pm} = 102 \text{ GeV} \quad m_{\chi_1^\pm} = 786 \text{ GeV} \quad M_{Z'} = 1285 \text{ GeV} \quad m_{\tilde{g}} = 338 \text{ GeV} \quad (\text{E.87})$$

CP-Even Higgs masses

$$m_{h_1}^{(2-loop)} = 119 \text{ GeV} \quad m_{h_1}^{(2-loop)} = 124 \text{ GeV} \quad (\text{E.88})$$

$$m_{h_2} = 748 \text{ GeV} \quad m_{h_3} = 1285 \text{ GeV} \quad (\text{E.89})$$

Inert Higgs, Higgsino and Singlet masses

$$m_{H_1}(1, 2) = 689 \text{ GeV} \quad m_{H_2}(1, 2) = 966 \text{ GeV} \quad (\text{E.90})$$

$$m_{\text{Singlet}}(1, 2) = 1351 \text{ GeV} \quad m_{\tilde{H}_1}(1, 2) = 323 \text{ GeV} \quad (\text{E.91})$$

E.7 Benchmark Point B3

$$\tan \beta = 30, \quad s = 5.0 \text{ TeV} \quad M_{1/2} = 725 \text{ GeV} \quad m_0 = 1074 \text{ GeV} \quad A = 1726 \text{ GeV} \quad (\text{E.92})$$

$$\lambda(M_X) = -0.38471 \quad \lambda(\mu_S) = -0.3788, \quad \lambda_{1,2}(M_X) = 0.1 \quad (\text{E.93})$$

$$\kappa_{1,2,3}(M_X) = 0.15788, \quad \kappa_{1,2,3}(\mu_S) = 0.4559 \quad (\text{E.94})$$

Squark and slepton masses

$$m_{\tilde{t}_1} = 837 \text{ GeV} \quad m_{\tilde{b}_1} = 1193 \text{ GeV} \quad m_{\tilde{\tau}_1} = 1363 \text{ GeV} \quad (\text{E.95})$$

$$m_{\tilde{t}_2} = 1248 \text{ GeV} \quad m_{\tilde{b}_2} = 1491 \text{ GeV} \quad m_{\tilde{\tau}_2} = 1102, \text{ GeV} \quad (\text{E.96})$$

$$m_{\tilde{u}_2, \tilde{d}_1} = 1595 \text{ GeV} \quad m_{\tilde{e}_2} = 1427 \text{ GeV} \quad (\text{E.97})$$

$$m_{\tilde{u}_1} = 1557 \text{ GeV} \quad m_{\tilde{d}_2} = 1664 \text{ GeV} \quad m_{\tilde{e}_1} = 1254 \text{ GeV} \quad (\text{E.98})$$

Exotic colored masses

$$m_{\tilde{D}_1}(3) = 312 \text{ GeV} \quad m_{\tilde{D}_2}(3) = 2623 \text{ GeV} \quad \mu_{\tilde{D}}(1, 2, 3) = 1612 \text{ GeV} \quad (\text{E.99})$$

Neutralinos, charginos, gluino and Z' masses

$$m_{\chi_1^0} = 116 \text{ GeV} \quad m_{\chi_2^0} = 206 \text{ GeV} \quad m_{\chi_3^0} = 1343 \text{ GeV} \quad (\text{E.100})$$

$$m_{\chi_4^0} = 1343 \text{ GeV} \quad m_{\chi_5^0} = 1832 \text{ GeV} \quad m_{\chi_6^0} = 1950 \text{ GeV} \quad (\text{E.101})$$

$$m_{\chi_{1\pm}} = 206 \text{ GeV} \quad m_{\chi_{1\pm}} = 1344 \text{ GeV} \quad M_{Z'} = 1889 \text{ GeV} \quad m_{\tilde{g}} = 642 \text{ GeV} \quad (\text{E.102})$$

CP-Even Higgs masses

$$m_{h_1}^{(2-loop)} = 114 \text{ GeV} \quad m_{h_1}^{(1-loop)} = 123 \text{ GeV} \quad (\text{E.103})$$

$$m_{h_2} = 988 \text{ GeV} \quad m_{h_3} = 1890 \text{ GeV} \quad (\text{E.104})$$

Inert Higgs, Higgsino and Singlet masses

$$m_{H_1}(1, 2) = 220 \text{ GeV} \quad m_{H_2}(1, 2) = 1117 \text{ GeV} \quad (\text{E.105})$$

$$m_{\text{Singlet}}(1, 2) = 1732 \text{ GeV} \quad m_{\tilde{H}_1}(1, 2) = 491 \text{ GeV} \quad (\text{E.106})$$

E.8 Benchmark Point C1

$$\tan \beta = 3, \quad s = 3.3 \text{ TeV} \quad M_{1/2} = 365 \text{ GeV} \quad m_0 = 640 \text{ GeV} \quad A = 798 \text{ GeV} \quad (\text{E.107})$$

$$\lambda(M_X) = -0.465 \quad \lambda(\mu_S) = -0.354, \quad \lambda_{1,2}(M_X) = 0.1 \quad (\text{E.108})$$

$$\kappa_{1,2,3}(M_X) = 0.3, \quad \kappa_{1,2,3}(\mu_S) = 0.628 \quad (\text{E.109})$$

Squark and slepton masses

$$m_{\tilde{t}_1} = 493 \text{ GeV} \quad m_{\tilde{b}_1} = 758 \text{ GeV} \quad m_{\tilde{\tau}_1} = 873 \text{ GeV} \quad (\text{E.110})$$

$$m_{\tilde{t}_2} = 821 \text{ GeV} \quad m_{\tilde{b}_2} = 974 \text{ GeV} \quad m_{\tilde{\tau}_2} = 651 \text{ GeV} \quad (\text{E.111})$$

$$m_{\tilde{u}_2, \tilde{d}_1} = 910 \text{ GeV} \quad m_{\tilde{e}_2} = 874 \text{ GeV} \quad (\text{E.112})$$

$$m_{\tilde{u}_1} = 893 \text{ GeV} \quad m_{\tilde{d}_2} = 975 \text{ GeV} \quad m_{\tilde{e}_1} = 762 \text{ GeV} \quad (\text{E.113})$$

Exotic colored masses

$$m_{\tilde{D}_1}(1, 2, 3) = 1797 \text{ GeV} \quad m_{\tilde{D}_2}(1, 2, 3) = 1156 \text{ GeV} \quad \mu_D(1, 2, 3) = 1466 \text{ GeV} \quad (\text{E.114})$$

Neutralinos, charginos, gluino and Z' masses

$$m_{\chi_1^0} = 59 \text{ GeV} \quad m_{\chi_2^0} = 107 \text{ GeV} \quad m_{\chi_3^0} = 829 \text{ GeV} \quad (\text{E.115})$$

$$m_{\chi_4^0} = 832 \text{ GeV} \quad m_{\chi_5^0} = 1220 \text{ GeV} \quad m_{\chi_6^0} = 1278 \text{ GeV} \quad (\text{E.116})$$

$$m_{\chi_1^\pm} = 107 \text{ GeV} \quad m_{\chi_2^\pm} = 832 \text{ GeV} \quad M_{Z'} = 1248 \text{ GeV} \quad m_{\tilde{g}} = 336 \text{ GeV} \quad (\text{E.117})$$

CP-Even Higgs masses

$$m_{h_1}^{(2-loop)} = 114 \text{ GeV} \quad m_{h_1}^{(1-loop)} = 119 \text{ GeV} \quad (\text{E.118})$$

$$m_{h_2} = 850 \text{ GeV} \quad m_{h_3} = 1249 \text{ GeV} \quad (\text{E.119})$$

Inert Higgs, Higgsino and Singlet masses

$$m_{H_1}(1, 2) = 165 \text{ GeV} \quad m_{H_2}(1, 2) = 468 \text{ GeV} \quad (\text{E.120})$$

$$m_{\text{Singlet}}(1, 2) = 1097 \text{ GeV} \quad m_{\tilde{H}_1}(1, 2) = 249 \text{ GeV} \quad (\text{E.121})$$

E.9 Benchmark Point C2

$$\tan \beta = 3, \quad s = 5.6 \text{ TeV} \quad M_{1/2} = 352 \text{ GeV} \quad m_0 = 1238 \text{ GeV} \quad A = 1194 \text{ GeV} \quad (\text{E.122})$$

$$\lambda(M_X) = -0.529 \quad \lambda(\mu_S) = -0.300, \quad \lambda_{1,2}(M_X) = 0.1 \quad (\text{E.123})$$

$$\kappa_{1,2,3}(M_X) = 0.492, \quad \kappa_{1,2,3}(\mu_S) = 0.716 \quad (\text{E.124})$$

Squark and slepton masses

$$m_{\tilde{t}_1} = 944 \text{ GeV} \quad m_{\tilde{b}_1} = 1260 \text{ GeV} \quad m_{\tilde{\tau}_1} = 1571 \text{ GeV} \quad (\text{E.125})$$

$$m_{\tilde{t}_2} = 1293 \text{ GeV} \quad m_{\tilde{b}_2} = 1625 \text{ GeV} \quad m_{\tilde{\tau}_2} = 1412 \text{ GeV} \quad (\text{E.126})$$

$$m_{\tilde{u}_2, \tilde{d}_1} = 1494 \text{ GeV} \quad m_{\tilde{e}_2} = 1571 \text{ GeV} \quad (\text{E.127})$$

$$m_{\tilde{u}_1} = 1484 \text{ GeV} \quad m_{\tilde{d}_2} = 1627 \text{ GeV} \quad m_{\tilde{e}_1} = 1412 \text{ GeV} \quad (\text{E.128})$$

Exotic colored masses

$$m_{\tilde{D}_1}(3) = 2635 \text{ GeV} \quad m_{\tilde{D}_2}(3) = 3105 \text{ GeV} \quad \mu_D(1, 2, 3) = 2835 \text{ GeV} \quad (\text{E.129})$$

Neutralinos, charginos, gluino and Z' masses

$$m_{\chi_1^0} = 57 \text{ GeV} \quad m_{\chi_2^0} = 103 \text{ GeV} \quad m_{\chi_3^0} = 1189 \text{ GeV} \quad (\text{E.130})$$

$$m_{\chi_4^0} = 1191 \text{ GeV} \quad m_{\chi_5^0} = 2089 \text{ GeV} \quad m_{\chi_6^0} = 2148 \text{ GeV} \quad (\text{E.131})$$

$$m_{\chi_{1\pm}} = 103 \text{ GeV} \quad m_{\chi_{1\pm}} = 1191 \text{ GeV} \quad M_{Z'} = 2119 \text{ GeV} \quad m_{\tilde{g}} = 342 \text{ GeV} \quad (\text{E.132})$$

CP-Even Higgs masses

$$m_{h_1}^{(2-loop)} = 117 \text{ GeV} \quad m_{h_1}^{(1-loop)} = 125 \text{ GeV} \quad (\text{E.133})$$

$$m_{h_2} = 1319 \text{ GeV} \quad m_{h_3} = 2119 \text{ GeV} \quad (\text{E.134})$$

Inert Higgs, Higgsino and Singlet masses

$$m_{H_1}(1, 2) = 560 \text{ GeV} \quad m_{H_2}(1, 2) = 877 \text{ GeV} \quad (\text{E.135})$$

$$m_{\text{Singlet}}(1, 2) = 1947 \text{ GeV} \quad m_{\tilde{H}_1}(1, 2) = 313 \text{ GeV} \quad (\text{E.136})$$

E.10 Benchmark Point C3

$$\tan \beta = 3, \quad s = 5.5 \text{ TeV} \quad M_{1/2} = 931 \text{ GeV} \quad m_0 = 918 \text{ GeV} \quad A = 751 \text{ GeV} \quad (\text{E.137})$$

$$\lambda(M_X) = -0.434 \quad \lambda(\mu_S) = -0.375, \quad \lambda_{1,2}(M_X) = 0.1 \quad (\text{E.138})$$

$$\kappa_{1,2,3}(M_X) = 0.23, \quad \kappa_{1,2,3}(\mu_S) = 0.56 \quad (\text{E.139})$$

Squark and slepton masses

$$m_{\tilde{t}_1} = 1056 \text{ GeV} \quad m_{\tilde{b}_1} = 1472 \text{ GeV} \quad m_{\tilde{\tau}_1} = 1409 \text{ GeV} \quad (\text{E.140})$$

$$m_{\tilde{t}_2} = 1511 \text{ GeV} \quad m_{\tilde{b}_2} = 1784 \text{ GeV} \quad m_{\tilde{\tau}_2} = 1172, \text{ GeV} \quad (\text{E.141})$$

$$m_{\tilde{u}_2, \tilde{d}_1} = 1724 \text{ GeV} \quad m_{\tilde{e}_2} = 1409 \text{ GeV} \quad (\text{E.142})$$

$$m_{\tilde{u}_1} = 1666 \text{ GeV} \quad m_{\tilde{d}_2} = 1785 \text{ GeV} \quad m_{\tilde{e}_1} = 1173 \text{ GeV} \quad (\text{E.143})$$

Exotic colored masses

$$m_{\tilde{D}_1}(1, 2, 3) = 1567 \text{ GeV} \quad m_{\tilde{D}_2}(1, 2, 3) = 2997 \text{ GeV} \quad \mu_D(1, 2, 3) = 2187 \text{ GeV} \quad (\text{E.144})$$

Neutralinos, charginos, gluino and Z' masses

$$m_{\chi_1^0} = 148 \text{ GeV} \quad m_{\chi_2^0} = 262 \text{ GeV} \quad m_{\chi_3^0} = 1463 \text{ GeV} \quad (\text{E.145})$$

$$m_{\chi_4^0} = 1464 \text{ GeV} \quad m_{\chi_5^0} = 2006 \text{ GeV} \quad m_{\chi_6^0} = 2155 \text{ GeV} \quad (\text{E.146})$$

$$m_{\chi_1^\pm} = 262 \text{ GeV} \quad m_{\chi_1^\pm} = 1464 \text{ GeV} \quad M_{Z'} = 2079 \text{ GeV} \quad m_{\tilde{g}} = 805 \text{ GeV} \quad (\text{E.147})$$

CP-Even Higgs masses

$$m_{h_1}^{(2-loop)} = 114 \text{ GeV} \quad m_{h_1}^{(1-loop)} = 125 \text{ GeV} \quad (\text{E.148})$$

$$m_{h_2} = 1508 \text{ GeV} \quad m_{h_3} = 2080 \text{ GeV} \quad (\text{E.149})$$

Inert Higgs, Higgsino and Singlet masses

$$m_{H_1}(1, 2) = 121 \text{ GeV} \quad m_{H_2}(1, 2) = 714 \text{ GeV} \quad (\text{E.150})$$

$$m_{\text{Singlet}}(1, 2) = 1763 \text{ GeV} \quad m_{\tilde{H}_1}(1, 2) = 471 \text{ GeV} \quad (\text{E.151})$$

E.11 Benchmark Point D1

$$\tan\beta = 10, \quad s = 2.7 \text{ TeV} \quad M_{1/2} = 388 \text{ GeV} \quad m_0 = 681 \text{ GeV} \quad A = 645 \text{ GeV} \quad (\text{E.152})$$

$$\lambda_{1,2}(M_X) = 0.1 \quad \lambda_3 = -0.378 \quad \lambda(\mu_S) = -0.348 \quad (\text{E.153})$$

$$\kappa_{1,2} = 0.06 \quad \kappa_3(M_X) = 0.42, \quad \kappa_3(\mu_S) = 0.915 \quad (\text{E.154})$$

Squark and slepton masses

$$m_{\tilde{t}_1} = 546 \text{ GeV} \quad m_{\tilde{b}_1} = 777 \text{ GeV} \quad m_{\tilde{\tau}_1} = 845 \text{ GeV} \quad (\text{E.155})$$

$$m_{\tilde{t}_2} = 829 \text{ GeV} \quad m_{\tilde{b}_2} = 955 \text{ GeV} \quad m_{\tilde{\tau}_2} = 757, \text{ GeV} \quad (\text{E.156})$$

$$m_{\tilde{u}_2, \tilde{d}_1} = 929 \text{ GeV} \quad m_{\tilde{e}_2} = 849 \text{ GeV} \quad (\text{E.157})$$

$$m_{\tilde{u}_1} = 911 \text{ GeV} \quad m_{\tilde{d}_2} = 964 \text{ GeV} \quad m_{\tilde{e}_1} = 765 \text{ GeV} \quad (\text{E.158})$$

Exotic colored masses

$$m_{\tilde{D}_1}(3) = 1464 \text{ GeV} \quad m_{\tilde{D}_2}(3) = 2086 \text{ GeV} \quad \mu_D(3) = 1747 \text{ GeV} \quad (\text{E.159})$$

$$m_{\tilde{D}_1}(1, 2) = 520 \text{ GeV} \quad m_{\tilde{D}_2}(2) = 906 \text{ GeV} \quad \mu_D(1, 2) = 300 \text{ GeV} \quad (\text{E.160})$$

Neutralinos, charginos, gluino and Z' masses

$$m_{\chi_1^0} = 61 \text{ GeV} \quad m_{\chi_2^0} = 109 \text{ GeV} \quad m_{\chi_3^0} = 671 \text{ GeV} \quad (\text{E.161})$$

$$m_{\chi_4^0} = 672 \text{ GeV} \quad m_{\chi_5^0} = 992 \text{ GeV} \quad m_{\chi_6^0} = 1054 \text{ GeV} \quad (\text{E.162})$$

$$m_{\chi_1^\pm} = 109 \text{ GeV} \quad m_{\chi_2^\pm} = 674 \text{ GeV} \quad M_{Z'} = 1021 \text{ GeV} \quad m_{\tilde{g}} = 353 \text{ GeV} \quad (\text{E.163})$$

CP-Even Higgs masses

$$m_{h_1}^{(2-loop)} = 115 \text{ GeV} \quad m_{h_1}^{(1-loop)} = 119 \text{ GeV} \quad (\text{E.164})$$

$$m_{h_2} = 765 \text{ GeV} \quad m_{h_3} = 1022 \text{ GeV} \quad (\text{E.165})$$

Inert Higgs, Higgsino and Singlet masses

$$m_{H_1}(1, 2) = 459 \text{ GeV} \quad m_{H_2}(1, 2) = 627 \text{ GeV} \quad (\text{E.166})$$

$$m_{\text{Singlet}}(1, 2) = 1001 \text{ GeV} \quad m_{\tilde{H}_1}(1, 2) = 233 \text{ GeV} \quad (\text{E.167})$$

E.12 Benchmark Point D2

$$\tan\beta = 10, \quad s = 2.7 \text{ TeV} \quad M_{1/2} = 358 \text{ GeV} \quad m_0 = 623 \text{ GeV} \quad A = 757 \text{ GeV} \quad (\text{E.168})$$

$$\lambda_{1,2}(M_X) = 0.1 \quad \lambda_3 = -0.395 \quad \lambda(\mu_S) = -0.355 \quad (\text{E.169})$$

$$\kappa_{1,2} = 0.08 \quad \kappa_3(M_X) = 0.43, \quad \kappa_3(\mu_S) = 0.915 \quad (\text{E.170})$$

Squark and slepton masses

$$m_{\tilde{t}_1} = 474 \text{ GeV} \quad m_{\tilde{b}_1} = 712 \text{ GeV} \quad m_{\tilde{\tau}_1} = 794 \text{ GeV} \quad (\text{E.171})$$

$$m_{\tilde{t}_2} = 772 \text{ GeV} \quad m_{\tilde{b}_2} = 894 \text{ GeV} \quad m_{\tilde{\tau}_2} = 704, \text{ GeV} \quad (\text{E.172})$$

$$m_{\tilde{u}_2, \tilde{d}_1} = 862 \text{ GeV} \quad m_{\tilde{e}_2} = 798 \text{ GeV} \quad (\text{E.173})$$

$$m_{\tilde{u}_1} = 845 \text{ GeV} \quad m_{\tilde{d}_2} = 903 \text{ GeV} \quad m_{\tilde{e}_1} = 712 \text{ GeV} \quad (\text{E.174})$$

Exotic colored masses

$$m_{\tilde{D}_1}(3) = 1445 \text{ GeV} \quad m_{\tilde{D}_2}(3) = 2059 \text{ GeV} \quad \mu_D(3) = 1747 \text{ GeV} \quad (\text{E.175})$$

$$m_{\tilde{D}_1}(1, 2) = 370 \text{ GeV} \quad m_{\tilde{D}_2}(1, 2) = 916 \text{ GeV} \quad \mu_D(1, 2) = 391 \text{ GeV} \quad (\text{E.176})$$

Neutralinos, charginos, gluino and Z' masses

$$m_{\chi_1^0} = 57 \text{ GeV} \quad m_{\chi_2^0} = 101 \text{ GeV} \quad m_{\chi_3^0} = 684 \text{ GeV} \quad (\text{E.177})$$

$$m_{\chi_4^0} = 684 \text{ GeV} \quad m_{\chi_5^0} = 994 \text{ GeV} \quad m_{\chi_6^0} = 1051 \text{ GeV} \quad (\text{E.178})$$

$$m_{\chi_1^\pm} = 101 \text{ GeV} \quad m_{\chi_2^\pm} = 686 \text{ GeV} \quad M_{Z'} = 1021 \text{ GeV} \quad m_{\tilde{g}} = 327 \text{ GeV} \quad (\text{E.179})$$

CP-Even Higgs masses

$$m_{h_1}^{(2-loop)} = 114 \text{ GeV} \quad m_{h_1}^{(1-loop)} = 118 \text{ GeV} \quad (\text{E.180})$$

$$m_{h_2} = 723 \text{ GeV} \quad m_{h_3} = 1022 \text{ GeV} \quad (\text{E.181})$$

Inert Higgs, Higgsino and Singlet masses

$$m_{H_1}(1, 2) = 345 \text{ GeV} \quad m_{H_2}(1, 2) = 561 \text{ GeV} \quad (\text{E.182})$$

$$m_{Singlet}(1, 2) = 961 \text{ GeV} \quad m_{\tilde{H}_1}(1, 2) = 229 \text{ GeV} \quad (\text{E.183})$$

E.13 Benchmark Point F1

$$\tan\beta = 10, \quad s = 4.0 \text{ TeV} \quad M_{1/2} = 426 \text{ GeV} \quad m_0 = 701 \text{ GeV} \quad A = -1652 \text{ GeV} \quad (\text{E.184})$$

$$\lambda_{1,2}(M_X) = 2.8 \quad \lambda_3(M_X) = -2.0 \quad \lambda_3(\mu_S) = -0.266 \quad (\text{E.185})$$

$$\kappa_{1,2} = 2.5 \quad \kappa_3(M_X) = 2.0, \quad \kappa_3(\mu_S) = 0.652 \quad (\text{E.186})$$

Squark and slepton masses

$$m_{\tilde{t}_1} = 784 \text{ GeV} \quad m_{\tilde{b}_1} = 918 \text{ GeV} \quad m_{\tilde{\tau}_1} = 1000 \text{ GeV} \quad (\text{E.187})$$

$$m_{\tilde{t}_2} = 932 \text{ GeV} \quad m_{\tilde{b}_2} = 1115 \text{ GeV} \quad m_{\tilde{\tau}_2} = 850, \text{ GeV} \quad (\text{E.188})$$

$$m_{\tilde{u}_{2,\tilde{d}_1}} = 1035 \text{ GeV} \quad m_{\tilde{e}_2} = 1005 \text{ GeV} \quad (\text{E.189})$$

$$m_{\tilde{u}_1} = 1015 \text{ GeV} \quad m_{\tilde{d}_2} = 1121 \text{ GeV} \quad m_{\tilde{e}_1} = 862 \text{ GeV} \quad (\text{E.190})$$

Exotic colored masses

$$m_{\tilde{D}_1}(3) = 1728 \text{ GeV} \quad m_{\tilde{D}_2}(3) = 2013 \text{ GeV} \quad \mu_D(3) = 1845 \text{ GeV} \quad (\text{E.191})$$

$$m_{\tilde{D}_1}(1,2) = 1980 \text{ GeV} \quad m_{\tilde{D}_2}(1,2) = 2263 \text{ GeV} \quad \mu_D(1,2) = 2106 \text{ GeV} \quad (\text{E.192})$$

Neutralinos, charginos, gluino and Z' masses

$$m_{\chi_1^0} = 65 \text{ GeV} \quad m_{\chi_2^0} = 115 \text{ GeV} \quad m_{\chi_3^0} = 758 \text{ GeV} \quad (\text{E.193})$$

$$m_{\chi_4^0} = 759 \text{ GeV} \quad m_{\chi_5^0} = 1487 \text{ GeV} \quad m_{\chi_6^0} = 1551 \text{ GeV} \quad (\text{E.194})$$

$$m_{\chi_{1\pm}} = 116 \text{ GeV} \quad m_{\chi_{1\pm}} = 761 \text{ GeV} \quad M_{Z'} = 1518 \text{ GeV} \quad m_{\tilde{g}} = 380 \text{ GeV} \quad (\text{E.195})$$

CP-Even Higgs masses

$$m_{h_1}^{(2-loop)} = 116 \text{ GeV} \quad m_{h_1}^{(1-loop)} = 120 \text{ GeV} \quad (\text{E.196})$$

$$m_{h_2} = 624 \text{ GeV} \quad m_{h_3} = 1518 \text{ GeV} \quad (\text{E.197})$$

Inert Higgs, Higgsino and Singlet masses

$$m_{H_1}(1,2) = 977 \text{ GeV} \quad m_{H_2}(1,2) = 1245 \text{ GeV} \quad (\text{E.198})$$

$$m_{Singlet}(1,2) = 1290 \text{ GeV} \quad m_{\tilde{H}_1}(1,2) = 1175 \text{ GeV} \quad (\text{E.199})$$

E.14 Benchmark Point F2

$$\tan\beta = 10, \quad s = 4.0 \text{ TeV} \quad M_{1/2} = 389 \text{ GeV} \quad m_0 = 725 \text{ GeV} \quad A = -1528 \text{ GeV} \quad (\text{E.200})$$

$$\lambda_{1,2}(M_X) = 2.6 \quad \lambda_3(M_X) = -2.0 \quad \lambda_3(\mu_S) = -0.259 \quad (\text{E.201})$$

$$\kappa_{1,2,3} = 2.5 \quad \kappa_3(\mu_S) = 0.728 \quad (\text{E.202})$$

Squark and slepton masses

$$m_{\tilde{t}_1} = 777 \text{ GeV} \quad m_{\tilde{b}_1} = 907 \text{ GeV} \quad m_{\tilde{\tau}_1} = 1012 \text{ GeV} \quad (\text{E.203})$$

$$m_{\tilde{t}_2} = 921 \text{ GeV} \quad m_{\tilde{b}_2} = 1108 \text{ GeV} \quad m_{\tilde{\tau}_2} = 867, \text{ GeV} \quad (\text{E.204})$$

$$m_{\tilde{u}_{2,\tilde{d}_1}} = 1023 \text{ GeV} \quad m_{\tilde{e}_2} = 1017 \text{ GeV} \quad (\text{E.205})$$

$$m_{\tilde{u}_1} = 1007 \text{ GeV} \quad m_{\tilde{d}_2} = 1113 \text{ GeV} \quad m_{\tilde{e}_1} = 879 \text{ GeV} \quad (\text{E.206})$$

Exotic colored masses

$$m_{\tilde{D}_1}(1, 2, 3) = 1948 \text{ GeV} \quad m_{\tilde{D}_2}(3) = 2200 \text{ GeV} \quad \mu_D(1, 2, 3) = 2060 \text{ GeV} \quad (\text{E.207})$$

Neutralinos, charginos, gluino and Z' masses

$$m_{\chi_1^0} = 59 \text{ GeV} \quad m_{\chi_2^0} = 106 \text{ GeV} \quad m_{\chi_3^0} = 738 \text{ GeV} \quad (\text{E.208})$$

$$m_{\chi_4^0} = 739 \text{ GeV} \quad m_{\chi_5^0} = 1490 \text{ GeV} \quad m_{\chi_6^0} = 1548 \text{ GeV} \quad (\text{E.209})$$

$$m_{\chi_1^\pm} = 106 \text{ GeV} \quad m_{\chi_1^\pm} = 740 \text{ GeV} \quad M_{Z'} = 1518 \text{ GeV} \quad m_{\tilde{g}} = 350 \text{ GeV} \quad (\text{E.210})$$

CP-Even Higgs masses

$$m_{h_1}^{(2-loop)} = 116 \text{ GeV} \quad m_{h_1}^{(1-loop)} = 120 \text{ GeV} \quad (\text{E.211})$$

$$m_{h_2} = 615 \text{ GeV} \quad m_{h_3} = 1518 \text{ GeV} \quad (\text{E.212})$$

Inert Higgs, Higgsino and Singlet masses

$$m_{H_1}(1, 2) = 903 \text{ GeV} \quad m_{H_2}(1, 2) = 1172 \text{ GeV} \quad (\text{E.213})$$

$$m_{Singlet}(1, 2) = 1290. \text{ GeV} \quad m_{\tilde{H}_1}(1, 2) = 1302 \quad (\text{E.214})$$

Bibliography

- [1] P. Athron and D. J. Miller, Phys. Rev. D **76**, 075010 (2007) [arXiv:0705.2241 [hep-ph]].
- [2] P. Athron and D. J. Miller, AIP Conf. Proc. **903**, 373 (2007).
- [3] P. Athron and D. J. Miller, arXiv:0710.2486 [hep-ph].
- [4] S. F. King, S. Moretti and R. Nevzorov, Phys. Rev. D **73** (2006) 035009 [arXiv:hep-ph/0510419].
- [5] S. F. King, S. Moretti and R. Nevzorov, Phys. Lett. B **634** (2006) 278 [arXiv:hep-ph/0511256].
- [6] P. Athron, S. F. King, D. J. Miller, S. Moretti and R. Nevzorov, “Constrained Exceptional Supersymmetric standard Model,” In preparation.
- [7] P. Athron, S. F. King, D. J. Miller, S. Moretti and R. Nevzorov, J. Phys. Conf. Ser. **110**, 072001 (2008) [arXiv:0708.3248 [hep-ph]].
- [8] C. Quigg, Front. Phys. **56**, 1 (1983).
- [9] S. Dawson, arXiv:hep-ph/9901280.
- [10] J. F. Gunion, H. E. Haber, G. L. Kane and S. Dawson,
- [11] I. J. R. Aitchison and A. J. G. Hey, *Bristol, UK: IOP (2004) 454 p*
- [12] I. J. R. Aitchison and A. J. G. Hey, *Bristol, UK: IOP (2003) 406 p*
- [13] M. E. Peskin and D. V. Schroeder, *Reading, USA: Addison-Wesley (1995) 842 p*

-
- [14] F. Mandl and G. Shaw, *Chichester, UK: Wiley (1984) 354 P. (A Wiley-Interscience Publication)*
- [15] S. Weinberg, *Cambridge, UK: Univ. Pr. (1995) 609 p*
- [16] S. Weinberg, *Cambridge, UK: Univ. Pr. (1996) 489 p*
- [17] S. P. Martin, arXiv:hep-ph/9709356.
- [18] I. J. R. Aitchison, arXiv:hep-ph/0505105.
- [19] D. J. H. Chung, L. L. Everett, G. L. Kane, S. F. King, J. Lykken, L. T. Wang, *Phys. Rept.* **407** (2005) 1.
- [20] M. Drees, arXiv:hep-ph/9611409.
- [21] H. E. Haber, arXiv:hep-ph/9306207.
- [22] J. R. Ellis, arXiv:hep-ph/0203114.
- [23] K. Intriligator and N. Seiberg, *Class. Quant. Grav.* **24**, S741 (2007) [arXiv:hep-ph/0702069].
- [24] H. Murayama, arXiv:hep-ph/0002232.
- [25] M. F. Sohnius, *Phys. Rept.* **128**, 39 (1985).
- [26] R. L. Arnowitt and P. Nath, arXiv:hep-ph/9309277.
- [27] J. Wess and J. Bagger, *Princeton, USA: Univ. Pr. (1992) 259 p*
- [28] S. Weinberg, *Cambridge, UK: Univ. Pr. (2000) 419 p*
- [29] T. Araki *et al.* [KamLAND Collaboration], *Phys. Rev. Lett.* **94** (2005) 081801.
- [30] Super-Kamiokande Collaboration (Y. Ashie *et al.*), *Phys. Rev. D* **71** (2005) 112005; Y. Ashie *et al.* [Super-Kamiokande Collaboration], *Phys. Rev. Lett.* **93** (2004) 101801; M. Ambrosio *et al.* [MACRO Collaboration], *Eur. Phys. J. C* **36** (2004) 323; M. C. Sanchez *et al.* [Soudan 2 Collaboration], *Phys. Rev. D* **68** (2003) 113004; [MINOS Collaboration], hep-ex/0512036.

- [31] E. Aliu *et al.* [K2K Collaboration], Phys. Rev. Lett. **94** (2005) 081802.
- [32] <http://www.physics.gla.ac.uk/ppt/research.htm>
- [33] C. Amsler *et al.* [Particle Data Group], Phys. Lett. B **667**, 1 (2008).
- [34] <http://pdg.lbl.gov>
- [35] P. Langacker, Comments Nucl. Part. Phys. **19**, 1 (1989).
- [36] J. Erler and P. Langacker, arXiv:0807.3023 [hep-ph].
- [37] J.J.Thompson Phil. Mag. **44**, 293 (1897)
- [38] J. C. Street and E. C. Stevenson, Phys. Rev. **52**, 1003 (1937).
- [39] M. L. Perl *et al.*, Phys. Rev. Lett. **35**, 1489 (1975).
- [40] F. Reines and C. L. Cowan, Phys. Rev. **92**, 830 (1953).
- [41] G. Danby, J. M. Gaillard, K. Goulianos, L. M. Lederman, N. B. Mistry, M. Schwartz and J. Steinberger, Phys. Rev. Lett. **9**, 36 (1962).
- [42] K. Kodama *et al.*, Nucl. Instrum. Meth. A **493**, 45 (2002).
- [43] M. Gell-Mann, Phys. Lett. **8**, 214 (1964).
- [44] G. Zweig CERN preprint **TH401**, 412 (1964)
- [45] M. Gell-Mann, “The Eightfold Way: A Theory Of Strong Interaction Symmetry,”
- [46] M. Gell-Mann and Y. Neeman, “The eightfold way: a review with a collection of reprints,”
- [47] G. Zweig, “An SU(3) Model For Strong Interaction Symmetry And Its Breaking. 2,”
- [48] E. D. Bloom *et al.*, Phys. Rev. Lett. **23**, 930 (1969).
- [49] M. Breidenbach *et al.*, Phys. Rev. Lett. **23**, 935 (1969).

- [50] J. D. Bjorken, Phys. Rev. **179**, 1547 (1969).
- [51] J. E. Augustin *et al.* [SLAC-SP-017 Collaboration], Phys. Rev. Lett. **33**, 1406 (1974).
- [52] J. J. Aubert *et al.* [E598 Collaboration], Phys. Rev. Lett. **33**, 1404 (1974).
- [53] S. W. Herb *et al.*, Phys. Rev. Lett. **39**, 252 (1977).
- [54] F. Abe *et al.* [CDF Collaboration], Phys. Rev. Lett. **73**, 225 (1994) [arXiv:hep-ex/9405005].
- [55] J. Bernstein, M. Ruderman and G. Feinberg, Phys. Rev. **132**, 1227 (1963).
- [56] S. N. Gninenko, N. V. Krasnikov and A. Rubbia, Phys. Rev. D **75**, 075014 (2007) [arXiv:hep-ph/0612203].
- [57] M. Marinelli and G. Morpurgo, Phys. Lett. B **137**, 439 (1984).
- [58] J. Baumann, J. Kalus, R. Gahler and W. Mampe, Phys. Rev. D **37**, 3107 (1988).
- [59] V. Meyer *et al.*, Phys. Rev. Lett. **84**, 1136 (2000) [arXiv:hep-ex/9907013].
- [60] G. Arnison *et al.* [UA1 Collaboration], Phys. Lett. B **122**, 103 (1983).
- [61] G. Arnison *et al.* [UA1 Collaboration], Phys. Lett. B **126**, 398 (1983).
- [62] F. J. Yndurain, Phys. Lett. B **345**, 524 (1995).
- [63] R. Barate *et al.* [LEP Working Group for Higgs boson searches and ALEPH Collaboration], Phys. Lett. B **565**, 61 (2003) [arXiv:hep-ex/0306033].
- [64] G. Bernardi *et al.* [Tevatron New Phenomena Higgs Working Group and CDF Collaboration and D], arXiv:0808.0534 [hep-ex].
- [65] P. Renton Talk given at ICHEP 2008 conference.
- [66] J. S. Schwinger, Phys. Rev. **74**, 1439 (1948).
- [67] J. S. Schwinger, Phys. Rev. **75**, 651 (1948).

-
- [68] J. S. Schwinger, Phys. Rev. **76**, 790 (1949).
- [69] S. Tomonaga, Phys. Rev. **74**, 224 (1948)
- [70] R. P. Feynman, Phys. Rev. **76**, 749 (1949).
- [71] R. P. Feynman, Phys. Rev. **76**, 769 (1949).
- [72] F. J. Dyson, Phys. Rev. **75**, 486 (1949).
- [73] T. Aoyama, M. Hayakawa, T. Kinoshita and M. Nio, Phys. Rev. D **77**, 053012 (2008) [arXiv:0712.2607 [hep-ph]].
- [74] Cladé et al. Phys. Rev. A. **74**, 052109 (2006)
- [75] Gerginov et al. Phys. Rev. A. **73**,032504 (2006)
- [76] G. Arnison *et al.* [UA1 Collaboration], Phys. Lett. B **166**, 484 (1986).
- [77] G. Abbiendi *et al.* [OPAL Collaboration], Eur. Phys. J. C **20**, 601 (2001) [arXiv:hep-ex/0101044].
- [78] J. Goldstone, Nuovo Cim. **19**, 154 (1961).
- [79] J. Goldstone, A. Salam and S. Weinberg, Phys. Rev. **127**, 965 (1962).
- [80] Y. Nambu, Phys. Rev. Lett. **4**, 380 (1960).
- [81] P. W. Higgs, Phys. Lett. **12**, 132 (1964).
- [82] P. W. Higgs, Phys. Rev. Lett. **13**, 508 (1964).
- [83] P. W. Higgs, Phys. Rev. **145**, 1156 (1966).
- [84] F. Englert and R. Brout, Phys. Rev. Lett. **13**, 321 (1964).
- [85] G. S. Guralnik, C. R. Hagen and T. W. B. Kibble, Phys. Rev. Lett. **13**, 585 (1964).
- [86] T. W. B. Kibble, Phys. Rev. **155**, 1554 (1967).
- [87] S. L. Glashow, Nucl. Phys. **22**, 579 (1961).

- [88] S. Weinberg, Phys. Rev. Lett. **19**, 1264 (1967).
- [89] A. Salam, *Originally printed in *Svartholm: Elementary Particle Theory, Proceedings Of The Nobel Symposium Held 1968 At Lerum, Sweden*, Stockholm 1968, 367-377*
- [90] J. S. Schwinger, Phys. Rev. **73**, 416 (1948).
- [91] R. P. Feynman, Phys. Rev. **74**, 1430 (1948).
- [92] G. 't Hooft and M. J. G. Veltman, Nucl. Phys. B **44**, 189 (1972).
- [93] W. Siegel, Phys. Lett. B **84**, 193 (1979).
- [94] D. Stockinger, *In the Proceedings of 2005 International Linear Collider Workshop (LCWS 2005), Stanford, California, 18-22 Mar 2005, pp 0203* [arXiv:hep-ph/0506258].
- [95] D. Stockinger, JHEP **0503**, 076 (2005) [arXiv:hep-ph/0503129].
- [96] G. 't Hooft, Nucl. Phys. B **35**, 167 (1971).
- [97] M. Gell-Mann and F. E. Low, Phys. Rev. **95**, 1300 (1954).
- [98] E. C. G. Stueckelberg and A. Petermann, Helv. Phys. Acta **26** (1953) 499.
- [99] W. Pauli and F. Villars, Rev. Mod. Phys. **21** (1949) 434.
- [100] S. Weinberg, Phys. Rev. D **13**, 974 (1976).
- [101] S. Weinberg, Phys. Rev. D **19**, 1277 (1979).
- [102] E. Gildener, Phys. Rev. D **14**, 1667 (1976).
- [103] L. Susskind, Phys. Rev. D **20**, 2619 (1979).
- [104] G. 't Hooft, C. Itzykson, A. Jaffe, H. Lehmann, P. K. Mitter, I. M. Singer and R. Stora, *New York, Usa: Plenum (1980) 438 P. (Nato Advanced Study Institutes Series: Series B, Physics, 59)*

- [105] G. Bertone, D. Hooper and J. Silk, Phys. Rept. **405**, 279 (2005) [arXiv:hep-ph/0404175].
- [106] A. D. Dolgov, arXiv:0803.3887 [hep-ph].
- [107] G. W. Bennett *et al.* [Muon G-2 Collaboration], Phys. Rev. D **73**, 072003 (2006) [arXiv:hep-ex/0602035].
- [108] J. P. Miller, E. de Rafael and B. L. Roberts, Rept. Prog. Phys. **70** (2007) 795.
- [109] M. Davier, Nucl. Phys. Proc. Suppl. **169** (2007) 288.
- [110] K. Hagiwara, A. D. Martin, D. Nomura and T. Teubner, Phys. Lett. B **649** (2007) 173.
- [111] F. Jegerlehner, arXiv:hep-ph/0703125.
- [112] B. T. Cleveland *et al.*, Astrophys. J. **496** (1998) 505; J. N. Abdurashitov *et al.* [SAGE Collaboration], J. Exp. Theor. Phys. **95** (2002) 181 [Zh. Eksp. Teor. Fiz. **122** (2002) 211]; W. Hampel *et al.* [GALLEX Collaboration], Phys. Lett. B **447** (1999) 127; J. Hosaka *et al.* [Super-Kamkiokande Collaboration], hep-ex/0508053; M. Altmann *et al.* [GNO COLLABORATION Collaboration], Phys. Lett. B **616** (2005) 174; SNO Collaboration (B. Aharmim *et al.*). *Phys. Rev. C* **72** (2005) 055502; Phys. Rev. D **72**, 052010 (2005).
- [113] R. Haag, J. T. Lopuszanski and M. Sohnius, Nucl. Phys. B **88**, 257 (1975).
- [114] S. R. Coleman and J. Mandula, Phys. Rev. **159**, 1251 (1967).
- [115] Yu. A. Golfand and E. P. Likhtman, JETP Lett. **13**, 323 (1971) [Pisma Zh. Eksp. Teor. Fiz. **13**, 452 (1971)].
- [116] N. Seiberg, JHEP **0306**, 010 (2003) [arXiv:hep-th/0305248].
- [117] T. Araki, K. Ito and A. Ohtsuka, Phys. Lett. B **573**, 209 (2003) [arXiv:hep-th/0307076].
- [118] I. Jack, D. R. T. Jones and L. A. Worthy, Phys. Lett. B **611**, 199 (2005) [arXiv:hep-th/0412009].

- [119] D. Stockinger, J. Phys. G **34**, R45 (2007) [arXiv:hep-ph/0609168].
- [120] J. Haestier, S. Heinemeyer, W. Hollik, D. Stockinger, A. M. Weber and G. Weiglein, AIP Conf. Proc. **903**, 291 (2007) [arXiv:hep-ph/0610318].
- [121] D. Stockinger, arXiv:0710.2429 [hep-ph].
- [122] S. Marchetti, S. Mertens, U. Nierste and D. Stockinger, arXiv:0808.1530 [hep-ph].
- [123] A. Czarnecki and W. J. Marciano, Phys. Rev. D **64**, 013014 (2001) [arXiv:hep-ph/0102122].
- [124] S. F. King, S. Moretti and R. Nevzorov, Phys. Lett. B **650**, 57 (2007) [arXiv:hep-ph/0701064].
- [125] J. R. Ellis, J. S. Hagelin, D. V. Nanopoulos, K. A. Olive and M. Srednicki, Nucl. Phys. B **238**, 453 (1984).
- [126] L. E. Ibanez and G. G. Ross, Phys. Lett. B **110**, 215 (1982).
- [127] K. Inoue, A. Kakuto, H. Komatsu and S. Takeshita, Prog. Theor. Phys. **68**, 927 (1982) [Erratum-ibid. **70**, 330 (1983)].
- [128] K. Inoue, A. Kakuto, H. Komatsu and S. Takeshita, Prog. Theor. Phys. **71**, 413 (1984).
- [129] L. Alvarez-Gaume, M. Claudson and M. B. Wise, Nucl. Phys. B **207**, 96 (1982).
- [130] L. Alvarez-Gaume, J. Polchinski and M. B. Wise, Nucl. Phys. B **221**, 495 (1983).
- [131] J. R. Ellis, J. S. Hagelin, D. V. Nanopoulos and K. Tamvakis, Phys. Lett. B **125**, 275 (1983).
- [132] A. Dedes and P. Slavich, Nucl. Phys. B **657**, 333 (2003) [arXiv:hep-ph/0212132].
- [133] M. R. Nolta *et al.* [WMAP Collaboration], Astrophys. J. **608**, 10 (2004) [arXiv:astro-ph/0305097].
- [134] V. A. Kuzmin, V. A. Rubakov and M. E. Shaposhnikov, Phys. Lett. B **155**, 36 (1985).

- [135] I. Affleck and M. Dine, Nucl. Phys. B **249**, 361 (1985).
- [136] J. Wess and B. Zumino, Nucl. Phys. B **70**, 39 (1974).
- [137] L. Girardello and M. T. Grisaru, Nucl. Phys. B **194**, 65 (1982).
- [138] P. Fayet and J. Iliopoulos, Phys. Lett. B **51**, 461 (1974); P. Fayet, Nucl. Phys. B **90**, 104 (1975).
- [139] L. O’Raifeartaigh, Nucl. Phys. B **96**, 331 (1975).
- [140] S. Ferrara, L. Girardello and F. Palumbo, Phys. Rev. D **20**, 403 (1979).
- [141] W. Fischler, H. P. Nilles, J. Polchinski, S. Raby and L. Susskind, Phys. Rev. Lett. **47**, 757 (1981).
- [142] E. Witten, Nucl. Phys. B **188**, 513 (1981).
- [143] L. Randall, arXiv:hep-ph/9706474.
- [144] H. Murayama, arXiv:0709.3041 [hep-ph].
- [145] H. Murayama and Y. Nomura, Phys. Rev. D **75**, 095011 (2007) [arXiv:hep-ph/0701231].
- [146] H. Murayama and Y. Nomura, Phys. Rev. Lett. **98**, 151803 (2007) [arXiv:hep-ph/0612186].
- [147] K. Intriligator, N. Seiberg and D. Shih, JHEP **0604**, 021 (2006) [arXiv:hep-th/0602239].
- [148] K. Intriligator, N. Seiberg and D. Shih, JHEP **0707**, 017 (2007) [arXiv:hep-th/0703281].
- [149] M. L. Brooks *et al.* [MEGA Collaboration], Phys. Rev. Lett. **83**, 1521 (1999) [arXiv:hep-ex/9905013].
- [150] M. Ahmed *et al.* [MEGA Collaboration], Phys. Rev. D **65**, 112002 (2002) [arXiv:hep-ex/0111030].

- [151] M. Ciuchini *et al.*, JHEP **9810**, 008 (1998) [arXiv:hep-ph/9808328].
- [152] F. Gabbiani and A. Masiero, Nucl. Phys. B **322**, 235 (1989);
- [153] J. Ellis, S. Ferrara and D.V. Nanopoulos, Phys. Lett. B **114**, 231 (1982);
- [154] J. Polchinski and M.B. Wise, Phys. Lett. B **125**, 393 (1983);
- [155] F. del Aguila, M.B. Gavela, J.A. Grifols and A. Méndez, Phys. Lett. B **126**, 71 (1983) [Erratum-ibid. B **129**, 473 (1983)];
- [156] G. 't Hooft, Phys. Rev. Lett. **37**, 8 (1976).
- [157] J. Abdallah *et al.* [LEP SUSY Working Group], <http://lepsusy.web.cern.ch/lepsusy/>.
- [158] [CDF Collaboration], <http://www-cdf.fnal.gov/physics/>
CDF Notes 9176; 9229;9332
- [159] V. M. Abazov *et al.* [D0 Collaboration], Phys. Lett. B **660**, 449 (2008);
- [160] J. Abdallah *et al.* [DELPHI Collaboration], Eur. Phys. J. C **36**, 1 (2004) [Eur. Phys. J. C **37**, 129 (2004)] [arXiv:hep-ex/0406009].
- [161] J. R. Ellis, K. A. Olive and Y. Santoso, New J. Phys. **4**, 32 (2002) [arXiv:hep-ph/0202110].
- [162] H. Baer, C. Balazs, A. Belyaev, J. K. Mizukoshi, X. Tata and Y. Wang, JHEP **0207**, 050 (2002) [arXiv:hep-ph/0205325].
- [163] L. Roszkowski, R. Ruiz de Austri, and T. Nihei, JHEP **08** (2001) 024, [hep-ph/0106334](http://arxiv.org/abs/hep-ph/0106334).
- [164] H. Baer, C. Balazs, and A. Belyaev, JHEP **03** (2002) 042, [hep-ph/0202076](http://arxiv.org/abs/hep-ph/0202076).
- [165] H. Baer and C. Balazs, JCAP **0305** (2003) 006, [hep-ph/0303114](http://arxiv.org/abs/hep-ph/0303114).
- [166] U. Chattopadhyay, A. Corsetti, and P. Nath, Phys. Rev. **D68** (2003) 035005, [hep-ph/0303201](http://arxiv.org/abs/hep-ph/0303201).

- [167] A. B. Lahanas and D. V. Nanopoulos, Phys. Lett. **B568** (2003) 55–62, hep-ph/0303130.
- [168] G. Belanger, F. Boudjema, A. Cottrant, A. Pukhov, and A. Semenov, hep-ph/0412309.
- [169] A. Belyaev, AIP Conf. Proc. **753**, 352 (2005) [arXiv:hep-ph/0410385].
- [170] B. C. Allanach and C. G. Lester, Phys. Rev. D **73**, 015013 (2006) [arXiv:hep-ph/0507283].
- [171] B. C. Allanach, Phys. Lett. B **635**, 123 (2006) [arXiv:hep-ph/0601089].
- [172] B. C. Allanach, K. Cranmer, C. G. Lester and A. M. Weber, JHEP **0708**, 023 (2007) [arXiv:0705.0487 [hep-ph]].
- [173] L. Roszkowski, R. R. de Austri, J. Silk and R. Trotta, *On prospects for dark matter indirect detection in the Constrained MSSM*, [arXiv:0707.0622].
- [174] R. R. de Austri, R. Trotta and L. Roszkowski, *A Markov chain Monte Carlo analysis of the CMSSM*, JHEP **0605** (2006) 002 [arXiv:hep-ph/0602028].
- [175] B. C. Allanach, C. G. Lester and A. M. Weber, *The dark side of mSUGRA*, JHEP **12** (2006) 065 [arXiv:hep-ph/0609295].
- [176] L. Roszkowski, R. R. de Austri and R. Trotta *Implications for the Constrained MSSM from a new prediction for $b \rightarrow s\gamma$* , JHEP **2007** (2007) 075 [arXiv:0705.2012].
- [177] F. Feroz, B. C. Allanach, M. Hobson, S. S. AbdusSalam, R. Trotta and A. M. Weber, arXiv:0807.4512 [hep-ph].
- [178] B. C. Allanach *et al.*, Eur. Phys. J. C **25** (2002) 113 [arXiv:hep-ph/0202233].
- [179] N. Ghodbane and H. U. Martyn, in *Proc. of the APS/DPF/DPB Summer Study on the Future of Particle Physics (Snowmass 2001)* ed. N. Graf, arXiv:hep-ph/0201233.
- [180] D. M. Pierce, J. A. Bagger, K. T. Matchev and R. j. Zhang, Nucl. Phys. B **491**, 3 (1997) [arXiv:hep-ph/9606211].

- [181] B. C. Allanach, *Comput. Phys. Commun.* **143**, 305 (2002) [arXiv:hep-ph/0104145].
- [182] V. D. Barger, M. S. Berger and P. Ohmann, *Phys. Rev. D* **49**, 4908 (1994) [arXiv:hep-ph/9311269].
- [183] B. C. Allanach <http://projects.hepforge.org/softsusy/>
- [184] S. Chang, P. J. Fox and N. Weiner, *JHEP* **0608**, 068 (2006) [arXiv:hep-ph/0511250].
- [185] K. Choi, K. S. Jeong and K. i. Okumura, *JHEP* **0509** (2005) 039 [arXiv:hep-ph/0504037].
- [186] Y. Nomura and B. Tweedie, *Phys. Rev. D* **72**, 015006 (2005) [arXiv:hep-ph/0504246].
- [187] K. Choi, K. S. Jeong, T. Kobayashi and K. i. Okumura, *Phys. Lett. B* **633** (2006) 355 [arXiv:hep-ph/0508029].
- [188] R. Kitano and Y. Nomura, *Phys. Lett. B* **631**, 58 (2005) [arXiv:hep-ph/0509039].
- [189] O. Lebedev, H. P. Nilles and M. Ratz, arXiv:hep-ph/0511320.
- [190] R. Kitano and Y. Nomura, *Phys. Rev. D* **73**, 095004 (2006) [arXiv:hep-ph/0602096].
- [191] S. Chang, L. J. Hall and N. Weiner, *Phys. Rev. D* **75**, 035009 (2007) [arXiv:hep-ph/0604076].
- [192] J. A. Casas, J. R. Espinosa and I. Hidalgo, *JHEP* **0503**, 038 (2005) [arXiv:hep-ph/0502066].
- [193] Z. Chacko, H. S. Goh and R. Harnik, *Phys. Rev. Lett.* **96**, 231802 (2006) [arXiv:hep-ph/0506256].
- [194] Z. Chacko, H. S. Goh and R. Harnik, *JHEP* **0601**, 108 (2006) [arXiv:hep-ph/0512088].

- [195] R. Barbieri and G. F. Giudice, Nucl. Phys. B **306**, 63 (1988).
- [196] J. R. Ellis, K. Enqvist, D. V. Nanopoulos and F. Zwirner, Mod. Phys. Lett. A **1** (1986) 57.
- [197] B. de Carlos and J. A. Casas, Phys. Lett. B **309**, 320 (1993) [arXiv:hep-ph/9303291].
- [198] B. de Carlos and J. A. Casas, arXiv:hep-ph/9310232.
- [199] P. H. Chankowski, J. R. Ellis and S. Pokorski, Phys. Lett. B **423**, 327 (1998) [arXiv:hep-ph/9712234].
- [200] K. Agashe and M. Graesser, Nucl. Phys. B **507**, 3 (1997) [arXiv:hep-ph/9704206].
- [201] D. Wright, arXiv:hep-ph/9801449.
- [202] G. L. Kane and S. F. King, Phys. Lett. B **451** (1999) 113 [arXiv:hep-ph/9810374].
- [203] M. Bastero-Gil, G. L. Kane and S. F. King, Phys. Lett. B **474**, 103 (2000) [arXiv:hep-ph/9910506].
- [204] J. L. Feng, K. T. Matchev and T. Moroi, Phys. Rev. D **61**, 075005 (2000) [arXiv:hep-ph/9909334].
- [205] B. C. Allanach, J. P. J. Hetherington, M. A. Parker and B. R. Webber, JHEP **0008**, 017 (2000) [arXiv:hep-ph/0005186].
- [206] T. Kobayashi, H. Terao and A. Tsuchiya, Phys. Rev. D **74**, 015002 (2006) [arXiv:hep-ph/0604091].
- [207] R. Dermisek and J. F. Gunion, Phys. Rev. Lett. **95**, 041801 (2005) [arXiv:hep-ph/0502105].
- [208] R. Barbieri and L. J. Hall, arXiv:hep-ph/0510243.
- [209] R. Barbieri, L. J. Hall and V. S. Rychkov, Phys. Rev. D **74**, 015007 (2006) [arXiv:hep-ph/0603188].

- [210] B. Gripaios and S. M. West, Phys. Rev. D **74**, 075002 (2006) [arXiv:hep-ph/0603229].
- [211] R. Dermisek, J. F. Gunion and B. McElrath, Phys. Rev. D **76** (2007) 051105 [arXiv:hep-ph/0612031].
- [212] G. W. Anderson and D. J. Castano, Phys. Lett. B **347**, 300 (1995) [arXiv:hep-ph/9409419].
- [213] G. W. Anderson and D. J. Castano, Phys. Rev. D **52**, 1693 (1995) [arXiv:hep-ph/9412322].
- [214] G. W. Anderson and D. J. Castano, Phys. Rev. D **53**, 2403 (1996) [arXiv:hep-ph/9509212].
- [215] G. W. Anderson, D. J. Castano and A. Riotto, Phys. Rev. D **55**, 2950 (1997) [arXiv:hep-ph/9609463].
- [216] J. A. Casas, J. R. Espinosa and I. Hidalgo, JHEP **0401**, 008 (2004) [arXiv:hep-ph/0310137].
- [217] J. A. Casas, J. R. Espinosa and I. Hidalgo, arXiv:hep-ph/0402017.
- [218] J. A. Casas, J. R. Espinosa and I. Hidalgo, JHEP **0411**, 057 (2004) [arXiv:hep-ph/0410298].
- [219] J. A. Casas, J. R. Espinosa and I. Hidalgo, Nucl. Phys. B **777** (2007) 226 [arXiv:hep-ph/0607279].
- [220] P. Ciafaloni and A. Strumia, Nucl. Phys. B **494**, 41 (1997) [arXiv:hep-ph/9611204].
- [221] K. L. Chan, U. Chattopadhyay and P. Nath, Phys. Rev. D **58**, 096004 (1998) [arXiv:hep-ph/9710473].
- [222] R. Barbieri and A. Strumia, Phys. Lett. B **433**, 63 (1998) [arXiv:hep-ph/9801353].

- [223] L. Giusti, A. Romanino and A. Strumia, Nucl. Phys. B **550**, 3 (1999) [arXiv:hep-ph/9811386].
- [224] P. H. Chankowski, J. R. Ellis, K. A. Olive and S. Pokorski, Phys. Lett. B **452**, 28 (1999) [arXiv:hep-ph/9811284].
- [225] S. F. King and J. P. Roberts, JHEP **0609** (2006) 036 [arXiv:hep-ph/0603095].
- [226] S. F. King and J. P. Roberts, JHEP **0701** (2007) 024 [arXiv:hep-ph/0608135].
- [227] P. H. Chankowski, J. R. Ellis, M. Olechowski and S. Pokorski, Nucl. Phys. B **544**, 39 (1999) [arXiv:hep-ph/9808275].
- [228] G. L. Kane, J. D. Lykken, B. D. Nelson and L. T. Wang, Phys. Lett. B **551**, 146 (2003) [arXiv:hep-ph/0207168].
- [229] P. C. Schuster and N. Toro, arXiv:hep-ph/0512189.
- [230] A. Salam, J. Strathdee, Phys. Rev. D **11** (1975) 1521; M. T. Grisaru, W. Siegel, M. Rocek, Nucl. Phys. B **159** (1979) 429.
- [231] M. B. Green, J. H. Schwarz, E. Witten, Superstring Theory (Cambridge Univ. Press, Cambridge, 1987).
- [232] P. Horava, E. Witten, Nucl. Phys. B **460** (1996) 506; Nucl. Phys. B **475** (1996) 94.
- [233] E. Witten, Nucl. Phys. B **471** (1996) 135; T. Banks, M. Dine, Nucl. Phys. B **479** (1996) 173; K. Choi, H. B. Kim, C. Muñoz, Phys. Rev. D **57** (1998) 7521.
- [234] F. del Aguila, G. A. Blair, M. Daniel, G. G. Ross, Nucl. Phys. B **272** (1986) 413.
- [235] Y. Hosotani, Phys. Lett. B **129** (1983) 193.
- [236] Ya. B. Zel'dovich, I. Yu. Kobzarev, L. B. Okun, Sov. Phys. JETP **40** (1975) 1.
- [237] T. Hambye, E. Ma, M. Raidal and U. Sarkar, Phys. Lett. B **512** (2001) 373 [arXiv:hep-ph/0011197].

- [238] S. F. King, R. Luo, D. J. Miller and R. Nevrozov, arXiv:0806.0330 [hep-ph].
- [239] R. Howl and S. F. King, Phys. Lett. B **652**, 331 (2007) [arXiv:0705.0301 [hep-ph]].
- [240] R. Howl and S. F. King, JHEP **0801**, 030 (2008) [arXiv:0708.1451 [hep-ph]].
- [241] S. R. Coleman and E. Weinberg, Phys. Rev. D **7**, 1888 (1973).
- [242] S. Weinberg, Phys. Rev. D **7** (1973) 2887.
- [243] F. Abe *et al* [CSF Collaboration] Phys. Rev. Lett. **79**, 2192 (1997).
- [244] P. Abreu *et al.* [DELPHI Collaboration], Phys. Lett. B **485**, 45 (2000) R. Barate *et al.* [ALEPH Collaboration] Eur. Phys. J. C **12**, 183 (2000)
- [245] L. Solmaz, arXiv:hep-ph/0609162.
- [246] J. R. Ellis, S. Heinemeyer, K. A. Olive and G. Weiglein, JHEP **0605**, 005 (2006) [arXiv:hep-ph/0602220].
- [247] H. Baer, A. Mustafayev, S. Profumo, A. Belyaev and X. Tata, JHEP **0507**, 065 (2005) [arXiv:hep-ph/0504001].
- [248] J. R. Ellis, A. Ferstl, K. A. Olive and Y. Santoso, Phys. Rev. D **67**, 123502 (2003) [arXiv:hep-ph/0302032].
- [249] J. R. Ellis, T. Falk, K. A. Olive and Y. Santoso, Nucl. Phys. B **652**, 259 (2003) [arXiv:hep-ph/0210205].
- [250] J. R. Ellis, K. A. Olive and Y. Santoso, Phys. Lett. B **539**, 107 (2002) [arXiv:hep-ph/0204192].
- [251] V. Berezhinsky, A. Bottino, J. R. Ellis, N. Fornengo, G. Mignola and S. Scopel, Astropart. Phys. **5**, 1 (1996) [arXiv:hep-ph/9508249].
- [252] P. Nath and R. L. Arnowitt, Phys. Rev. D **56**, 2820 (1997) [arXiv:hep-ph/9701301].
- [253] M. Drees, M. M. Nojiri, D. P. Roy and Y. Yamada, Phys. Rev. D **56**, 276 (1997) [Erratum-ibid. D **64**, 039901 (2001)] [arXiv:hep-ph/9701219].

- [254] J. R. Ellis, T. Falk, G. Ganis, K. A. Olive and M. Schmitt, Phys. Rev. D **58**, 095002 (1998) [arXiv:hep-ph/9801445].
- [255] J. R. Ellis, T. Falk, G. Ganis and K. A. Olive, Phys. Rev. D **62**, 075010 (2000) [arXiv:hep-ph/0004169].
- [256] [LEP Higgs Working Group for Higgs boson searches and ALEPH Collaboration], arXiv:hep-ex/0107031; A. Sopczac, Talk given at Charged Higgs 2006.
- [257] B. Schrempp and M. Wimmer, Prog. Part. Nucl. Phys. **37**, 1 (1996) [arXiv:hep-ph/9606386].
- [258] M. Carena, M. Quiros, C. E. M. Wagner, Nucl. Phys. B **461** (1996) 407.
- [259] U. Ellwanger, C. Hugonie, Eur. Phys. J. C **25** (2002) 297.
- [260] G. Passarino and M. J. G. Veltman, Nucl. Phys. B **160**, 151 (1979).
- [261] F. Abe *et al.* [CDF Collaboration], Phys. Rev. Lett. **79**, 2192 (1997).
- [262] A. Aktas *et al.* [H1 Collaboration], Phys. Lett. B **629**, 9 (2005) [arXiv:hep-ex/0506044].
- [263] S. Kermiche Heavy resonances search at Tevatron Talk given at the EPS 2007 conference
- [264] [CDF Collaboration], [http://www-cdf.fnal.gov/physics/CDF Notes 9246](http://www-cdf.fnal.gov/physics/CDF%20Notes%209246)
- [265] S. Wolfram, Phys. Lett. B **82** (1979) 65; C. B. Dover, T. K. Gaisser, G. Steigman, Phys. Rev. Lett. **42** (1979) 1117.
- [266] J. Rich, M. Spiro, J. Lloyd-Owen, Phys. Rept. **151** (1987) 239; P. F. Smith, Contemp. Phys. **29** (1988) 159; T. K. Hemmick *et al.*, Phys. Rev. D **41** (1990) 2074.
- [267] W. Gerlach and O. Stern Ann. Phys. **74**, 673 (1924), Ann. Phys. **76**, 163 (1925)
- [268] P.J.Mohr and B.N. Taylor, Rev. Mod. Phys. **77**, 1 (2005).

- [269] H. O. Back *et al.*, Phys. Lett. B **525**, 29 (2002).
- [270] M. L. Perl Ann. Rev. Nucl. Part. Sci.**30**, 229 (1980).
- [271] M. Passera, Nucl. Phys. Proc. Suppl. **169**, 213 (2007) [arXiv:hep-ph/0702027].
- [272] A. G. Cohen, T. S. Roy and M. Schmaltz, JHEP **0702**, 027 (2007) [arXiv:hep-ph/0612100].
- [273] S. A. Abel, C. Durnford, J. Jaeckel and V. V. Khoze, JHEP **0802**, 074 (2008) [arXiv:0712.1812 [hep-ph]].
- [274] J. R. Ellis, L. E. Ibanez and G. G. Ross, Phys. Lett. B **113**, 283 (1982).